UNIVERSITAT DE BARCELONA

# Analysis of the molecular bases that mediate the interplay between Multisubunit Tethering Complexes and P4-ATPases

Irene Pazos Capell

Aquesta tesi doctoral està subjecta a la llicència ***Reconeixement- NoComercial – SenseObraDerivada 3.0. Espanya de Creative Commons***.

Esta tesis doctoral está sujeta a la licencia ***Reconocimiento - NoComercial – SinObraDerivada 3.0. España de Creative* Commons**.

This doctoral thesis is licensed under the ***Creative Commons Attribution-NonCommercial-NoDerivs 3.0. Spain License***.

# Analysis of the molecular bases that mediate the interplay between Multisubunit Tethering Complexes and P4-ATPases

Tesis doctoral UB / 2018 - Programa de doctorado en Biomedicina

Institute for Research in Biomedicine (IRB) Barcelona


Irene Pazos Capell,

Doctoranda

Oriol Gallego Moli,
Co-director de Tesis

Raúl Méndez de la Iglesia,
Co-director de Tesis

Antonio Zorzano Olarte,
Tutor de Tesis

**A mis padres**

**y a mis hermanos.**

**ABSTRACT**

Vesicle trafficking is fundamental to distribute correctly lipids and proteins among cellular compartments. A complex network of interconnected pathways transport vesicles between organelles to satisfy the cellular demand. Multisubunit Tethering Complexes (MTCs) form a group of 9 protein assemblies that are conserved from yeast to human and that are essential for intracellular trafficking: Exocyst, Dls1, COG, GARP, HOPS, Corvet, TRAPPI, TRAPPII and TRAPPIII. Each MTC recognizes a specific type of vesicle and tether it to the appropriate acceptor membrane, providing specificity and directionality to the trafficking.

My research aimed to do a comparative analysis among all MTCs to shed light on the mechanism of action of these complexes. In my group we have developed PICT (Protein interaction from Imaging of Complexes after Translocation), a high sensitivity technique that allows us to study interactions between two proteins using live-cell imaging. We have used genetic interactions and PICT to search in the yeast genome for proteins that associate with MTCs and that are relevant for their function. I found that MTCs establish a network of interactions with P4-ATPases, lipid flippases that translocate phospholipids to the cytosolic leaflet of the membranes. P4-ATPases maintain the asymmetric distribution of phospholipids and they also play essential roles in vesicle trafficking. In yeast, there are 5 different P4-ATPases: Dnf1, Dnf2, Dnf2, Drs2 and NeoI. Dnf1 and Drs2 are the ones that concentrate most of the interactions with MTCs, mainly GARP and the TRAPPs. Up to date, no study had observed that MTCs and P4-ATPases might function together. In this Thesis I investigated the molecular mechanism that mediates the interplay in this network of essential components for the trafficking machinery.

I found that GARP is responsible to transport Dnf1 from late endosomes to *trans*-Golgi network during the recycling of Dnf1 to the plasma membrane, a transport step that is essential to maintain the correct distribution of PE in the plasma membrane. Furthermore, I have found that Drs2 is required for the proper functioning of the Cytoplasm-to-Vacuole Targeting (Cvt) pathway, a model historically used to study selective autophagy, and non-selective autophagy. The results of my thesis show that, in response to a temperature decrease, the cell induces the binding between TRAPPIII and Drs2 and that this interaction is required to sustain the adequate transport of Atg9. Drs2 is fundamental for the delivery of vesicles loaded with Atg9 from endocytic compartments, a new function of this flippase that might have important implications in other types of autophagy. I identified a short motif in the N- terminal tail of Drs2 that is required for the interaction TRAPPIII-Drs2. This is a motif highly conserved among P4-ATPases and other proteins that bind MTCs, suggesting that it might have a more general role in regulating the trafficking of vesicles that remains to be elucidated.

**CONTENTS**

# 1. INTRODUCTION

Eukaryotic cells contain numerous subcellular compartments bounded by membranes. The trafficking of proteins, lipids and other biomolecules among these compartments is constantly taking place to maintain the correct distribution of these components and fulfil the needs of the cell at any time (Bonifacino and Glick 2004). The primary carriers of these traffic routes are vesicles that bud in a cargo-dependent manner from a donor membrane, traffic and fuse with the acceptor membrane (See Figure 1.1). These processes require the concerted action of the trafficking machinery, a network of proteins that work together in a tightly regulated mode to ensure the correct functioning of this transport.

## 1.1. Multisubunit Tethering Complexes (MTCs)

Multisubunit Tethering Complexes (MTCs) are nine protein complexes evolutionary conserved in all eukaryotes that play a central role in vesicle trafficking. MTCs are compartment-specific complexes that promote the initial interaction between a vesicle and its acceptor membrane via binding of lipids and proteins on both membranes.

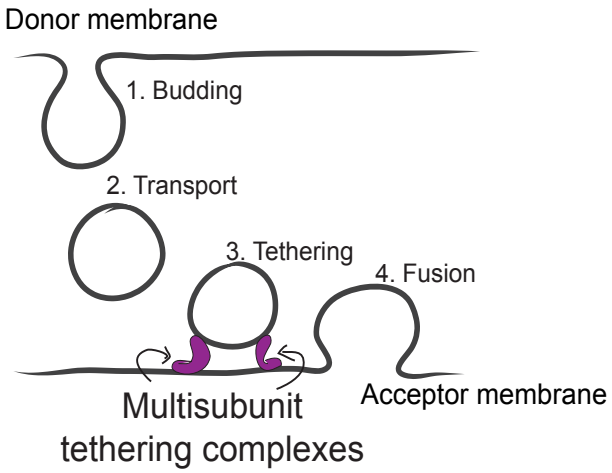


**Figure 1.1. Major steps in vesicle traffic**. Budding: the vesicle is generated from a donor membrane. Transport: the vesicle moves and reaches the target membrane. Tethering: the vesicle is docked to the acceptor membrane. MTCs are in charge of the tethering step. Fusion: the vesicle is fused with the membrane of the target compartment.

These interactions are critical to promote specific vesicle fusion at the proper target destination (Dubuke and Munson 2016). MTCs mode of action also requires the interaction with other components of the transport machinery such as GTPases, Soluble N-ethylmaleimide-sensitive factor Attachment protein REceptor (SNAREs), Sec1/Munc18 (SM) proteins and coat proteins. Thus, determining the network of interactions of MTCs has become indispensable to understand MTCs mechanism of action. However, many of these interactions are just transient associations, making them difficult to identify. A wider analysis to elucidate all the regulators that compose the whole network of interactions with MTCs, as

well as their cargo specificity, is still missing. This lack of information became our prime motivation to carry out a comparative analysis between MTCs and shed light in the network of interactions that are relevant for their function.

### 1.1.1. MTCs functions and subunit composition

MTCs define a heterologous group of 9 the large and flexible protein complexes that define the MTCs (See Figure 1.2). The 42 proteins that form MTCs are conserved in all eukaryotes.

MTCs are categorized into three groups: (1) the CATCHR family (collectively named Complexes Associated with Tethering Containing Helical Rods), comprised of Dsl1, the conserved oligomeric Golgi (COG) complex, the exocyst and the Golgi-associated retrograde protein (GARP). CATCHR tethering complexes play a role at compartments along the exocytic and endocytic pathways. (2) The class C core vacuole/endosome tethering (CORVET) complex and the homotypic fusion and vacuole protein sorting (HOPS) complex, both of them involved in the endolysosomal pathway. (3) The transport protein particle (TRAPP) complexes (TRAPPI, TRAPPII, and TRAPPIII), with tethering roles in both the secretory and endolysosomal pathways, as well as in autophagy.

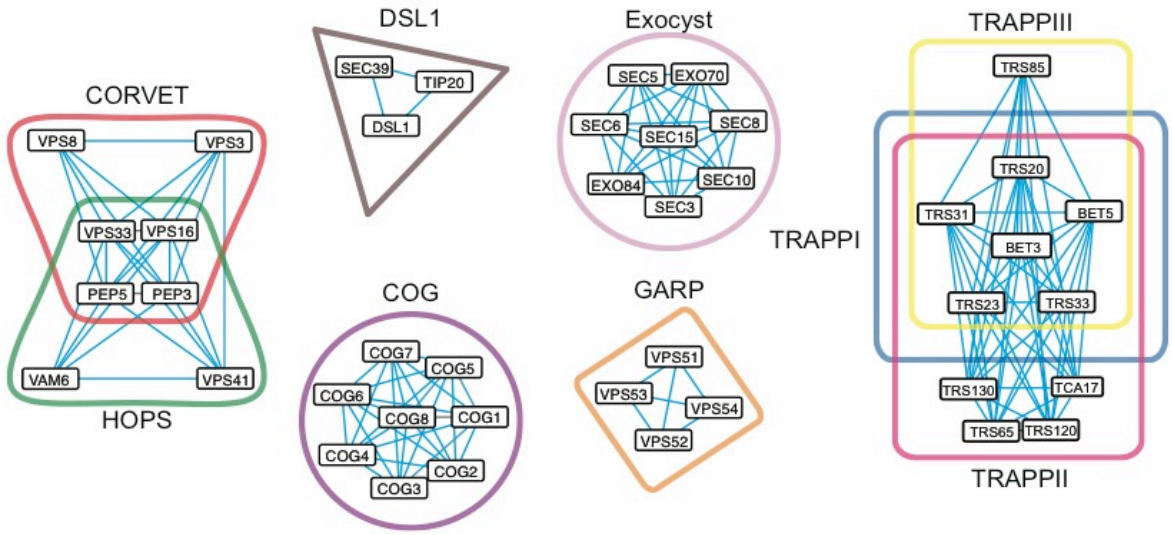


**Figure 1.2. Schematic representation of the 9 MTCs found in *Saccharomyces cerevisiae*.** Each MTC is represented by a different colour containing the subunits that comprise the complex (black rectangles). Blue lines represent physical interactions among MTCs subunits.

As shown in Figure 1.2, CORVET and HOPS complex share a common core of four subunits and each one contains two additional specific subunits. Both complexes act at the endolysosomal pathway. CORVET, which binds the Rab GTPase Vps21 (i.e. human Rab5 homolog), functions in early to late endosome fusion while HOPS, which interacts with Ypt7 (i.e. human Rab7 homolog), works downstream in late endosomes, homotypic vacuole-vacuole fusion and in the fusion of autophagosomes with the vacuole (Balderhaar and Ungermann 2013).

Regarding the CATCHR family, Dsl1 is composed of three different subunits and it is responsible to tether Golgi-derived COPI vesicles to the ER (Ren et al. 2010). The COG complex consists of eight subunits assembled in two subcomplexes, also called lobes A and B. This heterooctamer has been involved in retrograde transport between Golgi compartments (Suvorova, Duden, and Lupashin 2002), and from endosomes to the Golgi (Vanrheenen et al. 1999). The exocyst, composed of eight different subunits, is in charge of tethering secretory vesicles to exocytic sites at the plasma membrane (Heider et al. 2016). The exocyst binds the Rab GTPase Sec4 on secretory vesicles and the Rho GTPases Rho1, Rho3 and Cdc42 at the plasma membrane. The GARP complex is a heterotetramer that needs the Rab GTPase Ypt6 (i.e. human Rab6 homolog) to tether vesicles derived from early and late endosomes to the trans-Golgi network (TGN) (Conibear, Cleck, and Stevens 2003). GARP has been also shown to regulate the anterograde trafficking of Atg9 vesicles to promote biogenesis of the phagophore assembly site (PAS) during autophagy (Yang and Rosenwald 2016).

Finally, the TRAPP complexes have historically been classified as MTCs despite their major role as guanine nucleotide exchange factors (GEF) catalysing the GDP/GTP nucleotide exchange of Rab GTPases (Jones et al. 2000). It has been stablished so far that TRAPP complexes come in three forms in yeast and all of them share a core complex consisting of six different proteins (Bet3, Bet5, Trs20, Trs23, Trs31 and Trs33), the so called TRAPPI complex (Sacher et al. 2008). TRAPPI activates the Rab GTPase Ypt1 (i.e. human Rab1 homolog) during the tethering of ER-derived COPII vesicles to the Golgi (Sacher et al. 2001). TRAPPII, comprised of TRAPPI plus Trs120, Tr130, Tr65 and Tca17, activates Ypt31/32 to regulate the intra-Golgi trafficking and exocytic Golgi exit (Yip, Berscheminski, and Walz 2010). TRAPPIII involves TRAPPI complex plus one additional subunit (Trs85) and has a main role activating Ypt1 to regulate the transport of Atg9 vesicles and the biogenesis of the PAS during autophagy (J. J. Kim, Lipatova, and Segev 2016). However, in addition to its role in autophagy, TRAPPIII and Ypt1 have also been implicated in endosome to Golgi traffic (Lewis et al. 2000). Note that there are controversial reports about the exact number of different TRAPP complexes in yeast. In a recent publication (Thomas, Joiner, and Fromme 2018), the authors claimed that yeast possess only two TRAPP complexes (TRAPPII and TRAPIII) rather than three. Functional studies led them to conclude TRAPPIII has a major role in trafficking at the Golgi by carrying out the functions that had been historically assigned to TRAPPI. They show that TRAPPIII-catalyzed nucleotide exchange is an order of magnitude faster than that of TRAPPI in physiological enzyme activity assays. Correspondingly, Ypt1 activation and Golgi trafficking are significantly perturbed in TRAPPIII mutant cells. Therefore, it is likely that TRAPPIII activates Ypt1 to control multiple traffic events in the cell that range from facilitating normal ER–Golgi transport of COPII vesicles and at the medial/late Golgi to mediate normal endosome–Golgi trafficking to the PAS.

TRAPPIII is primary activator of Ypt1 at the Golgi. Furthermore, they suggest that TRAPPI may be an artefact of purification biochemical and localization analyses.

Figure 1.3 illustrates the canonical functions of MTCs in the cell and their corresponding GTPases counterparts:

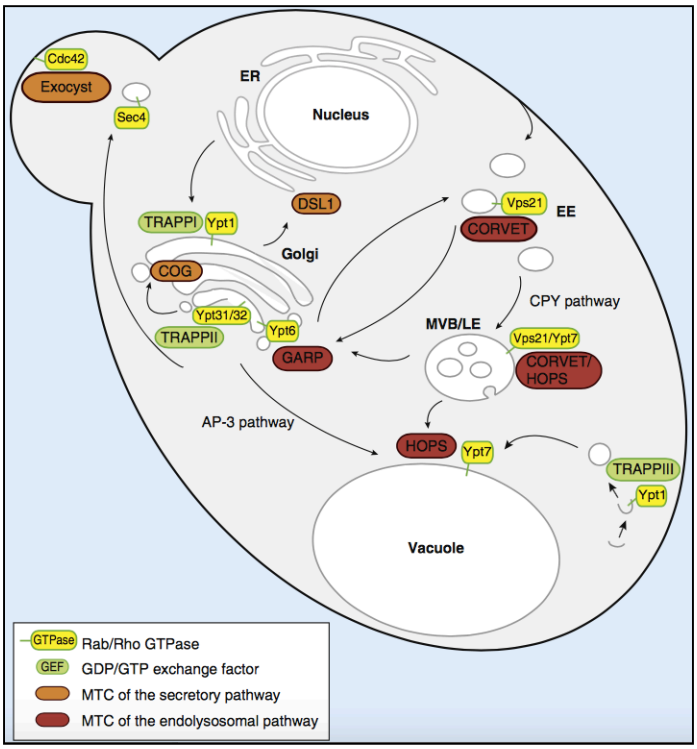


**Figure 1.3. Overall view of the trafficking routes (black arrows) controlled by MTCs in yeast**. Image from (Bröcker, Engelbrecht-Vandré, and Ungermann 2010).

### 1.1.2. Structural characterization of TRAPP complexes

Another fundamental requirement to better understand the mechanisms that mediate cellular pathways reside on the structural characterization of its biological complexes. Among those MTCs whose architecture has been studied, TRAPP complexes are some of the best characterized. Because of the relevance of TRAPPIII in this thesis, following I summarize what is known so far about TRAPP complexes at the structural level.

Crystal structures of two mammalian TRAPPI subcomplexes, the EM reconstruction of the yeast TRAPPI, together with the crystal structure of the core complex (Bet3, Bet5, Trs23, Trs31) bound to Ypt1, has generated an atomic reconstruction for TRAPPI (Y. G. Kim et al. 2006) (Cai et al. 2008). The model revealed an elongated complex with two large surfaces and a catalytic site to promote the GDP/GTP exchange of Ypt1. TRAPPI binds the GTPase Ypt1 through its Bet5 and Trs23 subunits and contains two copies of Bet3 (A and B). The C-terminus of Bet3-A plays a critical role in the catalytic mechanism (Figure 1.4).

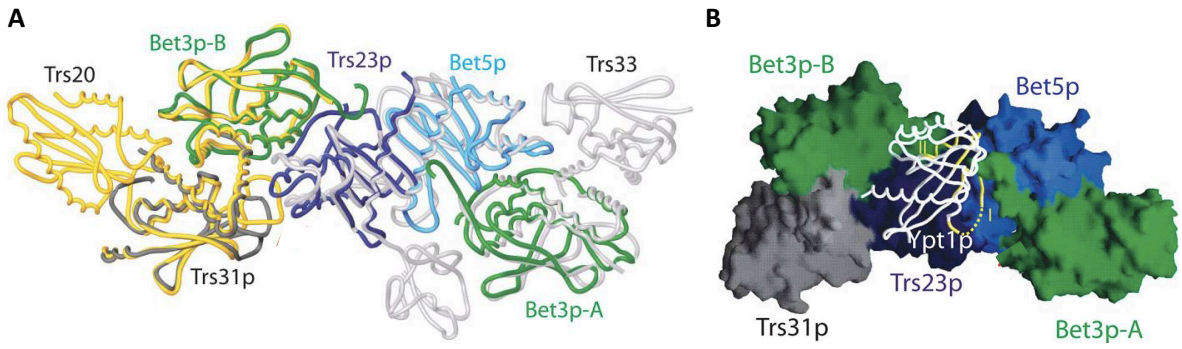


**Figure 1.4. (A)** Superposition of the yeast TRAPPI subcomplex containing Trs31/Bet3-B/Trs23/Bet5/Bet3-A with the Trs20/Trs31/Bet3-B (PDB ID 2J3W, yellow) and Trs23/Bet5/Bet3-A/Trs33 (2J32 white) complexes. **(B)** Surface representation of the TRAPPI complex together with Ypt1. Ypt1 is shown as a white backbone worm. Images adapted from Cai et al., 2008.

Yip et al. resolved the molecular architecture of the TRAPPII complex (Yip, Berscheminski, and Walz 2010). Based on single-particle electron microscopy from purified native TRAPPII, the characterization of TRAPPII showed a dimmer complex. In this model, TRAPPII-specific subunits are located in between two anti-parallel layers of TRAPPI, and Trs65 is required for dimerization of the complex. Trs130 is predicted to be interacting with Trs20 while Trs33 and Bet3 regulate the interaction of Trs120 with TRAPPI (Figure 1.5). Neither GST-Ypt31 nor GST-Ypt32 could pulled down TRAPPII, so the architecture reconstruction with these GTPases is still not generated.

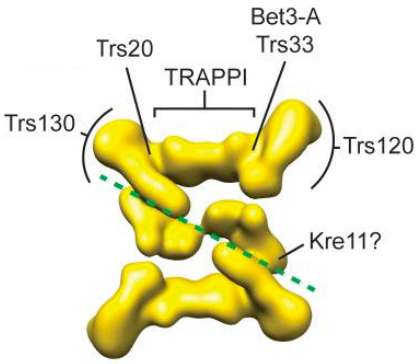


**Figure 1.5. TRAPPII reconstruction.** TRAPPI and TRAPPII specific subunits Trs120, Trs130 and Trs65 (Kre11) are indicated. The green dashed line represents the dimer interface. Image obtained from Yip et al., 2010.

TRAPPIII architecture was predicted based on negative EM staining and docking of the atomic model of TRAPPI in the EM density map of TRAPPIII (Tan et al. 2013). The model proposed locates Trs85 in one of the extremes of TRAPPI, interacting with Trs20, what gives rise an even more elongated shape than the observed for TRAPPI. Note that Trs85 is located in a position equivalent to Trs120 in TRAPPII (Figure 1.6). The binding site of Ypt1 is conserved in between TRAPPI and TRAPPIII.

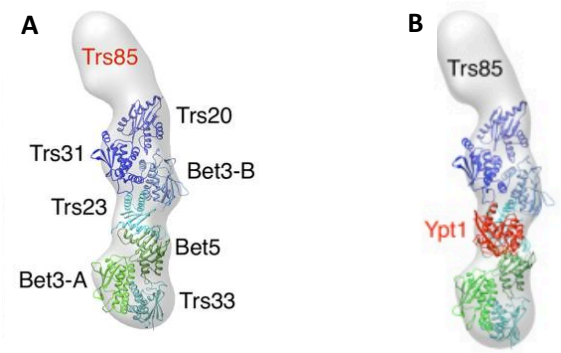


**Figure 1.6. Subunit organization of the TRAPPIII complex alone and with Ypt1. (A, B)** TRAPPI complex atomic model (generated from three crystal structures; PDB ID codes 2J3T, 2J3W, and 3CUE) fit into the EM density map of TRAPPIII. In A, TRAPPI subunits are shown in black, and the TRAPPIII-specific Trs85 subunit in red. In B, the TRAPPIII-specific Trs85 is labelled in black, and Ypt1 in red (From Tan D. et al).

Aside from TRAPP complexes, other MTCs such us HOPS, Dsl1, COG or exocyst have been tried to be either entirely or partially reconstructed at the structural level (Brocker et al. 2012) (Ren et al. 2009) (Lees et al. 2010) (Wu et al. 2005). However, in addition to the inherent difficulties of conventional approaches to isolate the complexes, most of the data available so far reside on approaches done *in vitro,* what can not truly represent the MTCs architecture in the cellular environment where the binding of other biomolecules (i.e. GTPases, vesicles, etc) is likely to affect MTCs structure. For this reason, our group has further participated in the reconstruction of the exocyst and COG *in vivo* (Picco et al. 2017), a work where I also contributed although it is not included in this Thesis.

### 1.1.3. Structural characterization of exocyst and COG

PICT (Protein interaction from Imaging Complexes after Translocation) technique can be used to detect protein-protein interactions (PPIs) directly in living cells (see a detailed explanation of the PICT technique in section 3.3.2-Materials and Methods). On the other side, localization microscopy can estimate the separation between two fluorophores with a precision below 5 nm (L. S. Churchman et al. 2005) (L. Stirling Churchman, Flyvbjerg, and Spudich 2006). In our group we combined PICT and fluorescence localization microscopy to determine the 3D architecture of protein complexes directly in living cells. In brief, cells where engineered with immobile anchoring platforms where the complex of interest can be recruited in a controlled manner (Gallego et al. 2013). Several strains were generated with the anchoring platform tagged with RFP, and the termini of each MTC subunit tagged to GFP (one at the time). The distances between these two fluorophores for different orientations were measured with high precision (< 5nm), and the data obtained was combined with the structural information available for each subunit (Russel et al. 2012). Finally, the reconstruction of the complete 3D molecular architecture of the exocyst and COG complexes could be generated.

### 1.1.4. Mammalian MTCs

MTCs functions are highly conserved in higher eukaryotes. However, some mammalian MTCs subunits are not present in yeast, others significantly differ from their yeast homologues and other proteins have evolved with high homology (Van Der Kant et al. 2015).

Firstly, CORVET and HOPS work in the endolysosomal system in mammalian cells as it has been described for their counterparts in yeast. CORVET is in charge of tethering vesicles to early endosome, while fusion of late endosome with lysosomes (mammalian vacuoles) is mediated by HOPS (Van Der Kant et al. 2015).

The members of the CATCHR family also conserve their tethering functions. The recently discovered endosome-associated recycling protein (EARP) complex, which shares three out of its four subunits with GARP (Schindler et al. 2015), and to a lesser extent, GARP itself, participate in the recycling of vesicles to the plasma membrane from the TGN. In mammals GARP also controls the retrograde transport from endosomes to the TGN (Schindler et al. 2015). The COG complex keeps playing important roles in determining the structure and function of the Golgi apparatus (Ungar et al. 2002). The metazoan homolog of the yeast DSL1 complex, called NRZ complex, has also been involved in Golgi-to-ER retrograde transport (Aoki et al. 2009). Furthermore, each of its three subunits has specific cellular functions including endosome-to-Golgi transport, cytokinesis, cell cycle checkpoint, autophagy, and mRNA decay (Tagaya et al. 2014). The exocyst has been shown to be required for diverse cellular processes where polarized exocytosis is essential including the establishment of epithelial polarity, neurite outgrowth, and ciliogenesis (Murthy et al. 2003) (Zuo, Guo, and Lipschutz 2009) (Das and Guo 2011).

Finally, two TRAPP complexes have been suggested to exist in mammalian cells based on genetic interactions maps and purification assays, however no evidences support the existence of TRAPPI in mammalian cells. Mammalian TRAPPII and TRAPPIII contain the core TRAPP subunits plus TrappC9-10 (Trs120-130), or TrappC8 (Trs85), respectively (Bassik et al. 2013). Furthermore, TRAPPIII possess two specific metazoan subunits (TrappC11-12) and the homolog of Trs65, TrappC13, which in yeast cells is a specific subunit for TRAPPII. Mammalian TRAPPII has been linked to ER-to-Golgi transport due to the defects caused by the mutations in the TrappC10 specific subunit (Yamasaki et al. 2009). TRAPPIII has also been proposed to have a role in ER-to-Golgi transport together with COPII vesicles (Bassik et al. 2013) and both TRAPPIII and the Ypt1 human homolog Rab1 have been shown to play essential roles in autophagy (Imai et al. 2016) (Ramírez-Peinado et al. 2017). In addition, TrappC8 was shown to be required for cell entry of the human papilloma virus, implying its role in endocytosis (Ishii et al. 2013) and for ciliogenesis (Schou et al. 2014).

Importantly, due to the essential function of these complexes in the cell, gene mutations in the MTCs subunits have been implicated in a broad range of human pathologies. Among them, mutation in several MTCs subunits have been related to cancer or carcinogenesis (HOPS, (An et al. 2012); TRAPPII,

(Zhang et al. 2015); TRAPP core (Weng et al. 2014)) and mental disorders (TRAPP core (Hamilton et al. 2011), (Mccarthy et al. 2014), (Chang et al. 2015); GARP (Feinstein et al. 2014); TRAPPII (Khattak and Mir 2014)); among others.

### 1.1.5. Role of MTCs in autophagy

#### 1.1.5.1. Autophagy: selective Vs non-selective

Autophagy is a membrane trafficking mechanism conserved from yeast to humans that delivers cytoplasmic cargo to the vacuole/lysosome for degradation and recycling (Kraft and Martens 2012). Autophagy pathways can be classified into the so-called non-selective autophagy (bulk degradation induced by nutrient deprivation) and selective autophagy (selective degradation of cellular components).

Therefore, autophagy *per se* (or bulk autophagy) refers to the degradation of random cytoplasmic components within the vacuole in response to stress conditions, such us starvation, to ensure cell viability. This process starts with the repression of TOR complex, what triggers many controlled steps that lead to the engulfment of big portions of the cytoplasm in a double membrane compartment called autophagosome (Baba, Osumi, and Ohsumi 1995).

On the other hand, selective autophagy takes place under normal conditions with the aim of maintaining cellular homeostasis by degrading specific cargos. To this end, selective targets such as unfolded proteins; damaged or dysfunctional organelles including mitochondria (Kanki and Klionsky 2008), parts of the nucleus (Krick et al. 2008), peroxisomes (Dunn et al. 2005), invasive bacteria and others are specifically removed from the cells (see Figure 1.7). Among them, the Cytoplasm-to-Vacuole Targeting (Cvt) pathway is the best studied and has been historically used as a model to study selective autophagy (M. A. Lynch-Day and Klionsky 2010). Selective autophagy has a housekeeping function maintaining organism's health and longevity in higher eukaryotes. Furthermore, it has been also demonstrated to be required for other physiological functions including development (Betin et al. 2013), cell death (Yu et al. 2004) and aging (Bergamini et al. 2004).

Giving the role of autophagy in so many biological functions, it is not surprising that alterations in these processes and mutations in autophagy related genes (ATG genes) have been linked to many human diseases such as neurodegeneration (Ravikumar et al. 2004), muscular disorders (T. Suzuki et al. 2002), pathogen infection (Suhy, Giddings, and Kirkegaard 2000) (Rich, Chelsea, and Webster 2003), liver diseases (Gao et al. 2014) and cancer (Amaravadi, Kimmelman, and White 2016), among others.

Some common features and many components of the autophagy molecular machinery are shared both in non-selective and selective autophagy pathways. For instance, they all can be divided into the same different steps that are represented in Figure 1.7: PAS formation and nucleation of the autophagosome (or Cvt vesicle), expansion or elongation of the double membrane to enwrap the cargo, closure of the autophagic vesicle, fusion with the vacuole/lysosome and cargo degradation (M. A. Lynch-Day and Klionsky 2010) (Su ab et al. 2015).

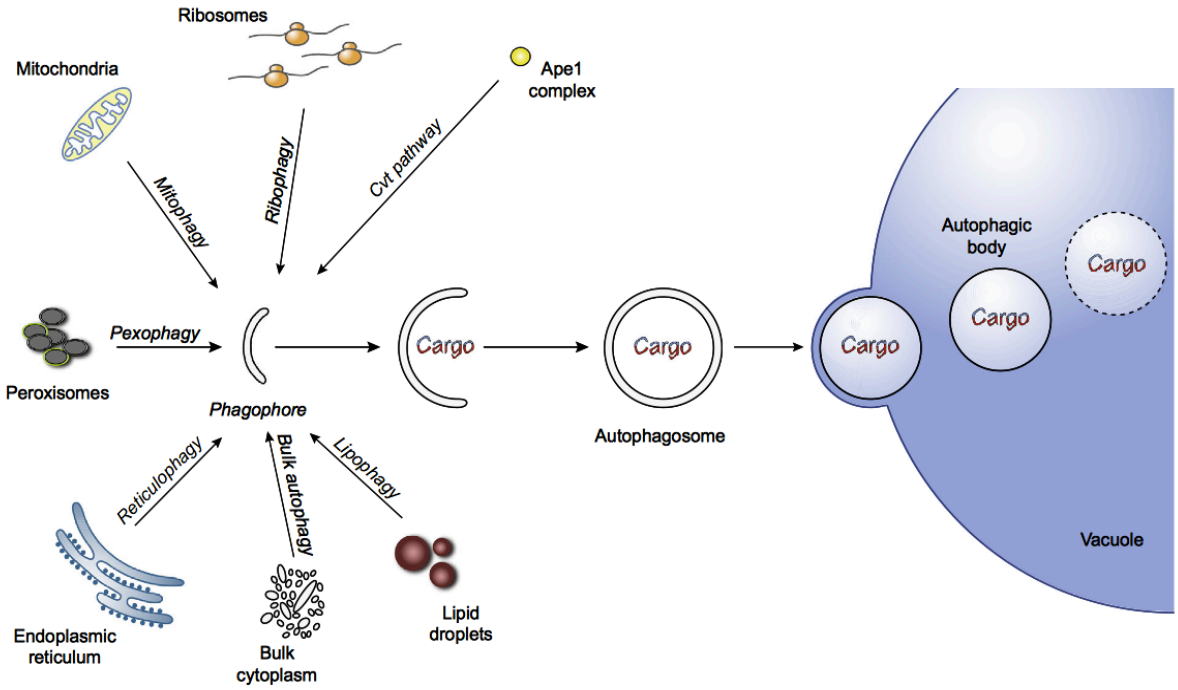


**Figure 1.7. Representation of non-selective and selective types of autophagy in yeast *Saccharomyces cerevisiae*.** Either bulk cytoplasm or specific cargo are targeted to the PAS, where the biogenesis of the autophagosome/Cvt vesicle takes place. A double-membrane expands to sequester the cargo and elongates until forming the autophagosome/Cvt vesicle. Once it is close, the outer membrane fuses with the vacuole and the inner membrane together with the cargo is released in the vacuole/lysosome lumen, what is called autophagic body/Cvt body. (Adapted from (Guimaraes et al. 2015).

The PAS has been described as the place where most of the Atg proteins and other members of the autophagy machinery localize (Klionsky et al. 2003), at least transiently, and where the expansion of a double membrane begins to generate the autophagosome (K. Suzuki et al. 2001) (K. Suzuki et al. 2007). This structure is close to the vacuole (Torggler et al. 2016). However, the process of biogenesis or nucleation has not been completely elucidated yet, and part of the reason is that the PAS has not been fully characterized. For instance, some questions as whether it is a permanent structure or if it becomes part of the incoming vesicle, remain unknown. Following the nucleation, the expansion of the autophagosome surrounding the cargo occurs, presumably thought membrane trafficking. The origin of the membrane(s) that drives this expansion, though, is still not well understood and there is some controversy in the field. In the last steps, the membrane of the newly generated vesicle is closed and the

outer leaflet is fused with the vacuole, releasing the autophagic body or Cvt body into the lumen of the vacuole to be degraded by resident hydrolases (Trumbly and Bradley 1983).

In the last year of my thesis, I had the opportunity to visit Prof. Tamotsu Yoshimori's laboratory in the Osaka University, where I was under the supervision of Dr. Maho Hamasaki for three months. Prof. Yoshimori is leading one of the worldwide top groups in the study of autophagy. In addition, Prof. Yoshimori's group is sibling of Prof. Yoshinori Oshumi's group, who was awarded with the 2016 Novel Prize in Physiology or Medicine 'for his discoveries of mechanism for autophagy' using yeast as model organism. Among other findings, he saw for the first time the accumulation of spherical bodies in the lumen of the vacuole under nutrient-deficient medium, what he called 'autophagic bodies'. Electron microscopy examination showed these spherical bodies ranged from 400 to 900 nm in size, surrounded by a unit membrane (Takeshige et al. 1992) (Figure 1.8).


**Figure 1.8. Morphology of vacuoles in nitrogen-deficient conditions.** Multiple protease-deficient cells were incubated for 2 hours in SD(-N) medium. Vesicles loaded with portions of the cytosol are observed inside the vacuole lumen (AB). *AB*, autophagic body; *V*, vacuole. Imaged from (Takeshige et al. 1992).

Overall, this short stay at Prof. Yoshimori's laboratory gave me the opportunity of learning from their long-standing experience in the employment of techniques applied to autophagy, as well as their remarkable knowledge in the field.

#### 1.1.5.2. The Cvt pathway

Studies of the Cvt pathway in *S. cerevisiae* have been key to discover important insights in the molecular and functional mechanisms of autophagy, and still today *S. cerevisiae* and the Cvt pathway remain a leading model system for investigations in the field.

In the Cvt pathway, three vacuolar hydrolases (aminopeptidase I (Ape1), Ape4 and α-mannosidase (Ams1) (M. A. Lynch-Day and Klionsky 2010)) are specifically transported to the vacuole, being Ape1 the principal cargo. Furthermore, it has been described that prApe1 is associated with Ty1 virus-like particles (VLPs) of around 35-50 nm diameter that can be detected within the Cvt vesicle, indicating that Ty1 is also a selective cargo of the Cvt pathway (Baba et al. 1997) (Yamasaki and Noda 2017) (Figure 1.9).

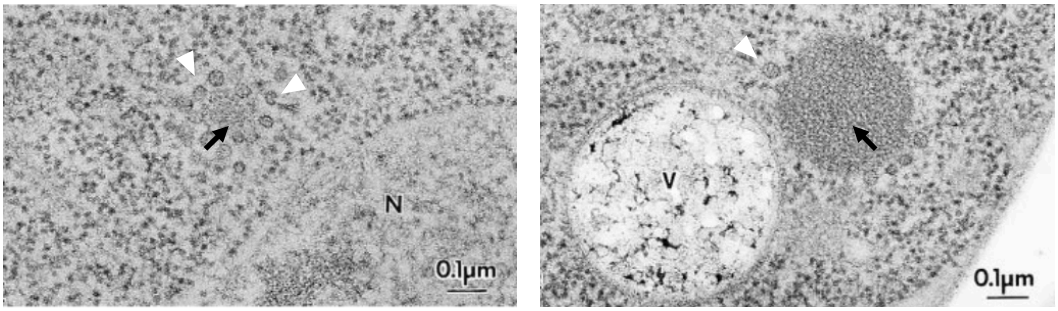


**Figure 1.9. Morphology of prApe1 in the cytosol.** Freeze substitution fixation images of cells lacking the vacuolar protease Pep4. White arrowheads point to VLPs; black arrows indicate prApe1 aggregates in the cytosol. *N*, nucleous; *V*, vacuole. Image adapted from (Baba et al. 1997).

Ape1 is firstly synthesized in the cytosol as inactive proenzyme (prApe). When the Cvt pathway is triggered, prApe1 oligomerizes in dodecamers that further assemble in the Cvt complex in the cytoplasm. It is then targeted to the PAS, where the *de novo* biogenesis of a Cvt vesicle (of around 150 nm in size) takes place (Baba et al. 1997) (K. Suzuki et al. 2001). After this step, the expansion and closure of the Cvt vesicle, as well as the fusion with the vacuole and cargo degradation happen as it has been described before (M. A. Lynch-Day and Klionsky 2010) (See Figure 1.10).

To undertake all these steps in a regulated manner, more than 40 proteins work together in budding yeast cells. The autophagy machinery encompasses more than 40 genes (Klionsky et al. 2003), 27 out them, ATG genes. The Atg proteins function at the PAS at different time points (K. Suzuki et al. 2001) (K. Suzuki et al. 2007), and they are classified into six functional groups: the Atg1 kinase complex, Atg9 vesicle, autophagy-specific phosphatidylinositol 3-kinase complex, Atg2–Atg18 protein complex, Atg12–Atg5 conjugation system, and Atg8 lipidation system (Mizushima, Yoshimori, and Ohsumi 2011) (N. N. Noda and Inagaki 2015). The Cvt pathway shares most of these proteins with bulk autophagy, however, some of them are different and specific for each process. For instance, while the Atg17–Atg29–Atg31 complex is specially required as scaffold in bulk autophagy, the Cvt pathway uses Atg11 (Mizushima, Yoshimori, and Ohsumi 2011) (M. A. Lynch-Day and Klionsky 2010), (K. Suzuki 2013). Furthermore, the receptor of the selective cargo prApe1, Atg19, is only required to generate the Cvt vesicle (Scott et al. 2001).

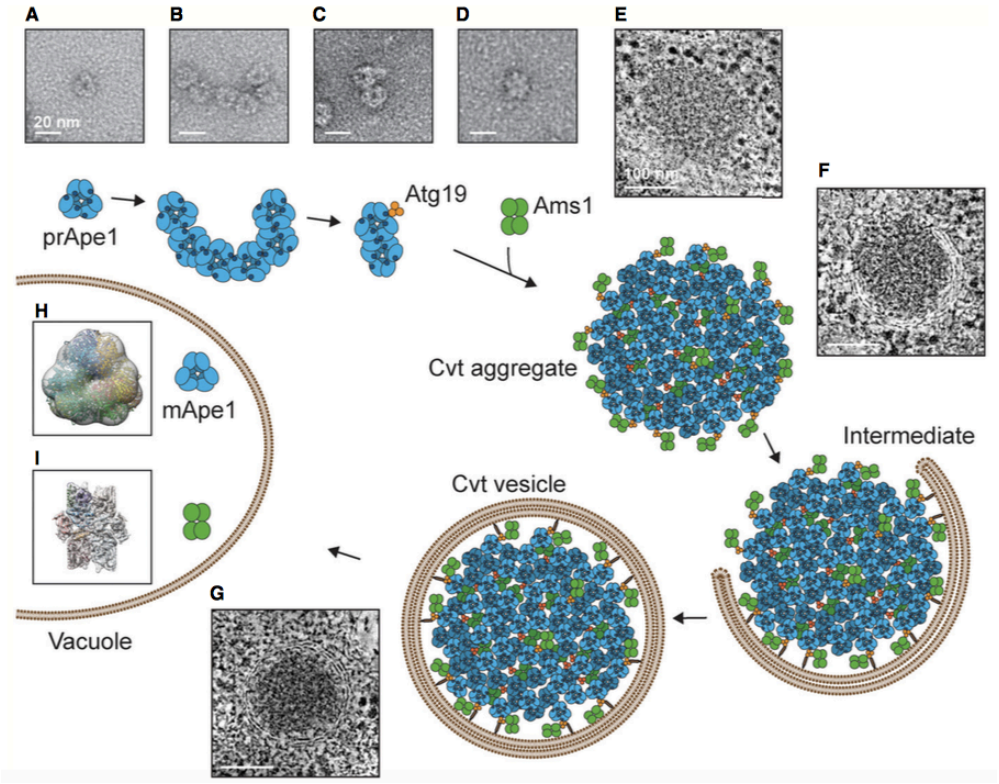


**Figure 1.10. Model of the Cvt pathway.** The major cargo of Cvt pathway, prApe1 (A) assembles to form dodecamers (B), which form higher order assemblies recognized by the prApe1 receptor Atg19 (C). Ams1 tetramers also bind Atg19, and together with other secondary cargo, they form the Cvt aggregate in the cytosol (E). At the PAS, the Cvt cargo is engulfed by a double membrane (F) to form the Cvt vesicle (G). After fusion with the vacuole, prApe1 is subjected to maturation giving rise to mApe1 (H), while Ams1 does not experiment the maturation process (I). Image from (Bertipaglia et al. 2016).

The cleavage of the propeptide portion of prApe1 (61 kDa) inside the vacuole lumen, gives rise to the mature form of the enzyme (mApe1), with a molecular mass of 56 kDa (see Figure 1.11).

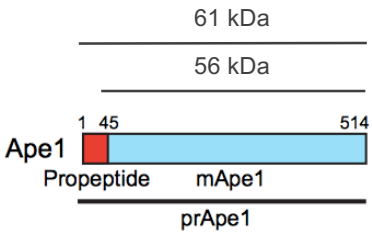


**Figure 1.11. Ape1 representation.** prApe length is 514 aa with a molecular mass of 61 kDa (Quinones, Winston, and Stromhaug 2012). The propeptide portion is shown in red. mApe length is 469 aa and has a molecular mass of 56 kDa (Quinones, Winston, and Stromhaug 2012). It is coloured in blue. Imaged adapted from (Yamasaki and Noda 2017).

#### 1.1.5.3. TRAPPIII in the Cvt pathway

As mentioned before, yeast TRAPPIII consists of the core TRAPP complex plus a specific subunit named Trs85, and it is a GEF for the Rab GTPase Ypt1. A part from its role in Golgi trafficking,

TRAPPIII has important functions both in selective and bulk autophagy.

The concerted action of TRAPPIII-Ypt1 is essential for the biogenesis of the Cvt vesicle. Trs85 is responsible for the recruitment of the TRAPPIII complex to the PAS, where it will further target and activate Ypt1. Ypt1 in its GTP-bound state, in turn, interacts with its downstream effector, the scaffold protein Atg11, who mediates the transport of the Ape1 cargo to the PAS (Yorimitsu and Klionsky 2005). The interaction Atg11-Ypt1 is required for the subsequent PAS assembly (Lipatova et al. 2012). Once at the PAS, Atg11 physically associates with the serine/threonine kinase Atg1. The kinase activity of Atg1 requires clustering on Ape1 cargo (Torggler et al. 2016), and it is necessary for membrane elongation during the formation of Cvt vesicles (Shintani et al. 2001).

TRAPPIII-Ypt1 complexes are transported in Atg9 vesicles to the PAS. Atg9 is a transmembrane protein that directly interacts with Trs85. Atg9 exits on cytoplasmic small vesicles termed Atg9 vesicles and cycle between the PAS and other subcellular compartments called reservoirs (e.g. TGN or endosomes) (T. Noda et al. 2000). They have been suggested to provide membrane for the elongation and closure of the Cvt vesicle. However, there are conflicting reports about the mechanisms controlling the trafficking of these vesicles and their interplay with the TRAPPIII complex in the Cvt pathway. On the one hand, it has been published that Trs85 directs Ypt1 and Atg9 vesicles to the PAS and on the other hand, that is Atg9 who recruits TRAPPIII and Ypt1 to the PAS (Shirahama-Noda et al. 2013), (Yamamoto et al. 2012) (Kakuta et al. 2012). In any case both Trs85 and Atg9 are essential for the Cvt pathway.

Since the role of TRAPPIII in the Cvt pathway is one of the most relevant topics of this thesis, I have compiled some key steps of the pathway and the specific role of TRAPPIII on it in the next scheme for further clarity (Figure 1.12).

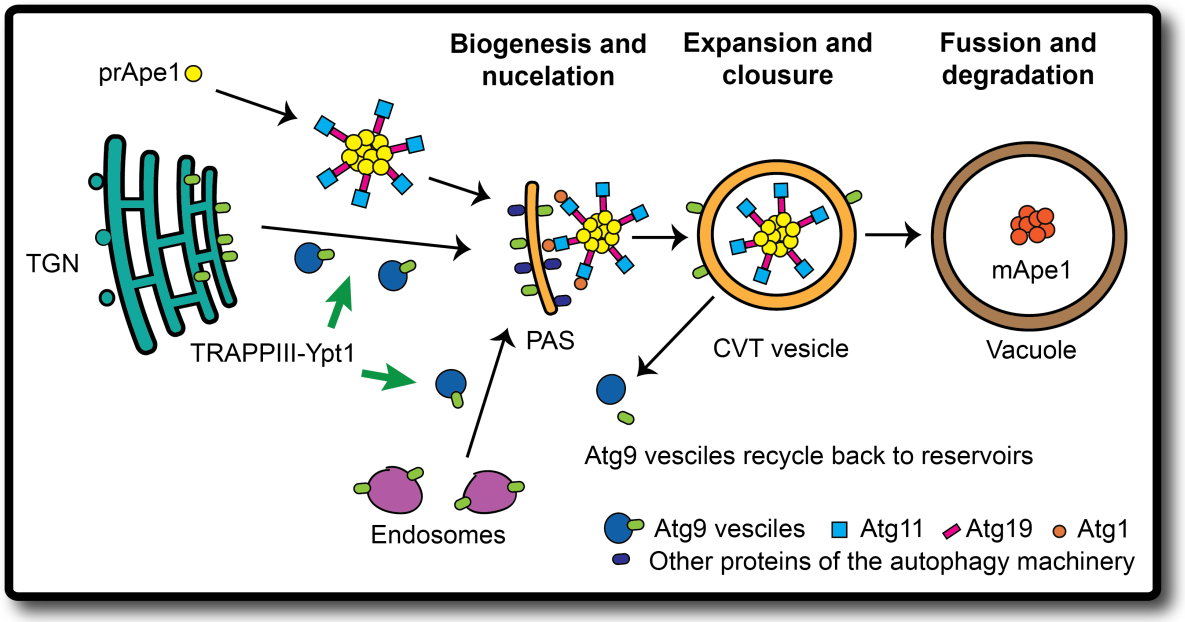

**Figure 1.12. Role of TRAPPIII in the Cvt pathway.** When the Cvt pathway is triggered, Atg9 vesicles leave their reservoirs (i.e. TGN or endosomes) to be targeted to the PAS in a TRAPPIII-Ypt1-dependent manner. Once at the PAS, TRAPPIII will further activate Ypt1, which in its GTP-bound state, interacts with the scaffold protein of prApe1 Atg11, what is required for Atg11 localization to the PAS and for subsequent assembly of the rest of the autophagy machinery (the PAS has not been put in proximity to the vacuole surface because of spatial constraints). Once at the PAS, Atg11 physically interacts with the serine/threonine kinase Atg1, whose kinase activity is required for the subsequent membrane elongation. Once the Cvt vesicle is completely mature and closed, Atg9 vesicles are recycle back to their reservoirs. Following, the outer membrane of the Cvt vesicle fuses with the vacuole membrane, and the inner membrane together with the cargo are delivered into the lumen and processed. At this point, prApe1 becomes mApe1.

#### 1.1.5.4. TRAPPIII in non-selective autophagy

A part from its essential role in selective autophagy, TRAPPIII has been also shown to have an important function in bulk autophagy. It has been reported to direct Ypt1 to the PAS (M. A. Lynch-Day and Klionsky 2010), which in its active form is also essential for the initial steps of bulk autophagy. Furthermore, Tan et al. demonstrated that TRAPPIII binds the COPII coat subunit Sec23, and recruits these vesicles to the PAS. COPII are also needed at early steps of the autophagosome formation, likely providing one of the membrane sources (Tan et al. 2013).

On the other hand, Atg9 vesicles are also essential players in bulk autophagy. Yamamoto et al. identified Atg9-containing structures as highly mobile vesicles within the cytoplasm both in normal and starvation conditions. In their studies under starvation conditions, they showed that these Atg9 vesicles provide membrane for the autophagosome growth. However, only 3 vesicles are needed to assemble to the PAS in a single round of autophagosome formation (Yamamoto et al. 2012). Noda and colleagues published a report showing a key role of TRAPIII in bulk autophagy tethering Atg9 vesicles from early endosome to TGN (Shirahama-Noda et al. 2013) rather than at the PAS. However, they observed that the lack of TRAPPIII did not completely perturb the pathway. Instead, they saw that when TRAPIII is abrogated, Atg9 vesicles are relocated from early to late endosomes and subsequently transported to the TGN, where the GARP complex tethers them. They concluded TRAPIII is only partially required for bulk autophagy because GARP complex can bypass TRAPPIII function. Note that in CVT pathway, GARP cannot bypass TRAPPIII. Therefore, disruption of both complexes produces additive defects. Nonetheless, even in the double mutant, bulk autophagy was not completely abolished, suggesting that other pathways must be involved in the process as well.

In mammalian cells, TRAPPIII and the Ypt1 human homolog Rab1 also plays essential roles in autophagy by controlling ATG9 in a similar way to their counterparts in yeast (Ramírez-Peinado et al. 2017). Removal of specific mammalian TRAPPIII subunits such us TRAPPC8 (Trs85 homolog) or TRAPPC13 revealed autophagy defects in autophagosome formation (Imai et al. 2016).

In conclusion, the studies published so far evidence an important function of the TRAPPIII complex for the correct functioning of non-selective autophagy, although unlike in the Cvt pathway, TRAPPIII

seems to be dispensable for this process.

#### 1.1.5.5. Other MTCs

Although TRAPPIII complex is the MTC with a more important role in both selective and non-selective autophagy, other MTCs have also been shown to be involved in these pathways by regulating Atg9 traffic.

- **GARP**

Further than its role in bulk autophagy bypassing the function of TRAPPIII (section 1.2.3), the GARP complex has been also shown to have an essential role in the Cvt pathway. Reggiori and colleagues demonstrated that mutations in GARP subunits completely inhibit the processing of Ape1, indicating a block in the Cvt pathway (Reggiori et al. 2003). The role of GARP in selective autophagy, though, is not completely understood yet. Although there are not direct evidences of the mammalian GARP complex in autophagy, it has been postulated that GARP complex may be involved in the recycling of Atg9 vesicles to the TGN (Young and Tooze 2007).

- **TRAPPII**

Very little is still known about the role of TRAPPII in autophagy. However, Shenshen Zou et al. demonstrated that the TRAPPII specific subunit Trs130, which is the GEF of Ypt31/Ypt32, is also required for both, the Cvt pathway and bulk autophagy (Zou et al. 2014). A strain harbouring a temperature sensitive mutant of Trs130, *trs130ts,* showed misslocalitation of Atg9 at restrictive temperatures. Instead of assembling at the PAS, Atg9 vesicles showed some accumulation at the TGN, defects partially caused by the reduced activity of Ypt31/32. Furthermore, combination of mutations in both TRAPPII and TRAPIII subunits produced greater defects in starvation-autophagy than in each single mutant, suggesting they are playing in parallel pathways.

## 1.2. Type IV P-type ATPases

P-type ATPases is a family of proteins that comprises a large group of membrane pumps that transport different substrates, such as ions, across biological membranes (Jencks 1989) (Kühlbrandt 2004). They are divided into four subfamilies (P1- to P4-ATPases) and further into smaller subgroups based on sequence homology and substrate specificity.

P4-ATPases (or flippases) subfamily is composed of a group of five genes, where DRS2, DNF1, DNF2 and DNF3 form an essential group of genes and NEO1 alone is an essential gene *per se* (Paulusma and Oude Elferink 2010) (van der Mark, Oude Elferink, and Paulusma 2013) (Hua, Fatheddin, and Graham 2002). P4-ATPases actively flip phospholipids across the lipid bilayer to the cytosolic leaflet of the membranes to generate and maintain asymmetric distributions. Phospholipid asymmetry is thought to

induce local membrane bending and recruitment of proteins such as coat proteins, two events required for vesicle budding (Lopez-Marques et al. 2014) (Sebastian et al. 2012). For instance, in a recent publication (Takada et al. 2018) authors showed that phosphatidylserine (PS)-flippase activity at the plasma membrane triggers the recruitment of several BAR domains that will promote membrane tubulation.

Although flipping phospholipids, the main function of P4-ATPases, requires hydrolysis of ATP, some cellular functions of P4-ATPases are ATP-independent (Van der Velden, Van de Graaf, and Klomp 2010). Furthermore, it is known that other P-type ATPases such as Na+/K+ ATPases bind intracellular and extracellular proteins to serve as scaffolds for PPIs in an energy-independent manner (Liang et al. 2007). It is likely that other similar pump-independent scaffold function would be feasible for other P-type ATPases (Andersen et al. 2016).

### 1.2.1. P4-ATP in higher eukaryotes

P4-ATPases are conserved in eukaryotes. The human genome which encodes a total of 14 P4-ATPases that are organized into five classes with each class having multiple members: Class 1a (ATP8A1, ATP8A2); Class 1b (ATP8B1, ATP8B2, ATP8B3, ATP8B4); Class 2 (ATP9A, ATP9B); Class 5 (ATP10A, ATP10B, ATP10D); and Class 6 (ATP11A, ATP11B, ATP11C).

P4-ATPases in humans also transport phospholipids across cellular membranes, and have essential roles in multiple vesicle-mediated protein transport steps. Furthermore, they are involved in a wide variety of cellular processes such as cell signaling, blood coagulation, apoptosis, bile and cholesterol homeostasis and neuronal cell survival, among others (Andersen et al. 2016). However, the importance of P4-ATPases is highlighted by the finding that genetic defects in two P4-ATPases (ATP8A2 and ATP8B1) are associated with severe human disorders.

ATP8A2 and ATP8B1 (also called FIC1), are closely related to its yeast orthologue Drs2. Mutations in ATP8B1 cause Progressive Familial Intrahepatic Cholestasis type 1 (PFIC1) and Benign Recurrent Intrahepatic Cholestasis type 1 (BRIC) (Bull et al. 1998). While BRIC is a milder form of the Cholestasis, in PFIC patients the liver disease may progress toward liver failure and death before adulthood. On the other hand, ATP8A2 mutations can produce severe mental disorders (Onat et al. 2013).

Drs2 is also nearly 50% identical to its mammalian homolog ATP8A1 (also called ATPase II), the founding member of the large subfamily of P4-ATPases in mammals (Tang et al. 1996). Although there are no as clear evidences for the implication of ATP8A1 in human diseases as for ATP8A2 and ATP8B1, ATP8A1 deficiency has been associated with delayed hippocampus-dependent learning in mice (Levano et al. 2012). Recently, aberrant hippocampal Atp8a1 levels in post-mortem cortex of

juvenile patients with autism, have been also associated with altered synaptic strength, electrical activity, and autistic-like behavior (Kerr et al. 2016).

Importantly, the molecular mechanism by which the loss of these flippases leads to human pathologies is still poorly understood (Folmer et al. 2009).

### 1.2.2. P4-ATPases/Cdc50 complexes, phospholipid specificity and transport mechanisms

Most flippases in the P4-ATPase family are comprised of a catalytic α-subunit (the P4-ATPase) and a non-catalytic β-subunit that belong to the CDC50/LEM3 family of evolutionary conserved proteins (Simonin et al. 2004) (Saito et al. 2004) (Figure 1.13). The binding affinity for each other fluctuates during the phospholipid transport cycle of P4-ATPases (Lenoir et al. 2009). There are three β-subunits in yeast (Cdc50, Lem3, Crf1) that are required for the export of P4-ATPases from the ER and for their catalytic activity (Saito et al. 2004) (Chen et al. 2006) (Puts et al. 2012).

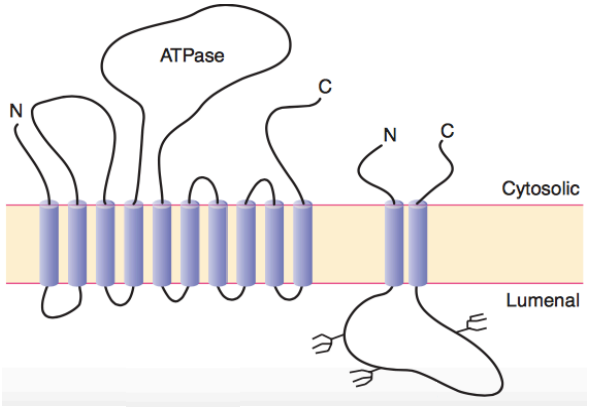


**Figure 1.13. Predicted topology of the α-β heterodimer formed by a P4ATP-ase and a protein of the CDC50/LEM3 family.** Image adapted from (Graham 2004).

In addition, P4-ATPases differ in their substrate specificity. As is shown in Table 1.1, each flippase recognizes and translocates specific phospholipids. P4-ATPases establish and maintain phospholipid asymmetry acting at different cellular membranes, so they are involved in different biological roles.

For instance, Drs2 and Dnf3 localize in the TGN as steady state, and to a lesser extent to endosomal compartments (Yamasaki and Noda 2017) (Furuta et al. 2007). They are necessary for the aminophospholipid transport and asymmetry in post-Golgi secretory vesicles. On the other hand, Neo1 resides in Golgi compartments and also accumulates in late endosomes of class E *vps* (vacuolar protein sorting) mutants (Hua, Fatheddin, and Graham 2002) (Wicky, Schwarz, and Singer-Kruger 2004).

Dnf1 and Dnf2 are paralogous that have aroused from the whole genome duplication and are 69% identical in amino acid sequence. Dnf1 and Dnf2 cycle between the plasma membrane, endosomes, and TGN, although its main function has been stablished at the plasma membrane. Loss of these flippases promotes an abnormal increment in the exposure of endogenous aminophospholipids (PE and PS) at

the outer leaflet of the plasma membrane (Chen et al. 2006) (Pomorski et al. 2003). Furthermore, they have redundant functions in the internalization step of endocytosis (at cold temperatures) and an in the exocytic v-SNARE Snc1 transport from early endosomes to TGN (Hua, Fatheddin, and Graham 2002) (Pomorski et al. 2003). Interestingly, it has been published that GARP is required for the proper localization of Dnf1 and Dnf2 at the plasma membrane, and for the correct asymmetric distribution of PE between its inner and outer leaflets. Furthermore, deletion mutants of the components of the GARP complex are also defective in the uptake of fluorescence-labeled-PE and accumulate Dnf2-GFP in intracellular compartments, suggesting that the GARP complex could be involved in the recycling of these phospholipid flippases through an unknown mechanism (Takagi et al. 2012b).

Therefore, P4-ATPases, like MTCs, are also required for vesicle traffic in several transport routes. However, although some studies such as the one published by Takagi et al. suggest a possible a concerted action in vesicular transport, very little is still known about the interplay between them.

| P4-ATPase | Cdc50 subunit | Substrates | Biological role |
|---|---|---|---|
| Drs2 | Cdc50 | PS, PE | Vesicle formation, cell polarity |
| Dnf1 | Lem3 | PC, PE, (PS), LPC, LPE, LPS | Endocytosis, cell polarity, lysolipid uptake, protein sorting |
| Dnf2 | Lem3 | PC, PE, (PS), LPC, LPE | Endocytosis, lysolipid uptake, protein sorting |
| Dnf3 | Crf1 | PC, PE | Vesicular transport |
| NeoI | - | - | Vesicular transport |

**Table 1.1. P4-ATPase/Cdc50 complexes and their substrate specificities and biological roles.** *PC* phosphatidylcholine, *PE* phosphatidylethanolamine, *PS* phosphatidylserine, *LPC* lyso-phosphatidylcholine, *LPE* lyso-phosphatidylethanolamine.

### 1.2.3. Drs2

Drs2 is one of the best characterized P4-ATPases, and an essential gene for cell growth at temperatures below 23ºC (Ripmaster, Vaughn, and Woolford 1993). Drs2 is required for the translocation of PS (Zhou and Graham 2009) (Natarajan et al. 2009) and, to a lesser extent, phosphatidylethanolamine (PE) (Alder-Baerens et al. 2006)(Xu et al. 2013) (R. D. Baldridge and Graham 2012). Although flipping PS is the main role of Drs2 for protein transport, Drs2 also regulates other traffic routes in an PS independent manner (Xu et al. 2013) (Muthusamy et al. 2009).

#### 1.2.3.1. Function

Drs2 cycles between the exocytic and endocytic pathways. However, although it transits the plasma membrane as part of its trafficking itinerary (Saito et al. 2004) (Alder-Baerens et al. 2006), Drs2 localizes to the TGN and early endosome membranes as steady state, where clathrin coated vesicles (CCVs) are actively budded. Drs2 has a critical role in the formation of the high-density, invertase-containing of CCVs from the TGN (Gall et al. 2002) and for the bidirectional transport of CCVs between the TGN and early endosome (Liu et al. 2008). All these clathrin-mediated pathways use the tetrameric clathrin adaptor protein AP-1 (β1-, γ-, μ1-, σ1-adaptin) (Liu et al. 2008) (Hinners 2003). In early endosomes, Drs2 also requires the F-box protein Rcy1 for the early endosome-Golgi sorting (Hanamatsu et al. 2014).

While PS-flipping translocation activity is essential for the transport routes between TGN and early endosomes, cells lacking the PS synthase Cho1 still require Drs2 to produce invertase-containing exocytic CCVs (Natarajan et al. 2004), suggesting Drs2 flips other substrates rather than PS across the TGN membrane with a critical role in vesicle formation.

Drs2 also regulates the lipid-based sorting of the light class of exocytic vesicles carrying Pma1, which are clathrin-independent. The production of this class of secretory vesicles (SVs) requires the PS-translocation activity, and in either *Δdrs2* or *Δcho1* cells, Pma1 is missorted from the TGN to the vacuole (Hankins et al. 2015). Additionally, Drs2 together with Dnf3 are copacked with Pma1 in these low-density class of SVs, where they maintain the asymmetric distribution of phospholipids (with ~80% of PE located in the cytosolic leaflet). It has been shown that removal of Drs2 and Dnf3 inhibits this PE arrangement (Alder-Baerens et al. 2006), what demonstrates Drs2 plays roles in protein transport flipping other PLs besides PS.

Drs2 is also involved in sorting processes from the TGN to the vacuole. On the one hand, Drs2 has a role in the generation of CCVs from the TGN to the late endosomes through the carboxypeptidase Y (CPY) pathway, a process mediated by the monomeric clathrin adaptor proteins Gga1 and Gga2 (Golgi associated, Gamma-ear containing, Arf-binding). Cheng et al, showed a delayed transport of CPY to the vacuole in *Δdrs2* cells (Chen et al. 2006). On the other hand, Drs2 also functions in the transport of cargos to the vacuole in the alkaline phosphatase pathway (ALP), which is clathrin-independent and mediated by AP-3 (β3-, δ-, μ3-, σ3-adaptin) adaptor (Greg Odorizzi, Cowles, and Emr 1998). Both pathways are PS-flipping independent.

As I have mentioned before Drs2 is required for the cell to grow at temperatures below 23ºC. While deletion of DRS2 abolish the formation of dense class of exocytic vesicles, and the bidirectional transport between the TGN and early endosomes at all temperatures, the ALP and CPY pathways are markedly perturb at low temperatures. It has been suggested that the inability of *Δdrs2* cells to grow at temperatures below 23ºC is caused by the failure in CPY pathway together with the transport defects

caused by the lack of Drs2 at all temperatures (Hua, Fatheddin, and Graham 2002) (Muthusamy et al. 2009).

A summary of Drs2 functions is represented in the following cartoon (Figure 1.14).

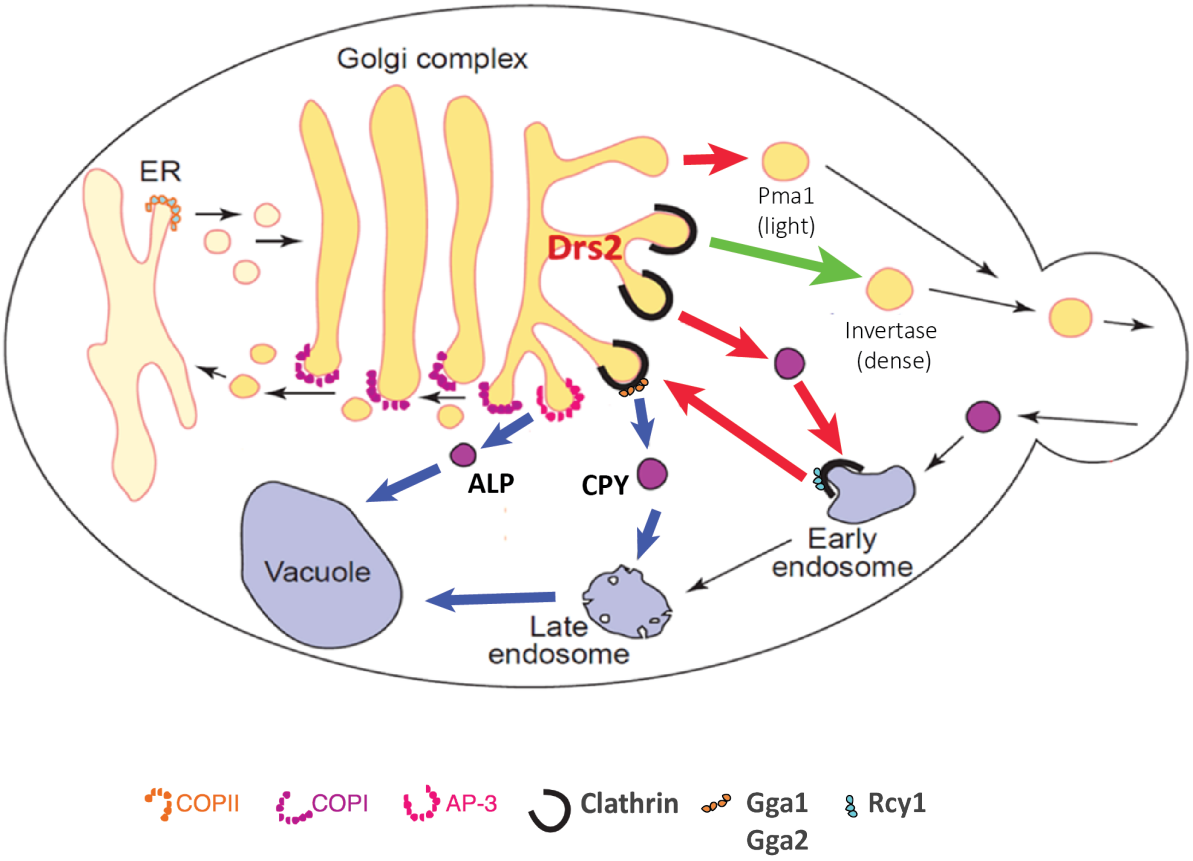


**Figure 1.14. Vesicle transport routes mediated by Drs2.** Pathways perturbed in cells lacking DRS2 gene are indicated by red, green and blue arrows. Red arrows represent those pathways that are Drs2 PS-flipping dependent while green and blue arrows indicate those transport routes that take place in a Drs2 PS-flipping independent manner. Blue arrows also define the pathways controlled by Drs2 together with other P4-ATPases and that are affected only at temperatures below 23ºC. Pathways that are affected at all temperatures are indicated by red and green arrows, with the exception of Pma1, for which the link with temperature is still not known. *ALP*, alkaline phosphatase; *CPY*, carboxypeptidase Y; *ER*, endoplasmic reticulum. Image adapted from Graham, 2004.

#### 1.2.3.2. Overlapping functions with other P4-ATPases

A functional redundancy between DRS2 and the DNF genes has been demonstrated in some Drs2-dependent pathways. Drs2 is the only flippase required for the exit from the TGN of dense secretory vesicles, vesicles targeted to early endosomes, and for the recycle back from early endosomes to the TGN. However, the ALP and CPY pathways are also controlled by Dnf1 and Dnf2 at temperatures higher than 23ºC. Hua and colleagues showed that although there is a modest defect in the ALP transport in *Δdrs2* cells, it is much exacerbated in the *Δdrs2Δdnf1* double mutant (Hua, Fatheddin, and Graham 2002). On the other hand, the *Δdrs2Δdnf1* mutant exhibited an increased kinetic delay in the CPY

transport compared to the *Δdrs2* single mutant. The inhability of Dnf P4-ATPases to functionally substitute for Drs2 at lower than 23ºC is likely the cause why *Δdrs2* cells have this cold sensitive growth defect.

#### 1.2.3.3. Drs2 structure and regulatory proteins

Drs2 is an integral membrane protein made up of 10 transmembrane segments (TM1-TM10) that comprise its transmembrane domain. Drs2 also has three cytosolic regions in the transmembrane domain that are involved in the ATP reaction cycle. These regions are coupled to the phospholipid flipping and are named nucleotide-binding (N), phosphorylation (P) and actuator (A) domains. In the TM4, residues 237-238 (QQ) define the substrate specificity of Drs2, and are thus required for its ability to translocate PS. Site-directed mutagenesis experiments showed that amino acid substitution to GA reverted specificity for PS to PE (Ryan D Baldridge and Graham 2013).

Moreover, Drs2 has relatively long N- and C-terminal cytosolic tails, where some relevant sequences have been mapped (Figure 1.15). Firstly, Drs2 has two NPFXD motifs (hereafter referred to as NPF) in its C-cytosolic tail that constitute some of its multiple endocytosis signals. Closer to the NPFXD motifs, Drs2 has a highly conserved motif (CM) among all, including mammalian Drs2 homologues. Although the function of the CM is still not well known, some studies based on growth complementary assays at low temperature suggest it is required for the proper function of Drs2 (Chantalat 2004). Adjacent to the CM, a segment called the Gea2 interaction motif (GIM) directly interacts with the ARF-GEF Gea2 and also with a phosphatidylinositol-4-phosphate (PI4P) at the TGN (Liu et al. 2007). The C-terminal domain of Drs2 acts as an auto-inhibitory domain. The interaction with either PI4P or Gea2 at the TGN releases the C-terminal tail from the catalytic domain of Drs2, letting the protein get active (Zhou, Sebastian, and Graham 2013). The Lee group showed that Drs2 and Gea2 form a stable complex with the Arf-like protein Arl1 required for the flippase activity of Drs2, and thus control of its PS-translocation dependent pathways. The ternary complex Gea2-Drs2-Arl1 is also required for Arfl1 functioning at the TGN (Tsai et al. 2013). Although lack of either the NPF or the GIM domains does not perturb growth of Drs2 at low temperature, deletion of both motifs fails to complement the growth defect of *Δdrs2* cells at temperatures below 23ºC.

In early endosomes, Drs2 interacts at trough an overlapping domain of the GIM motif with the F-box protein Rcy1, also required for the early endosome-Golgi sorting (Hanamatsu et al. 2014).

In its N-cytosolic tail, Drs2 possess an ISTTK sequence close to the first transmembrane domain (Todd Graham, personal communication). If this sequence is involved in Drs2 function, is still not known.

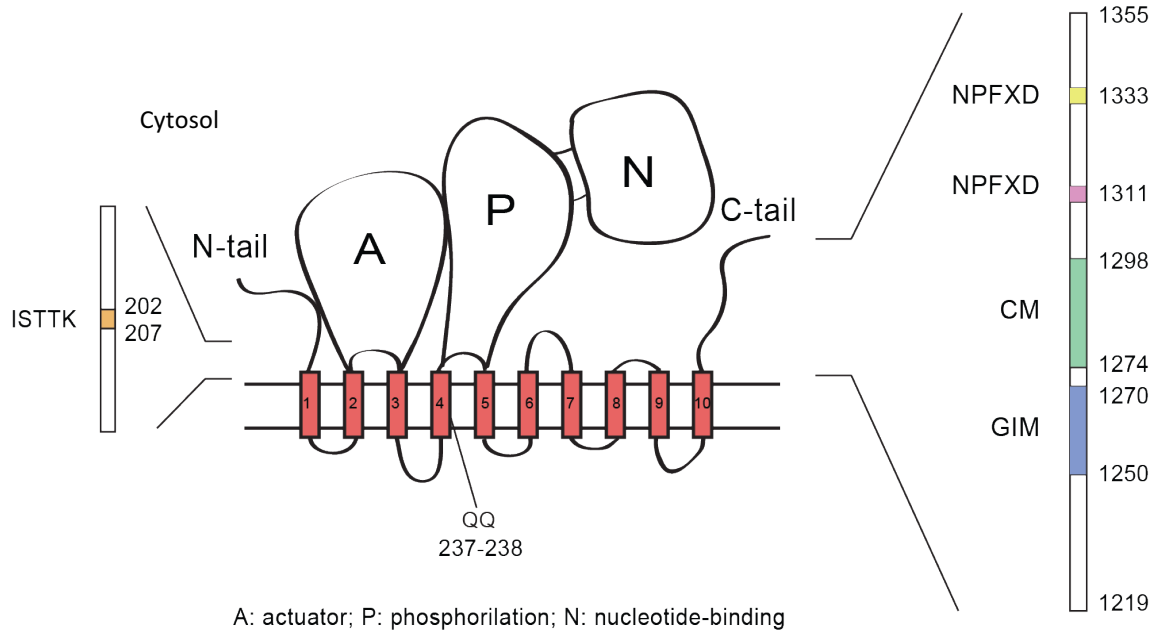


**Figure 1.15. Representation of Drs2 structure.** In red, transmembrane domains from TM1 to TM10. Parallel black lines denote the membrane boundaries. QQ residues in TM4 define substrate specificity. Cytoplasmic loops A, P and N are required for ATP reaction cycle; A, actuator domain; N, nucleotide-binding domain; P, phosphorylation domain. ISTTK sequence is located in the N-terminal tail. Endocytosis signals NPFXDs, the conserved motif (CM) and Gea2 interaction motif (GIM) are situated in the C-terminal tail. Numbers indicate amino acid positions.

On the other hand, the oxysterol binding protein homologue Kes1, which has been involved in non-vesicular sterol transport, negatively regulates Drs2 (Muthusamy et al. 2009). Kes1 hardly antagonizes Drs2 flippase activity at the TGN, and the loss of Kes1 reverts the cold-sensitive defect of *Δdrs2* cells. Interestingly, the depletion of KES1 can also suppress the defects of *Δdrs2* cells in the pathways where Drs2 has overlapping functions with other Dnfs (CPY and ALP transport). Muthusamy et al. suggest that the absence of Kes1 could improve Dnfs function to compensate for the loss of Drs2 in the ALP and CPY pathways, but this has not been demonstrated. On the other hand, the lack of Kes1 cannot recue those pathways that are restricted to Drs2 (the budding of dense exocytic vesicles and the AP-1 and Rcy1 mediated pathways).

At the same time, Drs2 also antagonizes Kes1 function in transporting sterol to intracellular membranes and maintaining physiological sterol levels in cellular compartments. Therefore, in *Δdrs2* cells Kes1 is hyperactive.

Ergosterol levels in exocytic vesicles are significantly increased relative to the TGN membrane from which they were budded (Zinser, Paltauf, and Daum 1993) (Klemm et al. 2009). It has been suggested that Kes1 can be in charge of this ergosterol enrichment since it is able of loading the TGN membrane (or the vesicle forming) with ergosterol in exchange for PI4P (Mesmin et al. 2013) (Von Filseck et al. 2015).

Hankins et al. reported there is a critical balance activity between Drs2 and Kes1 at the TGN to ensure the correct sorting of proteins and lipids (Hankins et al. 2015). Since Kes1 antagonizes PS-flipping activity of Drs2, in Δ*kes1* cells the Drs2 PS flippase activity is twofold higher in Golgi membranes purified compared to wild type cells (Muthusamy et al. 2009). The Kes1 inhibition of Drs2 function is probably due to the ability of Kes1 to extract PI4P from the TGN, which is a stimulator of Drs2 activity (Natarajan et al. 2009) (Zhou, Sebastian, and Graham 2013). On the other hand, PS-activity of Drs2 perturbs the ability of Kes1 to exchange sterol for PI4P (de Saint-Jean et al. 2011), likely diminishing Kes1's activity of loading ergosterol into the TGN.

Hankins et al. showed that *Δdrs2Δkes1* cells have wild type-like distribution of light class of vesicles containing Pma1, restoring the misslocalization of Pma1 to the vacuole seen in *Δdrs2* or *Δkes1* individual mutants. They claimed that Kes1 may be aberrantly increasing the levels of ergosterol at the TGN when either Drs2 is not present or it can not translocate PS. The similar phenotypes of Δ*kes1* and Δ*drs2* single mutants in Pma1 misslocalization to the vacuole suggest that unphysiological levels of ergosterol may disrupt the balance required for concentrating Pma1 into microdomains for their selective incorporation into exocytic vesicles.

# 1. OBJECTIVES

In spite of their essential role in the cell, MTCs mode of action is not fully characterize yet. The aim of this work was to perform a comparative analysis among MTCs to shed light on the molecular mechanism that govern their function. To this end, we carried out a screening between MTCs and proteins selected according to their genetic interaction profile with these complexes. The ultimate goal was to find new protein interactions that regulate their role in membrane trafficking. Given the high sensitivity of the PICT assay (see section 3.3.2-Materials and Methods) we expected to detect interactions that have been overlooked by previous analysis. Our results showed an interesting interplay between MTCs and P4-ATPases that led us to further investigate the biological role of some of these associations. On the basis of this, the main objectives of my thesis are listed below:

2.1. Screening for new protein interactions that are relevant for MTCs function.

2.2. Study the network of interactions between P4-ATPases and MTCs.

2.2.1. Characterization of the interplay between GARP and Dnf1.

2.2.2. Characterization of the interplay between TRAPPIII and Drs2 based on the following points:

2.2.2.1. Estimate the contribution of Drs2 in the Cvt pathway.

2.2.2.2. Evaluate whether Drs2 controls TRAPPIII function in the Cvt pathway.

2.2.2.3. Discern whether Drs2 role in the Cvt pathway is due to a canonical or a new function of this flippase.

2.2.2.4. Analyze the molecular mechanism that regulates Drs2 role in the Cvt pathway.

# 3. MATERIALS AND METHODS

## 3.1. Yeast media

Media used in this thesis are listed and described below:

- YPD liquid medium: 10% bacto-yeast extract (CONDA Pronadisa), 20% bacto-peptone (CONDA Pronadisa), 2% glucose (Formedium).
- Synthetic minimal liquid medium: 6.7% Yeast-Nitrogen Base (winthout Amino acids; Formedium), 2% Synthetic complete Mixture Drop-out (Formedium. Contains all essential amino acids except uracil, leucine, histidine and tryptophan) complemented with 0.01% uracil (Sigma-Aldrich), 0.05% leucine (Sigma-Aldrich), histidine 0.01% (Sigma-Aldrich), tryptophan 0.01% (Sigma-Aldrich) as required, and 2% glucose.
- Low florescent (Low Flo) liquid medium: 6.9% Yeast Nitrogen Base Low Florescence (without Amino acids, Folic Acid and Riboflavin; Formedium), 2% Synthetic complete Mixture Drop-out (Formedium. Contains all essential amino acids except uracil, leucine, histidine and tryptophan) and 2% glucose (Formedium) complemented with 0.01% uracil (Sigma-Aldrich), 0.05% leucine (Sigma-Aldrich), histidine 0.01% (Sigma-Aldrich), tryptophan 0.01% (Sigma-Aldrich) as required, and 2% glucose.
- SD (-N) liquid medium: 0.17% Yeast Nitrogen Base (without Amino acids and Ammoniumsulfat; Formedium), and 2% glucose (Formedium).
- YPD plates: 10% bacto-yeast extract (CONDA Pronadisa), 20% bacto-peptone (CONDA Pronadisa), 20% european bacteriological agar (CONDA Pronadisa) and 2% glucose (Formedium)
- Diploid plates: 6.7% Yeast Nitrogen Base (without Amino acids; Formedium), 2% Synthetic Complete Mixture Drop-Out mix lacking uracil and histidine, 2% european bacteriological agar (CONDA Pronadisa), and 2% glucose (Formedium).
- Sporulation minimal medium plates: 1% potassium acetate (Sigma-Aldrich), 0.01% uracil (Sigma-Aldrich), 0.05% leucine (Sigma-Aldrich), lysine 0.01% (Sigma-Aldrich), histidine 0.01% (Sigma-Aldrich) and methionine 0.02% (Sigma-Aldrich) and 20% european bacteriological agar (CONDA Pronadisa).
- Haploid plates: 1.7% Yeast Nitrogen Base w/o Amino acids and Ammoniumsulfat (Formedium), 2% Synthetic Complete Mixture Drop-Out mix lacking uracil, histidine, leucine, lysine and arginine, 100 µg/ml Thialysine (Sigma-Aldrich), 100 µg/ml Canavanine (Sigma-

Aldrich), 20% european bacteriological agar (CONDA Pronadisa), and 2% glucose (Formedium).

- Full haploid plates: 1.7% Yeast Nitrogen Base without Amino acids and Ammoniumsulfat (Formedium), 2% Synthetic Complete Mixture Drop-Out mix lacking uracil, histidine, leucine, lysine and arginine, 100 µg/ml Thialysine (Sigma-Aldrich), 100 µg/ml Canavanine (Sigma-Aldrich), 100 µg/ml cloNAT (Sigma-Aldrich), and 200 µg/ml G418 (Sigma-Aldrich), 20% european bacteriological agar (CONDA Pronadisa), and 2% glucose (Formedium).
- Synthetic minimal plates: 6.7% Yeast-Nitrogen Base without Amino acids (Formedium), 2% Synthetic complete Mixture Drop-out (lacking WHAT? Formedium), 20% european bacteriological agar (CONDA Pronadisa), and 2% glucose (Formedium).

### 3.2. Yeast strains generation

#### 3.2.1. Yeast transformation

*S. cerevisiae* strains are derivatives of BY4741 or BY4742 background. Strains with genes coding for C-terminal tags, deleted genes, and/or mutated alleles were generated by homologous recombination of the corresponding genes with PCR cassettes following standard PCR strategies (Janke et al. 2004) (Strains listed in Appendix I-Yeast strains). Yeast strains harboring exogenous genes coded in plasmids were generated by transformation. All plasmids used are listed in Appendix II-Plasmids. YPD liquid medium was inoculated with parental yeast strain and grown overnight at 30ºC and 220 rpm. The next morning culture was diluted to an optical density of $OD_{600}$=0.2 in 5ml of the same medium. 5 hours later, when cultures reached an optical density of $OD_{600}$0≈1, cells were harvested by centrifugation at 3000 rpm for 2 min at room temperature. Cells were washed in 1ml of sterile MiliQ water and harvested again. After discarding the supernatant, 5 µl of freshly denatured chilled salmon sperm DNA (10 mg/ml salmon sperm DNA (Sigma-Aldrich); 10 min denatured at 95ºC (cooled on ice), 30-40 µl of PCR product or 1 µl of plasmid miniprep and 500 µl of LP buffer (40% PEG 4000 (Sigma-Aldrich), 0.1 M LiAc (Sigma-Aldrich) and 1X TE) were added to the pellet. Cells were resuspended and heat-shocked for 40 min at 42ºC in a water bath. After, cells were washed twice with 700 µl of 1X sterile TE and harvested at 3000 rpm for 2 min at room temperature. Cells were resuspended in 70 µl 1X sterile TE and plated. Selection for auxotrophic markers was carried out directly on synthetic minimal medium plates lacking the amino acid of choice. For selection with antibiotic resistance, cells were first cultured overnight in liquid YPD at 30ºC and 220 rpm. The next morning, 200 µl of the culture was plated onto a plate containing the antibiotic of interest and grown at 30ºC for 2-3 days.

To check insertions and deletions, genomic DNA of transformants was analyzed by PCR. Tagging with fluorescent proteins was confirmed by live-cell imaging.

### 3.2.2. Synthetic Genetic Array (SGA)

Excluding those strains expressing GFP-tagged proteins from plasmids, the rest of PICT experiments (see Section 3.3.2) were done with yeast strains constructed with the SGA approach (Y. Tong and Boone 2005). Strains used for the PICT assay express the anchor Tub4-RFP-FKBP and harbor different combinations of baits (FRB fusions) and preys (GFP fusions at the C-terminus) (see Appendix I-Yeast strains). Parental cells expressing the anchoring platform and the bait-FRB and are constructed on the SGA7039 genetic background (Mating type α cells engineered to perform SGA). Parental cells expressing the prey-GFP were constructed in BY471 or obtained from the genomic C-terminal GFP fusion collection (Mating type A). Haploid yeast cells of opposite mating type (α+A) were mixed on YPD plates and grown for 1 day at 30ºC. Resulting cells were grown for 2 days at 30ºC on plates to select diploid cells. Subsequently, strains were grown overnight on YPD plates at 30ºC to recover from the selection. Recovered yeast strains were plated on sporulation minimal medium plates and incubated for seven days at room temperature. Cells were then plated on Haploid selection plates and grown for 2-3 days at 30ºC. Finally, cells were plated on Full Haploid selection plates and grown for 2-3 days at 30ºC to select those strains with the genotype of interest.

## 3.3. Fluorescence microscopy

Unless otherwise indicated, the images obtained from fluorescence microscopy experiments were acquired on an IX81 (Olympus) microscope equipped with 100x/1.40 objective lens, an Orca-ER camera (Hamamatsu) and two complete fluorescence filter cubes from AHF respectively optimized for GFP (ET Bandpass 470/40 + Beamsplitter 500 DVXRUV + ET Bandpass 525/50) and RFP (ET Bandpass 545/30 + Beamsplitter 580 DVXRUV + BrightLine HC 617/73). When both fluorescence channels were required, images were obtained sequentially by switching the filter cubes. Cells were imaged using Excellence as acquisition software. The RFP and GFP exposition times were manually adapted for each particular strain.

### 3.3.1. Localization and colocalization assays

Yeast cells were grown in YPD liquid medium containing the required nutrients at 30ºC and 220 rpm overnight. Those cells harboring plasmids were grown in synthetic minimal medium lacking the amino acid of choice. The next morning, cells were diluted to an optical density of $OD_{600}$=0.2 in Low Flo liquid medium and cultured at 30ºC and 220 rpm until they reached an early logarithmic phase ($OD_{600}\approx1$). In experiments with *Δcho1* cells, the medium was supplemented with 1 mM Ethanolamine (Sigma-Aldrich).

Cells were attached to Concanavalin A (0.1 µg/mL) (Sigma-Aldrich)-coated 96-well glass bottom plates (Zell-Kontakt). 100 µl of the Low Flo liquid medium was added to completely cover the cells. Strains were observed at room temperature, 23ºC or 37ºC as required.

Where indicated, cells were treated with 200 μM Latrunculin A (Lat A; Enzo Life Sciences) 10 to 20 minutes before imaging to induce actin depolymerization. Labeling the vacuole or the endocytic pathway was done with 8 μM FM4-64 in cells grown in YPD. Prior to imaging, cells were kept in the dark for 10 or 30 min to stain the endocytic pathway or the vacuole respectively. Then cells were washed twice with Low Flo medium to remove YPD and free FM4-64 before imaging.

Cells harboring the pDDFGP-2-(Drs2_1-212aa) under GAL1 promoter, were grown with 0.1% glucose until reaching the early logarithm phase. Expression of Drs2 N-terminus was induced with 2% galactose 30 min prior to imaging.

Imaris software was used to obtain the 3D reconstruction of yeast cells imaged with Z-stacks of 250 nm step size.

### 3.3.2. Protein interactions from Imaging Complexes after Translocation (PICT)

PICT technique allows the quantitative characterization of PPIs *in vivo,* as described in the work we recently published that is not included in this thesis (Torreira et al. 2017). PICT takes advantage of the inducible dimerization of FK506-binding protein (FKBP) and FKBP-rapamycin binding (FRB) domain to translocate protein assemblies to membrane associated anchoring platforms in yeast. Addition of rapamycin induces FRB-FKBP heterodimerization and subsequent translocation of the protein of interest tagged to FRB (bait-FRB) to the anchoring site. GFP-tagged proteins (prey-GFP) that are bound to the bait-FRB will be co-translocated to the anchoring platform. In that case, dual-color live-cell imaging will reveal those proteins by showing co-localization with the anchor-RFP-FKBP. These changes in localization can be subsequently quantified. As PICT experiments are performed in living cells, this method allows the detection of transient interactions that will not be detected using biochemical approaches because of the loss due to washing steps. First-engineered anchors (Pil1-RFP-FKBP) result in a large number of anchoring platforms at the plasma membrane. This allowed the detection of abundant complexes that once anchored accumulate enough prey-GFP in each of these anchoring platforms to be detected efficiently (Gallego et al. 2013). However, prior to my incorporation into the lab, the group designed a new anchor by tagging Tub4, a component of the spindle pole body, with RFP and FKBP (Tub4-RFP-FKBP). The resulting cells harbor only one or two anchoring platforms, thus increasing the PICT sensitivity by up to 200-fold. Even low abundant complexes, when they are anchor, accumulate enough prey-GFP in these 1-2 anchoring platforms to be detected and quantified (Torreira et al. 2017) (see Figure 3.1).

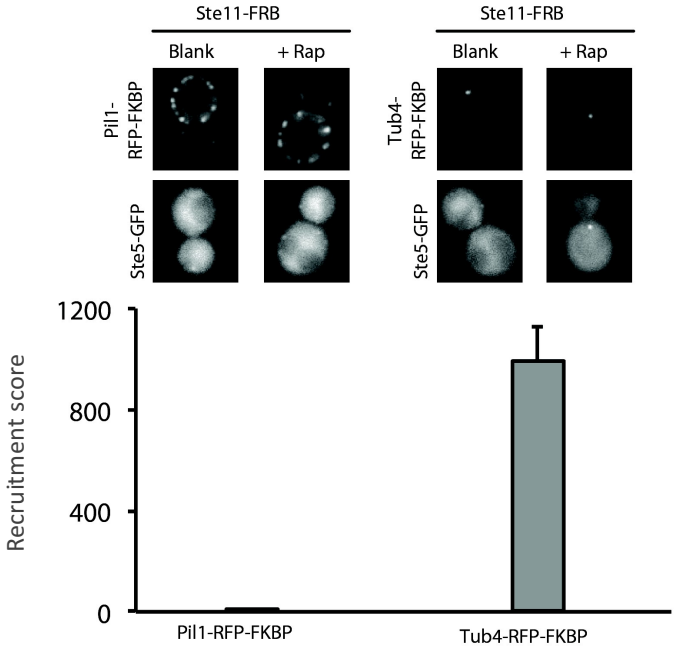


**Figure 3.1. A 200-fold more sensitive PICT assay to detect protein interactions.** Comparison of Pil1-RFP-FKBP (left) and Tub4-RFP-FKBP (right) anchoring platforms to detect the Ste11-Ste5 complex. Ste11-FRB was used as bait. Representative images of the anchor-RFP-FKBP (upper row) and Ste5-GFP (bottom row). Below, quantification of Ste5-GFP recruitment to the corresponding anchoring platform in rapamycin-treated cells (Mean ± SD). Figure adapted from (Torreira et al. 2017).

All PICT experiments were performed in rapamycin-insensitive strains carrying the *tor*1-1 mutation in the TOR1 gene and where the endogenous FPR1 gene was replaced by kanMXA cassette (Gallego et al. 2013).

#### 3.3.2.1. One-to-one PICT

For experiments involving one-to-one PICT assays, cells were grown and attached to plates as described in Section 3.3.1. Images were taken prior and after 20-30 minutes incubation with 10 µM rapamycin. The RFP imaging time was 200 ms for all the pictures. The GFP imaging time was manually adapted for each particular strain.

#### 3.3.2.2. Automated PICT

For screenings of PPIs, we have established in collaboration with the microscopy facility of the institute (IRB ADMCF) an automated pipeline for PICT assays.

Strains were inoculated in 96-well plates (Thermo-Scientific) and grown over night in Low Flo liquid medium at 30ºC. Five hours before imaging, cultures were diluted (1:25) in Low Flo liquid medium

and shacked at around 900 rpm at room temperature with a Mini-shaker PSU-2T (Biosan). Cells were attached to Concanavaline A-coated 96 well plates as described in Section 3.3.1. When required, 10 μM of rapamycin was added 20-30 minutes before imaging. Images were taken prior and after rapamycin addition. For automated imaging acquisition, ScanR software (Olympus) was set up to detect those cells' planes with highest RFP signal. This provided a focal plane that captured the highest number of anchoring platforms in focus. Strains were imaged in the RFP (200 ms) and GFP channels (200 and 1500 ms) and each well was imaged in at least 6 fields of view.

For the study of the association between P4-ATPases and MTCs, strains were inoculated in 96-well plates (Thermo-Scientific) and grown over night in Low Flo liquid medium at 30ºC. Twenty-four hours before the screening, cultures were diluted (1:1340000) on Low Flo liquid medium and shacked at around 900 rpm at 30ºC with a Teleshake Orbit Microplate Shaker (Vaiomag) kindly lent by the protein expression facility at IRB. Cells were attached to a 96 well plate as described in Section 3.3.1. For automated imaging acquisition, the ScanR software (Olympus) was also employed. Strains were imaged in the RFP (200 ms) and GFP channels (200 ms and 1000 ms) and each well was imaged in at least 6 fields of view.

### 3.3.3. Vesicle tracking

Yeast strains were grown and attached to 3.5 cm diameter glass-bottom petri dishes as described in Section 3.3.1. Cells were incubated at 23ºC for 2 hours. A single plane was chosen for imaging and 2D time-lapse sequences were acquired at 28 frames per second with 488 nm laser excitation at 80% power using an inverted microscope (IX71 Olympus), optimized for oblique illumination and fast acquisition (Hamamatsu Flash 4 sCMOS camera). Oblique illumination reduces background signal and the high-speed camera allowed high-temporal resolution. The microscope was equipped with 100x/1.45 objective lens. More than 290 trajectories of GFP puncta were collected in several movies for each strain.

### 3.3.4. Image analysis

#### 3.3.4.1. PICT assays

The software ImageJ (Schneider, Rasband, and Eliceiri 2012) was used to analyze the images. A custom image analysis workflow was developed and implemented together with the IRB ADMCF in ImageJ macro language to enable the automatic processing of complete data sets.

For each field of view, the segmentation of bright spots was performed individually in the RFP and the GFP channels by the following sequence of operations: 1) image smoothening, 2) background reduction (rolling ball), 3) local thresholding (mean intensity based), 4) median filtering and 5) connected

particles analysis to discard small particles (area threshold). For each experimental condition the functional parameters of this pipeline were manually optimized to lead to the most accurate segmentation masks upon visual inspection of few positions.

The area of overlap between prey (GFP) and anchors (RFP) was then estimated by applying a logical AND operation between the segmentation masks and by counting the number of foreground pixels. This area was normalized to the count of foreground pixels in the RFP segmentation mask only to lead to the "average fractional overlap", the main measurement of the screen.

The mean GFP intensity in the area of overlap between prey and anchors was subsequently calculated for each field of view and termed as "average overlap intensity".

Finally, an image sharpness quality factor was computed from the RFP channel as the standard deviation of the image intensity normalized to its mean intensity. Images that do not reach a minimum sharpness were excluded from the statistical analysis as likely out of focus or empty.

For the statistical analysis, a recruitment score was calculated for each strain both before and after adding rapamycin. It was defined as the result of multiplying the mean "average fractional overlap" by the mean "area overlap intensity" in each condition. Those strains with less than 18 focused anchors, were also excluded from the analysis. A fold change of the recruitment score was then measured. It was calculated as the division of the recruitment score upon adding rapamycin by the recruitment score prior to rapamycin for each particular strain. Finally, those pictures with a fold change higher than 3, were considered as potential positive interactions and they were manually validated.

#### 3.3.4.2. Colocalization assays

The same custom analysis workflow described in the previous section was applied in RFP-GFP colocalization assays. As described before, the area of overlap between the GFP and RFP was estimated by applying a logical AND operation between the segmentation masks and by counting the number of foreground pixels. This area was normalized to the count of foreground pixels in the RFP segmentation mask in experiments of Figures 4.16, 4.17, 4.18, and 4.20. In experiment of Figure 4.22, the area was normalized to the count of foreground pixels in the GFP segmentation mask.

For the statistical analysis, the colocalization score was estimated in cells harboring wild type or deleted DRS2, and normalized to the measurement of those strains with wild type DRS2.

#### 3.3.4.3. Vesicle tracking

GFP images were stacked and compensated for bleaching by applying ImageJ "Bleach Correction" plugin ("Exponential Fit" method). This last step was important to ensure correct vesicle detection throughout the whole time-lapses.

Individual vesicles were then identified and tracked by ImageJ TrackMate plugin (Tinevez et al. 2017), using "DoG" detector for spot detection (blob diameter set to 5 pixels), and a threshold manually optimized for each time-lapse. Tracks were reconstructed by selecting "simple LAP" tracker, a maximal linking distance of 5 pixels (> maximum vesicle speed observed), and no gap-closing allowed (a vesicle must be detected at every time frame for a track to be valid). Finally, only tracks containing a minimum of 5 spots were kept to discard spurious tracks.

For each time-lapse, average vesicle speeds were computed and these speeds represented as a 20 bin histogram spanning from 0 to 200 nm/frame.

The resulting histograms were fitted to a two-component Gaussian mixture model (GMM); the fits were optimized by the nonlinear least-squares regression method provided in MATLAB. From these models, we could estimate the means and standard deviations as well as the multiplicative weight factors of both Gaussian components.

Finally, to estimate the fraction of spots belonging to each population (Gaussian component), we derived two coefficients $\alpha_1$ and $\alpha_2$ defined as the fractional areas below each Gaussian component normalized to the overall area below the fitted curve.

### 3.4. Electron microscopy (EM)

Yeast cells were grown in YPD until reaching an early logarithmic phase ($OD_{600}\approx1$) as described before. Then they were grown at 23ºC for two hours. For non-selective autophagy analysis, rapamycin (0.2 µg/ml) was added to cells cultures overnight. The next morning, cells were cultured at 23ºC for two hours.

#### 3.4.1. High pressure freezing

Samples were cryo-immobilized by high-pressure freezing as described in literature (Müller-Reichert 2012). In brief, yeast cells were pelleted and the yeast paste was loaded into 200 µm depth planchettes and high-pressure frozen using the High Pressure Freezing Leica EM ICE. The planchette sandwich was disassembled under liquid nitrogen prior to freeze-substitution.

#### 3.4.2. Freeze-substitution and embedding

Samples were freeze-substituted using a temperature-controlling AFS2 (Leica) with an FPS robot. Freeze-substitution occurs at −90°C for 48–58 h with 1% (w/v) uranyl acetate in glass distilled acetone. The temperature was then raised to −45°C (5°C/h), samples are washed 3 times with acetone and infiltrated with increasing concentrations (10%, 25%, 50%, 75%, 4 h each) of Lowicryl HM20 in acetone while the temperature raised further to −25°C. 100% Lowicryl was exchanged 3 times in 10 h

steps, and UV-polymerized at −25°C for 48 h after which the temperature was raised to 20°C (5°C/h) and UV polymerization continued for 48 h.

### 3.4.3. EM imaging

EM pictures were taken at various magnifications in a JEOL JEM 1011 electron microscope equipped with a Veleta 2k x 2k side-mounted TEM CCD camera (Olympus).

### 3.4.4. Correlated Light and Electron Microscopy (CLEM)

Cells were grown as described in the Section 3.4.

### 3.4.5. High pressure freezing

The same protocol described in Section 3.4.1 was applied.

### 3.4.6. Freeze-substitution and embedding

The protocol described in Section 3.4.2 was applied with a difference: freeze-substitution occurs with 0.1% (w/v) uranyl acetate in glass distilled acetone.

### 3.4.7. Sectioning, Pick-Up and Application of Fluorescent Fiducial Markers

Samples were stored protected from light after polymerization and processed further within 2 days. Ultrathin sections were cut with a diamond knife in a microtome (Leica EM UC7) and picked up on carbon-coated 200 mesh copper grids. Fluorescent fiducial markers, 0.02 µm Blue FluoSpheres (Molecular Probes) (excitation 365 nm/emission 415 nm) were adhered to the section. FluoSpheres were diluted 20× in a 0.1% Tween-20 in PBS solution, incubated for 10 min at room temperature, washed twice by 30 min ultracentrifugation at 100,000 g, 4°C, resuspended in PBS, and sonicated for 5 min. Then grids were placed section-face down onto a 15 µl drop of FluoSpheres for 10 min, blotted with filter paper and washed with 3 drops of water with blotting between the washing steps.

### 3.4.8. Fluorescence Microscopy

To minimize bleaching, fluorescence images were taken with an IX83 (Olympus) during the next three days. From 2 to 5 images were taken in different focal planes for both channels (GFP and blue fluorescent fiducials). During imaging, the positions on the grid of the imaged areas of interest were recorded, so that they could be found back easily by EM.

### 3.4.9. Electron Microscopy and Correlation

EM pictures were taken as described in Section 3.4.3 then they were correlated to the corresponding GFP images with the Adobe Illustrator software.

### 3.5. Immunoblot analysis

Yeast cells were grown in YPD medium at 30ºC and 220 rpm overnight. Those cells expressing plasmids were grown in synthetic minimal medium lacking the amino acid of choice. The next morning, cells were diluted to an optical density of $OD_{600}$=0.2 in the media of interest and were grown at 30ºC and 220 rpm until they reached an early logarithmic phase ($OD_{600}$≈1). When needed, cell cultures were shifted to 23ºC for one, two, three or four hours or to 37ºC for two hours. For nitrogen starvation assays, after reaching an early logarithmic phase cell cultures were shifted to SD (-N) liquid medium and incubated for four hours.

To prepare the samples for western blot analysis, an alkaline extraction method described in (Kushnirov 2000) was followed. About 1 ml of 1 $OD_{600}$ of yeast cells were harvested by centrifugation at 3000 rpm for 2 min. After resuspending in 50 µl distilled water, 50 µl 0.2M NaOH was added and samples were incubated at room temperature for 5 min. After, cells were pelleted, resuspended in 50 µl 2X SDS sample buffer, boiled for 5 min and pelleted again. About 10 µl of the supernatant was loaded in each lane of a 1.5 mm 10% acrylamide SDS gel. Gels were run at 100 V until the migration front left the bottom of the gel with electrophoresis running buffer. Proteins of the gel were transferred to a 0.2 µm Nitrocellulose Blotting Membrane (GE Healthcare) for one hour at 400 mA in transfer buffer. The blocking step was done with 5% milk powder (Asturiana) in TBS-0.5% Tween 20 (Sigma-Aldrich) for one hour at room temperature. Incubation with primary anti-Ape1 antibody was done overnight at 4ºC (1:4000 antibody dilution in blocking solution). Antibody anti-Ape1 was kindly given by Dr. Maho Hamasaki (Osaka Univesristy). The membrane was rinse thrice for 15 min at room temperature with TBS-Tween. Incubation with secondary anti-Rabbit antibody was done for one hour at room temperature (1:2500 antibody dilution in blocking solution) and the membrane was rinse three more times for 15 min at room temperature with TBS-Tween. ECL from GE Healthcare was used as western blotting detection reagent.

### 3.6. Cold sensitive assay

Newly fresh yeast strains were streaked on YPD plates and tested for growth at 18ºC for two days. In parallel, they were also streaked on YPD plates at 30ºC as a regular growth control.

### 3.7. Yeast two-hybrid assay

For yeast two-hybrid assays, I used the MatchmakerTM GAL4 Two-Hybrid System from Clonotech and the AH109 as the host strain. The vectors I employed are listed in Apendix II-Plasmids. To generate pOG0279, pOG0280 and pOG0281, the first 633pb of DRS2 (N-terminal tail), BET3 full-length and TRS31 full-length were PCR-amplified from yeast genomic DNA with the following oligonucleotides: Oligonucleotides 5'gtaccagattacgctcatatggccatggagATGAATGACGACAGAGAA3' and 5'tgcagctcgagctcgatggatcccgtatcgTCACGCAAAATTATACTTGGT3' for DRS2. Oligonucleotides

5’tcagaggaggacctgcatatggccatggagATGGTTTCTACCACGCAA3’ and 5’ggccgctgcaggtcgacggatccccgggaaCTAATCTTCGCCGATCGG3’ for BET3. Oligonucleotides 5’tcagaggaggacctgcatatggccatggagATGGGGATATATTCATTT3’ and 5’ggccgctgcaggtcgacggatccccgggaaTCACTGATTAACCATTGG3’ for TRS31. PCR-generated inserts and linearized vectors (pGADT7 and pGBKT7) were cloned by using In-Fusion HD methodology (Clonotech) as described in the In Fusion HD Cloning Kit User Manual. N-terminal DRS2 (633 bp) was cloned into the Ndel-SaclI site of pGADT7. BET3 and TRS31 were cloned into the NdeI-BamHI site of plasmid pGBKT7. Cloning products were transformed in DH5α competent cells (Thermo Fisher Scientific) following the kit protocol. DNA plasmids were isolated from *E.coli* cultures using GenElute Plasmid Miniprep Kit from Sigma-Aldrich and confirmed by sequencing. Correct clones were then transformed in the AH109 strain following the yeast transformation procedures described in Section 3.2.1. AH109 transformants were selected on SD leucine$^-$ tryptophan$^-$ plates and tested for growth on SD histidine$^-$, leucine$^-$ and tryptophan$^-$ plates at 23ºC.

# 4. RESULTS

## 4.1. Screening for new proteins that associate with MTCs

Despite their essential role in the cellular trafficking of all eukaryotic cells, the molecular mechanisms that mediate MTCs mode of action are still not completely understood. This prompted us to carry out a comparative analysis of these molecular machines with the aim of finding new proteins that interact with MTCs and that regulate their function. As model organism, we used yeast *S. cerevisiae.*

### 4.1.1. *In silico* genome-wide screen to detect functionally relevant partners for MTCs

Genetic interactions provide functional information and have been widely used in the past to identify functionally related proteins. Although single deletions of genes can produce phenotypic consequences, some combinations of mutations may exacerbate or reduce these phenotypic changes, providing useful information about functional relationship between these genes (A. H. Y. Tong et al. 2001) (Ooi, Showmaker, and Boeke 2003). Genetic interactions, therefore, may underlie common effects in the same biological process or pathway. Previous studies have revealed that two proteins in the same genetic network are more likely to also physically interact with each other (A. H. Y. Tong et al. 2001) (Kelley and Ideker 2010). For these reason, we decided to conduct an *in silico* genome-wide screen to identify proteins that could be functionally related to MTCs and select them for protein interactions screen.

This genome-wide search was done for all genetic and PPIs that had been reported at the Saccharomyces Genome Database (www.yeastgenome.org) by September 2013. MTCs establish 2587 genetic interactions and 128 PPIs with proteins that do not form part of their complex. In order to increase the likelihood to select proteins that were relevant for MTCs function, together with the Biostatistics facility at the IRB Barcelona, we selected 676 (26.1%) genetic interactions that had a provability lower than $10^{-6}$ to occur randomly. With this cutoff, 71 (55.4%) of the reported PPIs for MTCs were selected, suggesting that this subset of proteins is also more likely to bind MTCs. Therefore, we selected the 505 proteins that had not been described to interact physically with MTCs subunits and that were available in the genomic collection of GFP C-terminus fusions.

### 4.1.2. PICT method and strains generation

We used the PICT technique to identify new PPIs that are relevant for MTCs function. As described in Material and Methods (Section 3.3.2), PICT let us detect interactions by dual-color live-cell imaging in a genetic background optimal to recruit cytosolic complexes to a plasma membrane associated anchoring platform (Tub4-FKBP-RFP). Given the high sensitivity of the assay and that the experiments were done directly in living cells, this method was prompt to detect interactions that have been

overlooked by previous analysis, such as indirect, transient or low abundant interactions.

We generated a collection of 524 yeast strains harbouring pairwise combinations of MTCs subunits tagged to FRB (bait-FRB) and the proteins selected based on their genetic interaction profile tagged to GFP (prey-GFP), in cells engineered with Tub4-FKBP-RFP. The MTCs subunits selected as baits include one bait for each complex (Figure 4.1). In preliminary experiments, each of these baits was shown to efficiently recruit the corresponding MTC to the anchoring platform.

We also generated control strains to analyze the interaction between two subunits of each MTC (i.e. 9 positive controls) and the interaction between each MTC and one protein with similar localization but that was not expected to interact (i.e. 9 negative controls) (Appendix I-Yeast strains).

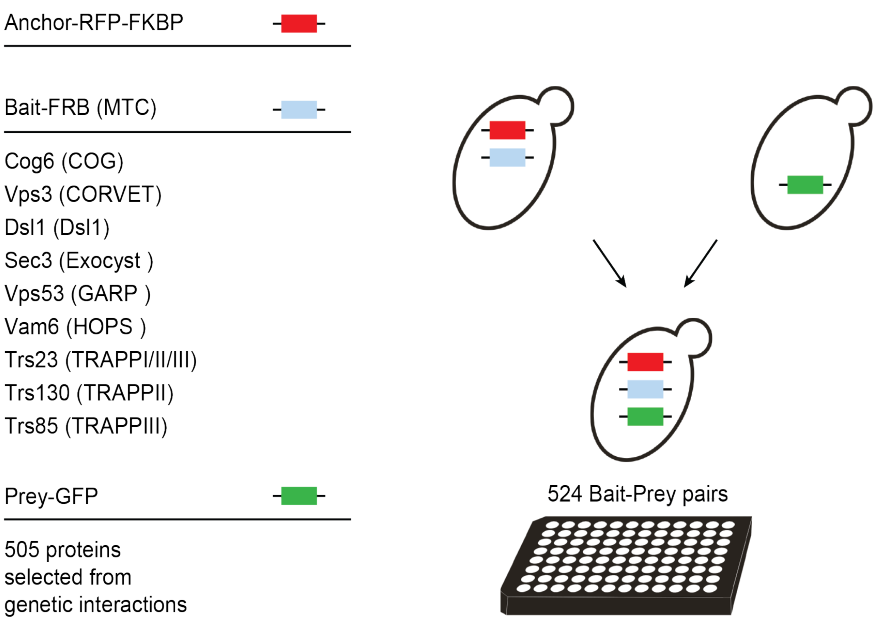


**Figure 4.1. Schema of the screening designed to detect new proteins that associate with MTCs.** A total of 524 yeast strains were generated. Using automated PICT we systematically analyzed the association of MTCs subunits (baits) and 505 proteins selected according to their genetic interaction profile (preys). Note that Trs23-FRB will translocate all three TRAPP complexes.

In collaboration with the microscopy facility of the institute (ADMF-IRB), we established an automated pipeline to screen PPIs using automated-PICT. We used image analysis to quantify the colocalization between preys and the anchoring platforms before and after adding rapamycin (see Section 3.3.4.1-Materials and Methods).

### 4.1.3. Validation of the method used to select preys based on genetic interactions

Before embarking on the entire screen, I confirmed that the approach used to select the 505 preys was useful to provide new insights on MTCs mechanisms of function. I analysed the interactions between CORVET and 79 proteins, including 40 prey-GFPs selected based on their genetic interaction profile and 39 prey-GFPs selected randomly. While no interactions were detected with those targets selected

randomly, we found 4 new interactions when analyzing preys selected based on their genetic interactions with CORVET. These results evidence the utility of conducting an *in silico* screening based on genetic interactions to increase the likelihood to identify new PPIs.

#### 4.1.4. Identification of 9 new interactions with MTCs

The 524 PPIs screened gave rise to the identification of 10 new interactions with MTCs (see Figure 4.2). As mentioned earlier, four of these interactions concerned CORVET: Hse1, Bro1, Vps45 and Vps9. Hse1 is part of a complex required for sorting of ubiquitinated membrane proteins into intraluminal vesicles prior to vacuolar degradation, as well as for recycling of Golgi proteins and formation of luminal membranes (Bilodeau et al. 2002) (Bilodeau et al. 2003); Bro1 is a cytoplasmic class E vacuolar protein sorting (VPS) factor, that coordinates deubiquitination in the multivesicular body (MVB) pathway (Nickas and Yaffe 1996) (G. Odorizzi 2003); Vps45 is a protein of the Sec1p/Munc-18 family, which is also essential for vacuolar protein sorting and for fusion of Golgi-derived vesicles with the prevacuolar compartment (Bryant et al. 1998) (Piper, Whitters, and Stevens 1994); and Vps9 is a GEF and ubiquitin receptor involved in vesicle-mediated vacuolar transport, including Golgi-endosome trafficking and sorting through the MVB, which has been described to be required for localization of the CORVET complex to endosomes (Burd et al. 1996) (Hama, Tall, and Horazdovsky 1999) (Cabrera et al. 2013).

We also detected the interaction between the COG complex and the vesicle membrane receptor protein (v-SNARE) involved in the fusion between Golgi-derived secretory vesicles with the plasma membrane (Protopopov et al. 1993) (Paumet, Rahimian, and Rothman 2004).

The remaining four interactions involve MTCs and members of the P4-ATPases family. We detected the association between GARP and the CDC50/LEM3 family protein Lem3, which specifically interacts with the flippases Dnf1 and Dnf2 (Riekhof et al. 2007) (Lenoir et al. 2009). We also identified the lipid flippase Drs2 binding all the three TRAPP complexes. This percentage of interactions with members of the P4-ATPases family suggested a more important interplay between MTCs and lipid asymmetry in cellular membranes than it had been anticipated, what led us to further study the linkage between them.

A

New interactions with MTCs

| MTC | Prey (Human homologos) |
|---|---|
| COG | Snc2 (VAMP1) |
| CORVET | Hse1 (STAM1/STAM2) |
| CORVET | Bro1 (PDCD61P) |
| CORVET | Vps45 (Vps45) |
| CORVET | Vps9 (Vpas9 domains) |
| GARP | Lem3 (TMEM30A/TMEM30B) |
| TRAPPI/II/III | Drs2 (ATP8A1) |
| TRAPPII | Drs2 (ATP8A1) |
| TRAPPIII | Drs2 (ATP8A1) |

B

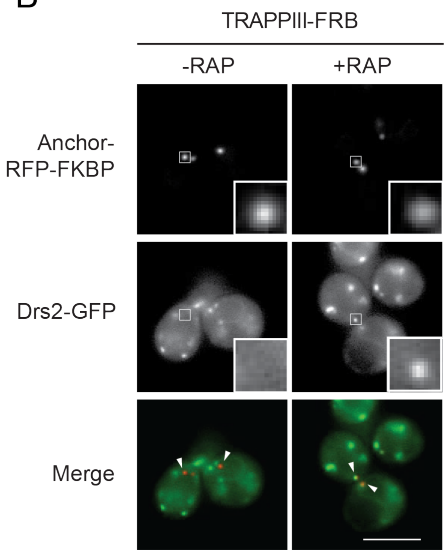


**Figure 4.2. Screen to find new interactions for each MTC *in vivo*. (A)** 9 new interactions with MTCs, and their human homologs shown in parentheses. **(B)** Representative images of the PICT assay with Trs85-FRB (TRAPPIII) as bait and Drs2-GFP as prey. The RFP-tagged Tub4 and the GFP-tagged Drs2 are shown in the upper and middle row, respectively. Overlap of RFP and GFP fluorescence (bottom row) indicates that the prey has been co-translocated with the bait to the anchoring platform (arrowheads). White squares show zoom of representative anchoring platforms. Zoom-in box is 0.9 µm wide. Scale bar, 5 µm.

## 4.2. Study of the interplay between P4-ATPases and MTCs

P4-ATPases play important roles in vesicle trafficking, and so far, very little is known about the interplay between flippases and MTCs (Takagi et al. 2012b). Given the number of associations between P4-ATPases and MTCs that we obtained in our screen, we decided to extend the analysis and examine the interactions among all the MTCs and the rest of P4-ATPases (see Figure 4.3).

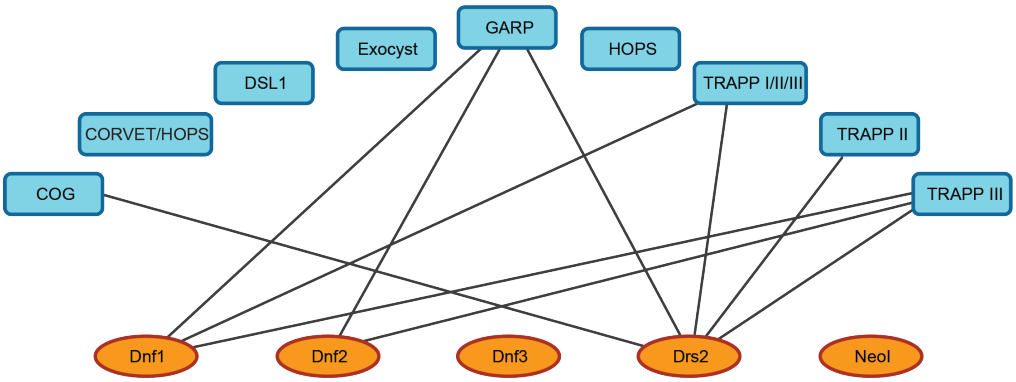


**Figure 4.3. Interactions between MTCs and P4-ATPases.** MTCs and P4-ATPases are represented in blue and orange, respectively. Black lines indicate PPIs obtained from our PICT assays.

To conduct this study, I generated new pairwise combinations with the same baits selected for the previous screening and the five phospholipid flippases that conform the P4-ATPases family in *S. cerevisiae*. The results of the PICT assay revealed that, Dnf1 and Drs2 on the one hand, and GARP and

TRAPPIII on the other hand, are the ones that concentrate most of the interactions. We subsequently decided to go further into the study of the biological relevance of two of these interactions, for what we focused on two main objectives:

### 4.2.1. Study of the interplay between GARP and Dnf1

It has been shown that GARP is important for the proper localization of Dnf1 and Dnf2 and thus to maintain the correct distribution of PE and PS in both leaflets of the plasma membrane. Nevertheless, so far it has not been described a direct role of GARP in this process (Takagi et al. 2012a). I found that Dnf1 and Dnf2 interact with GARP, suggesting a direct function of this complex in the transport of these flippases. Dnf1 and Dnf2 are recycled to the plasma membrane after they are internalized through endocytosis. For this reason, we purposed to characterize the role of GARP in the Dnf1 recycling. To do that, I first confirmed the changes in Dnf1 localization upon GARP deletion that had been reported before (Figure 4.4).

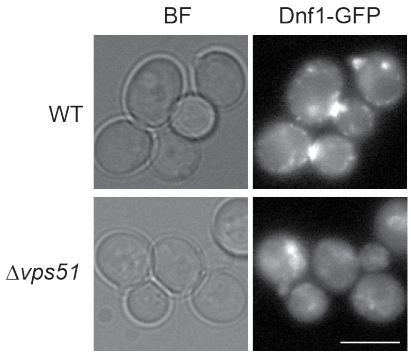


**Figure 4.4. Subcellular localization of Dnf1-GFP.** Representative images of GFP tagged Dnf1 in wild type and Δ*vps51* cells. *BF,* brightfield images**.** Scale bar, 5 µm.

To further investigate the interplay between GARP and Dnf1, I next conducted PICT assays to analyse the interaction between GARP and Dnf1-GFP when specific trafficking pathways were blocked (Figure 4.5). I examined the interaction between GARP and Dnf1 in wild type cells, cells treated with latrunculin A (Lat A) and a set of traffic mutants. Lat A induces actin polymerization, which blocks endocytosis (Smythe and Ayscough 2006). Snx4 is a sortin nexin required for the recycling from early endosomes to the Golgi (Hettema et al. 2003). Vps25 belongs to the class E vps (vacuolar protein sorting) family, and it is involved in the maturation of early endosomes (Ueno et al. 2014). Mon1 is a GEF that stimulates the activation of Ypt7, a Rab family GTPase involved in membrane tethering and fusion events at the vacuole (Ueno et al. 2014). Finally, Tlg2 is a syntaxin-like t-SNARE, which mediates the fusion of endosome-derived vesicles with trans-Golgi network (TGN) (Holthuis et al. 1998).

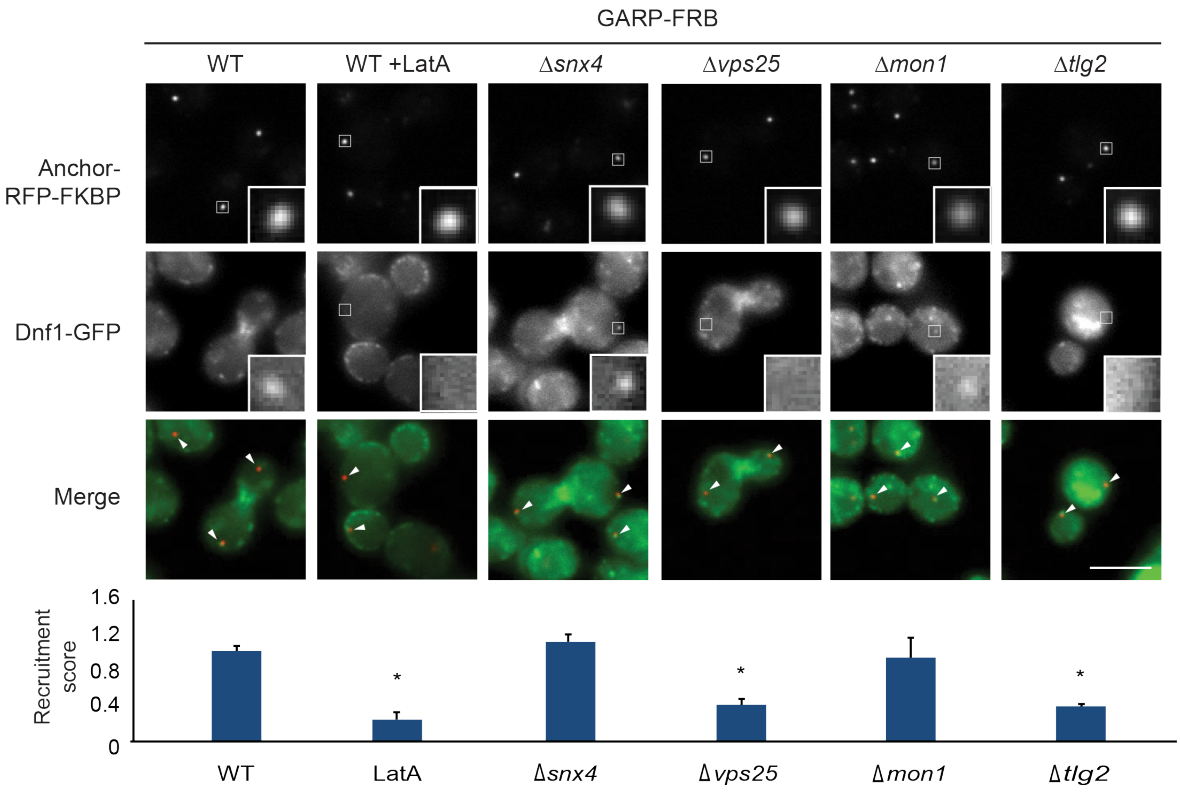


**Figure 4.5. Analysis of the interaction GARP-Dnf1.** The interaction between GARP and Dnf1 was analyzed by PICT in wild type cells, wild type cells treated with Lat A, and Δ*snx4*, Δ*vps25*, Δ*mon1* and Δ*tlg2* mutants. Representative PICT images of the RFP-tagged anchor and GFP-tagged Dnf1 are shown in the upper and middle row, respectively. White squares represent a zoom of a 0.9 × 0.9 µm square around the anchoring platforms. Overlap of RFP and GFP fluorescence (bottom row) indicates that Dnf1 has been co-translocated with GARP to the anchoring platform (arrowheads) upon addition of rapamycin. Scale bar, 5 µm. Below, quantification of the Dnf1-GFP recruitment score, normalized to the measurement of the wild type strain (Mean ± SD, p-value * < 0.05 t-test). Error bars indicate SD.

To better evaluate how the interaction between GARP and Dnf1 is affected under each condition, we quantified the PICT images by scoring the GFP-RFP overlapping area (see Section 3.3.4.1-Material and Methods for a detailed explanation). This recruitment score showed a significant decrease in GARP-Dnf1 interaction in cells treated with Lat A, in Δ*vps25* and in Δ*tlg2* mutants (Figure 4.5). These results suggest that GARP-Dnf1 binding takes place during the transport of Dnf1 from late endosomes to the TGN. To verify this possibility with another approach, we also examined the colocalization between Dnf1 and markers of late endosomes (Vps26) and the TGN (Sec7), both in wild type and GARP mutants (Δ*vps51*). While in wild type cells the flippase accumulates in the TGN, in cells lacking the GARP subunit Vps51 we could not detect Dnf1 in this organelle. (Figure 4.6). On the other hand, the colocalization between Dnf1 and the late endosome marker was higher in mutant cells. This result confirms that GARP is required for the transport of Dnf1 from late endosomes to TGN.

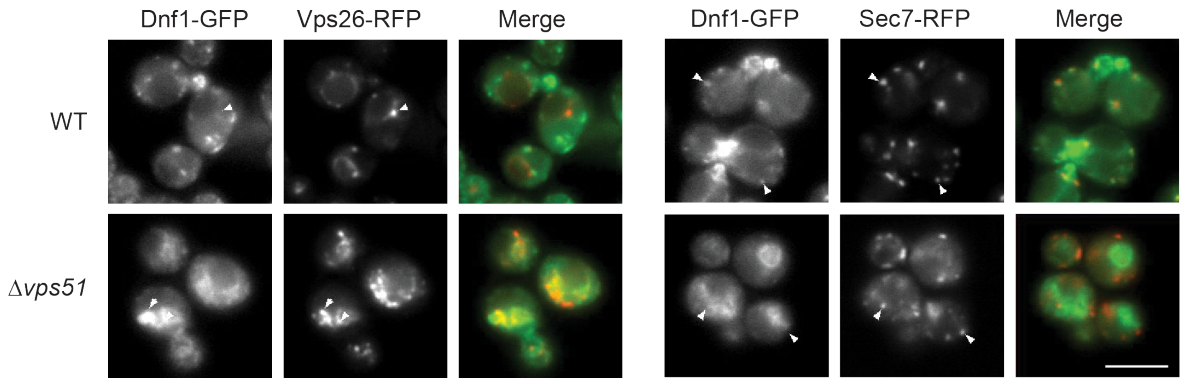


**Figure 4.6. Subcellular distribution of Dnf1-GFP.** Representative images of GFP tagged Dnf1 and RFP tagged Vps26 or RFP tagged Sec7 in wild type and Δ*vps51* cells are shown in the left and middle column, respectively. Arrowheads indicate organelle markers. Scale bar, 5 µm.

Altogether, our experiments imply that GARP tethers Dnf1 to the TGN when coming from late endosomes, what evidences its direct role in the recycling of this flippase.

### 4.2.2. Study of the interplay between TRAPPIII and Drs2

The other interaction we decided to further characterize is the one that takes place between TRAPPIII and Drs2 (Figure 4.2_B and Figure 4.3). TRAPPIII is required for the transport of Atg9 vesicles to the PAS during the biogenesis of the Cvt vesicle. In starvation, when non-selective autophagy takes place, TRAPPIII also participates in the transport of Atg9 vesicles to the PAS during the biogenesis of the autophagosome, but its contribution is minor (M. A. Lynch-Day and Klionsky 2010) (Shirahama-Noda et al. 2013). Drs2 is a PS flipasse that maintains membrane lipid asymmetry in post-Golgi secretory vesicles and that is essential for the trafficking between the Golgi and endosomal system (Hankins et al. 2015). Given the role of Drs2 in regulating some trafficking pathways, we wondered whether this flippase would be involved in TRAPPIII function during the trafficking of Atg9 vesicles.

#### 4.2.2.1. The cell regulates TRAPPIII-Drs2 interaction in response to temperature

Drs2 is essential for cell growth at temperatures below 23ºC (Ripmaster, Vaughn, and Woolford 1993). Even when grown at milder temperatures, cells lacking Drs2 present strong defects that are rescued when cells are grown at 37ºC (Hua, Fatheddin, and Graham 2002). The molecular details that mediate Drs2 function at lower temperatures are not clear. Some studies suggested that PS flipping is necessary to maintain membrane fluidity at low temperatures (Todd Graham, personal communication). However, cells expressing Drs2 mutants that kept their ability to flip phospholipids also show cold-sensitive phenotypes (Ryan D Baldridge and Graham 2013). In order to explore new molecular mechanisms that could be mediating Drs2 function at low temperatures, and to better describe the association TRAPPIII-Drs2, I analyzed the TRAPPIII-Drs2 interaction at 23ºC and 37ºC (Figure 4.7). Surprisingly, the interaction decreased more than 50% at higher temperature, although it was not completely blocked.

This difference suggests that Drs2 interplay with TRAPPIII could be regulated by temperature.

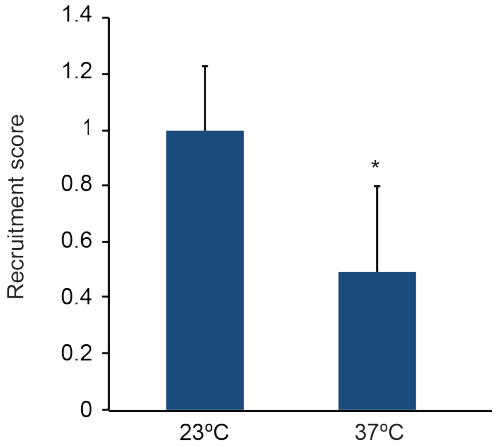


**Figure 4.7. Quantification of the TRAPPIII-Drs2 interaction.** Quantification of Drs2-GFP recruitment score normalized to the measurement at 23ºC. (Mean ± SD, p-value * < 0.05 t-test). Error bars indicate SD.

#### 4.2.2.2. Drs2 is required for a proper Cvt pathway at low temperatures

To first evaluate whether Drs2 could be involved in the correct functioning of the Cvt pathway, we monitored Ape1 processing. Since the lack of Drs2 produces temperature-sensitive growth and traffic defects (Hua, Fatheddin, and Graham 2002), and the interaction TRAPPIII-Drs2 is regulated in a temperature-dependent manner, I evaluated Ape1 maturation by Wester-blot in a range of temperatures. After reaching the log phase, cells were either maintained at 30ºC, or shifted to 23ºC or 37ºC for 2 hours. As positive and negative controls, I used wild type cells and cells lacking Trs85, the specific subunit of TRAPPIII that is required for Cvt pathway (Figure 4.8). While Ape1 is mostly processed in growing wild type cells, in *Δtrs85* cells no mature Ape1 was observed. *Δdrs2* cells, however, showed a partial and a strong inhibition at 30ºC and 23ºC, respectively, and behaved as wild type cells at 37ºC. These results are in agreement with our hypothesis that Drs2-TRAPPIII cooperate at low temperatures. For this reason, the rest of experiments involving Drs2 were carried out after two hours at 23ºC unless otherwise is indicated.

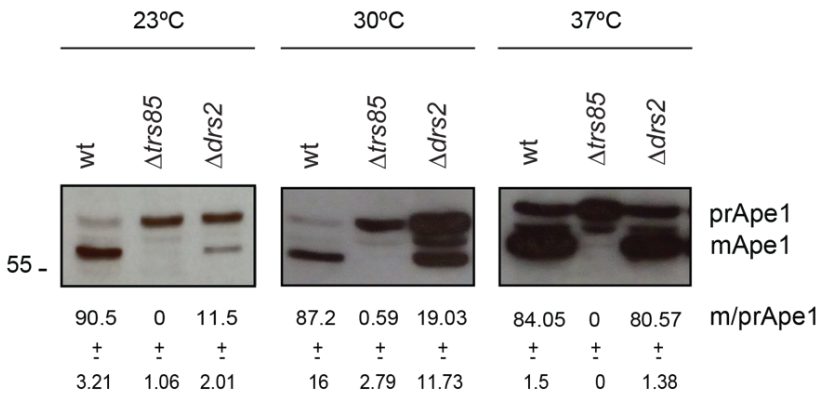

**Figure 4.8. Analysis of the requirement of Drs2 in the Cvt pathway at different temperatures.** Wild-type, *Δtrs85* and *Δdrs2* cells were grown at 30ºC until reaching the log phase and either maintained at 30ºC or shifted to 23ºC or 37ºC for 2 hours. The upper band shows the not processed Ape1 (prApe1) and the lower band shows the matured Ape1 (mApe1). Below, the quantification of the Ape1 processing (mApe1/(prApe+mApe1)) in 3 replicates ± SD.

Although we saw an important defect in Ape1 maturation of *Δdrs2* cells at 23ºC, the processing was not entirely inhibited. Instead, there is a slight band corresponding to mApe1 in these cells. We wondered whether this observation results from mApe1 that remains in the cells after the temperature shift to 23ºC. To solve this question, I did a time course assay where I took samples after 1,2,3, or 4 hours at 23ºC (Figure 4.9). However, the ratio between both bands is constant over time, what made us discard this possibility.

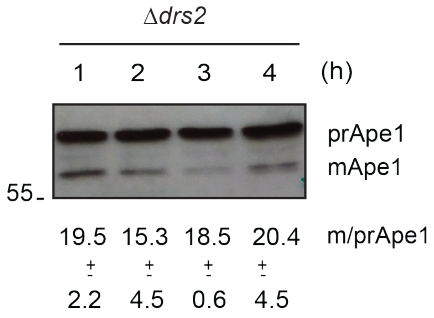


**Figure 4.9. Time course assay of Ape1 processing.** *Δdrs2* cells were grown at 30ºC until reaching the log phase and shifted to 23ºC. Immunoblot analysis anti Ape1 was done in cells after 1,2,3 or 4h at 23ºC. The upper band shows the not processed Ape1 (prApe1) and the lower band shows the matured Ape1 (mApe1). Below, the quantification of the Ape1 processing (mApe1/(prApe+mApe1)) in 3 replicates ± SD.

Ape1 can be processed through selective autophagy (i.e. Cvt pathway) or non-selective autophagy (i.e bulk autophagy). To further confirm whether this modest maturation of Ape1 was dependent on the Cvt pathway, we analyzed a strain lacking DRS2 and ATG19 (Figure 4.10). Atg19 is a receptor for prApe1 specific for the Cvt pathway, also required for the formation of the Cvt vesicle (Delorme-axford et al. 2016). In this case, we observed a fully processing inhibition, which indicates the Cvt pathway is not completely blocked upon Drs2 deletion at 23ºC, although it is highly perturbed.

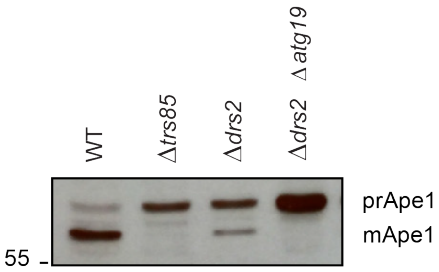


**Figure 4.10. Drs2 does not completely block the Cvt pathway.** Wild type, *Δtrs85, Δdrs2, Δdrs2Δatg19* strains were subjected to immunoblot analysis anti-Ape1. The upper band shows the not processed Ape1 (prApe1) and the lower band shows the matured Ape1 (mApe1).

In accordance with all these results, live-cell imaging showed that in *Δdrs2* cells Ape1-GFP forms brighter and bigger aggregates than in wild type cells, similar to the ones observed in cells lacking TRAPPIII. These big clusters advance important defects in the morphology of Ape1 oligomers (Figure 4.11).

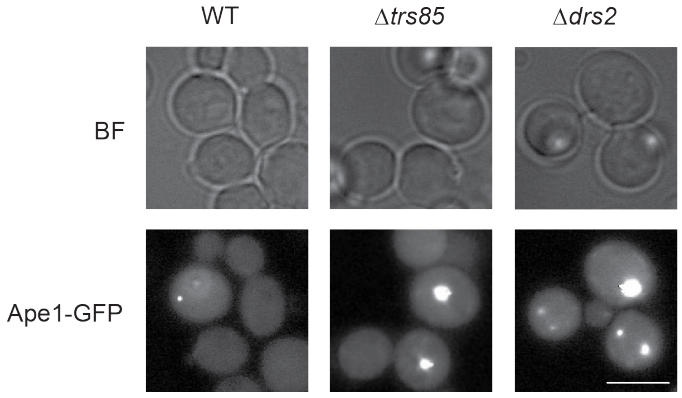


**Figure 4.11. Subcellular distribution of Ape1-GFP.** Representative images of GFP tagged Ape1 in wild type, *Δtrs85* and *Δdrs2* cells are shown in the lower raw. *BF* brightfield. Scale bar, 5 µm.

#### 4.2.2.3. Drs2 has a mild contribution in non-selective autophagy

We also wondered whether Drs2 could be involved in bulk autophagy, where TRAPPIII has also been involved (Shirahama-Noda et al. 2013). For this reason, we first confirmed by PICT assay that TRAPPIII and Drs2 also interact in cells grown under nitrogen (-N) starvation, where non-selective autophagy is activated (Figure 4.12).

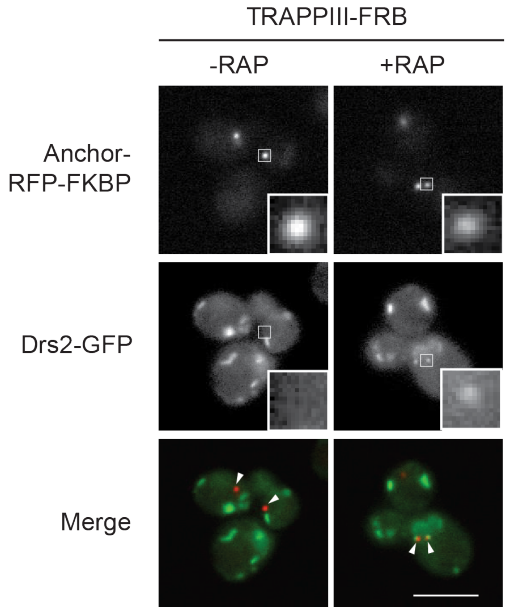


**Figure 4.12**. The interaction between TRAPPIII and Drs2 was analyzed by PICT in cells grown for 4h in SD (-N) liquid medium. Representative PICT images of the RFP-tagged anchor and GFP-tagged Drs2 are shown in the upper and middle row, respectively. White squares show zoom of representative anchoring platforms. Zoom-in box is 0.9 µm

wide. Overlap of RFP and GFP fluorescence (bottom row) on the right column, indicates that the prey has been co-translocated with the bait to the anchoring platform (arrowheads) upon addition of rapamycin. Scale bar, 5 µm.

I then evaluated the processing of Ape1 under starvation conditions (SD (-N)) in wild type, *Δtrs85* and *Δdrs2* cells (Figure 4.13). As expected, while in wild type cells Ape1 was almost completely processed, cells lacking Trs85 showed a 21.62% inhibition in the processing of the proenzyme. Similarly, *Δdrs2* cells showed 26.7% inhibition in the maturation of Ape1, supporting our hypothesis that Drs2 and TRAPPIII cooperate in the same pathway.

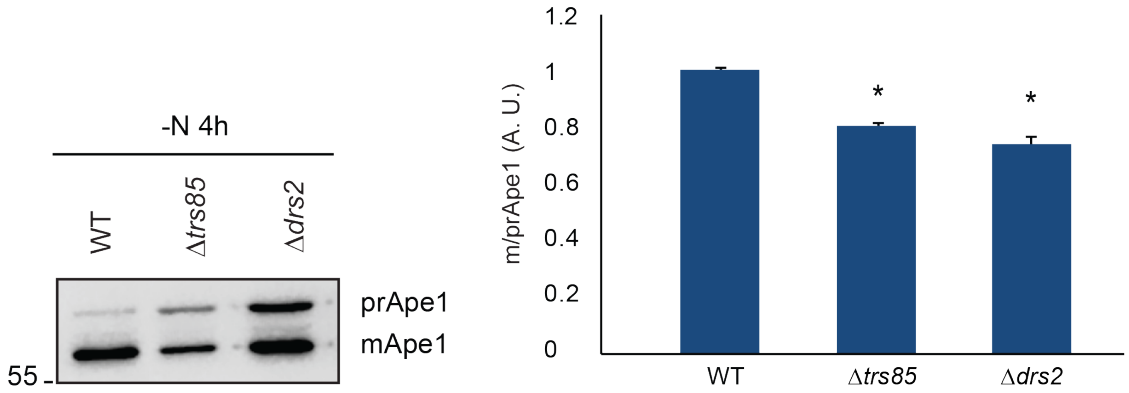


**Figure 4.13. Immunoblot anti Ape1 upon starvation conditions.** Left, wild type, *Δtrs85* and *Δdrs2* cells were grown in YPD until reaching the log phase and shifted to SD(–N) starvation conditions for 4 hours. The upper band shows the not processed Ape1 (preApe1) and the lower band shows the matured Ape1 (mApe1). Right, plot of m/prApe1 quantification normalized to m/prApe1 in wild type cells. (Mean ± SD, p-value * < 0.01 t-test). Error bars indicate SD.

#### 4.2.2.4. Drs2 is necessary for the biogenesis of the Cvt vesicle

As both TRAPPIII and Drs2 have a more relevant role in selective autophagy we decided to further study their interplay in this pathway. The Cvt pathway can be divided into different steps: PAS formation, elongation of the Cvt vesicle, closure, fusion with the vacuole and cargo degradation (M. Lynch-Day and Klionsky 2011).

To identify the precise stage of the Cvt pathway affected by the lack of Drs2, I first conducted EM experiments to compare the structure of Cvt bodies in strains with or without Drs2. Both of them lacked Pep4, a vacuolar enzyme required for processing of vacuolar deliveries (Ammerer et al. 1986). While I could observe Cvt bodies (Figure 4.14_A, arrowheads) in 89.29% of *Δpep4* cells, I could not detect any Cvt body in *Δpep4Δdrs2* cells, indicating that Drs2 is involved in a step before Cvt vesicle fuses with the vacuole:

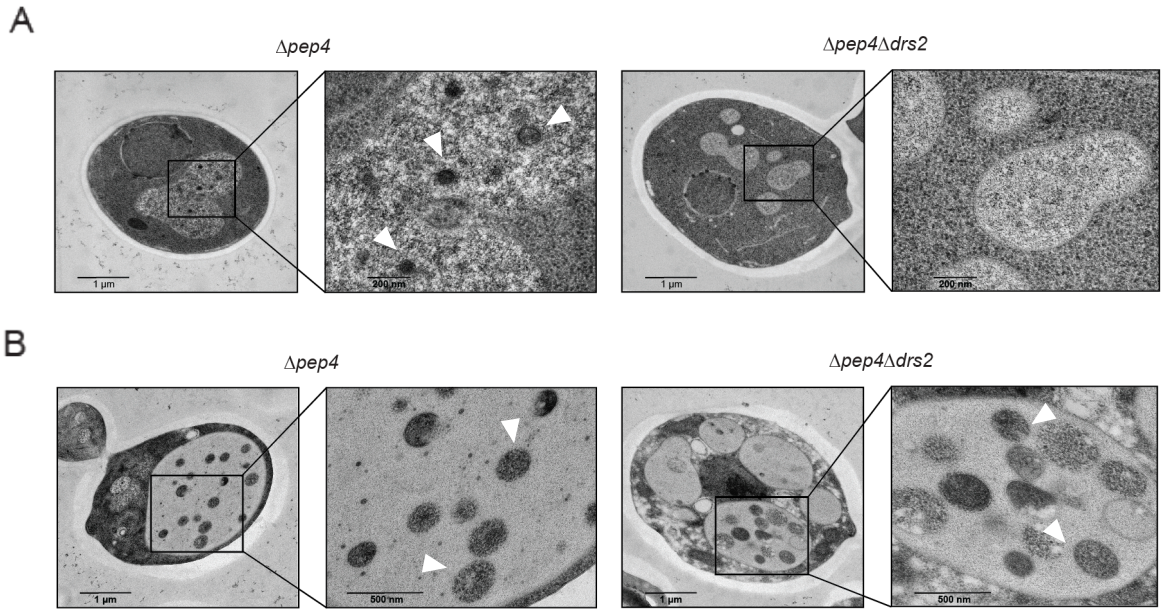


**Figure 4.14. Morphological studies of Cvt bodies in the vacuole. (A)** *Δpep4* and *Δpep4Δdrs2* cells were prepared for electron microscopy. Arrowheads point to mature Cvt bodies in higher magnification images. **(B)** *Δpep4* and *Δpep4Δdrs2* cells were treated with rapamycin (0.2 µg/ml) overnight to induce bulk autophagy and prepared for electron microscopy. Arrowheads point to autophagic bodies inside the vacuole in higher magnification images.

Instead, under starvation conditions *Δdrs2* cells present normal autophagic bodies. As shown in Figure 4.14_B, we detected autophagic bodies (arrowheads) in the vacuoles of both *Δpep4* and *Δpep4Δdrs2* strains after 15h treated with rapamycin. This is in accordance with my previous result showing that Drs2, similarly to Trs85, has a limited impact in non-selective autophagy but it is required for efficient selective autophagy of Ape1 mediated by the Cvt pathway.

To gain more precise insights of the role of Drs2, I continued with the study of the role of Drs2 in previous steps of the Cvt pathway using flurescence microscopy and Correlative Light-Electron Microscopy (CLEM). Labelling the vacuole with FM4-64 showed that in *Δdrs2* cells Ape1-GFP accumulate in large aggregates outside the lumen of this organelle. Fluorescent images were collected at different focal planes, allowing the 3D reconstruction of the entire cell volume. A three-dimensional representation showed large cytosolic aggregates of Ape1-GFP (Figure 4.15_A). This observation is in agreement with the EM analysis and pointed towards a critical role of Drs2 in early steps of the biogenesis of the Cvt vesicle.

CLEM allowed evaluating the ultrastructure of Cvt vesicles in cells lacking Drs2. I detected Ape1-GFP aggregates in around 2% of the 660 cells analyzed. 91.4% of these spots correlated with a membrane-free ribosome exclusion area (Figure 4.15_B). However, in none of the cells analyzed, the GFP signal correlated with a double-membrane vesicle as expected for a Cvt vesicle. It has been described that prApe1 is associated with Ty1 virus-like particles (VLPs) of around 35-50 nm diameter in the so called Cvt complex (Baba et al. 1997) (Yamasaki and Noda 2017). My results showed a correlation between

the GFP signal and amorphous structures, that in most of the cases were adjacent to an accumulation of spherical particles compatible with VLPs. These results denote the key role of Drs2 in the very early stages of the biogenesis of the Cvt vesicle, as is the case with TRAPPIII (Yorimitsu and Klionsky 2005) (Shirahama-Noda et al. 2013).

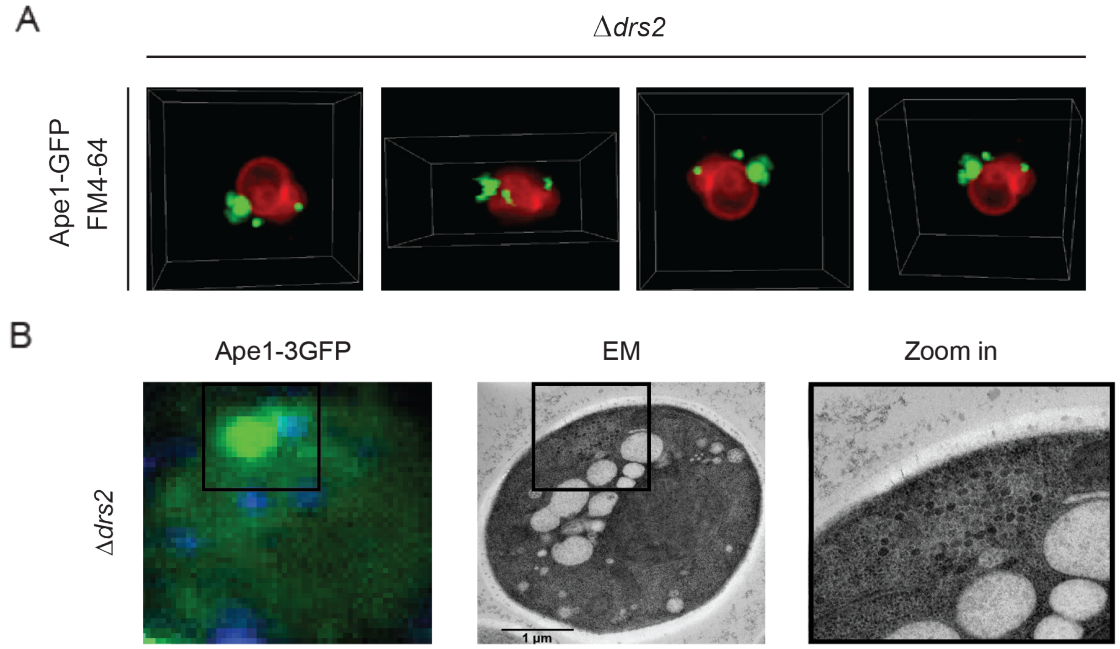


**Figure 4.15. Analysis of the Ape1 oligomers. (A)** 3D reconstruction of GFP tagged Ape1 and vacuole stained with the lipophilic dye FM4-64 in *Δdrs2* cells. Z-stacks of GFP and RFP pictures were taken in 250 nm incremental steps. **(B)** GFP tagged Ape1 (left), correlates with a membrane-free ribosome exclusion area mixed with a large number of Ty1 virus-like particles (middle). The zoom-in box shows a higher magnification of the black squares in the previous picture (1.59 µm wide).

I performed the EM and CLEM at the Prof. Tamotsu Yoshimori Lab (Osaka University, Japan) under the supervision of Dr. Maho Hamasaki.

#### 4.2.2.5. Drs2 is required for the arrival of TRAPPIII-Atg9 vesicles to the PAS

To keep investigating the precise role of Drs2 in the Cvt pathway, we decided to evaluate whether the lack of Drs2 specifically affects TRAPPIII function. To do that, I first assessed if the absence of the flippase could impact on the arrival of this complex at the PAS.

On this basis, I analyzed the colocalization between Trs85 and the PAS marker Atg11 in *Δatg1* and *Δatg1Δdrs2* cells (Figure 4.16). Atg1 has a critical role in early steps of the Cvt pathway allowing Cvt vesicle elongation. The abrogation of Atg1 leads to the accumulation of autophagy machinery at the PAS, what is often required to image some of its components (K. Suzuki et al. 2007). While in *Δatg1* cells I could observe the accumulation of Trs85 in Atg11 spots, *Δatg1Δdrs2* cells exhibited defective Trs85 transport to the PAS.

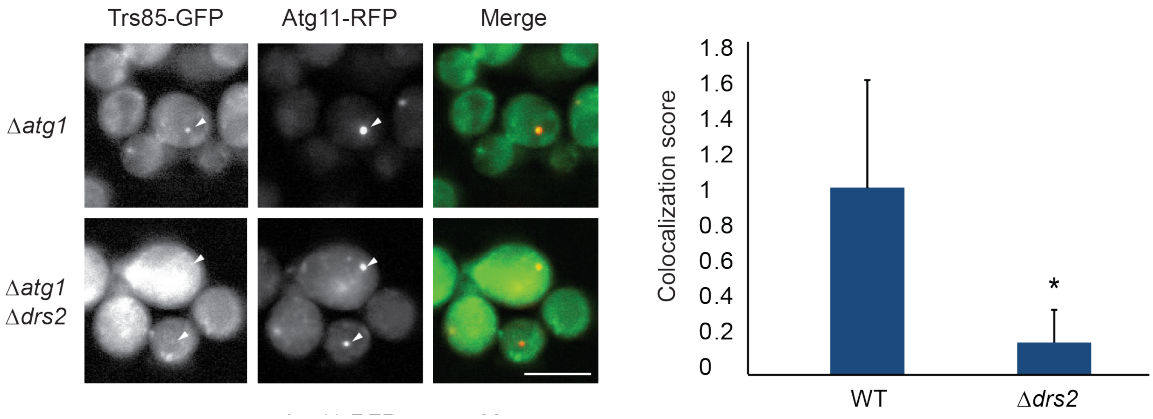


**Figure 4.16. Colocalization assay of TRAPPIII and the PAS.** Left, representative fluorescent images of GFP tagged Trs85 and RFP tagged Atg11 in *Δatg1* and *Δatg1Δdrs2* cells. Arrowheads point to Atg11-RFP spots. Scale bar, 5 µm. Right, quantification of the Atg11-RFP spots area colocalizing with Trs85-GFP, and normalized to the measurement of the *Δatg1* strain (Mean ± SD, p-value * < 0.05 t-test). Error bars indicate SD.

Interestingly, I noted higher intensity levels of both Trs85-GFP and Atg11-RFP in the strain lacking Drs2 due to an unknown reason. Nevertheless, this fact did not favour an increase in the colocalization between the two proteins, indicating that Drs2 is required for TRAPPIII to localize in the PAS.

Since it has been reported that TRAPPIII is essential to transport Atg9 vesicles to the PAS, I also analyzed whether Atg9 vesicles were still being translocated to the PAS in cells lacking Drs2 (Figure 4.17). Again, I observed higher intensity levels of Atg9-GFP in *Δdrs2* cells. But still, although Atg9 vesicles arrived and colocalized with Atg11 spots in wild type cells, they were hardly seen in the PAS of those cells where Drs2 was abrogated.

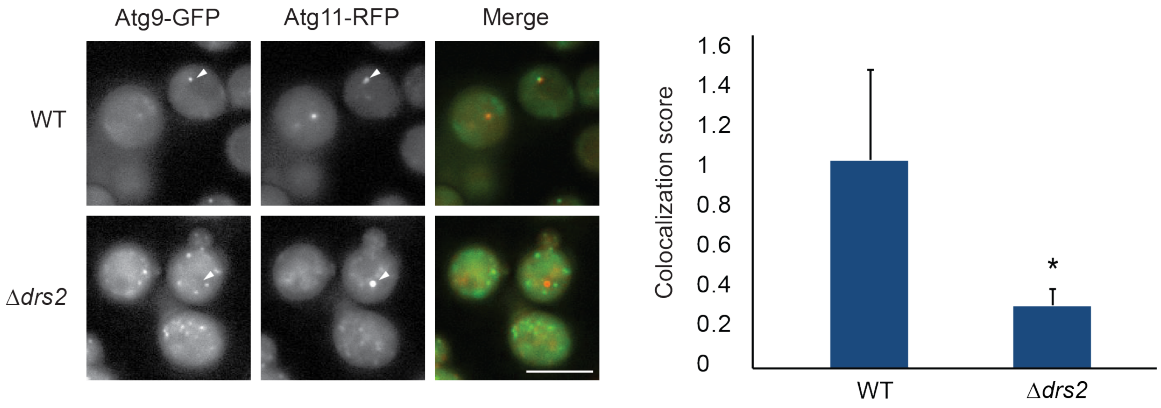


**Figure 4.17. Colocalization assay of Atg9 puncta and the PAS.** Left, representative fluorescent images of GFP tagged Atg9 and RFP tagged Atg11 and *Δdrs2* cells. Arrowheads point to Atg11-RFP spots. Scale bar, 5 µm. Right, quantification of the Atg11-RFP spots area colocalizing with Atg9-GFP, and normalized to the measurement of the wild type strain (Mean ± SD, p-value * < 0.05 t-test). Error bars indicate SD.

To further verify these results, I examined the influx of Atg9 vesicles to Ape1 structures. In line with the preceding experiments, a lower Atg9-Ape1 colocalization was detected in *Δdrs2* cells (Figure 4.18).

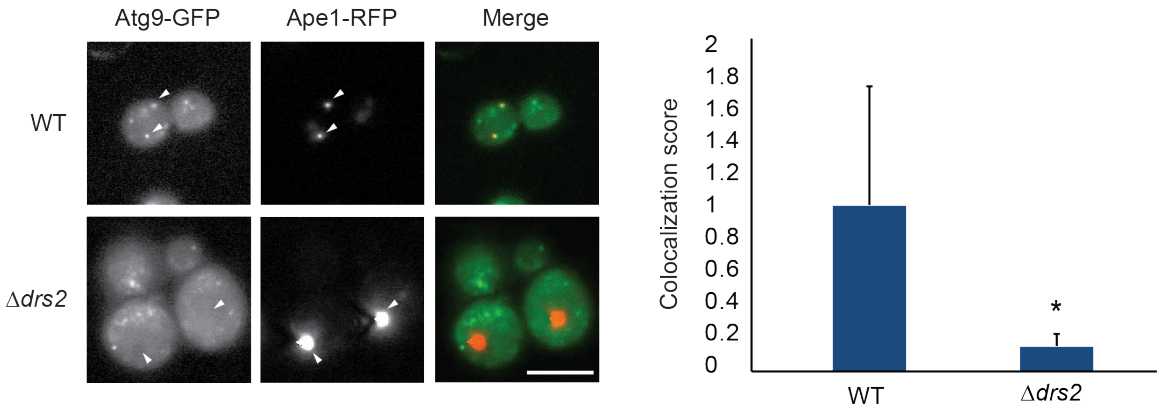


**Figure 4.18. Colocalization assay of Atg9 and Ape1 structures.** Left, representative fluorescent images of endogenous GFP tagged Atg9 and RFP tagged Ape1 expressed from plasmid in wild type and *Δdrs2* cells in the left and middle columns, respectively. Arrowheads point to Ape1-GFP spots. Scale bar, 5 µm. Right, quantification of the Ape1-RFP spots area colocalizing with Atg9-GFP, and normalized to the measurement of the wild type strain (Mean ± SD, p-value * < 0.05 t-test). Error bars indicate SD.

Altogether, these results reveal that Atg9 transport to the PAS mediated by TRAPIII during the Cvt pathway is abolished when Drs2 is not present. This fits with previous results indicating Drs2 is required for the proper biogenesis of the Cvt vesicle, and suggests that TRAPPIII is downstream of Drs2 function in this selective autophagy pathway.

To confirm Drs2 acts upstream TRAPPIII, I used yeast genetics. The oxysterol binding protein Kes1 is a negative regulator of vesicle budding in the TGN-early endosomal system by repressing Dnfs and Drs2 function. Furthermore, it is hyperactive in *Δdrs2* cells and previous studies have showed that deletion of KES1 suppresses some traffic defects caused by the lack of Drs2 (Villasmil, Bankaitis, and Mousley 2012) (Muthusamy et al. 2009). To better understand the role of Drs2 in the Cvt pathway, and so the interplay with TRAPPIII, we first combined the deletion of both DRS2 and KES1 to find out whether the abrogation of Kes1 could also compensate for the lack of Drs2 in the Cvt pathway. Therefore, we checked the processing of Ape1 in the *Δdrs2Δkes1* double mutant and, interestingly, we observed a recovery in the Ape1 maturation impairment typical from *Δdrs2* cells (Figure 4.19).

To ensure the lack of Kes1 can only compensate for the absence of Drs2, but Trs85 is still essential for the pathway, we also checked the Ape1 processing in *Δdrs2Δkes1Δtrs85* triple mutant. We observed a complete block in Ape1 maturation. This result, together with the previous experiments, confirms that TRAPPIII is downstream Drs2 function in the Cvt pathway.

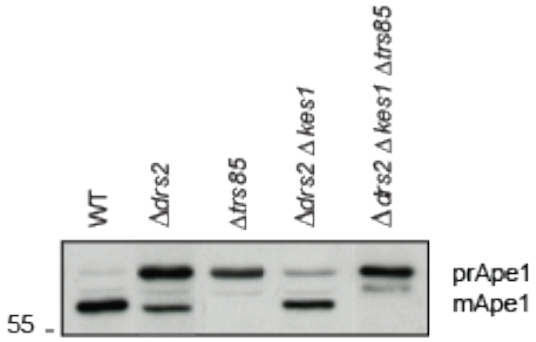


**Figure 4.19. Evaluation of the hierarchy between Trs85 and Drs2 in the Cvt pathway.** Wild type, *Δtrs85, Δdrs2, Δdrs2Δkes1 and Δdrs2Δkes1Δtrs85* strains were subjected to immunoblot analysis anti-Ape1. The upper band shows the not processed Ape1 (prApe1) and the lower band, the matured Ape1 (mApe1).

Given the relevance of Drs2 in the biogenesis of the Cvt pathway, we wondered whether the flippase localizes to the PAS to regulate TRAPPIII function. However, fluorescent microscopy could not reveal any colocalization of Drs2-GFP with the PAS marker Atg11-RFP in *Δatg1* cells (Figure 4.20).

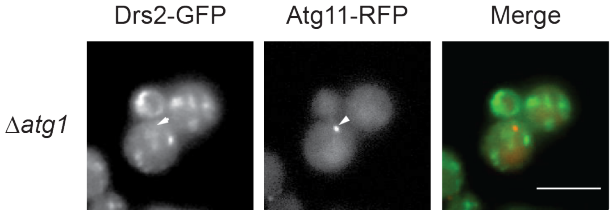


**Figure 4.20. Colocalization assay of Drs2 and the PAS.** Representative fluorescent images of endogenous GFP tagged Drs2 and RFP tagged Atg11 in *Δatg1* cells in the left and middle pictures, respectively. Arrowheads point to Atg11-RFP spots. Scale bar, 5 µm.

#### 4.2.2.6. Drs2 controls the delivery of Atg9 vesicles from the endocytic pathway

In yeast cells, Atg9-GFP can be observed in several punctate structures, which have been postulated to directly contribute to the delivery of lipids required for autophagosome formation. As described by the group of Prof. Ohsumi, the vast majority of these punctate structures are single-membrane vesicles highly mobile within the cytoplasm (Yamamoto et al. 2012).

In order to better understand the implication of Drs2 in the traffic of Atg9-GFP vesicles, we decided to quantify the dynamics of these vesicles by particle tracking experiments using a high-sensitivity microscopy system with high-temporal resolution (28 frames/second) (see Section 3.3.3-Materials and Methods). I collected >290 trajectories of Atg9-GFP puncta in wild type, *Δtrs85,* and *Δdrs2* cells and subjected them to the single-particle tracking analysis with ImageJ (see Section 3.3.4.3- Materials and Methods) (Figure 4.21). In accordance with Yamamoto et al, the mobility of Atg9-GFP puncta detected

in our wild type cells could be roughly classified into two groups: a larger population (86.2% of tracks) with higher mobility (mean speed 111.14 ± 35.5 nm/frame) that likely corresponds to freely diffusing vesicles in the cytoplasm and a smaller population (13.8% of tracks) with lower mobility (mean speed 34.23 ± 7.58 nm/frame). *Δdrs2* cells, in contrast, showed an opposite phenotype with a major population of Atg9-GFP particles (54.39% of tracks) with low mobility (mean speed 31.48 ± 12.5 nm/frame). This data indicates that Atg9-GFP accumulates in more static subcellular compartments upon Drs2 deletion, demonstrating that Drs2 regulates Atg9 traffic and suggesting that this flippase could be involved in Atg9-vesicles biogenesis. In *Δtrs85* cells, there is a population with high mobility similar to the one observed in wild type cells, but interestingly, we also observed that the population with lower mobility increases twice compared to wild type cells (26.6% of tracks with a mean speed of 40.95 nm/frame SD± 17). Since only very few Atg9 vesicles might be reaching the PAS according to the literature (Yamamoto et al. 2012), these results could reflect the traffic perturbation of those vesicles that cannot be correctly targeted in the Cvt pathway upon TRS85 deletion.

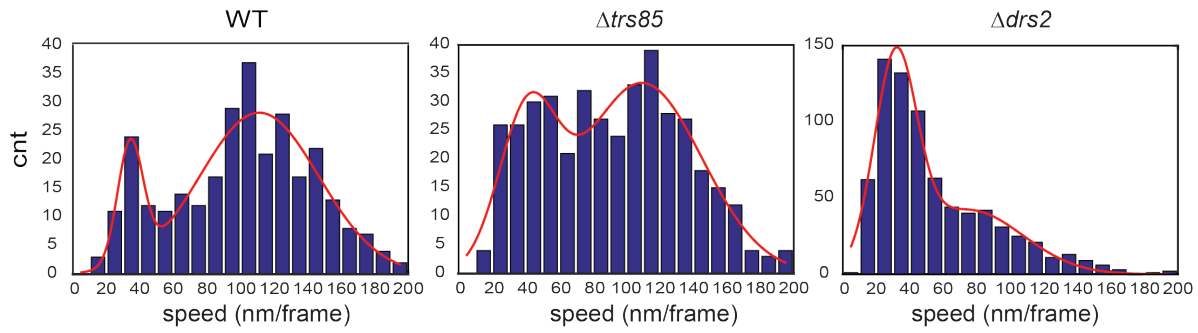


**Figure 4.21. Speed histograms of Atg9 puncta.** 2D time-lapse sequences of endogenous Atg9-3GFP were taken in wild type, *Δtrs85 and Δdrs2* cells at 28 frames per second. Individual spots were tracked with TrackMate (ImageJ) and fitted to Gaussian distributions. The y axis indicates the number of puncta belonging to each specific speed range represented in the x axis.

Since both TGN and endosomes have been postulated as reservoirs of Atg9 vesicles, we decided to analyze whether Atg9-GFP was been accumulated in these compartments. To this end, we used Sec7 as TGN marker and FM4-64 to label the endocytic pathway. While we observed the same colocaliztion rate between Atg9-GFP and Sec7-RFP in both wild type and *Δdrs2* cells, we detected a higher accumulation of Atg9-GFP in FM4-64 labelled structures in cells lacking Drs2. Altogether, these results imply that Drs2 is necessary for the delivery of Atg9 loaded vesicles from endocytic compartments (Figure 4.22).

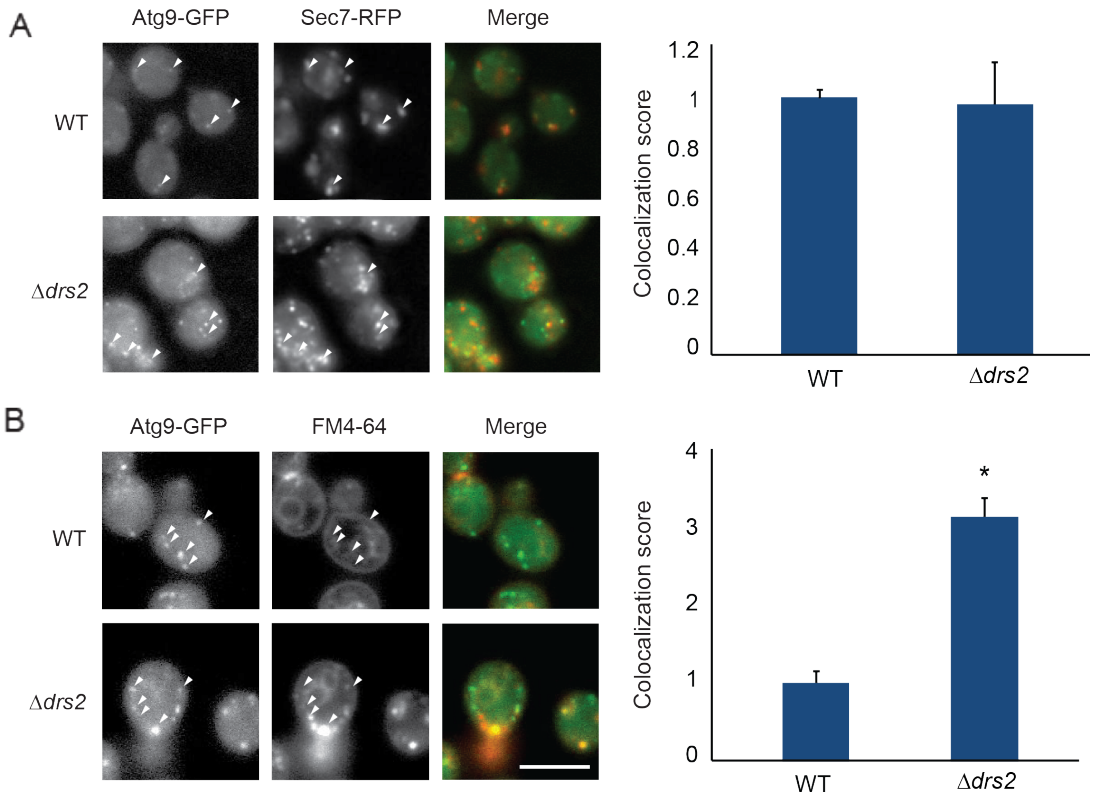


**Figure 4.22. Analysis of the accumulation of Atg9 vesicles on either the TGN or endocytic compartments. (A)** Left, representative fluorescent images of GPF tagged Atg9 and RFP tagged Sec7 in wild type and *Δdrs2* cells. Arrowheads point to Atg9-GFP pucta. Scale bar, 5 µm. Right, quantification of colocalization between Atg9-GFP and Sec7-RFP normalized to the measurement of the wild type strain (Mean ± SD, p-value * < 0.05 t-test). Error bars indicate STDEV. **(B)** Left, representative fluorescent images of endogenous Atg9-GFP or FM4-64 dye to label the endocytic pathway in wild type and *Δdrs2* cells. Arrowheads point to Atg9-GFP puncta. Scale bar, 5 µm. Right, quantification of colocalization between Atg9-GFP puncta and FM4-64 normalized to the measurement of the wild type strain (Mean ± SD, p-value * < 0.05 t-test). Error bars indicate SD.

### 4.2.2.7. Drs2 function in the Cvt pathway is a new role of the flippase

Drs2 is known to regulate a plethora of trafficking pathways. For this reason, we thought that Drs2 role in the transport of Atg9 vesicles was likely to be a consequence of one of its well-known functions, probably in endosomes. To evaluate if the role of Drs2 in the Cvt pathway is due to a canonical function of this protein, I used genetics to generate mutants that blocked specifically each of the pathways where Drs2 is involved (Figure 4.23). I exanimated Ape1 processing in *Δrcy1, Δapl4, Δapl5 and Δgga1Δgga2* cells. Rcy1 is required for the recycling pathway from early endosomes to TGN (Hua, Fatheddin, and Graham 2002). Apl4 (γ-adaptin) is an AP-1 subunit, necessary for the AP-1/clathrin trafficking between the TGN and early endosomes (Liu et al. 2008). Apl5 (δ-adaptin) functions in the AP-3 pathway, a route from TGN to the vacuole (Greg Odorizzi, Cowles, and Emr 1998). Finally, the GGA pathway (where Gga1 and Gga2 are involved), controls the traffic from TGN to late endosomes (Chen et al. 2006) (Hankins et al. 2015). Surprisingly, Ape1 processing was normal in all mutant cells tested.

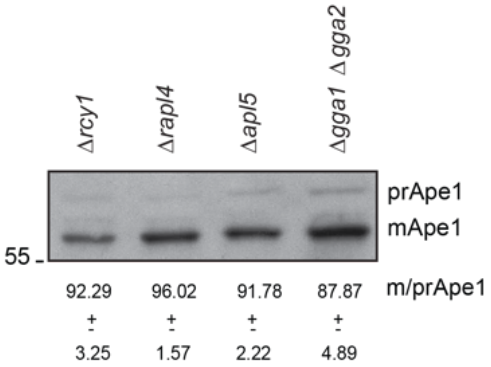


**Figure 4.23. Participation of Drs2 controlled-transport routes in Ape1 processing.** *Δrcy1, Δapl4, Δapl5* and *Δgga1Δgga2* cells were subjected to immunoblot analysis anti-Ape1. The upper band shows the not processed Ape1 (prApe1) and the lower band, the matured Ape1 (mApe1). Below, the quantification of the Ape1 processing (mApe1/(prApe+mApe1)) in 3 replicates ± SD.

These results open up two possibilities: either the defect in Atg9 vesicles transport in *Δdrs2* cells is caused by the multiple inhibition of these pathways or Atg9 vesicles transport is a new function of Drs2 that had not been described before. To discern between these two possibilities and better understand the role of Drs2 controlling Atg9 traffic, I analyzed yeast strains expressing Drs2 harbouring mutations that specifically target one of the multiple molecular mechanisms that have been reported to mediate the different functions of the flippase. We first evaluated the PS-flipping activity of Drs2. The mechanism of phospholipid recognition and translocation has been extensively studied with Drs2. Drs2 appears to be the primary PS flippase in the cell. Residues defining its substrates specificity have been mapped, and the substitution of QQ in the fourth transmembrane segment of Drs2 for GA has been shown to disrupt its ability to flip PS (Hankins et al. 2015). PS flip by Drs2 was shown to be critical for TGN-endosomes associated trafficking pathways and for the secretion of the dense class of exocytic vesicles from the TGN. However, our results indicated that loss of PS flipping does not appear to perturb the rate of Ape1 processing (Figure 4.24_A). To further confirm this, we checked the maturation of Ape1 in a strain lacking Cho1. CHO1-encodes the PS synthase (CDP-diacylglycerol:l-serine O-phosphatidyltransferase), an ER-associated enzyme that catalyzes the formation of PS. Hence, *Δcho1* cells are deficient in synthesis of PS (Choi, Han, and Carman 2010). Consistent with the results obtained for the Drs2-GA mutant, the *Δcho1* cells showed no defects in the maturation of Ape1 (Figure 4.24_B).

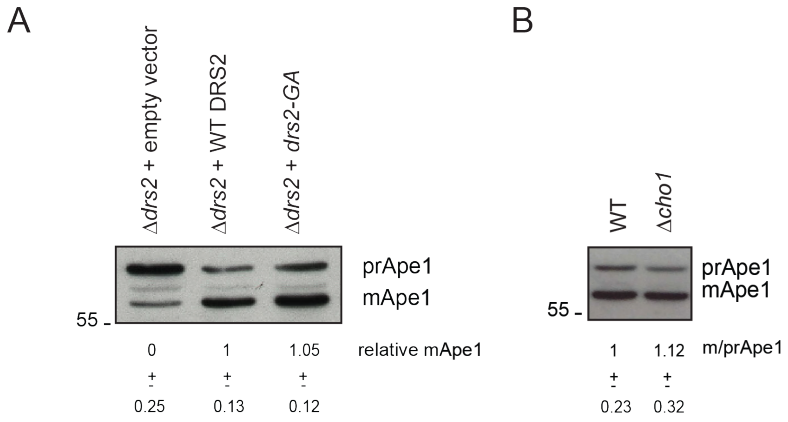


**Figure 4.24. Analysis of PS requirement for Ape1 processing**. **(A)** *Δdrs2* cells harbouring an empty vector, a vector coding for wild type DRS2 or *drs2*-GA were subjected to immunoblot analysis anti-Ape1. The upper band shows not processed Ape1 (prApe1) and the lower band, the matured Ape1 (mApe1). Below, the quantification of the Ape1 processing (mApe1/(prApe+mApe1)) in 3 replicates ± SD, normalized to *Δdrs2* cells harbouring wild type DRS2 plasmid. **(B)** wild type and *Δcho1* cells subjected to immunoblot analysis anti-Ape1. Below, the quantification of the Ape1 processing (mApe1/(prApe+mApe1)) in 2 replicates ± SD, normalized to the Ape1 processing in wild type cells.

Flipping PS is thought to be the main role of Drs2, but this flippase is also required for the formation of exocytic vesicles even in the absence of PS (*Δcho1* cells), suggesting PS is not required for some Drs2 functions (Natarajan et al. 2004). Furthermore, Drs2 plays crucial roles in trafficking by mediating PPIs. For instance, Arl1-Gea2-Drs2 multiprotein complex formation regulates the function of the Arf-like protein Arl, which in turn regulates multiple membrane trafficking pathways at the TGN (Tsai et al. 2013).

To explore if the role of Drs2 in the Cvt pathway is related to other known functions of the flippase and to further confirm it does not require PS translocation activity, I analyzed *Δdrs2* strains harbouring Drs2 plasmids with mutations in specific motifs of its sequence. Although some of these motifs have been widely studied and liked to Drs2 functions, others still need to be further characterize. Anyway, cold-sensitive assays have revealed that all of them make essential contributions to its function (See Figure 4.25_A).

Drs2 directly interacts with the ARF-GEF Gea2 through a short motif in its C-tail called GIM, which regulates its PS flippase activity. Furthermore, it is required to form the Arl1-Gea2-Drs2 multiprotein complex (Natarajan et al. 2009). *drs2*-ΔGIM plasmid restores cold-sensitive defect typical from *Δdrs2* cells (Liu et al. 2007). Adjacent to GIM, there is a region highly conserved among all, including mammalian, Drs2 homologues. Function of this conserved motif (CM) is still unknown, although a mutational analysis suggested that the CM is primarily responsible for the essential functions of the C-tail of Drs2 in protein trafficking (Chantalat 2004). *drs2*-ΔCM partially abrogated the ability of the *drs2* allele to complement the cold-sensitive growth defect of *Δdrs2* (Liu et al. 2007). Close to the end

of the C-tail, there are two NPFX(1,2)D motifs (hereafter referred to as NPF), which are potential endocytosis signals. However, they do not appear to perturb Drs2 function and *drs2*-ΔNPF restores cold-sensitive defect. On the other hand, the *drs2*-ΔGIMΔNPF double mutant has been suggested to be much more defective in Drs2 functions than either *drs2*-ΔNPF or *drs2*-ΔGIM single mutants, since it can not complement the cold-sensitive defect of *Δdrs2* cells (Liu et al. 2007). A truncation of the last 96 amino acids of the C-tail (ΔCT), what includes the NPF, CM and part of the GIM domain, markedly perturbs Drs2 function in protein traffic from the TGN (Liu et al. 2007). *drs2*-ΔCT plasmid can no restore cold-sensitive growth defect. Finally, a mutation in aspartate at position 560 by asparagine (D560N) completely blocks the ATPase activity of Drs2. *drs2*-D560N can no complement the cold-sensitive growth defect of *Δdrs2* cells either (Chantalat 2004).

All plasmids tested, regardless of the Drs2 mutant that they coded, could rescue the processing of Ape1 in *Δdrs2* cells (Figure 4.25_B), suggesting that Drs2 function in the Cvt pathway is not only a new role of the flippase but it is also mediated by a new molecular mechanism that had not been described before.

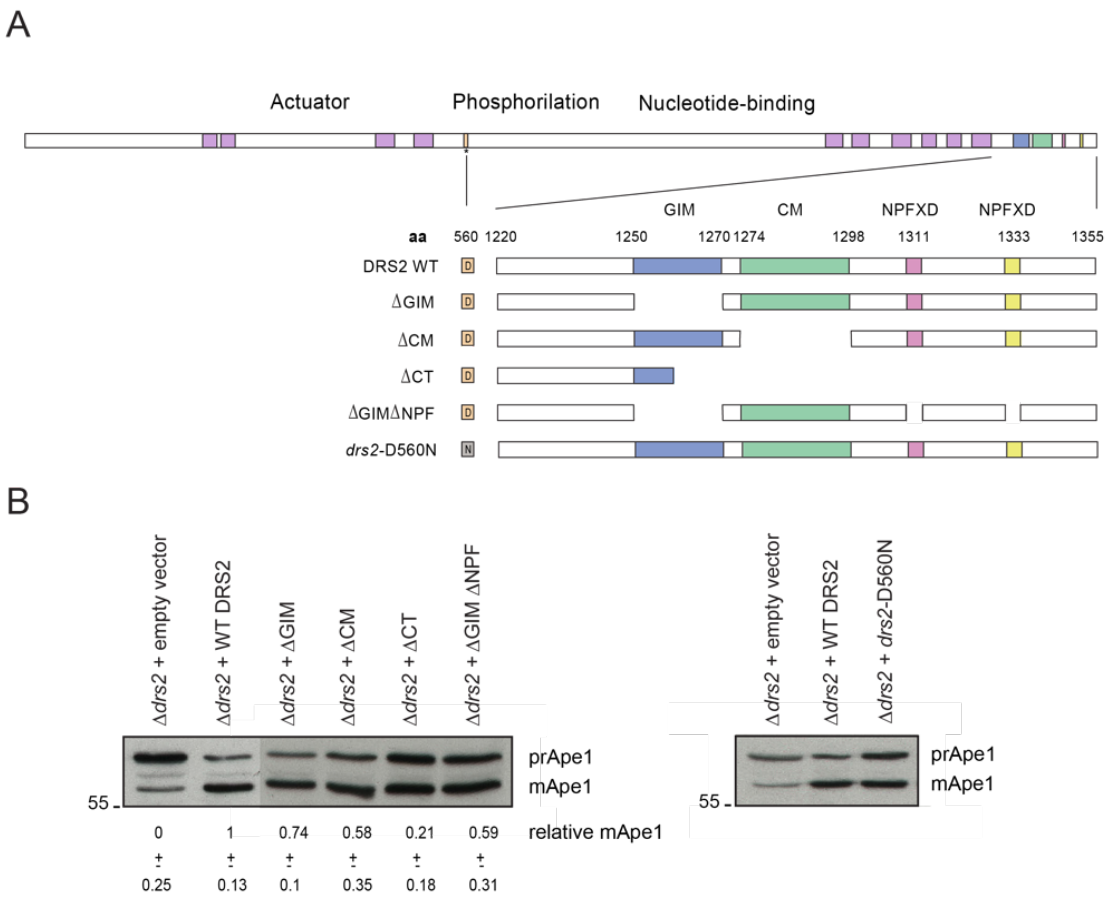


**Figure 4.25. Mutational analysis of Drs2 structural features (A)** Above, scheme of DRS2 gene and plasmids coding *drs2* mutants. **(B)** Immunoblot anti Ape1 in *Δdrs2* cells harbouring an empty vector, or plasmids coding for wild type DRS2 or mutant *drs2*. The upper band shows the not processed Ape1 (prApe1) and the lower band, the matured Ape1 (mApe1). Below, m/prApe1 quantification (mApe1/(prApe+mApe1)) in 3 replicates ± SD was normalized to *Δdrs2* cells harbouring wild type DRS2 plasmid (left panel).

### 4.2.2.8. TRAPPIII-Drs2 interaction is required for the Cvt pathway

Over the years of my PhD, we have been in contact with Prof. Todd Graham, who has a wide expertise in the field of P4-ATPases. In one of our talks we realized about the relevance of a sequence analysis he had carried out in the past. He found that Drs2 has an ISTTK motif in its N-terminal tail, which is located in a flexible loop upstream its first transmembrane domain (Figure 1.6-Introduction). Importantly, this motif also exists in Trs120, the specific subunit of TRAPPII. Although this observation did not attract the attention when was first discovered, it became an interesting point on the basis of my results. As explained in the Introduction, Trs120 has been suggested to interact with the Trs33 and Bet3 subunits of the TRAPPI when TRAPPII complex assembles (Yip, Berscheminski, and Walz 2010). Trs85 binds the TRAPPI complex through the Trs20 protein, so the binding site of both Bet3 and Trs33 subunits are free in the TRAPPIII complex. On the basis of this, we hypothesized that Drs2 could be substituting Trs120 when interacting with TRAPPIII through its ISTTK motif. Interestingly, Dnf1 and Dnf2, the other two flippases which also interact with TRAPPIII, conserve this ISTTK motif with one mismatch (Figure 4.26). This motif is the sole conserved motif in the N-terminal of P4-ATPases.

```
NEO1      -----------------PIELSD-------QHIEREIHPDTTPVYDRNRYVSNELSNAKY
DNF3      TILDRRRTFHSKDGRHIPIILDHNAIEYKQAATKRDGHLIDER--FNKPYCDNRITSSRY
DRS2      NYLDSRNKFNIKI-LFNRYILRKNVGDAEGNGEPRVIHINDSLANSSFGYSDNHISTTKY
DNF1      PGAINRA-QELRT-VYYNMPLPK--------------DMIDEEGNPIMQYPRNKIRTTKY
DNF2      SALQNRS-DELRT-VYYNLPLPE--------------DMLDEDGLPLAVYPRNKIRTTKY
                               * .              .           *  *.: .::*
```

**Figure 4.26. Alignment of yeast P4-ATPases by Clustal Omega.** A P4-ATPases protein sequences alignment revealed the ISTTK motif present in Drs2 is highly conserved among flippases (yellow highlight).

To test the potential TRAPPIII-Drs2 binding through the ISTTK motif of Drs2, we generated a plasmid with a Drs2 mutant where these five amino acids were substituted by AAAAA (*drs2*-5A). But as pervious control, we wanted to ensure that this *drs2*-5A mutant remains active in its canonical functions. Therefore, I evaluated the growth capability of *Δdrs2* cells expressing either Drs2 wild type or *drs2*-5A from respective plasmids at 18ºC. After two days, *Δdrs2* cells expressing *drs2*-5A grew as well as wild type cells and *Δdrs2* cells expressing Drs2 wild type from a plasmid at both 30ºC and 18ºC (Figure 4.27).

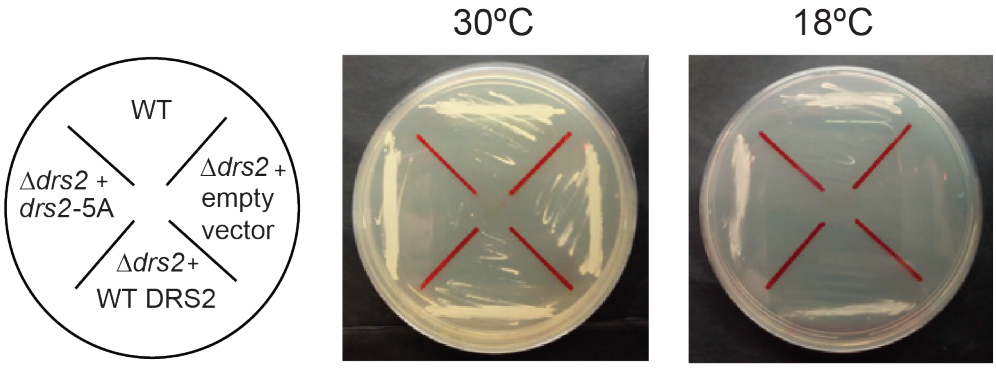

**Figure 4.27. Cold sensitive assay for cells expressing** ***drs2*****-5A.** wild type and *Δdrs2* cells expressing an empty vector, or plasmids coding for wild type DRS2 or *drs2*-5A mutant plasmids, were streaked onto YPD plates and left at 30ºC and 18ºC for two days.

Giving that *drs2*-5A can rescue the cold-sensitive phenotype of *Δdrs2* cells, we proceed to analyze the interaction between TRAPPIII and the *drs2*-5A mutant. Interestingly, PICT assays showed no association between them, suggesting the ISTTK motif in the N-terminal tail of Drs2 is required for the interaction with TRAPPIII (Figure 4.28).

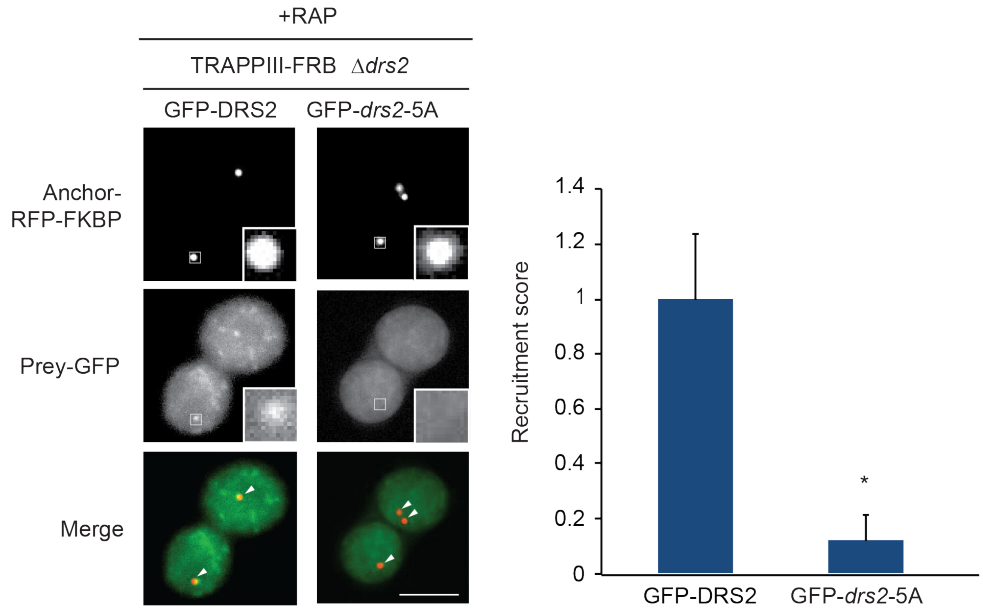


**Figure 4.28. Analysis of the interaction between TRAPPIII and** ***drs2*****-5A.** Trs85-Drs2 interaction is demonstrated in cells expressing Tub4-RFP-FKBP, Trs85-FRB and GFP-Drs2, but it is lost in cells expressing GFP-*drs2*-5A. Left, representative images of the PICT assay with Trs85-FRB as bait and either GFP-Drs2 or GFP-*drs2*-5A as prey. The RFP-tagged Tub4 and the GFP-tagged prey are shown in the upper and middle row, respectively. Overlap of RFP and GFP fluorescence (bottom row) indicates when the prey has been co-translocated with the bait to the anchoring platform (arrowheads). White squares show zoom of representative anchoring platforms. Zoom-in box is 0.9 µm wide. Scale bar, 5 µm. Right, quantification of the GFP-prey recruitment score, normalized to the measurement of the GFP-Drs2 (Mean ± SD, p-value * < 0.01 t-test). Error bars indicate SD.

Since this result support a model where Drs2 interacts directly with TRAPPIII, we decided to use the yeast two-hybrid system to further confirm this hypothesis. We first asked Hybrigenics to test the interaction between Trs85 and Drs2. However, they did not detect binding between both proteins, probably because they are supposed to be located at opposites sides of the complex. Later, we wanted to check the interaction between Drs2 and other subunits of the complex. Because Drs2 has several transmembrane domains, and the interaction is supposed to take place through a motif in its N-tail, we cloned only its cytosolic N-terminal tail (633 bp) into the plasmid pGADT7. On the other hand, we cloned two subunits of the TRAPP complex TRS31 and BET3, into the plasmid pGBKT7. Note that

TRS31 and BET3 are located to different sites of the elongated form of TRAPPIII (Figure 1.4 and 1.6-Introduction). Positive transformants were tested for growth on SD histidine$^-$, leucine$^-$ and tryptophan$^-$ plates at 23ºC. But again, we did not see positive results for the strains carrying the N-terminal tail of Drs2 and any of the two TRAPP core subunits (Figure 4.29).

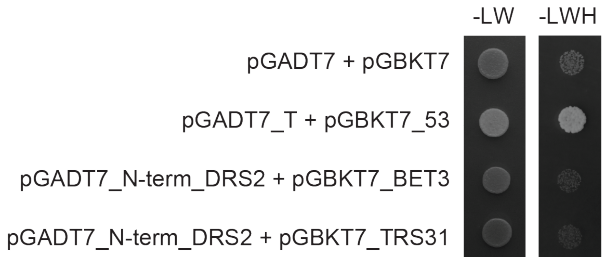


**Figure 4.29. Yeast two-hybrid assays between the N-terminal of Drs2 and Bet3 and Trs31 TRAPP complexes subunits.** N-terminal tail of Drs2 was fused with the Gal4 activation domain. Bet3 and Trs31 were fused with the DNA-binding domain. AH109 strains transformed with each vector were grown on SD lacking either leucine and tryptophan (-LEU -TRP) or histidine, leucine and tryptophan (-LEU-TRP-HIS) for 3 days. The empty vectors pGADT7 and pGBKT7 were used as negative control. pGADT7-T and pGBKT7-53, which encode the Gal4 AD fused with SV40 large T-antigen and the Gal4 DNA-BD fused with murine p53, respectively, were used as positive control.

We then decided to examine the localization of the N-terminal tail of Drs2 tagged to GFP in an effort to try to clarify these negative results. We used cells lacking Drs2 to introduce a vector coding for the N-terminal tail of Drs2 (aa 1-212) tagged to GFP. Surprisingly, we observed a majority of the construct was localizing to the plasma membrane (Figure 4.30). Thus, the negative results obtained by Yeast two-hybrid assay could be explained by the fact the N-terminal of Drs2 was trapped in the plasma membrane. This observation prevented us to continue investigating direct PPIs of the Drs2 N-terminal domain.

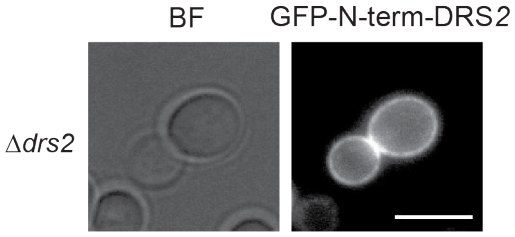


**Figure 4.30. Subcellular localization of the GFP-N-terminal domain of Drs2.** *Δdrs2* cells harbouring a pDDFGP_N-term_DRS2 (aa 1-212) were grown at 30ºC. After reaching an early logarithmic phase, they were shifted to 23ºC for 2 hours. Scale bar, 5 µm.

Given that the ISTTK motif in the N-terminal tail of Drs2 is required for the interaction with TRAPPIII, we wanted to determine whether this binding is actually necessary for the Cvt pathway. For this reason, I subsequently examined if mutating these five amino acids the Ape1 processing was affected. Importantly, the *Δdrs2* strain harbouring the *drs2*-5A mutant plasmid, showed the same Ape1 processing defect than the absence of the whole Drs2 (Figure 4.31).

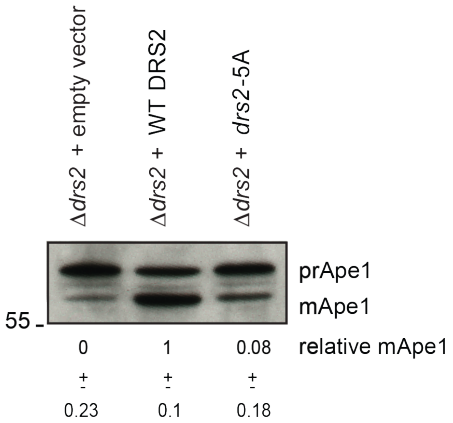


**Figure 4.31. Analysis of the requirement of the ISTTK motif for Ape1 processing.** *Δdrs2* cells harbouring an empty vector, wild type DRS2 or *drs2*-5A plasmids, were subjected to immunoblot analysis anti-Ape1. The upper band shows the not processed Ape1 (preApe1) and the lower band, the matured Ape1 (mApe1). Below, m/prApe1 quantification (mApe1/(prApe+mApe1)) in 3 replicates ± SD was normalized to *Δdrs2* cells harbouring wild type DRS2 plasmid.

Furthermore, I also checked Atg9 dynamics in these cells, and I observed the same phenotype that in cells lacking Drs2, with a major population of Atg9-GFP particles (50.23% of tracks) with low mobility (mean 27.77 ± 9.4 nm/frame) (Figure 4.32).

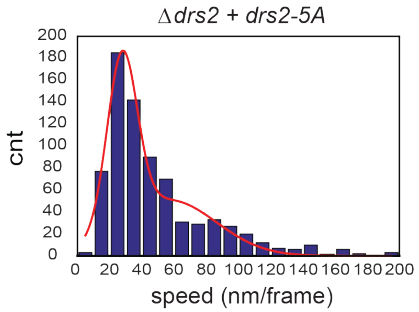


**Figure 4.32. Speed histogram of Atg9 vesicles.** 2D time-lapse sequences of endogenous Atg9-3GFP were taken at 28 frames per second in *Δdrs2* cells harbouring a *drs2-5A* plasmid. Individual puncta were tracked with TrackMate (ImageJ) and fitted to Gaussian distributions. The y axis indicates the number of puncta belonging to each specific range of speed represented in the x axis.

Altogether, our results indicate that the TRAPPIII-Drs2 interaction is necessary for the correct delivery of Atg9 vesicles from the endocytic compartments, a fundament step in the early steps of the Cvt pathway. Nonetheless, the mechanism that mediates TRAPPIII-Drs2 function has not yet been entirely characterized, but our work indicates it is a new function for the lipid flippase Drs2.

# 5. DISCUSSION

It is essential to maintain the proper distribution of lipids and proteins among the different organelles to ensure the correct functioning of the cell (Bonifacino and Glick 2004). Therefore, a wide variety of membrane trafficking mechanisms are constantly taking place to guarantee that the different processes the cell needs to execute are smoothly running at any time. These processes require the tight coordination of many components of the trafficking machinery. Among them, MTCs are essential players for vesicle trafficking, which together with other components of the transport machinery such as GTPases, specifically recognize the carrier vesicle and dock it to the appropriate acceptor membrane (Bröcker, Engelbrecht-Vandré, and Ungermann 2010). P4-ATPases, also play essential roles in cellular trafficking by maintaining phospholipid asymmetric distribution in cellular membranes (Lopez-Marques et al. 2014). P4-ATPases can deform membranes by creating an imbalance in the phospholipid number between the two leaflets, what in turn can induce the recruitment of the coating machinery as it has been described for BAR domains at the plasma membrane (Takada et al. 2018). However, P-type ATPases such as Na+/K+ ATPases have been shown to work as scaffolds for PPIs in an energy-independent manner (Liang et al. 2007), denoting that pump-independent functions are also remarkable to understand the mechanism of action of P-type ATPases. Interestingly, despite their fundamental role in membrane trafficking, no one had revealed a direct functional link between MTCs and P4-ATPases.

Our lab has developed the PICT technique, a fluorescence microscopy technique to analyse protein interactions in living cells. Although the amount of methodologies to study protein-protein interactions has raised in the last decades, most of these approaches have limitations that lead to miss the most challenging interactions. In *in vitro* techniques, complexes are usually difficult to purify and they are far from their physiological environment. Furthermore, those interactions that are transient or low abundant are hard to detect. On the other hand, *in vivo* approaches are usually technically challenging (i.e. Föster resonance energy transfer (FRET) and fluorescence cross-correlation spectroscopy) or non-quantitative (Y2H). Conventional Y2H may also incur a large number of false positives and negatives interactions, and hamper the study of transmembrane proteins interactions. Therefore, it is not surprising that interactions we have found in this study to be required for proper MTCs function have been overlooked in the past.

The PICT methodology, however, overcomes most of the limitations of conventional techniques. PICT allows the quantitative detection of low abundant, indirect or even transient protein interactions on both sides of the nuclear envelope under different physiological conditions or upon perturbations. For instance, in our recent publication we used PICT to investigate the levels of RNA polymerase I (Pol I) homodimers and the complexes formed between PolI and its activator factor Rrn3 in response to nutrient availability (Torreira et al. 2017). In this thesis, we have further automated PICT for high-

throughput studies to encompass the almost simultaneous analysis of several PPIs in conditions close to physiological.

Thanks to all this, the PICT experiments carried out in this thesis discovered an important interplay between MTCs and P4-ATPases that had not been reported before. We first performed a genome-wide screening to identify proteins based on the genetic interaction profile that are likely to be relevant for MTCs function (Figure 4.2). Importantly, a control experiment conducted with CORVET emphasizes the importance of implementing an *in silico* screen to increase the likelihood of finding new physical interactions.

From the 524 protein-protein interactions analyzed, we discover 9 new interactions involving MTCs, and 4 of them concerned P4-ATPases. This observation led us to expand the analysis between MTCs and P4-ATPases to determine the entire network of interactions between both families of trafficking machines. The outcome of the study resulted in the discovery of a network of 10 MTCs-P4-ATPases interactions (Figure 4.3). Dnf1 and Drs2 on the one hand, and GARP and TRAPPIII on the other hand, concentrate most of the interactions.

### 5.1. Interaction GARP-Dnf1

GARP showed interaction with three flippases: Dnf1, Dnf2 and Drs2 (Figure 4.3). We further investigated the interaction GARP-Dnf1 to get insight into the function of GARP in binding Dnf1. It had been previously advanced that GARP is required for the proper localization of Dnf1 and Dnf2 at the plasma membrane, as well as for the correct asymmetric distribution of PE between its inner and outer leaflets (Takagi et al. 2012b). However, as cells lacking GARP present various defects in the trafficking of vesicles, it had not been anticipated a direct role of this protein complex in controlling these flippases. Our experiments suggest for the first time the function of this complex in recycling Dnf1 from late endosomes to the TGN (Figures 4.5 and 4.6), what not only sheds light in the function of GARP in the transport of Dnf1 back to the plasma membrane, but also opens up the possibility of a wider function of GARP in tethering additional P4-ATPases to the TGN. Since we also detected the interaction between GARP and both Dnf2 and Drs2, it would be plausible to think that the function of GARP in recycling P4-ATPases is not only limited to Dnf1. However, if GARP is also necessary for the arrival of Dnf2 and Drs2 vesicles to the TGN needs to be examined. Furthermore, experiments to better characterize the interaction GARP-Dnf1 such as exploring whether it is either direct or indirect, are still missing.

### 5.2. Interaction TRAPPIII-Drs2

The interaction TRAPPIII-Drs2 has been the main target of my research. TRAPPIII has a critical role in selective autophagy, and to a less extent, in bulk autophagy. It interacts with Atg9 vesicles, another crucial component of both pathways, and together reach the PAS to initiate the Cvt vesicle or

autophagosome biogenesis. Atg9 trafficking has been investigated for decades due to its critical role in selective and non-selective autophagy. Many studies have focused on the function of Atg9 at the PAS, but the precise transport mechanism of this transmembrane protein is not completely clear (Shirahama-Noda et al. 2013), (Yamamoto et al. 2012), (Kakuta et al. 2012). On the other hand, Drs2 is a flippase essential for cell growth at low temperatures (Ripmaster, Vaughn, and Woolford 1993). Drs2 maintains PS membrane asymmetry and controls the exit of different vesicles from the TGN and early endosomes, functions that are in some cases regulated in response to temperature shifts. While the lack of Drs2 blocks the exit of dense class secretory vesicles and the traffic between TGN and early endosomes at all temperatures, the ALP and CPY pathway are only affected at temperatures lower than 23ºC (Gall et al. 2002), (Liu et al. 2008), (Chen et al. 2006) (Greg Odorizzi, Cowles, and Emr 1998). Since both, the TGN and early endosomes have been postulated as Atg9 reservoirs, and giving the interaction with TRAPPIII, we wondered whether Drs2 and TRAPPIII could be cooperating together in the Cvt pathway.

### 5.2.1. Role of Drs2 in the biogenesis of the Cvt vesicle at low temperatures

The strong inhibition of Ape1 processing in *Δdrs2* cells and the accumulation of prApe1-GFP in cytosolic clusters, together with the lack of mature Cvt vesicles in the vacuoles of *Δpep4Δdrs2* cells and the correlation of Ape1-GFP signal with amorphous structures, indicate major perturbations in the Cvt vesicle biogenesis when Drs2 is not present at 23ºC (Figures 4.8, 4.11, 4.14_A and 4.15_B).

However, the Western Blot assays anti-Ape1 showed a slight processing of Ape1 in the absence of Drs2 (Figure 4.8). By doing time course assays I ruled out the possibility that this mApe1 had been processed before the temperature shift (Figure 4.9). On the other hand, the analysis of the double mutant *Δdrs2Δatg19* indicated that Ape1 is not been processed through other mechanisms different than the Cvt pathway as it could be bulk autophagy (Figure 4.10). This means that the lack of Drs2 does not completely block the Cvt pathway at 23ºC although it is highly perturbed. It is likely that at lower temperatures the Cvt pathway would have been totally inhibited, but since *Δdrs2* cells are not viable below 21ºC, I preferred to conduct my experiments at 23ºC to prevent artifacts. Therefore, even though we could not detect Cvt bodies inside the vacuole of our EM experiments or prApe1 structures associate to double membranes in CLEM experiments (Figures 4.14_A and 4.15_B), we cannot discard that a small population of Cvt vesicles are eventually formed and fused with the vacuole. But, why is this low amount of Ape1 still being process? As mentioned, my experiments are done at a permissive temperature for *Δdrs2* cells, so we cannot exclude the possibility of a more exacerbated defect in Ape1 maturation at lower temperature. But it has also been shown that Drs2 controls some traffic routes together with other P4-ATPases (Hua, Fatheddin, and Graham 2002). It is possible that other flippases partially compensate for the lack of Drs2 in the Cvt pathway. It would be interesting to combine the deletion of DRS2 together with the deletion of other flipasses to explore this option. In line with this,

the recovery of Ape1 processing in *Δdrs2Δkes1* double mutant support this hypothesis (Figure 4.19) since some studies have revealed that the suppression of *Δdrs2* growth defects by *Δkes1* requires the presence of the Dnf1,2,3 P4-ATPases (Muthusamy et al. 2009). At the moment, we are trying to generate *Δkes1Δdrs2* strains lacking other P4-ATPases to evaluate this possibility.

### 5.2.2. Drs2 controls the function of TRAPPIII in the CVT pathway

Fluorescent microscopy assays showed that the lack of Drs2 sharply perturbs the arrival of both, TRAPPIII and Atg9 to the PAS, and also impairs the binding between Ape1 clusters and Atg9 (Figures 4.16, 4.17 and 4.18). Collectively, our results support a model where Drs2 is required for the arrival of both TRAPPIII and Atg9 to the PAS, what evidences a key role of Drs2 in the Cvt pathway by controlling TRAPPIII function. These data, together with the block of Ape1 processing in the *Δdrs2Δkes1Δtrs85* triple mutant cells (Figure 4.19), demonstrate that Drs2 is working upstream TRAPPIII in the Cvt pathway. If TRAPPIII was working upstream Drs2, Ape1 maturation should have been restored upon KES1 deletion as it did for the *Δdrs2Δkes1* double mutant.

Another striking point is that the defect on Ape1 maturation in cells lacking Drs2 is reverted when increasing the temperature (Figure 4.8). In line with this, our PICT experiments showed the interaction TRAPPIII-Drs2 also changes upon temperature shift (Figure 4.7). Indeed, the interaction detected was twice higher at 23ºC than at 37ºC. These differences could reflect a regulated increment in the TRAPPIII-Drs2 interaction in response to a particular cellular demand, i.e to specifically control the Cvt pathway at low temperatures. In addition, this does not exclude the possibility that the concerted action TRAPPIII-Drs2 regulates other processes independent of the Atg9 transport. Since both of them are located to the TGN, it is plausible they work together in other trafficking events in this organelle.

How the cell regulates the interaction between TRAPPIII and Drs2 and why Drs2 is specifically required for the proper functioning of the Cvt pathway at low temperatures, is not known. Either Drs2 might have no effect on the Cvt pathway at high temperatures, or its abrogation triggers other compensatory mechanism to support its function, just as Dnf1 has shown to do at 30ºC in the ALP and CPY pathways (Hua, Fatheddin, and Graham 2002).

Our experiments showed that TRAPPIII and Drs2 also interact in cells deprived of nutrients (Figure 4.12). Interestingly, the same mild defect in bulk autophagy was observed in both *Δdrs2* and *Δtrs85* cells, suggesting that the interplay between them also takes place in starved cells. It has been demonstrated that under starvation conditions, GARP bypasses TRAPPIII function in Atg9 vesicles transport. Furthermore, it has been suggested that COG complex may function as a tethering factor at the PAS under starvation conditions, allowing Atg9-containing vesicles to fuse with the expanding phagophore (Yen et al. 2010). Thus, TRAPPIII is dispensable for bulk autophagy and its abrogation causes minor defects in Ape1 processing of starved cells, what explain why the interplay TRAPPIII-

Drs2 is not as essential in this context as in selective autophagy (Shirahama-Noda et al. 2013). In line with this, we could observe the presence of autophagic bodies in the lumen of vacuoles of *Δdrs2Δpep4* cells and the processing of Ape1 only decreased about 27% in *Δdrs2* cells (Figures 4.13 and 4.14_B). A deeper study on the role of Drs2-TRAPPIII interplay in bulk autophagy is missing, but the present data favors a hypothesis where Drs2 would be regulating TRAPPIII function in both the Cvt pathway and bulk autophagy. However, since GARP cannot compensate the lack of TRAPPIII in the trafficking of Atg9 vesicles during Cvt pathway, *Δdrs2* cells grown in rich media present a larger defect in Ape1 processing than *Δdrs*2 cells deprived of nutrients. If Drs2 is also necessary to control TRAPPIII complex in other type of selective autophagy pathways would be interesting to determine in the future. Nevertheless, as TRAPPIII has been shown to be required for other types of autophagy such us pexophagy, I postulate that Drs2 would have a similar role (Nazarko et al. 2005).

### 5.2.3. Drs2 controls the traffic of Atg9 vesicles

When both, selective and non-selective autophagy pathways are activated, the *de novo* formation of a double membrane takes place engulfing the cargo that will be eventually degraded into the lumen of the vacuole (M. A. Lynch-Day and Klionsky 2010) (Su ab et al. 2015). The source of these membranes is still a topic of discussion and an unsolved question. Although several organelles have been reported as putative membrane sources of autophagosomal membranes in yeast, the molecular mechanisms of membrane supply remain unclear. Atg9 is a conserved transmembrane protein essential for Cvt vesicles and autophagosomes formation that exist in vesicles of around 30-40 nm in diameter (Yamamoto et al. 2012). These vesicles have been postulated to be a source of lipids for the membrane elongation. Actually, Yamamoto and colleagues reported that Atg9 vesicles become part of the autophagosomal membrane. Atg9 is continuously cycling between several puncta dispersed throughout the cytoplasm (the putative Atg9 reservoirs) and the PAS. However, there are contradicting reports about the nature of these reservoirs and the molecular mechanism that mediate the delivery of these vesicles to the PAS (Mari et al. 2010). In this thesis, we tried to bring a little more clarity to the biology of Atg9 vesicles, and the mechanisms that control their traffic in the cell.

As it had been reported before (Yamamoto et al. 2012), I found that in wild type cells the vast majority of Atg9 puncta belongs to a larger population (86.2% of tracks) with high mobility (mean speed 111.14 nm/frame ± 35.5) that likely corresponds to freely diffusing vesicles in the cytoplasm, while a smaller population (13.8% of tracks) exist in puncta of lower mobility (mean speed 34.23 ± 7.58 nm/frame) (Figure 4.21). I found that in *Δtrs85* cells the population of Atg9 puncta with reduced mobility increases twice (26.6% of tracks - mean speed 40.95 ± 17 nm/frame). This probably reflects the defect in Atg9 trafficking to the PAS in the Cvt pathway that has been previously demonstrated upon deletion of TRS85. This phenotype is further exacerbated in *Δdrs2* cells, where the larger population of Atg9 puncta present a lower mobility (mean speed 31.48 ± 12.5 nm/frame - 54.39% of tracks). This data implies

some similitudes between *Δtrs85* and *Δdrs2* mutant strains since both display a rising of the slow population compared to wild type cells. It goes in accordance with previous results where TRAPPIII and Drs2 seem to be cooperating together for the correct transport of Atg9 to the PAS. Nevertheless, in *Δdrs2* cells the phenotype is more striking than in *Δtrs85* since the quantity of highly immobile vesicle is almost double. This suggest Drs2 further regulates other Atg9 vesicle transport routes in the cell where TRAPPIII is not required. In fact, Drs2 interacts with other MTCs that have also been related to Atg9 transport in the cell such as TRAPPII, COG or GARP (Figure 4.3) (Zou et al. 2014) (Yen et al. 2010) (Reggiori et al. 2003) (Young and Tooze 2007). Therefore, it would be interesting to evaluate whether Drs2 also controls the Atg9 traffic mediated by these complexes.

Since Drs2 controls trafficking pathways in organelles that been postulated as Atg9 reservoirs, we hypothesized that this population of Atg9 puncta highly immobile found in *Δdrs2* cells could be trapped in some of these organelles. Based on our colocalization assays between Atg9 and TGN or structures of the endocytic pathway labelled with FM4-64, Drs2 is apparently involved in the biogenesis of Atg9 vesicles from endocytic compartments (Figure 4.22). However, FM4-64 is a lipophilic dye that can be used as a tracer for detecting endosome to vacuole membrane transport, so it labels different endocytic intermediates (Thomas A 1995). For a better characterization of the structures where Atg9 is stuck upon DRS2 deletion, a more detailed analysis with markers of specific endocytic compartments should be conducted.

Nonetheless, if this increase in the amount of Atg9 on endocytic compartments directly contributes to the defect caused by the lack of Drs2 in the Cvt pathway, needs to be further confirm. Yamamoto et al showed that only 3 Atg9 vesicles are targeted to the PAS in response to starvation conditions (Yamamoto et al. 2012). Assuming that this can be extrapolated to the Cvt pathway, very few vesicles reach the PAS compared to the total amount of Atg9 vesicles that exits in the cell. This makes difficult to track these GFP punctate to control where they actually come from.

In any case, and on the basis of my results, we can affirm that Drs2 affects the physiological movement of the Atg9 vesicles in cell, and *Δdrs2* cells show a more exacerbated phenotype in the slow population of Atg9 vesicles than *Δtrs85* cells. Therefore, it would be plausible to think in a scenario where Drs2 on the one hand controls the global traffic of Atg9 vesicles in the cells by favoring their biogenesis from endocytic structures, and on the other hand, has a specific function in the Cvt pathway by regulating the arrival of Atg9 vesicles to the PAS controlled by TRAPPIII, a function that becomes more relevant at low temperatures.

### 5.2.4. The role of Drs2 in the Cvt pathway is a new function of the flippase

Drs2 is required for budding of a dense class of exocytic vesicles from the TGN (Gall et al. 2002) and clathrin coated vesicles mediating vesicle transport between the TGN and early endosomes (Liu et al.

2008), two of the postulated Atg9 reservoirs. Furthermore, Drs2 is involved in the transport of vacuole cargos from the TGN (ALP and CPY pathways) (Chen et al. 2006) (Greg Odorizzi, Cowles, and Emr 1998). Due to the role of Drs2 in regulating such a wide range of trafficking pathways, Drs2 function in the Cvt pathway might have been connected to one of its canonical functions. However, when we analyzed mutants blocking specifically each of the pathways controlled by Drs2, results showed that none of these traffic pathways is actually relevant for the Cvt pathway (Figure 4.23). Moreover, the analysis of a yeast strain expressing a mutated Drs2 with perturbed PS-flippase activity showed no defects in Ape processing (Figures 4.24_A). In line with this, although flipping PS is thought to be the main role of Drs2, some trafficking events controlled by Drs2 has been shown to be PS-translocation independent (Natarajan et al. 2004). For instance, Alder-Barens et al. demonstrated that Drs2 together with Dnf3 translocate PE substrate in the low-density class of SVs budded from the TGN (Alder-Baerens et al. 2006). We then carried out a later analysis of *Δdrs2* cells harbouring Drs2 plasmids whit mutations in specific motifs of its sequence. Mutations in these motifs block multiple trafficking functions of the flippase. Surprisingly, all the strains showed a recovery in Ape1 processing, even the one where the whole ATPase activity of the flippase was abrogated (*Δdrs2* + *drs2*-D560N). Although Ape1 maturation was not completely restored in all the strains, this result demonstrates the effect of Drs2 in the Cvt pathway is due to an unknown mechanism of the protein (Figure 4.25_B).

Beyond their role in flipping phospholipids, which requires hydrolysis of ATP, P4-ATPases have been also related to some cellular functions that are ATP-independent (Van der Velden, Van de Graaf, and Klomp 2010). For example, Chantalat et al. demonstrated that only when two Drs2 mutants were expressed concomitantly, one capable to flip PS but with a C-tail truncation (which localizes properly) and a second one harboring a point mutation that abrogates the ATPase activity, the growth defect of *Δdrs2* cells at low temperatures could not be rescued. Either mutant expressed individually could not restore the cold-sensitive phenotype (Chantalat 2004). This indicates a dual function of Drs2 in the cell. On the one hand, the C-terminal truncation mutant provides the enzymatic transport function of Drs2, whereas the enzymatic dead mutant complements the pump-independent function of the C-terminal tail of Drs2.

In agreement with this, other P-type ATPases such as Na+/K+ ATPases have been shown to serve as scaffolds for protein-protein interactions in an energy-independent manner (Liang et al. 2007), what could be extrapolated for other P-type ATPases. Collectively, my results and the evidences found in the literature indicate that the role of Drs2 in the Cvt pathway that is ATPase independent.

### 5.2.5. ISTTK motif of Drs2 is required to bind TRAPPIII

The existence of the ISTTK sequence in the N-terminal flexible tail of Drs2 had been notice before, but this sequence had never been linked to any known function of Drs2. Furthermore, the ISTTK motif also exists in Trs120, a specific subunit of TRAPII. It has been postulated that in TRAPPII complex Trs120

binds Trs33 and Bet3 subunits (Yip, Berscheminski, and Walz 2010), while in TRAPPIII the binding site for Trs33 and Bet3 remain free (Tan et al. 2013). Whit all this in mind, I hypothesised that Drs2 could be replacing Trs120 when interacting when TRAPPIII through its ISTTK motif. To evaluate this possibility, we decided to conduct PICT assays with a Drs2 mutant lacking this amino acid sequence. Interestingly, after confirming by a cold-sensitive assay that the Drs2 mutant lacking the ISTTK motif remains partially active in *Δdrs2* cells (Figure 4.27), the PICT assay demonstrated that *drs2*-5A does no longer interact with TRAPPIII (Figure 4.28). This result goes in agreement with our hypothesis in which Drs2 would be substituting Trs120 when binding TRAPPIII complex, what is further supported by the fact the interaction between Trs85 and Drs2 full length could not be detected by MBMATE Y2H. MBMATE Y2H is a variant of Y2H designed to detect interactions with transmembrane protein, however since Trs85 and Drs2 are located at opposites sides of the complex according to our model, they would be too far from each other to interact.

Nevertheless, we cannot discard a scenario where Drs2 would be interacting with TRAPPIII through an intermediate. Unfortunately, I could not interpret the results from Y2H experiments because Drs2 N-term is bound to the plasma membrane (Figures 4.29 and 4.30). To clearly discern whether the interaction between TRAPPIII and Drs2 is direct or not, we should perform different approaches, such as MBMATE Y2H between Drs2 and subunits of the TRAPPIII complex including Trs33 and Bet3, or by crosslinking and mass spectrometry experiments.

In any case, our results evidence that ISTTK motif is required for the Drs2-TRAPPIII interaction whether it is direct or indirect. Furthermore, the *drs2*-5A mutant also showed the same defect in the processing of Ape1 than the whole absence of Drs2, in agreement with our hypothesis that TRAPPIII and Drs2 cooperate together in the Cvt pahway. Drs2 could be binding the TRAPPIII complex and operating as an intermediate to promote the connection between TRAPPIII and Atg9 vesicles, what is consistent with our previous results where Atg9 vesicles cannot reach the PAS in the absence of Drs2. Additionally, the ISTTK motif could be also mediating the interaction between Drs2 with the other MTCs that control other Atg9 trafficking routes in the cell (such as COG and GARP), since the *drs2*-5A mutant exhibited the same the Atg9 movement pattern than the Δ*drs2* strain.

Interestingly, the ISTTK motif is highly conserved among other P4ATP-ases, namely Dnf1 and Dnf2, which also interact with TRAPPIII (Figures 4.26 and 4.3). Therefore, it would be interesting to also asses if these flippases interact with TRAPIII trough the same motif. If so, it could provide another hint of a possible role of other Dnfs in compensating for the loss of function of Drs2 when KES1 is deleted. If by mutating the ISTTK motif in other Dnfs we could no longer recover the functioning of the Cvt pathway in Δ*drs2*Δ*kes1* cells, it would further support a model where the ISSTK motif is required for some P4-ATPases to interact with TRAPPIII and promote the binding between this complex and Atg9 vesicles.

Taking all together, it is likely the ISTTK motif has key implications in a multitude of trafficking pathways beyond the Cvt pahtway. Further investigations on this sequence could elucidate the molecular mechanism that regulates the network of interactions between MTCs and P4-ATPases described in this thesis.

### 5.3. Conclusions

Although in this thesis we have mainly focused on the study of the biological relevance of the interactions between GARP-Dnf1 and TRAPPIII-Drs2, it would be also interesting to further characterize the rest of associations detected between MTCs and P4-ATPases. Here, I have demonstrated Drs2 is not just a cargo of TRAPIII, but directly participates in the regulation of its function. Therefore, it is indispensable to keep working to elucidate the interplay between the rest of MTCs-P4-ATPases interactions, to better understand the molecular mechanism that controls the traffic routes mediated by this trafficking machinery in yeast cells. Furthermore, a deeper characterization on how yeast cells govern the trafficking pathways may also shed light in the traffic regulation of higher eukaryotic cells. Actually, Drs2 and TRAPPIII are conserved human cells, where they play similar functions that in yeast (Ramírez-Peinado et al. 2017) (Imai et al. 2016). Therefore, experiments conducted in human cells to study whether the interaction and interplay between TRAPPIII-Drs2 is conserved in higher eukaryotes, would be interesting.

In conclusion, my results provide new insight into the connected action between MTCs and P4-ATPases that could be extrapolated to mammalian cells. Future work will be essential to elucidate the molecular mechanism that govern all the interactions between MTCs and P4-ATPases to better understand the biological significance of these associations.

# 6. CONCLUSIONS

- The PICT method combined with a genome-wide screening based on genetic interactions discovered 10 new interactions with MTCs that are relevant for their function.
- MTCs and P4-ATPases establish an extended network of interactions.
- Dnf1 and Drs2 on the one hand, and GARP and TRAPPIII on the other hand, are central hubs of his network.
- GARP binds Dnf1 during the transport of the flippase from late endosomes to the TGN.
- Cell induces the interaction TRAPPIII-Drs2 in response to temperature decrease.
- Drs2, like Trs85, is required for the biogenesis of the Cvt vesicle at low temperature.
- Drs2 has the same mild contribution in non-selective autophagy as TRAPIII, suggesting they cooperate in the same pathway.
- Drs2 acts upstream TRAPIII in the Cvt pathway, controlling its function in the transport of Atg9 vesicles to the PAS.
- Drs2 regulates the dynamics of Atg9 vesicles, particularly in their release from endocytic compartments.
- The binding of Drs2 to TRAPPIII is required for the transport of Atg9 vesicles in the biogenesis of the Cvt vesicle. This is a new function for Drs2.
- The ISTTK motif is conserved among P4-ATPases and other proteins that bind MTCs.
- The ISTTK motif in the N-terminal tail of Drs2 is required for the interaction with TRAPPIII and for the role of Drs2 in the Cvt pathway.

## 7. BIBLIOGRAPHY


Alder-Baerens, Nele et al. 2006. "Loss of P4 ATPases Drs2p and Dnf3p Disrupts Aminophospholipid Transport and Asymmetry in Yeast Post-Golgi Secretory Vesicles." *Molecular biology of the cell* 17: 1632–42.

Amaravadi, Ravi, Alee C. Kimmelman, and Eileen White. 2016. "Recent Insights into the Function of Autophagy in Cancer." *Genes & development* 30(17): 1913–30. http://www.ncbi.nlm.nih.gov/pubmed/27664235.

Ammerer, G et al. 1986. "PEP4 Gene of Saccharomyces Cerevisiae Encodes Proteinase A, a Vacuolar Enzyme Required for Processing of Vacuolar Precursors." *Molecular and cellular biology* 6(7): 2490–99.

An, Chang Hyeok et al. 2012. "Frameshift Mutations of Vacuolar Protein Sorting Genes in Gastric and Colorectal Cancers with Microsatellite Instability." *Human Pathology* 43(1): 40–47. http://dx.doi.org/10.1016/j.humpath.2010.03.015.

Andersen, Jens P. et al. 2016. "P4-ATPases as Phospholipid Flippases-Structure, Function, and Enigmas." *Frontiers in Physiology* 7(JUL): 1–23.

Aoki, Takehiro et al. 2009. "Identification of the Neuroblastoma-Amplified Gene Product as a Component of the Syntaxin 18 Complex Implicated in Golgi-to-Endoplasmic Reticulum Retrograde Transport." *Molecular Biology of the Cell* 20(10): 2639–49.

Baba, Misuzu et al. 1997. "Two Distinct Pathways for Targeting Proteins from the Cytoplasm to the Vacuole/lysosome." *Journal of Cell Biology* 139(7): 1687–95.

Baba, Misuzu, Masako Osumi, and Yoshinori Ohsumi. 1995. "Analysis of the Membrane Structures Involved in Autophagy in Yeast by Freeze-Replica Method." *Cell Structure and Function* 20(6): 465–71. http://joi.jlc.jst.go.jp/JST.Journalarchive/csf1975/20.465?from=CrossRef.

Balderhaar, H. J. k., and C. Ungermann. 2013. "CORVET and HOPS Tethering Complexes - Coordinators of Endosome and Lysosome Fusion." *Journal of Cell Science* 126(6): 1307–16. http://jcs.biologists.org/cgi/doi/10.1242/jcs.107805.

Baldridge, R. D., and T. R. Graham. 2012. "PNAS Plus: Identification of Residues Defining Phospholipid Flippase Substrate Specificity of Type IV P-Type ATPases." *Proceedings of the National Academy of Sciences* 109(6): E290–98.

Baldridge, Ryan D, and Todd R Graham. 2013. "Two-Gate Mechanism for Phospholipid Selection and Transport by Type IV P-Type ATPases." *Proceedings of the National*

*Academy of Sciences of the United States of America* 110(5): E358-67. http://www.pubmedcentral.nih.gov/articlerender.fcgi?artid=3562821&tool=pmcentrez&rendertype=abstract.

Bassik, Michael C et al. 2013. "A Systematic Mammalian Genetic Interaction Map Reveals Pathways Underlying Ricin Susceptibility." 152(4): 909–22.

Bergamini, E., G. Cavallini, A. Donati, and Z. Gori. 2004. "The Role of Macroautophagy in the Ageing Process, Anti-Ageing Intervention and Age-Associated Diseases." *International Journal of Biochemistry and Cell Biology* 36(12): 2392–2404.

Bertipaglia, Chiara et al. 2016. "Higher-order Assemblies of Oligomeric Cargo Receptor Complexes Form the Membrane Scaffold of the Cvt Vesicle." *EMBO reports* 17(7): 1044–60. http://embor.embopress.org/lookup/doi/10.15252/embr.201541960.

Betin, Virginie M S et al. 2013. "Autophagy Facilitates Organelle Clearance during Differentiation of Human Erythroblasts: Evidence for a Role for ATG4 Paralogs during Autophagosome Maturation." *Autophagy* 9(6): 881–93.

Bilodeau, Patricia S. et al. 2003. "Vps27-Hse1 and ESCRT-I Complexes Cooperate to Increase Efficiency of Sorting Ubiquitinated Proteins at the Endosome." *Journal of Cell Biology* 163(2): 237–43.

Bilodeau, Patricia S., Jennifer L. Urbanowski, Stanley C. Winistorfer, and Robert C. Piper. 2002. "The Vps27p Hse1p Complex Binds Ubiquitin and Mediates Endosomal Protein Sorting." *Nature Cell Biology* 4: 534–39.

Bonifacino, Juan S., and Benjamin S. Glick. 2004. "The Mechanisms of Vesicle Budding and Fusion." *Cell* 116(2): 153–66.

Brocker, C. et al. 2012. "Molecular Architecture of the Multisubunit Homotypic Fusion and Vacuole Protein Sorting (HOPS) Tethering Complex." *Proceedings of the National Academy of Sciences* 109(6): 1991–96. http://www.pnas.org/cgi/doi/10.1073/pnas.1117797109.

Bröcker, Cornelia, Siegfried Engelbrecht-Vandré, and Christian Ungermann. 2010. "Multisubunit Tethering Complexes and Their Role in Membrane Fusion." *Current Biology* 20(21): 943–52.

Bryant, Nia J., Robert C. Piper, Sonja R. Gerrard, and Tom H. Stevens. 1998. "Traffic into the Prevacuolar/endosomal Compartment of Saccharomyces Cerevisiae: A VPS45-Dependent Intracellular Route and a VPS45-Independent, Endocytic Route." *European Journal of Cell Biology* 76(1): 43–52.

Bull, Laura N. et al. 1998. “A Gene Encoding a P-Type ATPase Mutated in Two Forms of Hereditary Cholestasis.” *Nature Genetics* 18(3): 219–24.

Burd, C G, P a Mustol, P V Schu, and S D Emr. 1996. “A Yeast Protein Related to a Mammalian Ras-Binding Protein, Vps9p, Is Required for Localization of Vacuolar Proteins.” *Molecular and cellular biology* 16(5): 2369–77.

Cabrera, Margarita et al. 2013. “Functional Separation of Endosomal Fusion Factors and the Class C Core Vacuole/endosome Tethering (Corvet) Complex in Endosome Biogenesis.” *Journal of Biological Chemistry* 288(7): 5166–75.

Cai, Yiying et al. 2008. “The Structural Basis for Activation of the Rab Ypt1p by the TRAPP Membrane Tethering Complexes.” 133(7): 1202–13.

Chang, Jean-Yun et al. 2015. “Trafficking Protein Particle Complex 6A Delta (TRAPPC6AΔ) Is an Extracellular Plaque-Forming Protein in the Brain.” *Oncotarget* 6(6): 3578–89. http://oncotarget.com/abstract/2876.

Chantalat, S. 2004. “The Arf Activator Gea2p and the P-Type ATPase Drs2p Interact at the Golgi in Saccharomyces Cerevisiae.” *Journal of Cell Science* 117(5): 711–22. http://jcs.biologists.org/cgi/doi/10.1242/jcs.00896.

Chen, Sophie et al. 2006. “Roles for the Drs2p-Cdc50p Complex in Protein Transport and Phosphatidylserine Asymmetry of the Yeast Plasma Membrane.” *Traffic* 7(11): 1503–17.

Choi, Hyeon Son, Gil Soo Han, and George M. Carman. 2010. “Phosphorylation of Yeast Phosphatidylserine Synthase by Protein Kinase A: Identification of SER46 and SER47 as Major Sites of Phosphorylation.” *Journal of Biological Chemistry* 285(15): 11526–36.

Churchman, L. S. et al. 2005. “Single Molecule High-Resolution Colocalization of Cy3 and Cy5 Attached to Macromolecules Measures Intramolecular Distances through Time.” *Proceedings of the National Academy of Sciences* 102(5): 1419–23. http://www.pnas.org/cgi/doi/10.1073/pnas.0409487102.

Churchman, L. Stirling, Henrik Flyvbjerg, and James A. Spudich. 2006. “A Non-Gaussian Distribution Quantifies Distances Measured with Fluorescence Localization Techniques.” *Biophysical Journal* 90(2): 668–71.

Conibear, Elizabeth, Jessica N. Cleck, and Tom H. Stevens. 2003. “Vps51p Mediates the Association of the GARP (Vps52/53/54) Complex with the Late Golgi T-SNARE Tlg1p.” *Molecular Biology of the Cell* 14(4): 1610–23.

Das, Amlan, and Wei Guo. 2011. “Rabs and the Exocyst in Ciliogenesis, Tubulogenesis, and

Beyond Amlan." 21(7): 383–386.

Delorme-axford, Elizabeth, Daniel J Klionsky, Elizabeth Delorme-axford, and Daniel J Klionsky. 2016. "A Missing Piece of the Puzzle : Atg11 Functions as a Scaffold to Activate Atg1 for Selective Autophagy A Missing Piece of the Puzzle : Atg11 Functions as a Scaffold to Activate Atg1 for Selective Autophagy." 8627(April): 11–14.

Dubuke, Michelle L., and Mary Munson. 2016. "The Secret Life of Tethers: The Role of Tethering Factors in SNARE Complex Regulation." *Frontiers in Cell and Developmental Biology* 4(May): 1–8. http://journal.frontiersin.org/Article/10.3389/fcell.2016.00042/abstract.

Dunn, William A et al. 2005. "Key Words Es Introduction Rib Identification of Genes." *Landes Bioscience* 1(2): 75–83.

Feinstein, Miora et al. 2014. "VPS53 Mutations Cause Progressive Cerebello-Cerebral Atrophy Type 2 (PCCA2)." *Journal of epidemiology & Community Health* 51(5): 303–8.

Von Filseck, Joachim Moser et al. 2015. "A Phosphatidylinositol-4-Phosphate Powered Exchange Mechanism to Create a Lipid Gradient between Membranes." *Nature Communications* 6.

Folmer, Dineke E. et al. 2009. "Differential Effects of Progressive Familial Intrahepatic Cholestasis Type 1 and Benign Recurrent Intrahepatic Cholestasis Type 1 Mutations on Canalicular Localization of ATP8B1." *Hepatology* 50(5): 1597–1605.

Furuta, Nobumichi et al. 2007. "Endocytic Recycling in Yeast Is Regulated by Putative Phospholipid Translocases and the Ypt31p/32p–Rcy1p Pathway." *Molecular Biology of the Cell* 18(1): 295–312.

Gall, Walter E. et al. 2002. "Drs2p-Dependent Formation of Exocytic Clathrin-Coated Vesicles in Vivo." *Current Biology* 12(18): 1623–27.

Gallego, Oriol et al. 2013. "Detection and Characterization of Protein Interactions In Vivo by a Simple Live-Cell Imaging Method." *PLoS ONE* 8(5): 1–6.

Gao, Lu et al. 2014. "Activation of Autophagy Protects against Cholestasis-Induced Hepatic Injury." *Cell and Bioscience* 4(1): 1–10.

Graham, Todd R. 2004. "Flippases and Vesicle-Mediated Protein Transport." *Trends in cell biology* 14(12): 670–77.

Guimaraes, Rodrigo Soares, Elizabeth Delorme-Axford, Daniel J. Klionsky, and Fulvio Reggiori. 2015. "Assays for the Biochemical and Ultrastructural Measurement of Selective and Nonselective Types of Autophagy in the Yeast Saccharomyces

Cerevisiae." *Methods* 75: 141–50. http://dx.doi.org/10.1016/j.ymeth.2014.11.023.

Hama, H, G G Tall, and B F Horazdovsky. 1999. "Vps9p Is a Guanine Nucleotide Exchange Factor Involved in Vesicle-Mediated Vacuolar Protein Transport." *The Journal of biological chemistry* 274(21): 15284–91.

Hamilton, Gillian et al. 2011. "Alzheimer's Disease Genes Are Associated with Measures of Cognitive Ageing in the Lothian Birth Cohorts of 1921 and 1936." *International Journal of Alzheimer's Disease* 2011: 1–11. http://www.hindawi.com/journals/ijad/2011/505984/.

Hanamatsu, Hisatoshi et al. 2014. "Interaction of the Phospholipid Flippase Drs2p with the F-Box Protein Rcy1p Plays an Important Role in Early Endosome to Trans-Golgi Network Vesicle Transport in Yeast." *The Journal of Biochemistry* 155(1): 51–62.

Hankins, H. M. et al. 2015. "Phosphatidylserine Translocation at the Yeast Trans-Golgi Network Regulates Protein Sorting into Exocytic Vesicles." *Molecular Biology of the Cell* 26(25): 4674–85. http://www.molbiolcell.org/cgi/doi/10.1091/mbc.E15-07-0487.

Heider, Margaret R et al. 2016. "Of the Yeast Exocyst Complex." 23(1): 59–66.

Hettema, Ewald H., Michael J. Lewis, Michael W. Black, and Hugh R.B. Pelham. 2003. "Retromer and the Sorting Nexins Snx4/41/42 Mediate Distinct Retrieval Pathways from Yeast Endosomes." *EMBO Journal* 22(3): 548–57.

Hinners, I. 2003. "Changing Directions: Clathrin-Mediated Transport between the Golgi and Endosomes." *Journal of Cell Science* 116(5): 763–71. http://jcs.biologists.org/cgi/doi/10.1242/jcs.00270.

Holthuis, J. C M, Benjamin J. Nichols, Sadhana Dhruvakumar, and H. R B Pelham. 1998. "Two Syntaxin Homologues in the TGN/endosomal System of Yeast." *EMBO Journal* 17(1): 113–26.

Hua, Zhaolin, Parvin Fatheddin, and Todd R. Graham. 2002. "An Essential Subfamily of Drs2p-Related P-Type ATPases Is Required for Protein Trafficking between Golgi Complex and Endosomal/Vacuolar System." *Molecular Biology of the Cell* 13: 3162–77.

Imai, Kenta et al. 2016. "Atg9A Trafficking through the Recycling Endosomes Is Required for Autophagosome Formation." *Journal of Cell Science* 129(20): 3781–91. http://jcs.biologists.org/lookup/doi/10.1242/jcs.196196.

Ishii, Yoshiyuki et al. 2013. "Identification of TRAPPC8 as a Host Factor Required for Human Papillomavirus Cell Entry." *PLoS ONE* 8(11).

Janke, Carsten et al. 2004. "A Versatile Toolbox for PCR-Based Tagging of Yeast Genes:

New Fluorescent Proteins, More Markers and Promoter Substitution Cassettes." *Yeast* 21(11): 947–62.

Jencks, William P. 1989. "Utilization of Binding Energy and Coupling Rules for Active Transport and Other Coupled Vectorial Processes." *Methods in Enzymology* 171: 145–64.

Jones, Sara, Christina Newman, Fengli Liu, and Nava Segev. 2000. "The TRAPP Complex Is a Nucleotide Exchanger for Ypt1 and Ypt31/32." *Molecular Biology of the Cell* 11(12): 4403–11.

Kakuta, Soichiro et al. 2012. "Atg9 Vesicles Recruit Vesicle-Tethering Proteins Trs85 and Ypt1 to the Autophagosome Formation Site." *Journal of Biological Chemistry* 287(53): 44261–69.

Kanki, Tomotake, and Daniel J. Klionsky. 2008. "Mitophagy in Yeast Occurs through a Selective Mechanism." *Journal of Biological Chemistry* 283(47): 32386–93.

Van Der Kant, Rik et al. 2015. "Characterization of the Mammalian CORVET and HOPS Complexes and Their Modular Restructuring for Endosome Specificity." *Journal of Biological Chemistry* 290(51): 30280–90.

Kelley, Ryan, and Trey Ideker. 2010. "Systematic Interpretation of Genetic Interactions Using Protein Networks." *Nat Biotechnol* 23(5): 1–14. http://www.pubmedcentral.nih.gov/articlerender.fcgi?artid=2814446&tool=pmcentrez&rendertype=abstract.

Kerr, Daniel J. et al. 2016. "Aberrant Hippocampal Atp8a1 Levels Are Associated with Altered Synaptic Strength, Electrical Activity, and Autistic-like Behavior." *Biochimica et Biophysica Acta - Molecular Basis of Disease* 1862(9): 1755–65. http://dx.doi.org/10.1016/j.bbadis.2016.06.005.

Khattak, Naureen, and Asif Mir. 2014. "Computational Analysis of TRAPPC9: Candidate Gene for Autosomal Recessive Non-Syndromic Mental Retardation." *CNS & Neurological Disorders - Drug Targets* 13(4): 699–711. http://www.eurekaselect.com/openurl/content.php?genre=article&issn=1871-5273&volume=13&issue=4&spage=699.

Kim, Jane J., Zhanna Lipatova, and Nava Segev. 2016. "TRAPP Complexes in Secretion and Autophagy." *Frontiers in Cell and Developmental Biology* 4(March): 1–10. http://journal.frontiersin.org/Article/10.3389/fcell.2016.00020/abstract.

Kim, Yeon Gil et al. 2006. "The Architecture of the Multisubunit TRAPP I Complex Suggests a Model for Vesicle Tethering." *Cell* 127(4): 817–30.

Klemm, Robin W. et al. 2009. “Segregation of Sphingolipids and Sterols during Formation of Secretory Vesicles at the Trans-Golgi Network.” *Journal of Cell Biology* 185(4): 601–12.

Klionsky, Daniel J. et al. 2003. “A Unified Nomenclature for Yeast Autophagy-Related Genes.” *Developmental Cell* 5(4): 539–45.

Kraft, Claudine, and Sascha Martens. 2012. “Mechanisms and Regulation of Autophagosome Formation.” *Current Opinion in Cell Biology* 24(4): 496–501. http://dx.doi.org/10.1016/j.ceb.2012.05.001.

Krick, R. et al. 2008. “Piecemeal Microautophagy of the Nucleus Requires the Core Macroautophagy Genes.” *Molecular Biology of the Cell* 19: 4492–4505.

Kühlbrandt, Werner. 2004. “Biology, Structure and Mechanism of P-Type ATPases.” *Nature reviews. Molecular cell biology* 5: 282–95.

Kushnirov, Vitaly V. 2000. “Rapid and Reliable Protein Extraction from Yeast.” *Yeast* 16(9): 857–60.

Lees, Joshua A., Calvin K. Yip, Thomas Walz, and Frederick M. Hughson. 2010. “Molecular Organization of the COG Vesicle Tethering Complex.” *Nature Structural and Molecular Biology* 17(11): 1292–97.

Lenoir, Guillaume, Patrick Williamson, Catheleyne F. Puts, and Joost C.M. Holthuis. 2009. “Cdc50p Plays a Vital Role in the ATPase Reaction Cycle of the Putative Aminophospholipid Transporter Drs2p.” *Journal of Biological Chemistry* 284(27): 17956–67.

Levano, Kelly et al. 2012. “Atp8a1 Deficiency Is Associated with Phosphatidylserine Externalization in Hippocampus and Delayed Hippocampus- Dependent Learning Kelly.” *Journal of neurochemistry* 120(2): 302–13.

Lewis, M. J. et al. 2000. “Specific Retrieval of the Exocytic SNARE Snc1p from Early Yeast Endosomes.” *Molecular Biology of the Cell* 11(1): 23–38. http://www.molbiolcell.org/cgi/doi/10.1091/mbc.11.1.23.

Liang, Man et al. 2007. “Identification of a Pool of Non-Pumping Na/K-ATPase.” *Journal of Biological Chemistry* 282(14): 10585–93.

Lipatova, Z. et al. 2012. “Regulation of Selective Autophagy Onset by a Ypt/Rab GTPase Module.” *Proceedings of the National Academy of Sciences* 109(18): 6981–86. http://www.pnas.org/cgi/doi/10.1073/pnas.1121299109.

Liu, Ke, Zhaolin Hua, Joshua A. Nepute, and Todd R. Graham. 2007. “Yeast P4-ATPases Drs2p and Dnf1p Are Essential Cargos of the NPFXD/Sla1p Endocytic Pathway.”

*International Journal of Biological Sciences* 18: 487–500.

Liu, Ke, Kavitha Surendhran, Steven F. Nothwehr, and Todd R. Graham. 2008. "P4-ATPase Requirement for AP-1/Clathrin Function in Protein Transport from the Trans-Golgi Network and Early Endosomes." *Molecular Biology of the Cell* 19: 3526–35.

Lopez-Marques, Rosa L., Lisa Theorin, Michael G. Palmgren, and Thomas Günther Pomorski. 2014. "P4-ATPases: Lipid Flippases in Cell Membranes." *Pflugers Archiv European Journal of Physiology* 466(7): 1227–40.

Lynch-Day, Melinda A., and Daniel J. Klionsky. 2010. "The Cvt Pathway as a Model for Selective Autophagy." *FEBS Letters* 584(7): 1359–66. http://dx.doi.org/10.1016/j.febslet.2010.02.013.

Lynch-Day, Melinda, and Daniel J Klionsky. 2011. "The Cvt Pathway as a Model for Selective Autophagy." *FEBS letters* 584(7): 1359–66.

Mari, Muriel et al. 2010. "An Atg9-Containing Compartment That Functions in the Early Steps of Autophagosome Biogenesis." *Journal of Cell Biology* 190(6): 1005–22.

van der Mark, Vincent A., Ronald P.J. Oude Elferink, and Coen C. Paulusma. 2013. "P4 ATPases: Flippases in Health and Disease." *International Journal of Molecular Sciences* 14(4): 7897–7922.

Mccarthy, Shane E et al. 2014. "De Novo Mutations in Schizophrenia Implicate Chromatin Remodeling and Support a Genetic Overlap with Autism and Intellectual Disability." 19(6): 652–58.

Mesmin, Bruno et al. 2013. "XA Four-Step Cycle Driven by PI(4)P Hydrolysis Directs sterol/PI(4)P Exchange by the ER-Golgi Tether OSBP." *Cell* 155(4).

Mizushima, Noboru, Tamotsu Yoshimori, and Yoshinori Ohsumi. 2011. "The Role of Atg Proteins in Autophagosome Formation." *Annual Review of Cell and Developmental Biology* 27: 107–32.

Müller-Reichert, Müller. 2012. *Correlative Light and Electron Microscopy*. eds. Müller Müller-Reichert and Paul Verkade.

Murthy, Mala, Dan Garza, Richard H. Scheller, and Thomas L. Schwarz. 2003. "Mutations in the Exocyst Component Sec5 Disrupt Neuronal Membrane Traffic, but Neurotransmitter Release Persists." *Neuron* 37(3): 433–47.

Muthusamy, Baby-Periyanayaki et al. 2009. "Control of Protein and Sterol Trafficking by Antagonistic Activities of a Type IV P-Type ATPase and Oxysterol Binding Protein Homologue." *Molecular Biology of the Cell* 20: 2920–31.

Natarajan, Paramasivam et al. 2009. "Regulation of a Golgi Flippase by Phosphoinositides

and an ArfGEF." 11(12): 1421–26.

Natarajan, Paramasivam, Jiyi Wang, Zhaolin Hua, and Todd R Graham. 2004. "Drs2p-Coupled Aminophospholipid Translocase Activity in Yeast Golgi Membranes and Relationship to in Vivo Function." *Proceedings of the National Academy of Sciences of the United States of America* 101(29): 10614–19.

Nazarko, Taras Y. et al. 2005. "Trs85 Is Required for Macroautophagy, Pexophagy and Cytoplasm to Vacuole Targeting in Yarrowia Lipolytica and Saccharomyces Cerevisiae." *Autophagy* 1(1): 37–45.

Nickas, M E, and M P Yaffe. 1996. "BRO1, a Novel Gene That Interacts with Components of the Pkc1p-Mitogen-Activated Protein Kinase Pathway in Saccharomyces Cerevisiae." *Molecular and cellular biology* 16(6): 2585–93. http://www.ncbi.nlm.nih.gov/pubmed/8649366%5Cnhttp://www.pubmedcentral.nih.gov/articlerender.fcgi?artid=PMC231249.

Noda, Nobuo N., and Fuyuhiko Inagaki. 2015. "Mechanisms of Autophagy." *Annual Review of Biophysics* 44: 101–22.

Noda, Takeshi et al. 2000. "Apg9p/Cvt7p Is an Integral Membrane Protein Required for Transport Vesicle Formation in the Cvt and Autophagy Pathways." *Journal of Cell Biology* 148(3): 465–79.

Odorizzi, G. 2003. "Bro1 Is an Endosome-Associated Protein That Functions in the MVB Pathway in Saccharomyces Cerevisiae." *Journal of Cell Science* 116(10): 1893–1903. http://jcs.biologists.org/cgi/doi/10.1242/jcs.00395.

Odorizzi, Greg, Christopher R. Cowles, and Scott D. Emr. 1998. "The AP-3 Complex: A Coat of Many Colours." *Trends in cell biology* 8(7): 282–88.

Onat, Onur Emre et al. 2013. "Missense Mutation in the ATPase, Aminophospholipid Transporter Protein ATP8A2 Is Associated with Cerebellar Atrophy and Quadrupedal Locomotion." *European Journal of Human Genetics* 21(3): 281–85. http://dx.doi.org/10.1038/ejhg.2012.170.

Ooi, Siew Loon, Daniel D Showmaker, and Jef D Boeke. 2003. "DNA Helicase Gene Interaction Network Defined Using Synthetic Lethality Analyzed by Microarray." *Nature Genetics2* 35(3): 277–86.

Paulusma, Coen C., and Ronald P J Oude Elferink. 2010. "P4 ATPases - The Physiological Relevance of Lipid Flipping Transporters." *FEBS Letters* 584(13): 2708–16. http://dx.doi.org/10.1016/j.febslet.2010.04.071.

Paumet, F., V. Rahimian, and J. E. Rothman. 2004. "The Specificity of SNARE-Dependent

Fusion Is Encoded in the SNARE Motif." *Proceedings of the National Academy of Sciences* 101(10): 3376–80. http://www.pnas.org/cgi/doi/10.1073/pnas.0400271101.

Picco, Andrea et al. 2017. "The In Vivo Architecture of the Exocyst Provides Structural Basis for Exocytosis." *Cell* 168(3): 400–412.e18.

Piper, Robert C., EA Whitters, and Tom H. Stevens. 1994. "Yeast Vps45p Is a Sec1p-like Protein Required for the Consumption of Vacuole-Targeted, Post-Golgi Transport Vesicles." *European Journal of Human Genetics* 65(2): 305–18.

Pomorski, Thomas Günther et al. 2003. "Drs2p-Related P-Type ATPases Dnf1p and Dnf2p Are Required for Phospholipid Translocation across the Yeast Plasma Membrane and Serve a Role in Endocytosis." *Molecular Biology of the Cell* 14(February): 2372–84.

Protopopov, Vladimir, Brinda Govidan, Peter Novick, and Jeffrey E. Gerst. 1993. "Homologs of the synaptobrevin/VAMP Family of Synaptic Vesicle Proteins Function on the Late Secretory Pathway in S. Cerevisiae." *Cell* 74(5): 855–61.

Puts, Catheleyne F. et al. 2012. "Mapping Functional Interactions in a Heterodimeric Phospholipid Pump." *Journal of Biological Chemistry* 287(36): 30529–40.

Quinones, Mariana Morales, Jared T. Winston, and Per E. Stromhaug. 2012. "Propeptide of Aminopeptidase 1 Protein Mediates Aggregation and Vesicle Formation in Cytoplasm-to-Vacuole Targeting Pathway." *Journal of Biological Chemistry* 287(13): 10121–33.

Ramírez-Peinado, Silvia et al. 2017. "TRAPPC13 Modulates Autophagy and the Response to Golgi Stress." *Journal of Cell Science* 130(14): 2251–65.

Ravikumar, Brinda et al. 2004. "Inhibition of mTOR Induces Autophagy and Reduces Toxicity of Polyglutamine Expansions in Fly and Mouse Models of Huntington Disease." *Nature Genetics* 36(6): 585–95.

Reggiori, Fulvio et al. 2003. "Vps51 Is Part of the Yeast Vps Fifty-Three Tethering Complex Essential for Retrograde Traffic from the Early Endosome and Cvt Vesicle Completion." *Journal of Biological Chemistry* 278(7): 5009–20.

Ren, Yi et al. 2009. "A Structure-Based Mechanism for Vesicle Capture by the Multisubunit Tethering Complex Dsl1." *Cell* 139(6): 1119–29. http://dx.doi.org/10.1016/j.cell.2009.11.002.

———. 2010. "NIH Public Access." 139(6): 1119–29.

Rich, Kathryn A., Burkett Chelsea, and Paul Webster. 2003. "Cytoplasmic Bacteria Can Be Targets for Autophagy." *Cellular Microbiology* 5(7): 455–68.

Riekhof, Wayne R. et al. 2007. "Lysophosphatidylcholine Metabolism in Saccharomyces Cerevisiae: The Role of P-Type ATPases in Transport and a Broad Specificity

Acyltransferase in Acylation." *Journal of Biological Chemistry* 282(51): 36853–61.

Ripmaster, T L, G P Vaughn, and J L Woolford. 1993. "DRS1 to DRS7, Novel Genes Required for Ribosome Assembly and Function in Saccharomyces Cerevisiae." *Molecular and cellular biology* 13(12): 7901–12. http://www.pubmedcentral.nih.gov/articlerender.fcgi?artid=364862&tool=pmcentrez&rendertype=abstract.

Russel, Daniel et al. 2012. "Putting the Pieces Together: Integrative Modeling Platform Software for Structure Determination of Macromolecular Assemblies." *PLoS Biology* 10(1): 1–5.

Sacher, Michael et al. 2001. "TRAPP I Implicated in the Specificity of Tethering in ER-to-Golgi Transport." *Molecular Cell* 7(2): 433–42.

———. 2008. "The TRAPP Complex: Insights into Its Architecture and Function." *Traffic* 9(12): 2032–42.

de Saint-Jean, Maud et al. 2011. "Osh4p Exchanges Sterols for Phosphatidylinositol 4-Phosphate between Lipid Bilayers." *Journal of Cell Biology* 195(6): 965–78.

Saito, Koji et al. 2004. "Cdc50p, a Protein Required for Polarized Growth, Associates with the Drs2p P-Type ATPase Implicated in Phospholipid Translocation in Saccharomyces Cerevisiae." *Molecular Biology of the Cell* 15(7): 3418–32.

Schindler, Christina et al. 2015. "EARP Is a Multisubunit Tethering Complex Involved in Endocytic Recycling." *Nature Cell Biology* 17(5): 639–50.

Schneider, Caroline A., Wayne S. Rasband, and Kevin W. Eliceiri. 2012. "NIH Image to ImageJ: 25 Years of Image Analysis." *Nature Methods* 9(7): 671–75. http://dx.doi.org/10.1038/nmeth.2089.

Schou, Kenneth B, Stine K Morthorst, Søren T Christensen, and Lotte B Pedersen. 2014. "Identification of Conserved, Centrosome-Targeting ASH Domains in TRAPPII Complex Subunits and TRAPPC8." *Cilia* 3: 6. http://www.pubmedcentral.nih.gov/articlerender.fcgi?artid=4094338&tool=pmcentrez&rendertype=abstract.

Scott, Sidney V. et al. 2001. "Cvt19 Is a Receptor for the Cytoplasm-to-Vacuole Targeting Pathway." *Molecular Cell* 7(6): 1131–41.

Sebastian, Tessy T., Ryan D. Baldridge, Peng Xu, and Todd R. Graham. 2012. "Phospholipid Flippases: Building Asymmetric Membranes and Transport Vesicles." *Biochim Biophys Acta.*: 1068–1077.

Shintani, Takahiro et al. 2001. "Apg2p Functions in Autophagosome Formation on the

Perivacuolar Structure." *Journal of Biological Chemistry* 276(32): 30452–60.

Shirahama-Noda, K., S. Kira, T. Yoshimori, and T. Noda. 2013. "TRAPPIII Is Responsible for Vesicular Transport from Early Endosomes to Golgi, Facilitating Atg9 Cycling in Autophagy." *Journal of Cell Science* 126(21): 4963–73. http://jcs.biologists.org/cgi/doi/10.1242/jcs.131318.

Simonin, Frederic et al. 2004. "Identification of a Novel Family of G Protein-Coupled Receptor Associated Sorting Proteins." *Journal of neurochemistry* 89(3): 766–75. http://www.ncbi.nlm.nih.gov/pubmed/15086532 (June 18, 2014).

Smythe, E., and K. R. Ayscough. 2006. "Actin Regulation in Endocytosis." *Journal of Cell Science* 119(22): 4589–98. http://jcs.biologists.org/cgi/doi/10.1242/jcs.03247.

Su ab, Ming-Yuan et al. 2015. "Structure of Yeast Ape1 and Its Role in Autophagic Vesicle Formation): Structure of Yeast Ape1 and Its Role in Autophagic Vesicle Formation." 11(9): 1580–93. http://www.tandfonline.com/loi/kaup20%5Cnhttp://dx.doi.org/10.1080/15548627.2015.1067363.

Suhy, David A, Thomas H Giddings, and Karla Kirkegaard. 2000. "Remodeling the Endoplasmic Reticulum by Poliovirus Infection and by Individual Viral Proteins: An Autophagy-Like Origin for Virus-Induced Vesicles." *Journal of Virology* 74(19): 8953–65.

Suvorova, Elena S., Rainer Duden, and Vladimir V. Lupashin. 2002. "The Sec34/Sec35p Complex, a Ypt1p Effector Required for Retrograde Intra-Golgi Trafficking, Interacts with Golgi SNAREs and COPI Vesicle Coat Proteins." *Journal of Cell Biology* 157(4): 631–43.

Suzuki, Kuninori et al. 2001. "The Pre-Autophagosomal Structure Organized by Concerted Functions of APG Genes Is Essential for Autophagosome Formation." *EMBO Journal* 20(21): 5971–81.

———. 2013. "Selective Autophagy in Budding Yeast." *Cell Death and Differentiation* 20(1): 43–48. http://dx.doi.org/10.1038/cdd.2012.73.

Suzuki, Kuninori, Yuka Kubota, Takayuki Sekito, and Yoshinori Ohsumi. 2007. "Hierarchy of Atg Proteins in Pre-Autophagosomal Structure Organization." *Genes to Cells* 12(2): 209–18.

Suzuki, Takashi et al. 2002. "The First Molecular Evidence That Autophagy Relates Rimmed Vacuole Formation in Chloroquine Myopathy." *Journal of Biochemistry* 131(5): 647–51.

Tagaya, Mitsuo, Kohei Arasaki, Hiroki Inoue, and Hana Kimura. 2014. "Moonlighting Functions of the NRZ (Mammalian Dsl1) Complex." *Frontiers in Cell and Developmental Biology* 2(June): 1–9. http://journal.frontiersin.org/article/10.3389/fcell.2014.00025/abstract.

Takada, Naoto et al. 2018. "Phospholipid-flipping Activity of P4-ATPase Drives Membrane Curvature." *The EMBO Journal*.

Takagi, Keiko et al. 2012a. "Biochemical and Biophysical Research Communications Involvement of Golgi-Associated Retrograde Protein Complex in the Recycling of the Putative Dnf Aminophospholipid Flippases in Yeast." *Biochemical and Biophysical Research Communications* 417(1): 490–94. http://dx.doi.org/10.1016/j.bbrc.2011.11.147.

———. 2012b. "Involvement of Golgi-Associated Retrograde Protein Complex in the Recycling of the Putative Dnf Aminophospholipid Flippases in Yeast." *Communications* 417(1): 490–94.

Takeshige, K. et al. 1992. "Autophagy in Yeast Demonstrated with Proteinase-Deficient Mutants and Conditions for Its Induction." *Journal of Cell Biology* 119(2): 301–12.

Tan, D. et al. 2013. "The EM Structure of the TRAPPIII Complex Leads to the Identification of a Requirement for COPII Vesicles on the Macroautophagy Pathway." *Proceedings of the National Academy of Sciences* 110(48): 19432–37. http://www.pnas.org/cgi/doi/10.1073/pnas.1316356110.

Tang, Xiaojing, Margaret S. Halleck, Robert A. Schlegel, and Patrick Williamson. 1996. "A Subfamily of P-Type ATPases with Aminophospholipid Transporting Activity." *Sicence* 272(5267): 1495–97.

Thomas, Laura L., Aaron M.N. Joiner, and J. Christopher Fromme. 2018. "The TRA PPI II Complex Activates the GTPase Ypt1 (Rab1) in the Secretory Pathway." *Journal of Cell Biology* 217(1): 283–98.

Tinevez, Jean Yves et al. 2017. "TrackMate: An Open and Extensible Platform for Single-Particle Tracking." *Methods* 115: 80–90. http://dx.doi.org/10.1016/j.ymeth.2016.09.016.

Tong, Amy Hin Yan et al. 2001. "Systematic Genetic Analysis with Ordered Arrays of Yeast Deletion Mutants." *Science* 294(5550): 2364–68.

Tong, Yan, and Charles Boone. 2005. "Synthetic Genetic Array Analysis in Saccharomyces Cerevisiae." *Methods in Molecular Biology* 313(1): 171–92.

Torggler, Raffaela et al. 2016. "Two Independent Pathways within Selective Autophagy

Converge to Activate Atg1 Kinase at the Vacuole." *Molecular Cell* 64(2): 221–35.

Torreira, Eva et al. 2017. 6 eLife *The Dynamic Assembly of Distinct RNA Polymerase I Complexes Modulates rDNA Transcription*.

Trumbly, R. J., and G. Bradley. 1983. "Isolation and Characterization of Aminopeptidase Mutants of Saccharomyces Cerevisiae." *Journal of Bacteriology* 156(1): 36–48.

Tsai, P.-C. et al. 2013. "Arl1p Regulates Spatial Membrane Organization at the Trans-Golgi Network through Interaction with Arf-GEF Gea2p and Flippase Drs2p." *Proceedings of the National Academy of Sciences* 110(8): E668–77. http://www.pnas.org/cgi/doi/10.1073/pnas.1221484110.

Ueno, Kazuma et al. 2014. "V-ATPase-Dependent Luminal Acidification Is Required for Endocytic Recycling of a Yeast Cell Wall Stress Sensor, Wsc1p." *Biochemical and Biophysical Research Communications* 443(2): 549–55. http://dx.doi.org/10.1016/j.bbrc.2013.12.008.

Ungar, Daniel et al. 2002. "Characterization of a Mammalian Golgi-Localized Protein Complex, COG, That Is Required for Normal Golgi Morphology and Function." *Journal of Cell Biology* 157(3): 405–15.

Vanrheenen, Susan M et al. 1999. "Apparatus , Is in a Complex with Sec35p." 147(4): 729–42. http://jcb.rupress.org/content/147/4/729.full.pdf.

Van der Velden, Lieke M., Stan F. J. Van de Graaf, and Leo W. J. Klomp. 2010. "Biochemical and Cellular Functions of P4 ATPases." *Biochemical Journal* 143(1): 1–11.

Villasmil, Michelle L, Vytas A Bankaitis, and Carl J Mousley. 2012. "The Oxysterol-Binding Protein Superfamily: New Concepts and Old Proteins." *Biochemical Society transactions* 40(2): 469–73. http://www.pubmedcentral.nih.gov/articlerender.fcgi?artid=3996832&tool=pmcentrez&rendertype=abstract.

Weng, Yu Rong et al. 2014. "The Role of ERK2 in Colorectal Carcinogenesis Is Partly Regulated by TRAPPC4." *Molecular Carcinogenesis* 53(S1): 72–84.

Wicky, S, H Schwarz, and B Singer-Kruger. 2004. "Molecular Interactions of Yeast Neo1p, an Essential Member of the Drs2 Family of Aminophospholipid Translocases, and Its Role in Membrane Trafficking within the Endomembrane System." *Molecular and Cellular Biology* 24(17): 7402–18. http://mcb.asm.org/cgi/reprint/24/17/7402.pdf.

Wu, Shuya et al. 2005. "Sec15 Interacts with Rab11 via a Novel Domain and Affects Rab11 Localization in Vivo." *Nature Structural and Molecular Biology* 12(10): 879–85.

Xu, Peng et al. 2013. “Phosphatidylserine Flipping Enhances Membrane Curvature and Negative Charge Required for Vesicular Transport.” *Journal of Cell Biology* 202(6): 875–86.

Yamamoto, Hayashi et al. 2012. “Atg9 Vesicles Are an Important Membrane Source during Early Steps of Autophagosome Formation.” *Journal of Cell Biology* 198(2): 219–33.

Yamasaki, Akinori et al. 2009. “mTrs130 Is a Component of a Mammalian TRAPPII Complex, a Rab1 GEF That Binds to COPI-Coated Vesicles.” *Molecular biology of the cell* 20: 4205–15.

Yamasaki, Akinori, and Nobuo N. Noda. 2017. “Structural Biology of the Cvt Pathway.” *Journal of Molecular Biology* 429(4): 531–42. http://dx.doi.org/10.1016/j.jmb.2017.01.003.

Yang, Shu, and Anne G. Rosenwald. 2016. “Autophagy in Saccharomyces Cerevisiae Requires the Monomeric GTP-Binding Proteins, Arl1 and Ypt6.” *Autophagy* 12(10): 1721–37. http://dx.doi.org/10.1080/15548627.2016.1196316.

Yen, Wei Lien et al. 2010. “The Conserved Oligomeric Golgi Complex Is Involved in Double-Membrane Vesicle Formation during Autophagy.” *Journal of Cell Biology* 188(1): 101–14.

Yip, Calvin K., Julia Berscheminski, and Thomas Walz. 2010. “Molecular Architecture of the TRAPPII Complex and Implications for Vesicle Tethering.” *Nature Structural and Molecular Biology* 17(11): 1298–1304. http://dx.doi.org/10.1038/nsmb.1914.

Yorimitsu, Tomohiro, and Daniel J. Klionsky. 2005. “Atg11 Links Cargo to the Vesicle-Forming Machinery in the Cytoplasm to Vacuole Targeting Pathway.” *Molecular Biology of the Cell* 16(4): 1593–1605.

Young, Andrew R J, and Sharon A Tooze. 2007. “Atg9 Trafficking in Mammalian Cells ND ES SC.” *Autophagy* 3(1): 54–56.

Yu, Li et al. 2004. “Regulation of an ATG7-Beclin 1 Program of Autophagic Cell Death by Caspase-8.” *Science* 304(5676): 1500–1502.

Zhang, Yonggang et al. 2015. “Elevated NIBP/TRAPPC9 Mediates Tumorigenesis of Cancer Cells through NFκB Signaling.” *Oncotarget* 6(8): 6160–78. http://www.oncotarget.com/fulltext/3349.

Zhou, Xiaoming, and Todd R Graham. 2009. “Reconstitution of Phospholipid Translocase Activity with Purified Drs2p, a Type-IV P-Type ATPase from Budding Yeast.” *Proceedings of the National Academy of Sciences of the United States of America* 106: 16586–91.

Zhou, Xiaoming, Tessy T. Sebastian, and Todd R. Graham. 2013. “Auto-Inhibition of Drs2p, a Yeast Phospholipid Flippase, by Its Carboxyl-Terminal Tail.” *Journal of Biological Chemistry* 288(44): 31807–15.

Zinser, E., F. Paltauf, and G. Daum. 1993. “Sterol Composition of Yeast Organelle Membranes and Subcellular Distribution of Enzymes Involved in Sterol Metabolism.” *Journal of Bacteriology* 175(10): 2853–58.

Zou, Shenshen et al. 2014. “NIH Public Access.” 14(2): 233–46.

Zuo, Xiaofeng, Wei Guo, and Joshua H. Lipschutz. 2009. “The Exocyst Protein Sec10 Is Necessary for Primary Ciliogenesis and Cystogenesis in Vitro.” *Molecular Biology of the Cell* 20(10): 2522–29.

# APPENDIX I – YEAST STRAINS

| Strains manually generated | | | |
|---|---|---|---|
| **Number** | **Genotype** | **Strain** | **Source** |
| From GFP collection | MATa, his3Δ1, leu2Δ0, met15Δ0, ura3Δ0, DNF1-myeGFP::HIS3 | Dnf1-GFP | GFP collection |
| OGY0582 | MATa, his3Δ1, leu2Δ0, met15Δ0, ura3Δ0, DNF1-myeGFP::HIS3, vps51Δ::hphNT1 | Dnf1-GFP Δ*vps51* | This study |
| OGY0629 | MATa, his3Δ1, leu2Δ0, ura3Δ0, LYS+, can1Δ::STE2pr-LEU2, lyp1Δ::, tor1-1, fpr1Δ::klURA, Tub4-(6)-RFP-(24)-FKBP::natNT2, MTC33-FRB::hphNT1NT1, DNF1-myeGFP::HIS3, tlg2Δ::kanMX4 | Vps53-FRB Dnf1-GFP *Δtlg2* | This study |
| OGY0630 | MATa, his3Δ1, leu2Δ0, ura3Δ0, LYS+, can1Δ::STE2pr-LEU2, lyp1Δ::, tor1-1, fpr1Δ::klURA, Tub4-(6)-RFP-(24)-FKBP::natNT2, MTC33-FRB::hphNT1NT1, DNF1-myeGFP::HIS3, snx4Δ::kanMX4 | Vps53-FRB Dnf1-GFP *Δsnx4* | This study |
| OGY0633 | MATa, his3Δ1, leu2Δ0, ura3Δ0, LYS+, can1Δ::STE2pr-LEU2, lyp1Δ::, tor1-1, fpr1Δ::klURA, Tub4-(6)-RFP-(24)-FKBP::natNT2, MTC33-FRB::hphNT1NT1, DNF1-myeGFP::HIS3, mon1Δ::kanMX4 | Vps53-FRB Dnf1-GFP *Δmon1* | This study |
| OGY0634 | MATa, his3Δ1, leu2Δ0, ura3Δ0, LYS+, can1Δ::STE2pr-LEU2, lyp1Δ::, tor1-1, fpr1Δ::klURA, Tub4-(6)-RFP-(24)-FKBP::natNT2, MTC33-FRB::hphNT1NT1, DNF1-myeGFP::HIS3, vps25Δ::kanMX4 | Vps53-FRB Dnf1-GFP *Δvps25* | This study |
| OGY0866 | MATa, his3Δ1, leu2Δ0, met15Δ0, ura3Δ0, DNF1-3xmyeGFP::kanMX4, VPS26-3xmCherry | Dnf1-3GFP Vps26-3RFP | This study |
| OGY0867 | MATa, his3Δ1, leu2Δ0, met15Δ0, ura3Δ0, DNF1-3xmyeGFP::kanMX4, VPS26-3xmCherry, vps51Δ::hphNT1 | Dnf1-3GFP Vps26-3RFP *vps51Δ* | This study |
| OGY0868 | MATa, his3Δ1, leu2Δ0, met15Δ0, ura3Δ0, DNF1-3xmyeGFP::kanMX4, SEC7-3xmCherry | Dnf1-3GFP Sec7-3RFP | This study |
| OGY0869 | MATa, his3Δ1, leu2Δ0, met15Δ0, ura3Δ0, DNF1-3xmyeGFP::kanMX4, SEC7-3xmCherry, vps51Δ::hphNT1 | Dnf1-3GFP Sec7-3RFP *vps51Δ* | This study |
| OGY0596 | MATa, his3Δ1, leu2Δ0, met15Δ0, ura3Δ0 | Wild-type | Provided by Dr. Graham T |
| OGY0598 | MATα, his3Δ1, leu2Δ0, met15Δ0, ura3Δ0, drs2Δ::kanMX4 | *Δdrs2* | Provided by Dr. Graham T |
| OGY0686 | MATa, his3Δ1, leu2Δ0, met15Δ0, ura3Δ0, trs85Δ::klURA | *Δtrs85* | This study |
| OGY0676 | MATa, his3Δ1, leu2Δ0, met15Δ0, ura3Δ0, APE1-myeGFP::HIS3::natNT2 | Ape1-GFP | This study |
| OGY0423 | MATα, his3Δ1, leu2Δ0, met15Δ0, ura3Δ0, trs85Δ::kanMX4, APE1-myeGFP::HIS3::natNT2 | *Δtrs85* Ape1-GFP | This study |
| OGY0683 | MATα, his3Δ1, leu2Δ0, met15Δ0, ura3Δ0, drs2Δ::kanMX4, APE1-myeGFP::HIS3::natNT2 | *Δdrs2* Ape1-GFP | This study |
| OGY0700 | MATα, his3Δ1, leu2Δ0, met15Δ0, ura3Δ0, drs2Δ::kanMX4, atg19Δ::hphNT1 | *Δdrs2 Δatg19* | This study |
| OGY0684 | MATα, his3Δ1, leu2Δ0, met15Δ0, ura3Δ0, drs2Δ::kanMX4, atg17Δ::hphNT1 | *Δdrs2 Δatg17* | This study |
| OGY0678 | MATa, his3Δ1, leu2Δ0, met15Δ0, ura3Δ0, pep4Δ::hphNT1 | *Δpep4* | KO collection (provided by Dr. Vilardell J) |
| OGY0685 | MATα, his3Δ1, leu2Δ0, met15Δ0, ura3Δ0, drs2Δ::kanMX4, pep4Δ::hphNT1 | *Δdrs2 Δpep4* | This study |
| OGY0782 | MATa, his3Δ1, leu2Δ0, met15Δ0, ura3Δ0, APE1-3xmyeGFP::kanMX4, drs2Δ::kanMX4, pep4Δ::hphNT1 | *Δdrs2 Δpep4* Ape1-3GFP | This study |
| OGY0709 | MATa, his3Δ1, leu2Δ0, met15Δ0, ura3Δ0, DRS2-3xmyeGFP::kanMX4, ATG11-3xmCherry::natNT2 | Drs2-3GFP Atg11-3RFP | This study |
| OGY0710 | MATa, his3Δ1, leu2Δ0, met15Δ0, ura3Δ0, DRS2-3xmyeGFP::kanMX4, ATG11-3xmCherry::natNT2, ATG1Δ::hphNT1 | Drs2-3GFP Atg11-3RFP *Δatg1* | This study |
| OGY0711 | MATa, his3Δ1, leu2Δ0, met15Δ0, ura3Δ0, TRS85-3xmyeGFP::kanMX4, ATG11-3xmCherry::natNT2, ATG1Δ::hphNT1 | Trs85-3GFP Atg11-3RFP *Δatg1* | This study |

## APPENDIX I – YEAST STRAINS

| | | | |
|---|---|---|---|
| OGY0712 | MATa, his3Δ1, leu2Δ0, met15Δ0, ura3Δ0, TRS85-3xmyeGFP::kanMX4, ATG11-3xmCherry::natNT2, ATG1Δ::hphNT1, drs2Δ::LEU2 | Trs85-3GFP Atg11-3RFP *Δatg1 Δdrs2* | This study |
| OGY0675 | MATα, his3Δ1, leu2Δ0, met15Δ0, ura3Δ0, ATG9-3xmyeGFP::kanMX4, ATG11-3xmCherry::natNT2 | Atg9-3GFP Atg11-3RFP | This study |
| OGY0723 | MATα, his3Δ1, leu2Δ0, met15Δ0, ura3Δ0, drs2Δ::LEU2, ATG9-3xmyeGFP::kanMX4, ATG11-3xmCherry::natNT2 | Atg9-3GFP Atg11-3RFP *Δdrs2* | This study |
| From OGY0674 | MATa, his3Δ1, leu2Δ0, met15Δ0, ura3Δ0, ATG9-3xmyeGFP::kanMX4 + p.RS416-APE1-mCherry::KlURA | Atg9-3GFP + Ape1-Cherry | This study |
| From OGY0716 | MATα, his3Δ1, leu2Δ0, met15Δ0, ura3Δ0, drs2Δ::LEU2, ATG9-3xmyeGFP::kanMX4 + p.RS416-APE1-mCherry::KlURA | Atg9-3GFP + Ape1-Cherry *Δdrs2* | This study |
| OGY0674 | MATa, his3Δ1, leu2Δ0, met15Δ0, ura3Δ0, ATG9-3xmyeGFP::kanMX4 | Atg9-3GFP | This study |
| OGY0465 | MATα, his3Δ1, leu2Δ0, met15Δ0, ura3Δ0, trs85Δ::klURA, ATG9-3xmyeGFP::kanMX4 | Atg9-3GFP *Δdrs2* | This study |
| OGY0716 | MATα, his3Δ1, leu2Δ0, met15Δ0, ura3Δ0, drs2Δ::LEU2, ATG9-3xmyeGFP::kanMX4 | Atg9-3GFP *Δdrs2* | This study |
| OGY0820 | MATα, his3Δ1, leu2Δ0, met15Δ0, ura3Δ0, ATG9-3xmyeGFP::kanMX4, SEC7-3xmCherry::natNT2 | Atg9-3GFP Sec7-3RFP | This study |
| OGY0821 | MATα, his3Δ1, leu2Δ0, met15Δ0, ura3Δ0, drs2Δ::LEU2, ATG9-3xmyeGFP::kanMX4, SEC7-3xmCherry::natNT2 | Atg9-3GFP Sec7-3RFP *Δdrs2* | This study |
| OGY0434 | MATα, his3Δ1, leu2Δ0, met15Δ0, ura3Δ0, rcy1Δ::kanMX6 | *Δrcy1* | Provided by Dr. Graham T |
| OGY0699 | MATa, his3Δ1, leu2Δ0, met15Δ0, ura3Δ0, apl4Δ::hphNT1 | *Δapl4* | KO collection (provided by Dr. Vilardell J) |
| OGY0766 | MATα, his3Δ1, leu2Δ0, met15Δ0, ura3Δ0, apl5Δ::kanMX8 | *Δapl5* | KO collection (provided by Dr. Vilardell J) |
| OGY0768 | MATα, his3Δ1, leu2Δ0, met15Δ0, ura3Δ0, gga2Δ::kanMX10 | *Δgga2* | KO collection (provided by Dr. Vilardell J) |
| OGY0769 | MATα, his3Δ1, leu2Δ0, met15Δ0, ura3Δ0, gga2Δ::kanMX10, gga1Δ::hphNT1 | *Δgga2 Δgga1* | This study |
| From OGY0598 | MATα, his3Δ1, leu2Δ0, met15Δ0, ura3Δ0, drs2Δ::kanMX4 + pRS313 | *Δdrs2* + empty vector | This study |
| From OGY0598 | MATα, his3Δ1, leu2Δ0, met15Δ0, ura3Δ0, drs2Δ::kanMX4 + pRS313-DRS2 | *Δdrs2* + WT DRS2 | This study |
| From OGY0598 | MATα, his3Δ1, leu2Δ0, met15Δ0, ura3Δ0, drs2Δ::kanMX4 + pRS313-drs2-QQ>GA | *Δdrs2* + *drs2-GA* | This study |
| OGY0370 | MATα, his3Δ1, leu2Δ0, ura3Δ0, LYS+, can1Δ::STE2pr-LEU2, lyp1Δ::, cho1Δ::hphNT1 | *Δcho1* | Provided by Dr. Maeda K |
| From OGY0598 | MATα, his3Δ1, leu2Δ0, met15Δ0, ura3Δ0, drs2Δ::kanMX4 + pRS315-drs2-ΔGIM | *Δdrs2* + ΔGIM | This study |
| From OGY0598 | MATα, his3Δ1, leu2Δ0, met15Δ0, ura3Δ0, drs2Δ::kanMX4 + pRS315-drs2-ΔCM | *Δdrs2* + ΔCM | This study |
| From OGY0598 | MATα, his3Δ1, leu2Δ0, met15Δ0, ura3Δ0, drs2Δ::kanMX4 + pRS315-drs2-ΔCT | *Δdrs2* + ΔCT | This study |
| From OGY0598 | MATα, his3Δ1, leu2Δ0, met15Δ0, ura3Δ0, drs2Δ::kanMX4 + pRS315-drs2-ΔGIM-ΔNPF | *Δdrs2* + ΔGIMΔNPF | This study |
| OGY0433 | MATα, his3Δ1, leu2Δ0, lys2Δ0, ura3Δ0, drs2Δ::kanMX4, kes1Δ::his3 | *Δdrs2 Δkes1* | Provided by Dr. Graham T |
| OGY0680 | MATα, his3Δ1, leu2Δ0, lys2Δ0, ura3Δ0, drs2Δ::kanMX4, kes1Δ::his3, trs85Δ::klURA | *Δdrs2 Δkes1 Δtrs85* | This study |
| From OGY0451 | MATα, his3Δ1, leu2Δ0, ura3Δ0, LYS+, can1Δ::STE2pr-LEU2, lyp1Δ::, tor1-1, fpr1Δ::klURA, Tub4-(6)-RFP-(24)-FKBP::natNT2, MTC30-FRB::hphNT1NT1, drs2Δ::kanMX4 + pRS313-GFP-DRS2 | Trs85-FRB GFP-Drs2 | This study |

## APPENDIX I – YEAST STRAINS

| | | | |
|---|---|---|---|
| From OGY0451 | MATα, his3Δ1, leu2Δ0, ura3Δ0, LYS+, can1Δ::STE2pr-LEU2, lyp1Δ::, tor1-1, fpr1Δ::klURA, Tub4-(6)-RFP-(24)-FKBP::natNT2, MTC30-FRB::hphNT1NT1, drs2Δ::kanMX4 + pRS313-GFP-drs2-5A | Trs85-FRB GFP-*drs2-5A* | This study |
| OGY0727 | MATa trp1–901 LEU22–3,112 ura3–52 his3–200 gal4Δ gal80Δ LYS2::GAL1UAS–GAL1TATA–HIS3 GAL2UAS–GAL2TATA–ADE2 URA3::MEL1UAS –MEL1TATA–lacZ MEL1 | AH109 | Clonotech (provided by Dr. Hamasaki M) |
| From OGY0727 | MATa trp1–901 LEU22–3,112 ura3–52 his3–200 gal4Δ gal80Δ LYS2::GAL1UAS–GAL1TATA–HIS3 GAL2UAS–GAL2TATA–ADE2 URA3::MEL1UAS –MEL1TATA–lacZ MEL1 + pGADT7 + pGBKT7 | pGADT7 + pGBKT7 | This study |
| From OGY0727 | MATa trp1–901 LEU22–3,112 ura3–52 his3–200 gal4Δ gal80Δ LYS2::GAL1UAS–GAL1TATA–HIS3 GAL2UAS–GAL2TATA–ADE2 URA3::MEL1UAS –MEL1TATA–lacZ MEL1 + pGADT7_T + pGBKT7_53 | pGADT7_T + pGBKT7_53 | This study |
| From OGY0727 | MATa trp1–901 LEU22–3,112 ura3–52 his3–200 gal4Δ gal80Δ LYS2::GAL1UAS–GAL1TATA–HIS3 GAL2UAS–GAL2TATA–ADE2 URA3::MEL1UAS –MEL1TATA–lacZ MEL1 + pGADT7_N term_DRS2 + pGBKT7_BET3 | pGADT7_N term_DRS2 + pGBKT7_BET3 | This study |
| From OGY0727 | MATa trp1–901 LEU22–3,112 ura3–52 his3–200 gal4Δ gal80Δ LYS2::GAL1UAS–GAL1TATA–HIS3 GAL2UAS–GAL2TATA–ADE2 URA3::MEL1UAS –MEL1TATA–lacZ MEL1 + pGADT7_N term_DRS2 + pGBKT7_TRS31 | pGADT7_N term_DRS2 + pGBKT7_TRS31 | This study |
| From OGY0598 | MATα, his3Δ1, leu2Δ0, met15Δ0, ura3Δ0, drs2Δ::kanMX4 + pDDFGP_N-term_DRS2 | *Δdrs2* | This study |
| From OGY0598 | MATα, his3Δ1, leu2Δ0, met15Δ0, ura3Δ0, drs2Δ::kanMX4 + pRS315-drs2-5A | *Δdrs2* + *drs2*-5A | This study |
| From OGY0716 | MATα, his3Δ1, leu2Δ0, met15Δ0, ura3Δ0, drs2Δ::LEU2, ATG9-3xmyeGFP::kanMX4 + pRS315-drs2-5A | Atg9-3GFP *Δdrs2* | This study |
| OGY0762 | MATα, his3Δ1, leu2Δ0, lys2Δ0, ura3Δ0, drs2Δ::kanMX4, kes1Δ::his3, vps51Δ::hphNT1 | *Δdrs2 Δkes1 Δvps51* | This study |

| **Strains crosses with SGA** | | |
|---|---|---|
| **Number** | **Genotype** | **Source** |
| OGY0003 | *MATα, his3Δ1 leu2Δ0 ura3Δ0 LYS+, can1Δ::STE2pr-LEU2, lyp1Δ::* | Provided by Dr. Boone C. |
| MKY2127 | *MATα, his3Δ1 leu2Δ0 ura3Δ0 LYS+, can1Δ::STE2pr-LEU2, lyp1Δ::, tor1-1* | Gallegp O. et al, 2013 |
| MKY2128 | *MATα, his3Δ1 leu2Δ0 ura3Δ0 LYS+, can1Δ::STE2pr-LEU2, lyp1Δ::, tor1-1, fpr1Δ::klURA* | Gallegp O. et al, 2013 |
| OGY0307 | *MATα, his3Δ1 leu2Δ0 ura3Δ0 LYS+, can1Δ::STE2pr-LEU2, lyp1Δ::, tor1-1, fpr1Δ::klURA, Tub4-(6)-RFP-(24)-FKBP::natNT2* | This study and Torreira E. 2017 |
| OGY0314 | *MATα, his3Δ1 leu2Δ0 ura3Δ0 LYS+, can1Δ::STE2pr-LEU2, lyp1Δ::, tor1-1, fpr1Δ::klURA, Tub4-(6)-RFP-(24)-FKBP::natNT2, DSL1-FRB::hphNT1* | This study |
| OGY0315 | *MATα, his3Δ1 leu2Δ0 ura3Δ0 LYS+, can1Δ::STE2pr-LEU2, lyp1Δ::, tor1-1, fpr1Δ::klURA, Tub4-(6)-RFP-(24)-FKBP::natNT2, COG6-FRB::hphNT1* | This study |
| OGY0524 | *MATα, his3Δ1 leu2Δ0 ura3Δ0 LYS+, can1Δ::STE2pr-LEU2, lyp1Δ::, tor1-1, fpr1Δ::klURA, Tub4-(6)-RFP-(24)-FKBP::natNT2, VPS3-FRB::hphNT1* | This study |
| OGY0317 | *MATα, his3Δ1 leu2Δ0 ura3Δ0 LYS+, can1Δ::STE2pr-LEU2, lyp1Δ::, tor1-1, fpr1Δ::klURA, Tub4-(6)-RFP-(24)-FKBP::natNT2, VAM6-FRB::hphNT1* | This study |
| OGY0318 | *MATα, his3Δ1 leu2Δ0 ura3Δ0 LYS+, can1Δ::STE2pr-LEU2, lyp1Δ::, tor1-1, fpr1Δ::klURA, Tub4-(6)-RFP-(24)-FKBP::natNT2, TRS23-FRB::hphNT1* | This study |
| OGY0536 | *MATα, his3Δ1 leu2Δ0 ura3Δ0 LYS+, can1Δ::STE2pr-LEU2, lyp1Δ::, tor1-1, fpr1Δ::klURA, Tub4-(6)-RFP-(24)-FKBP::natNT2, TRS130-FRB::hphNT1* | This study |
| OGY0320 | *MATα, his3Δ1 leu2Δ0 ura3Δ0 LYS+, can1Δ::STE2pr-LEU2, lyp1Δ::, tor1-1, fpr1Δ::klURA, Tub4-(6)-RFP-(24)-FKBP::natNT2, TRS85-FRB::hphNT1* | This study |

## APPENDIX I – YEAST STRAINS

| | | |
|---|---|---|
| OGY0321 | *MATα, his3Δ1 leu2Δ0 ura3Δ0 LYS+, can1Δ::STE2pr-LEU2, lyp1Δ::, tor1-1, fpr1Δ::klURA, Tub4-(6)-RFP-(24)-FKBP::natNT2, VPS53-FRB::hphNT1* | This study |
| OGY0326 | *MATα, his3Δ1 leu2Δ0 ura3Δ0 LYS+, can1Δ::STE2pr-LEU2, lyp1Δ::, tor1-1, fpr1Δ::klURA, Tub4-(6)-RFP-(24)-FKBP::natNT2, SEC3-FRB::hphNT1* | This study |
| OGYSGA1641 | *MATa, his3Δ1, leu2Δ0, ura3Δ0, LYS+, can1Δ::STE2pr-LEU2, lyp1Δ::, tor1-1, fpr1Δ::klURA, Tub4-(6)-RFP-(24)-FKBP::natNT2, DSL1-FRB::hphNT1, YKL033W-myeGFP::HIS3* | This study |
| OGYSGA1642 | *MATa, his3Δ1, leu2Δ0, ura3Δ0, LYS+, can1Δ::STE2pr-LEU2, lyp1Δ::, tor1-1, fpr1Δ::klURA, Tub4-(6)-RFP-(24)-FKBP::natNT2, DSL1-FRB::hphNT1, YNL287W-myeGFP::HIS3* | This study |
| OGYSGA1643 | *MATa, his3Δ1, leu2Δ0, ura3Δ0, LYS+, can1Δ::STE2pr-LEU2, lyp1Δ::, tor1-1, fpr1Δ::klURA, Tub4-(6)-RFP-(24)-FKBP::natNT2, DSL1-FRB::hphNT1, YGL054C-myeGFP::HIS3* | This study |
| OGYSGA1644 | *MATa, his3Δ1, leu2Δ0, ura3Δ0, LYS+, can1Δ::STE2pr-LEU2, lyp1Δ::, tor1-1, fpr1Δ::klURA, Tub4-(6)-RFP-(24)-FKBP::natNT2, DSL1-FRB::hphNT1, YMR224C-myeGFP::HIS3* | This study |
| OGYSGA1645 | *MATa, his3Δ1, leu2Δ0, ura3Δ0, LYS+, can1Δ::STE2pr-LEU2, lyp1Δ::, tor1-1, fpr1Δ::klURA, Tub4-(6)-RFP-(24)-FKBP::natNT2, COG6-FRB::hphNT1, YHL020C-myeGFP::HIS3* | This study |
| OGYSGA1646 | *MATa, his3Δ1, leu2Δ0, ura3Δ0, LYS+, can1Δ::STE2pr-LEU2, lyp1Δ::, tor1-1, fpr1Δ::klURA, Tub4-(6)-RFP-(24)-FKBP::natNT2, COG6-FRB::hphNT1, YPR051W-myeGFP::HIS3* | This study |
| OGYSGA1647 | *MATa, his3Δ1, leu2Δ0, ura3Δ0, LYS+, can1Δ::STE2pr-LEU2, lyp1Δ::, tor1-1, fpr1Δ::klURA, Tub4-(6)-RFP-(24)-FKBP::natNT2, COG6-FRB::hphNT1, YJL123C-myeGFP::HIS3* | This study |
| OGYSGA1648 | *MATa, his3Δ1, leu2Δ0, ura3Δ0, LYS+, can1Δ::STE2pr-LEU2, lyp1Δ::, tor1-1, fpr1Δ::klURA, Tub4-(6)-RFP-(24)-FKBP::natNT2, COG6-FRB::hphNT1, YFR051C-myeGFP::HIS3* | This study |
| OGYSGA1649 | *MATa, his3Δ1, leu2Δ0, ura3Δ0, LYS+, can1Δ::STE2pr-LEU2, lyp1Δ::, tor1-1, fpr1Δ::klURA, Tub4-(6)-RFP-(24)-FKBP::natNT2, COG6-FRB::hphNT1, YDL058W-myeGFP::HIS3* | This study |
| OGYSGA1650 | *MATa, his3Δ1, leu2Δ0, ura3Δ0, LYS+, can1Δ::STE2pr-LEU2, lyp1Δ::, tor1-1, fpr1Δ::klURA, Tub4-(6)-RFP-(24)-FKBP::natNT2, COG6-FRB::hphNT1, YGL137W-myeGFP::HIS3* | This study |
| OGYSGA1651 | *MATa, his3Δ1, leu2Δ0, ura3Δ0, LYS+, can1Δ::STE2pr-LEU2, lyp1Δ::, tor1-1, fpr1Δ::klURA, Tub4-(6)-RFP-(24)-FKBP::natNT2, COG6-FRB::hphNT1, YGL020C-myeGFP::HIS3* | This study |
| OGYSGA1652 | *MATa, his3Δ1, leu2Δ0, ura3Δ0, LYS+, can1Δ::STE2pr-LEU2, lyp1Δ::, tor1-1, fpr1Δ::klURA, Tub4-(6)-RFP-(24)-FKBP::natNT2, COG6-FRB::hphNT1, YJR032W-myeGFP::HIS3* | This study |
| OGYSGA1653 | *MATa, his3Δ1, leu2Δ0, ura3Δ0, LYS+, can1Δ::STE2pr-LEU2, lyp1Δ::, tor1-1, fpr1Δ::klURA, Tub4-(6)-RFP-(24)-FKBP::natNT2, COG6-FRB::hphNT1, YER083C-myeGFP::HIS3* | This study |
| OGYSGA1654 | *MATa, his3Δ1, leu2Δ0, ura3Δ0, LYS+, can1Δ::STE2pr-LEU2, lyp1Δ::, tor1-1, fpr1Δ::klURA, Tub4-(6)-RFP-(24)-FKBP::natNT2, COG6-FRB::hphNT1, YGR187C-myeGFP::HIS3* | This study |
| OGYSGA1655 | *MATa, his3Δ1, leu2Δ0, ura3Δ0, LYS+, can1Δ::STE2pr-LEU2, lyp1Δ::, tor1-1, fpr1Δ::klURA, Tub4-(6)-RFP-(24)-FKBP::natNT2, COG6-FRB::hphNT1, YIL109C-myeGFP::HIS3* | This study |
| OGYSGA1656 | *MATa, his3Δ1, leu2Δ0, ura3Δ0, LYS+, can1Δ::STE2pr-LEU2, lyp1Δ::, tor1-1, fpr1Δ::klURA, Tub4-(6)-RFP-(24)-FKBP::natNT2, COG6-FRB::hphNT1, YJL004C-myeGFP::HIS3* | This study |
| OGYSGA1657 | *MATa, his3Δ1, leu2Δ0, ura3Δ0, LYS+, can1Δ::STE2pr-LEU2, lyp1Δ::, tor1-1, fpr1Δ::klURA, Tub4-(6)-RFP-(24)-FKBP::natNT2, COG6-FRB::hphNT1, YGL054C-myeGFP::HIS3* | This study |
| OGYSGA1658 | *MATa, his3Δ1, leu2Δ0, ura3Δ0, LYS+, can1Δ::STE2pr-LEU2, lyp1Δ::, tor1-1, fpr1Δ::klURA, Tub4-(6)-RFP-(24)-FKBP::natNT2, COG6-FRB::hphNT1, YDL100C-myeGFP::HIS3* | This study |
| OGYSGA1659 | *MATa, his3Δ1, leu2Δ0, ura3Δ0, LYS+, can1Δ::STE2pr-LEU2, lyp1Δ::, tor1-1, fpr1Δ::klURA, Tub4-(6)-RFP-(24)-FKBP::natNT2, COG6-FRB::hphNT1, YPL051W-myeGFP::HIS3* | This study |
| OGYSGA1660 | *MATa, his3Δ1, leu2Δ0, ura3Δ0, LYS+, can1Δ::STE2pr-LEU2, lyp1Δ::, tor1-1, fpr1Δ::klURA, Tub4-(6)-RFP-(24)-FKBP::natNT2, COG6-FRB::hphNT1, YMR292W-myeGFP::HIS3* | This study |
| OGYSGA1661 | *MATa, his3Δ1, leu2Δ0, ura3Δ0, LYS+, can1Δ::STE2pr-LEU2, lyp1Δ::, tor1-1, fpr1Δ::klURA, Tub4-(6)-RFP-(24)-FKBP::natNT2, COG6-FRB::hphNT1, YOR216C-myeGFP::HIS3* | This study |
| OGYSGA1662 | *MATa, his3Δ1, leu2Δ0, ura3Δ0, LYS+, can1Δ::STE2pr-LEU2, lyp1Δ::, tor1-1, fpr1Δ::klURA, Tub4-(6)-RFP-(24)-FKBP::natNT2, COG6-FRB::hphNT1, YJR060W-myeGFP::HIS3* | This study |
| OGYSGA1663 | *MATa, his3Δ1, leu2Δ0, ura3Δ0, LYS+, can1Δ::STE2pr-LEU2, lyp1Δ::, tor1-1, fpr1Δ::klURA, Tub4-(6)-RFP-(24)-FKBP::natNT2, COG6-FRB::hphNT1, YBR164C-myeGFP::HIS3* | This study |
| OGYSGA1664 | *MATa, his3Δ1, leu2Δ0, ura3Δ0, LYS+, can1Δ::STE2pr-LEU2, lyp1Δ::, tor1-1, fpr1Δ::klURA, Tub4-(6)-RFP-(24)-FKBP::natNT2, COG6-FRB::hphNT1, YOR070C-myeGFP::HIS3* | This study |
| OGYSGA1665 | *MATa, his3Δ1, leu2Δ0, ura3Δ0, LYS+, can1Δ::STE2pr-LEU2, lyp1Δ::, tor1-1, fpr1Δ::klURA, Tub4-(6)-RFP-(24)-FKBP::natNT2, COG6-FRB::hphNT1, YGR261C-myeGFP::HIS3* | This study |

## APPENDIX I – YEAST STRAINS

| | | |
|---|---|---|
| OGYSGA1666 | *MATa, his3Δ1, leu2Δ0, ura3Δ0, LYS+, can1Δ::STE2pr-LEU2, lyp1Δ::, tor1-1, fpr1Δ::klURA, Tub4-(6)-RFP-(24)-FKBP::natNT2, COG6-FRB::hphNT1, YDR137W-myeGFP::HIS3* | This study |
| OGYSGA1667 | *MATa, his3Δ1, leu2Δ0, ura3Δ0, LYS+, can1Δ::STE2pr-LEU2, lyp1Δ::, tor1-1, fpr1Δ::klURA, Tub4-(6)-RFP-(24)-FKBP::natNT2, COG6-FRB::hphNT1, YCR053W-myeGFP::HIS3* | This study |
| OGYSGA1668 | *MATa, his3Δ1, leu2Δ0, ura3Δ0, LYS+, can1Δ::STE2pr-LEU2, lyp1Δ::, tor1-1, fpr1Δ::klURA, Tub4-(6)-RFP-(24)-FKBP::natNT2, COG6-FRB::hphNT1, YAL019W-myeGFP::HIS3* | This study |
| OGYSGA1669 | *MATa, his3Δ1, leu2Δ0, ura3Δ0, LYS+, can1Δ::STE2pr-LEU2, lyp1Δ::, tor1-1, fpr1Δ::klURA, Tub4-(6)-RFP-(24)-FKBP::natNT2, COG6-FRB::hphNT1, YBL102W-myeGFP::HIS3* | This study |
| OGYSGA1670 | *MATa, his3Δ1, leu2Δ0, ura3Δ0, LYS+, can1Δ::STE2pr-LEU2, lyp1Δ::, tor1-1, fpr1Δ::klURA, Tub4-(6)-RFP-(24)-FKBP::natNT2, COG6-FRB::hphNT1, YDR153C-myeGFP::HIS3* | This study |
| OGYSGA1671 | *MATa, his3Δ1, leu2Δ0, ura3Δ0, LYS+, can1Δ::STE2pr-LEU2, lyp1Δ::, tor1-1, fpr1Δ::klURA, Tub4-(6)-RFP-(24)-FKBP::natNT2, COG6-FRB::hphNT1, YLR360W-myeGFP::HIS3* | This study |
| OGYSGA1672 | *MATa, his3Δ1, leu2Δ0, ura3Δ0, LYS+, can1Δ::STE2pr-LEU2, lyp1Δ::, tor1-1, fpr1Δ::klURA, Tub4-(6)-RFP-(24)-FKBP::natNT2, COG6-FRB::hphNT1, YPL195W-myeGFP::HIS3* | This study |
| OGYSGA1673 | *MATa, his3Δ1, leu2Δ0, ura3Δ0, LYS+, can1Δ::STE2pr-LEU2, lyp1Δ::, tor1-1, fpr1Δ::klURA, Tub4-(6)-RFP-(24)-FKBP::natNT2, COG6-FRB::hphNT1, YER074W-myeGFP::HIS3* | This study |
| OGYSGA1674 | *MATa, his3Δ1, leu2Δ0, ura3Δ0, LYS+, can1Δ::STE2pr-LEU2, lyp1Δ::, tor1-1, fpr1Δ::klURA, Tub4-(6)-RFP-(24)-FKBP::natNT2, COG6-FRB::hphNT1, YOR132W-myeGFP::HIS3* | This study |
| OGYSGA1675 | *MATa, his3Δ1, leu2Δ0, ura3Δ0, LYS+, can1Δ::STE2pr-LEU2, lyp1Δ::, tor1-1, fpr1Δ::klURA, Tub4-(6)-RFP-(24)-FKBP::natNT2, COG6-FRB::hphNT1, YNL297C-myeGFP::HIS3* | This study |
| OGYSGA1676 | *MATa, his3Δ1, leu2Δ0, ura3Δ0, LYS+, can1Δ::STE2pr-LEU2, lyp1Δ::, tor1-1, fpr1Δ::klURA, Tub4-(6)-RFP-(24)-FKBP::natNT2, COG6-FRB::hphNT1, YMR272C-myeGFP::HIS3* | This study |
| OGYSGA1677 | *MATa, his3Δ1, leu2Δ0, ura3Δ0, LYS+, can1Δ::STE2pr-LEU2, lyp1Δ::, tor1-1, fpr1Δ::klURA, Tub4-(6)-RFP-(24)-FKBP::natNT2, COG6-FRB::hphNT1, YKR094C-myeGFP::HIS3* | This study |
| OGYSGA1678 | *MATa, his3Δ1, leu2Δ0, ura3Δ0, LYS+, can1Δ::STE2pr-LEU2, lyp1Δ::, tor1-1, fpr1Δ::klURA, Tub4-(6)-RFP-(24)-FKBP::natNT2, COG6-FRB::hphNT1, YPL120W-myeGFP::HIS3* | This study |
| OGYSGA1679 | *MATa, his3Δ1, leu2Δ0, ura3Δ0, LYS+, can1Δ::STE2pr-LEU2, lyp1Δ::, tor1-1, fpr1Δ::klURA, Tub4-(6)-RFP-(24)-FKBP::natNT2, COG6-FRB::hphNT1, YLR039C-myeGFP::HIS3* | This study |
| OGYSGA1680 | *MATa, his3Δ1, leu2Δ0, ura3Δ0, LYS+, can1Δ::STE2pr-LEU2, lyp1Δ::, tor1-1, fpr1Δ::klURA, Tub4-(6)-RFP-(24)-FKBP::natNT2, COG6-FRB::hphNT1, YDL115C-myeGFP::HIS3* | This study |
| OGYSGA1681 | *MATa, his3Δ1, leu2Δ0, ura3Δ0, LYS+, can1Δ::STE2pr-LEU2, lyp1Δ::, tor1-1, fpr1Δ::klURA, Tub4-(6)-RFP-(24)-FKBP::natNT2, COG6-FRB::hphNT1, YHR012W-myeGFP::HIS3* | This study |
| OGYSGA1682 | *MATa, his3Δ1, leu2Δ0, ura3Δ0, LYS+, can1Δ::STE2pr-LEU2, lyp1Δ::, tor1-1, fpr1Δ::klURA, Tub4-(6)-RFP-(24)-FKBP::natNT2, COG6-FRB::hphNT1, YGL225W-myeGFP::HIS3* | This study |
| OGYSGA1683 | *MATa, his3Δ1, leu2Δ0, ura3Δ0, LYS+, can1Δ::STE2pr-LEU2, lyp1Δ::, tor1-1, fpr1Δ::klURA, Tub4-(6)-RFP-(24)-FKBP::natNT2, COG6-FRB::hphNT1, YOL009C-myeGFP::HIS3* | This study |
| OGYSGA1684 | *MATa, his3Δ1, leu2Δ0, ura3Δ0, LYS+, can1Δ::STE2pr-LEU2, lyp1Δ::, tor1-1, fpr1Δ::klURA, Tub4-(6)-RFP-(24)-FKBP::natNT2, COG6-FRB::hphNT1, YDR310C-myeGFP::HIS3* | This study |
| OGYSGA1685 | *MATa, his3Δ1, leu2Δ0, ura3Δ0, LYS+, can1Δ::STE2pr-LEU2, lyp1Δ::, tor1-1, fpr1Δ::klURA, Tub4-(6)-RFP-(24)-FKBP::natNT2, COG6-FRB::hphNT1, YIL160C-myeGFP::HIS3* | This study |
| OGYSGA1686 | *MATa, his3Δ1, leu2Δ0, ura3Δ0, LYS+, can1Δ::STE2pr-LEU2, lyp1Δ::, tor1-1, fpr1Δ::klURA, Tub4-(6)-RFP-(24)-FKBP::natNT2, COG6-FRB::hphNT1, YIL090W-myeGFP::HIS3* | This study |
| OGYSGA1687 | *MATa, his3Δ1, leu2Δ0, ura3Δ0, LYS+, can1Δ::STE2pr-LEU2, lyp1Δ::, tor1-1, fpr1Δ::klURA, Tub4-(6)-RFP-(24)-FKBP::natNT2, COG6-FRB::hphNT1, YDR202C-myeGFP::HIS3* | This study |
| OGYSGA1688 | *MATa, his3Δ1, leu2Δ0, ura3Δ0, LYS+, can1Δ::STE2pr-LEU2, lyp1Δ::, tor1-1, fpr1Δ::klURA, Tub4-(6)-RFP-(24)-FKBP::natNT2, COG6-FRB::hphNT1,, YAL011W-myeGFP::HIS3* | This study |
| OGYSGA1689 | *MATa, his3Δ1, leu2Δ0, ura3Δ0, LYS+, can1Δ::STE2pr-LEU2, lyp1Δ::, tor1-1, fpr1Δ::klURA, Tub4-(6)-RFP-(24)-FKBP::natNT2, COG6-FRB::hphNT1, YDR293C-myeGFP::HIS3* | This study |
| OGYSGA1690 | *MATa, his3Δ1, leu2Δ0, ura3Δ0, LYS+, can1Δ::STE2pr-LEU2, lyp1Δ::, tor1-1, fpr1Δ::klURA, Tub4-(6)-RFP-(24)-FKBP::natNT2, COG6-FRB::hphNT1, YOL111C-myeGFP::HIS3* | This study |
| OGYSGA1691 | *MATa, his3Δ1, leu2Δ0, ura3Δ0, LYS+, can1Δ::STE2pr-LEU2, lyp1Δ::, tor1-1, fpr1Δ::klURA, Tub4-(6)-RFP-(24)-FKBP::natNT2, COG6-FRB::hphNT1, YOR007C-myeGFP::HIS3* | This study |
| OGYSGA1692 | *MATa, his3Δ1, leu2Δ0, ura3Δ0, LYS+, can1Δ::STE2pr-LEU2, lyp1Δ::, tor1-1, fpr1Δ::klURA, Tub4-(6)-RFP-(24)-FKBP::natNT2, COG6-FRB::hphNT1, YOR327C-myeGFP::HIS3* | This study |

## APPENDIX I – YEAST STRAINS

| | | |
|---|---|---|
| OGYSGA1693 | *MATa, his3Δ1, leu2Δ0, ura3Δ0, LYS+, can1Δ::STE2pr-LEU2, lyp1Δ::, tor1-1, fpr1Δ::klURA, Tub4-(6)-RFP-(24)-FKBP::natNT2, COG6-FRB::hphNT1, YEL042W-myeGFP::HIS3* | This study |
| OGYSGA1694 | *MATa, his3Δ1, leu2Δ0, ura3Δ0, LYS+, can1Δ::STE2pr-LEU2, lyp1Δ::, tor1-1, fpr1Δ::klURA, Tub4-(6)-RFP-(24)-FKBP::natNT2, COG6-FRB::hphNT1, YDL074C-myeGFP::HIS3* | This study |
| OGYSGA1695 | *MATa, his3Δ1, leu2Δ0, ura3Δ0, LYS+, can1Δ::STE2pr-LEU2, lyp1Δ::, tor1-1, fpr1Δ::klURA, Tub4-(6)-RFP-(24)-FKBP::natNT2, COG6-FRB::hphNT1, YJL053W-myeGFP::HIS3* | This study |
| OGYSGA1696 | *MATa, his3Δ1, leu2Δ0, ura3Δ0, LYS+, can1Δ::STE2pr-LEU2, lyp1Δ::, tor1-1, fpr1Δ::klURA, Tub4-(6)-RFP-(24)-FKBP::natNT2, COG6-FRB::hphNT1, YDR334W-myeGFP::HIS3* | This study |
| OGYSGA1697 | *MATa, his3Δ1, leu2Δ0, ura3Δ0, LYS+, can1Δ::STE2pr-LEU2, lyp1Δ::, tor1-1, fpr1Δ::klURA, Tub4-(6)-RFP-(24)-FKBP::natNT2, COG6-FRB::hphNT1, YML041C-myeGFP::HIS3* | This study |
| OGYSGA1698 | *MATa, his3Δ1, leu2Δ0, ura3Δ0, LYS+, can1Δ::STE2pr-LEU2, lyp1Δ::, tor1-1, fpr1Δ::klURA, Tub4-(6)-RFP-(24)-FKBP::natNT2, COG6-FRB::hphNT1, YHR004C-myeGFP::HIS3* | This study |
| OGYSGA1699 | *MATa, his3Δ1, leu2Δ0, ura3Δ0, LYS+, can1Δ::STE2pr-LEU2, lyp1Δ::, tor1-1, fpr1Δ::klURA, Tub4-(6)-RFP-(24)-FKBP::natNT2, COG6-FRB::hphNT1, YBR288C-myeGFP::HIS3* | This study |
| OGYSGA1700 | *MATa, his3Δ1, leu2Δ0, ura3Δ0, LYS+, can1Δ::STE2pr-LEU2, lyp1Δ::, tor1-1, fpr1Δ::klURA, Tub4-(6)-RFP-(24)-FKBP::natNT2, COG6-FRB::hphNT1, YNR051C-myeGFP::HIS3* | This study |
| OGYSGA1701 | *MATa, his3Δ1, leu2Δ0, ura3Δ0, LYS+, can1Δ::STE2pr-LEU2, lyp1Δ::, tor1-1, fpr1Δ::klURA, Tub4-(6)-RFP-(24)-FKBP::natNT2, COG6-FRB::hphNT1, YDL145C-myeGFP::HIS3* | This study |
| OGYSGA1702 | *MATa, his3Δ1, leu2Δ0, ura3Δ0, LYS+, can1Δ::STE2pr-LEU2, lyp1Δ::, tor1-1, fpr1Δ::klURA, Tub4-(6)-RFP-(24)-FKBP::natNT2, COG6-FRB::hphNT1, YJL154C-myeGFP::HIS3* | This study |
| OGYSGA1703 | *MATa, his3Δ1, leu2Δ0, ura3Δ0, LYS+, can1Δ::STE2pr-LEU2, lyp1Δ::, tor1-1, fpr1Δ::klURA, Tub4-(6)-RFP-(24)-FKBP::natNT2, COG6-FRB::hphNT1, YOR069W-myeGFP::HIS3* | This study |
| OGYSGA1704 | *MATa, his3Δ1, leu2Δ0, ura3Δ0, LYS+, can1Δ::STE2pr-LEU2, lyp1Δ::, tor1-1, fpr1Δ::klURA, Tub4-(6)-RFP-(24)-FKBP::natNT2, COG6-FRB::hphNT1, YLL040C-myeGFP::HIS3* | This study |
| OGYSGA1705 | *MATa, his3Δ1, leu2Δ0, ura3Δ0, LYS+, can1Δ::STE2pr-LEU2, lyp1Δ::, tor1-1, fpr1Δ::klURA, Tub4-(6)-RFP-(24)-FKBP::natNT2, COG6-FRB::hphNT1, YJR073C-myeGFP::HIS3* | This study |
| OGYSGA1706 | *MATa, his3Δ1, leu2Δ0, ura3Δ0, LYS+, can1Δ::STE2pr-LEU2, lyp1Δ::, tor1-1, fpr1Δ::klURA, Tub4-(6)-RFP-(24)-FKBP::natNT2, COG6-FRB::hphNT1, YDR320C-myeGFP::HIS3* | This study |
| OGYSGA1707 | *MATa, his3Δ1, leu2Δ0, ura3Δ0, LYS+, can1Δ::STE2pr-LEU2, lyp1Δ::, tor1-1, fpr1Δ::klURA, Tub4-(6)-RFP-(24)-FKBP::natNT2, COG6-FRB::hphNT1, YKL212W-myeGFP::HIS3* | This study |
| OGYSGA1708 | *MATa, his3Δ1, leu2Δ0, ura3Δ0, LYS+, can1Δ::STE2pr-LEU2, lyp1Δ::, tor1-1, fpr1Δ::klURA, Tub4-(6)-RFP-(24)-FKBP::natNT2, COG6-FRB::hphNT1, YOR109W-myeGFP::HIS3* | This study |
| OGYSGA1709 | *MATa, his3Δ1, leu2Δ0, ura3Δ0, LYS+, can1Δ::STE2pr-LEU2, lyp1Δ::, tor1-1, fpr1Δ::klURA, Tub4-(6)-RFP-(24)-FKBP::natNT2, COG6-FRB::hphNT1, YKL004W-myeGFP::HIS3* | This study |
| OGYSGA1710 | *MATa, his3Δ1, leu2Δ0, ura3Δ0, LYS+, can1Δ::STE2pr-LEU2, lyp1Δ::, tor1-1, fpr1Δ::klURA, Tub4-(6)-RFP-(24)-FKBP::natNT2, COG6-FRB::hphNT1, YIL033C-myeGFP::HIS3* | This study |
| OGYSGA1711 | *MATa, his3Δ1, leu2Δ0, ura3Δ0, LYS+, can1Δ::STE2pr-LEU2, lyp1Δ::, tor1-1, fpr1Δ::klURA, Tub4-(6)-RFP-(24)-FKBP::natNT2, COG6-FRB::hphNT1, YFL024C-myeGFP::HIS3* | This study |
| OGYSGA1712 | *MATa, his3Δ1, leu2Δ0, ura3Δ0, LYS+, can1Δ::STE2pr-LEU2, lyp1Δ::, tor1-1, fpr1Δ::klURA, Tub4-(6)-RFP-(24)-FKBP::natNT2, COG6-FRB::hphNT1, YOR123C-myeGFP::HIS3* | This study |
| OGYSGA1713 | *MATa, his3Δ1, leu2Δ0, ura3Δ0, LYS+, can1Δ::STE2pr-LEU2, lyp1Δ::, tor1-1, fpr1Δ::klURA, Tub4-(6)-RFP-(24)-FKBP::natNT2, COG6-FRB::hphNT1, YDR146C-myeGFP::HIS3* | This study |
| OGYSGA1714 | *MATa, his3Δ1, leu2Δ0, ura3Δ0, LYS+, can1Δ::STE2pr-LEU2, lyp1Δ::, tor1-1, fpr1Δ::klURA, Tub4-(6)-RFP-(24)-FKBP::natNT2, COG6-FRB::hphNT1, YER031C-myeGFP::HIS3* | This study |
| OGYSGA1715 | *MATa, his3Δ1, leu2Δ0, ura3Δ0, LYS+, can1Δ::STE2pr-LEU2, lyp1Δ::, tor1-1, fpr1Δ::klURA, Tub4-(6)-RFP-(24)-FKBP::natNT2, COG6-FRB::hphNT1, YGL115W-myeGFP::HIS3* | This study |
| OGYSGA1716 | *MATa, his3Δ1, leu2Δ0, ura3Δ0, LYS+, can1Δ::STE2pr-LEU2, lyp1Δ::, tor1-1, fpr1Δ::klURA, Tub4-(6)-RFP-(24)-FKBP::natNT2, COG6-FRB::hphNT1, YOR089C-myeGFP::HIS3* | This study |
| OGYSGA1717 | *MATa, his3Δ1, leu2Δ0, ura3Δ0, LYS+, can1Δ::STE2pr-LEU2, lyp1Δ::, tor1-1, fpr1Δ::klURA, Tub4-(6)-RFP-(24)-FKBP::natNT2, COG6-FRB::hphNT1, YNL271C-myeGFP::HIS3* | This study |
| OGYSGA1718 | *MATa, his3Δ1, leu2Δ0, ura3Δ0, LYS+, can1Δ::STE2pr-LEU2, lyp1Δ::, tor1-1, fpr1Δ::klURA, Tub4-(6)-RFP-(24)-FKBP::natNT2, COG6-FRB::hphNT1, YKL119C-myeGFP::HIS3* | This study |
| OGYSGA1719 | *MATa, his3Δ1, leu2Δ0, ura3Δ0, LYS+, can1Δ::STE2pr-LEU2, lyp1Δ::, tor1-1, fpr1Δ::klURA, Tub4-(6)-RFP-(24)-FKBP::natNT2, COG6-FRB::hphNT1, YMR123W-myeGFP::HIS3* | This study |

## APPENDIX I – YEAST STRAINS

| | | |
|---|---|---|
| OGYSGA1720 | *MATa, his3Δ1, leu2Δ0, ura3Δ0, LYS+, can1Δ::STE2pr-LEU2, lyp1Δ::, tor1-1, fpr1Δ::klURA, Tub4-(6)-RFP-(24)-FKBP::natNT2, COG6-FRB::hphNT1, YEL002C-myeGFP::HIS3* | This study |
| OGYSGA1721 | *MATa, his3Δ1, leu2Δ0, ura3Δ0, LYS+, can1Δ::STE2pr-LEU2, lyp1Δ::, tor1-1, fpr1Δ::klURA, Tub4-(6)-RFP-(24)-FKBP::natNT2, COG6-FRB::hphNT1, YBR036C-myeGFP::HIS3* | This study |
| OGYSGA1722 | *MATa, his3Δ1, leu2Δ0, ura3Δ0, LYS+, can1Δ::STE2pr-LEU2, lyp1Δ::, tor1-1, fpr1Δ::klURA, Tub4-(6)-RFP-(24)-FKBP::natNT2, COG6-FRB::hphNT1, YEL031W-myeGFP::HIS3* | This study |
| OGYSGA1723 | *MATa, his3Δ1, leu2Δ0, ura3Δ0, LYS+, can1Δ::STE2pr-LEU2, lyp1Δ::, tor1-1, fpr1Δ::klURA, Tub4-(6)-RFP-(24)-FKBP::natNT2, COG6-FRB::hphNT1, YHR090C-myeGFP::HIS3* | This study |
| OGYSGA1724 | *MATa, his3Δ1, leu2Δ0, ura3Δ0, LYS+, can1Δ::STE2pr-LEU2, lyp1Δ::, tor1-1, fpr1Δ::klURA, Tub4-(6)-RFP-(24)-FKBP::natNT2, COG6-FRB::hphNT1, YNL136W-myeGFP::HIS3* | This study |
| OGYSGA1725 | *MATa, his3Δ1, leu2Δ0, ura3Δ0, LYS+, can1Δ::STE2pr-LEU2, lyp1Δ::, tor1-1, fpr1Δ::klURA, Tub4-(6)-RFP-(24)-FKBP::natNT2, COG6-FRB::hphNT1, YDL185W-myeGFP::HIS3* | This study |
| OGYSGA1726 | *MATa, his3Δ1, leu2Δ0, ura3Δ0, LYS+, can1Δ::STE2pr-LEU2, lyp1Δ::, tor1-1, fpr1Δ::klURA, Tub4-(6)-RFP-(24)-FKBP::natNT2, COG6-FRB::hphNT1, YPL057C-myeGFP::HIS3* | This study |
| OGYSGA1727 | *MATa, his3Δ1, leu2Δ0, ura3Δ0, LYS+, can1Δ::STE2pr-LEU2, lyp1Δ::, tor1-1, fpr1Δ::klURA, Tub4-(6)-RFP-(24)-FKBP::natNT2, COG6-FRB::hphNT1, YJL183W-myeGFP::HIS3* | This study |
| OGYSGA1728 | *MATa, his3Δ1, leu2Δ0, ura3Δ0, LYS+, can1Δ::STE2pr-LEU2, lyp1Δ::, tor1-1, fpr1Δ::klURA, Tub4-(6)-RFP-(24)-FKBP::natNT2, COG6-FRB::hphNT1, YBR080C-myeGFP::HIS3* | This study |
| OGYSGA1729 | *MATa, his3Δ1, leu2Δ0, ura3Δ0, LYS+, can1Δ::STE2pr-LEU2, lyp1Δ::, tor1-1, fpr1Δ::klURA, Tub4-(6)-RFP-(24)-FKBP::natNT2, COG6-FRB::hphNT1, YBR168W-myeGFP::HIS3* | This study |
| OGYSGA1730 | *MATa, his3Δ1, leu2Δ0, ura3Δ0, LYS+, can1Δ::STE2pr-LEU2, lyp1Δ::, tor1-1, fpr1Δ::klURA, Tub4-(6)-RFP-(24)-FKBP::natNT2, COG6-FRB::hphNT1, YLR350W-myeGFP::HIS3* | This study |
| OGYSGA1731 | *MATa, his3Δ1, leu2Δ0, ura3Δ0, LYS+, can1Δ::STE2pr-LEU2, lyp1Δ::, tor1-1, fpr1Δ::klURA, Tub4-(6)-RFP-(24)-FKBP::natNT2, COG6-FRB::hphNT1, YNL169C-myeGFP::HIS3* | This study |
| OGYSGA1732 | *MATa, his3Δ1, leu2Δ0, ura3Δ0, LYS+, can1Δ::STE2pr-LEU2, lyp1Δ::, tor1-1, fpr1Δ::klURA, Tub4-(6)-RFP-(24)-FKBP::natNT2, COG6-FRB::hphNT1, YHR181W-myeGFP::HIS3* | This study |
| OGYSGA1733 | *MATa, his3Δ1, leu2Δ0, ura3Δ0, LYS+, can1Δ::STE2pr-LEU2, lyp1Δ::, tor1-1, fpr1Δ::klURA, Tub4-(6)-RFP-(24)-FKBP::natNT2, COG6-FRB::hphNT1, YLR085C-myeGFP::HIS3* | This study |
| OGYSGA1734 | *MATa, his3Δ1, leu2Δ0, ura3Δ0, LYS+, can1Δ::STE2pr-LEU2, lyp1Δ::, tor1-1, fpr1Δ::klURA, Tub4-(6)-RFP-(24)-FKBP::natNT2, COG6-FRB::hphNT1, YGL167C-myeGFP::HIS3* | This study |
| OGYSGA1735 | *MATa, his3Δ1, leu2Δ0, ura3Δ0, LYS+, can1Δ::STE2pr-LEU2, lyp1Δ::, tor1-1, fpr1Δ::klURA, Tub4-(6)-RFP-(24)-FKBP::natNT2, COG6-FRB::hphNT1, YLL038C-myeGFP::HIS3* | This study |
| OGYSGA1736 | *MATa, his3Δ1, leu2Δ0, ura3Δ0, LYS+, can1Δ::STE2pr-LEU2, lyp1Δ::, tor1-1, fpr1Δ::klURA, Tub4-(6)-RFP-(24)-FKBP::natNT2, COG6-FRB::hphNT1, YGR089W-myeGFP::HIS3* | This study |
| OGYSGA1737 | *MATa, his3Δ1, leu2Δ0, ura3Δ0, LYS+, can1Δ::STE2pr-LEU2, lyp1Δ::, tor1-1, fpr1Δ::klURA, Tub4-(6)-RFP-(24)-FKBP::natNT2, COG6-FRB::hphNT1, YMR004W-myeGFP::HIS3* | This study |
| OGYSGA1738 | *MATa, his3Δ1, leu2Δ0, ura3Δ0, LYS+, can1Δ::STE2pr-LEU2, lyp1Δ::, tor1-1, fpr1Δ::klURA, Tub4-(6)-RFP-(24)-FKBP::natNT2, COG6-FRB::hphNT1, YBR231C-myeGFP::HIS3* | This study |
| OGYSGA1739 | *MATa, his3Δ1, leu2Δ0, ura3Δ0, LYS+, can1Δ::STE2pr-LEU2, lyp1Δ::, tor1-1, fpr1Δ::klURA, Tub4-(6)-RFP-(24)-FKBP::natNT2, COG6-FRB::hphNT1, YMR307W-myeGFP::HIS3* | This study |
| OGYSGA1740 | *MATa, his3Δ1, leu2Δ0, ura3Δ0, LYS+, can1Δ::STE2pr-LEU2, lyp1Δ::, tor1-1, fpr1Δ::klURA, Tub4-(6)-RFP-(24)-FKBP::natNT2, COG6-FRB::hphNT1, YGR106C-myeGFP::HIS3* | This study |
| OGYSGA1741 | *MATa, his3Δ1, leu2Δ0, ura3Δ0, LYS+, can1Δ::STE2pr-LEU2, lyp1Δ::, tor1-1, fpr1Δ::klURA, Tub4-(6)-RFP-(24)-FKBP::natNT2, COG6-FRB::hphNT1, YJL024C-myeGFP::HIS3* | This study |
| OGYSGA1742 | *MATa, his3Δ1, leu2Δ0, ura3Δ0, LYS+, can1Δ::STE2pr-LEU2, lyp1Δ::, tor1-1, fpr1Δ::klURA, Tub4-(6)-RFP-(24)-FKBP::natNT2, COG6-FRB::hphNT1, YOR244W-myeGFP::HIS3* | This study |
| OGYSGA1743 | *MATa, his3Δ1, leu2Δ0, ura3Δ0, LYS+, can1Δ::STE2pr-LEU2, lyp1Δ::, tor1-1, fpr1Δ::klURA, Tub4-(6)-RFP-(24)-FKBP::natNT2, COG6-FRB::hphNT1, YOL012C-myeGFP::HIS3* | This study |
| OGYSGA1744 | *MATa, his3Δ1, leu2Δ0, ura3Δ0, LYS+, can1Δ::STE2pr-LEU2, lyp1Δ::, tor1-1, fpr1Δ::klURA, Tub4-(6)-RFP-(24)-FKBP::natNT2, COG6-FRB::hphNT1, YHR059W-myeGFP::HIS3* | This study |
| OGYSGA1745 | *MATa, his3Δ1, leu2Δ0, ura3Δ0, LYS+, can1Δ::STE2pr-LEU2, lyp1Δ::, tor1-1, fpr1Δ::klURA, Tub4-(6)-RFP-(24)-FKBP::natNT2, COG6-FRB::hphNT1, YGR105W-myeGFP::HIS3* | This study |
| OGYSGA1746 | *MATa, his3Δ1, leu2Δ0, ura3Δ0, LYS+, can1Δ::STE2pr-LEU2, lyp1Δ::, tor1-1, fpr1Δ::klURA, Tub4-(6)-RFP-(24)-FKBP::natNT2, COG6-FRB::hphNT1, YCL001W-myeGFP::HIS3* | This study |

## APPENDIX I – YEAST STRAINS

| | | |
|---|---|---|
| OGYSGA1747 | *MATa, his3Δ1, leu2Δ0, ura3Δ0, LYS+, can1Δ::STE2pr-LEU2, lyp1Δ::, tor1-1, fpr1Δ::klURA, Tub4-(6)-RFP-(24)-FKBP::natNT2, COG6-FRB::hphNT1, YNL322C-myeGFP::HIS3* | This study |
| OGYSGA1748 | *MATa, his3Δ1, leu2Δ0, ura3Δ0, LYS+, can1Δ::STE2pr-LEU2, lyp1Δ::, tor1-1, fpr1Δ::klURA, Tub4-(6)-RFP-(24)-FKBP::natNT2, COG6-FRB::hphNT1, YPR057W-myeGFP::HIS3* | This study |
| OGYSGA1749 | *MATa, his3Δ1, leu2Δ0, ura3Δ0, LYS+, can1Δ::STE2pr-LEU2, lyp1Δ::, tor1-1, fpr1Δ::klURA, Tub4-(6)-RFP-(24)-FKBP::natNT2, COG6-FRB::hphNT1, YIR005W-myeGFP::HIS3* | This study |
| OGYSGA1750 | *MATa, his3Δ1, leu2Δ0, ura3Δ0, LYS+, can1Δ::STE2pr-LEU2, lyp1Δ::, tor1-1, fpr1Δ::klURA, Tub4-(6)-RFP-(24)-FKBP::natNT2, COG6-FRB::hphNT1, YGL212W-myeGFP::HIS3* | This study |
| OGYSGA1751 | *MATa, his3Δ1, leu2Δ0, ura3Δ0, LYS+, can1Δ::STE2pr-LEU2, lyp1Δ::, tor1-1, fpr1Δ::klURA, Tub4-(6)-RFP-(24)-FKBP::natNT2, COG6-FRB::hphNT1, YCR063W-myeGFP::HIS3* | This study |
| OGYSGA1752 | *MATa, his3Δ1, leu2Δ0, ura3Δ0, LYS+, can1Δ::STE2pr-LEU2, lyp1Δ::, tor1-1, fpr1Δ::klURA, Tub4-(6)-RFP-(24)-FKBP::natNT2, COG6-FRB::hphNT1, YPL234C-myeGFP::HIS3* | This study |
| OGYSGA1753 | *MATa, his3Δ1, leu2Δ0, ura3Δ0, LYS+, can1Δ::STE2pr-LEU2, lyp1Δ::, tor1-1, fpr1Δ::klURA, Tub4-(6)-RFP-(24)-FKBP::natNT2, COG6-FRB::hphNT1, YDR331W-myeGFP::HIS3* | This study |
| OGYSGA1754 | *MATa, his3Δ1, leu2Δ0, ura3Δ0, LYS+, can1Δ::STE2pr-LEU2, lyp1Δ::, tor1-1, fpr1Δ::klURA, Tub4-(6)-RFP-(24)-FKBP::natNT2, COG6-FRB::hphNT1, YJL062W-myeGFP::HIS3* | This study |
| OGYSGA1755 | *MATa, his3Δ1, leu2Δ0, ura3Δ0, LYS+, can1Δ::STE2pr-LEU2, lyp1Δ::, tor1-1, fpr1Δ::klURA, Tub4-(6)-RFP-(24)-FKBP::natNT2, COG6-FRB::hphNT1, YJR075W-myeGFP::HIS3* | This study |
| OGYSGA1756 | *MATa, his3Δ1, leu2Δ0, ura3Δ0, LYS+, can1Δ::STE2pr-LEU2, lyp1Δ::, tor1-1, fpr1Δ::klURA, Tub4-(6)-RFP-(24)-FKBP::natNT2, COG6-FRB::hphNT1, YKL139W-myeGFP::HIS3* | This study |
| OGYSGA1757 | *MATa, his3Δ1, leu2Δ0, ura3Δ0, LYS+, can1Δ::STE2pr-LEU2, lyp1Δ::, tor1-1, fpr1Δ::klURA, Tub4-(6)-RFP-(24)-FKBP::natNT2, COG6-FRB::hphNT1, YML097C-myeGFP::HIS3* | This study |
| OGYSGA1758 | *MATa, his3Δ1, leu2Δ0, ura3Δ0, LYS+, can1Δ::STE2pr-LEU2, lyp1Δ::, tor1-1, fpr1Δ::klURA, Tub4-(6)-RFP-(24)-FKBP::natNT2, COG6-FRB::hphNT1, YKL048C-myeGFP::HIS3* | This study |
| OGYSGA1759 | *MATa, his3Δ1, leu2Δ0, ura3Δ0, LYS+, can1Δ::STE2pr-LEU2, lyp1Δ::, tor1-1, fpr1Δ::klURA, Tub4-(6)-RFP-(24)-FKBP::natNT2, COG6-FRB::hphNT1, YLR200W-myeGFP::HIS3* | This study |
| OGYSGA1760 | *MATa, his3Δ1, leu2Δ0, ura3Δ0, LYS+, can1Δ::STE2pr-LEU2, lyp1Δ::, tor1-1, fpr1Δ::klURA, Tub4-(6)-RFP-(24)-FKBP::natNT2, COG6-FRB::hphNT1, YDR225W-myeGFP::HIS3* | This study |
| OGYSGA1761 | *MATa, his3Δ1, leu2Δ0, ura3Δ0, LYS+, can1Δ::STE2pr-LEU2, lyp1Δ::, tor1-1, fpr1Δ::klURA, Tub4-(6)-RFP-(24)-FKBP::natNT2, COG6-FRB::hphNT1, YPL069C-myeGFP::HIS3* | This study |
| OGYSGA1762 | *MATa, his3Δ1, leu2Δ0, ura3Δ0, LYS+, can1Δ::STE2pr-LEU2, lyp1Δ::, tor1-1, fpr1Δ::klURA, Tub4-(6)-RFP-(24)-FKBP::natNT2, COG6-FRB::hphNT1, YKR001C-myeGFP::HIS3* | This study |
| OGYSGA1763 | *MATa, his3Δ1, leu2Δ0, ura3Δ0, LYS+, can1Δ::STE2pr-LEU2, lyp1Δ::, tor1-1, fpr1Δ::klURA, Tub4-(6)-RFP-(24)-FKBP::natNT2, COG6-FRB::hphNT1, YGR157W-myeGFP::HIS3* | This study |
| OGYSGA1764 | *MATa, his3Δ1, leu2Δ0, ura3Δ0, LYS+, can1Δ::STE2pr-LEU2, lyp1Δ::, tor1-1, fpr1Δ::klURA, Tub4-(6)-RFP-(24)-FKBP::natNT2, COG6-FRB::hphNT1, YPL158C-myeGFP::HIS3* | This study |
| OGYSGA1765 | *MATa, his3Δ1, leu2Δ0, ura3Δ0, LYS+, can1Δ::STE2pr-LEU2, lyp1Δ::, tor1-1, fpr1Δ::klURA, Tub4-(6)-RFP-(24)-FKBP::natNT2, COG6-FRB::hphNT1, YIL076W-myeGFP::HIS3* | This study |
| OGYSGA1766 | *MATa, his3Δ1, leu2Δ0, ura3Δ0, LYS+, can1Δ::STE2pr-LEU2, lyp1Δ::, tor1-1, fpr1Δ::klURA, Tub4-(6)-RFP-(24)-FKBP::natNT2, COG6-FRB::hphNT1, YDR434W-myeGFP::HIS3* | This study |
| OGYSGA1767 | *MATa, his3Δ1, leu2Δ0, ura3Δ0, LYS+, can1Δ::STE2pr-LEU2, lyp1Δ::, tor1-1, fpr1Δ::klURA, Tub4-(6)-RFP-(24)-FKBP::natNT2, COG6-FRB::hphNT1, YPR017C-myeGFP::HIS3* | This study |
| OGYSGA1768 | *MATa, his3Δ1, leu2Δ0, ura3Δ0, LYS+, can1Δ::STE2pr-LEU2, lyp1Δ::, tor1-1, fpr1Δ::klURA, Tub4-(6)-RFP-(24)-FKBP::natNT2, COG6-FRB::hphNT1, YLL006W-myeGFP::HIS3* | This study |
| OGYSGA1769 | *MATa, his3Δ1, leu2Δ0, ura3Δ0, LYS+, can1Δ::STE2pr-LEU2, lyp1Δ::, tor1-1, fpr1Δ::klURA, Tub4-(6)-RFP-(24)-FKBP::natNT2, COG6-FRB::hphNT1, YDR485C-myeGFP::HIS3* | This study |
| OGYSGA1770 | *MATa, his3Δ1, leu2Δ0, ura3Δ0, LYS+, can1Δ::STE2pr-LEU2, lyp1Δ::, tor1-1, fpr1Δ::klURA, Tub4-(6)-RFP-(24)-FKBP::natNT2, COG6-FRB::hphNT1, YJL034W-myeGFP::HIS3* | This study |
| OGYSGA1771 | *MATa, his3Δ1, leu2Δ0, ura3Δ0, LYS+, can1Δ::STE2pr-LEU2, lyp1Δ::, tor1-1, fpr1Δ::klURA, Tub4-(6)-RFP-(24)-FKBP::natNT2, COG6-FRB::hphNT1, YJL210W-myeGFP::HIS3* | This study |
| OGYSGA1772 | *MATa, his3Δ1, leu2Δ0, ura3Δ0, LYS+, can1Δ::STE2pr-LEU2, lyp1Δ::, tor1-1, fpr1Δ::klURA, Tub4-(6)-RFP-(24)-FKBP::natNT2, COG6-FRB::hphNT1, YER111C-myeGFP::HIS3* | This study |
| OGYSGA1773 | *MATa, his3Δ1, leu2Δ0, ura3Δ0, LYS+, can1Δ::STE2pr-LEU2, lyp1Δ::, tor1-1, fpr1Δ::klURA, Tub4-(6)-RFP-(24)-FKBP::natNT2, COG6-FRB::hphNT1, YDR186C-myeGFP::HIS3* | This study |

## APPENDIX I – YEAST STRAINS

| | | |
|---|---|---|
| OGYSGA1774 | *MATa, his3Δ1, leu2Δ0, ura3Δ0, LYS+, can1Δ::STE2pr-LEU2, lyp1Δ::, tor1-1, fpr1Δ::klURA, Tub4-(6)-RFP-(24)-FKBP::natNT2, COG6-FRB::hphNT1, YNL008C-myeGFP::HIS3* | This study |
| OGYSGA1775 | *MATa, his3Δ1, leu2Δ0, ura3Δ0, LYS+, can1Δ::STE2pr-LEU2, lyp1Δ::, tor1-1, fpr1Δ::klURA, Tub4-(6)-RFP-(24)-FKBP::natNT2, COG6-FRB::hphNT1, YOR112W-myeGFP::HIS3* | This study |
| OGYSGA1776 | *MATa, his3Δ1, leu2Δ0, ura3Δ0, LYS+, can1Δ::STE2pr-LEU2, lyp1Δ::, tor1-1, fpr1Δ::klURA, Tub4-(6)-RFP-(24)-FKBP::natNT2, COG6-FRB::hphNT1, YLR208W-myeGFP::HIS3* | This study |
| OGYSGA1777 | *MATa, his3Δ1, leu2Δ0, ura3Δ0, LYS+, can1Δ::STE2pr-LEU2, lyp1Δ::, tor1-1, fpr1Δ::klURA, Tub4-(6)-RFP-(24)-FKBP::natNT2, COG6-FRB::hphNT1, YER151C-myeGFP::HIS3* | This study |
| OGYSGA1778 | *MATa, his3Δ1, leu2Δ0, ura3Δ0, LYS+, can1Δ::STE2pr-LEU2, lyp1Δ::, tor1-1, fpr1Δ::klURA, Tub4-(6)-RFP-(24)-FKBP::natNT2, COG6-FRB::hphNT1, YJL002C-myeGFP::HIS3* | This study |
| OGYSGA1779 | *MATa, his3Δ1, leu2Δ0, ura3Δ0, LYS+, can1Δ::STE2pr-LEU2, lyp1Δ::, tor1-1, fpr1Δ::klURA, Tub4-(6)-RFP-(24)-FKBP::natNT2, COG6-FRB::hphNT1, YAL009W-myeGFP::HIS3* | This study |
| OGYSGA1780 | *MATa, his3Δ1, leu2Δ0, ura3Δ0, LYS+, can1Δ::STE2pr-LEU2, lyp1Δ::, tor1-1, fpr1Δ::klURA, Tub4-(6)-RFP-(24)-FKBP::natNT2, COG6-FRB::hphNT1, YHL033C-myeGFP::HIS3* | This study |
| OGYSGA1781 | *MATa, his3Δ1, leu2Δ0, ura3Δ0, LYS+, can1Δ::STE2pr-LEU2, lyp1Δ::, tor1-1, fpr1Δ::klURA, Tub4-(6)-RFP-(24)-FKBP::natNT2, COG6-FRB::hphNT1, YEL043W-myeGFP::HIS3* | This study |
| OGYSGA1782 | *MATa, his3Δ1, leu2Δ0, ura3Δ0, LYS+, can1Δ::STE2pr-LEU2, lyp1Δ::, tor1-1, fpr1Δ::klURA, Tub4-(6)-RFP-(24)-FKBP::natNT2, COG6-FRB::hphNT1, YJL082W-myeGFP::HIS3* | This study |
| OGYSGA1783 | *MATa, his3Δ1, leu2Δ0, ura3Δ0, LYS+, can1Δ::STE2pr-LEU2, lyp1Δ::, tor1-1, fpr1Δ::klURA, Tub4-(6)-RFP-(24)-FKBP::natNT2, COG6-FRB::hphNT1, YPL105C-myeGFP::HIS3* | This study |
| OGYSGA1784 | *MATa, his3Δ1, leu2Δ0, ura3Δ0, LYS+, can1Δ::STE2pr-LEU2, lyp1Δ::, tor1-1, fpr1Δ::klURA, Tub4-(6)-RFP-(24)-FKBP::natNT2, COG6-FRB::hphNT1, YBL022C-myeGFP::HIS3* | This study |
| OGYSGA1785 | *MATa, his3Δ1, leu2Δ0, ura3Δ0, LYS+, can1Δ::STE2pr-LEU2, lyp1Δ::, tor1-1, fpr1Δ::klURA, Tub4-(6)-RFP-(24)-FKBP::natNT2, COG6-FRB::hphNT1, YDR372C-myeGFP::HIS3* | This study |
| OGYSGA1786 | *MATa, his3Δ1, leu2Δ0, ura3Δ0, LYS+, can1Δ::STE2pr-LEU2, lyp1Δ::, tor1-1, fpr1Δ::klURA, Tub4-(6)-RFP-(24)-FKBP::natNT2, COG6-FRB::hphNT1, YJR033C-myeGFP::HIS3* | This study |
| OGYSGA1787 | *MATa, his3Δ1, leu2Δ0, ura3Δ0, LYS+, can1Δ::STE2pr-LEU2, lyp1Δ::, tor1-1, fpr1Δ::klURA, Tub4-(6)-RFP-(24)-FKBP::natNT2, COG6-FRB::hphNT1, YDR141C-myeGFP::HIS3* | This study |
| OGYSGA1788 | *MATa, his3Δ1, leu2Δ0, ura3Δ0, LYS+, can1Δ::STE2pr-LEU2, lyp1Δ::, tor1-1, fpr1Δ::klURA, Tub4-(6)-RFP-(24)-FKBP::natNT2, COG6-FRB::hphNT1, YGL219C-myeGFP::HIS3* | This study |
| OGYSGA1789 | *MATa, his3Δ1, leu2Δ0, ura3Δ0, LYS+, can1Δ::STE2pr-LEU2, lyp1Δ::, tor1-1, fpr1Δ::klURA, Tub4-(6)-RFP-(24)-FKBP::natNT2, COG6-FRB::hphNT1, YBR127C-myeGFP::HIS3* | This study |
| OGYSGA1790 | *MATa, his3Δ1, leu2Δ0, ura3Δ0, LYS+, can1Δ::STE2pr-LEU2, lyp1Δ::, tor1-1, fpr1Δ::klURA, Tub4-(6)-RFP-(24)-FKBP::natNT2, COG6-FRB::hphNT1, YOR078W-myeGFP::HIS3* | This study |
| OGYSGA1791 | *MATa, his3Δ1, leu2Δ0, ura3Δ0, LYS+, can1Δ::STE2pr-LEU2, lyp1Δ::, tor1-1, fpr1Δ::klURA, Tub4-(6)-RFP-(24)-FKBP::natNT2, COG6-FRB::hphNT1, YDR432W-myeGFP::HIS3* | This study |
| OGYSGA1792 | *MATa, his3Δ1, leu2Δ0, ura3Δ0, LYS+, can1Δ::STE2pr-LEU2, lyp1Δ::, tor1-1, fpr1Δ::klURA, Tub4-(6)-RFP-(24)-FKBP::natNT2, COG6-FRB::hphNT1, YDR069C-myeGFP::HIS3* | This study |
| OGYSGA1793 | *MATa, his3Δ1, leu2Δ0, ura3Δ0, LYS+, can1Δ::STE2pr-LEU2, lyp1Δ::, tor1-1, fpr1Δ::klURA, Tub4-(6)-RFP-(24)-FKBP::natNT2, COG6-FRB::hphNT1, YKL110C-myeGFP::HIS3* | This study |
| OGYSGA1794 | *MATa, his3Δ1, leu2Δ0, ura3Δ0, LYS+, can1Δ::STE2pr-LEU2, lyp1Δ::, tor1-1, fpr1Δ::klURA, Tub4-(6)-RFP-(24)-FKBP::natNT2, COG6-FRB::hphNT1, YLR260W-myeGFP::HIS3* | This study |
| OGYSGA1795 | *MATa, his3Δ1, leu2Δ0, ura3Δ0, LYS+, can1Δ::STE2pr-LEU2, lyp1Δ::, tor1-1, fpr1Δ::klURA, Tub4-(6)-RFP-(24)-FKBP::natNT2, COG6-FRB::hphNT1, YMR060C-myeGFP::HIS3* | This study |
| OGYSGA1796 | *MATa, his3Δ1, leu2Δ0, ura3Δ0, LYS+, can1Δ::STE2pr-LEU2, lyp1Δ::, tor1-1, fpr1Δ::klURA, Tub4-(6)-RFP-(24)-FKBP::natNT2, COG6-FRB::hphNT1, YGR072W-myeGFP::HIS3* | This study |
| OGYSGA1797 | *MATa, his3Δ1, leu2Δ0, ura3Δ0, LYS+, can1Δ::STE2pr-LEU2, lyp1Δ::, tor1-1, fpr1Δ::klURA, Tub4-(6)-RFP-(24)-FKBP::natNT2, COG6-FRB::hphNT1, YCR094W-myeGFP::HIS3* | This study |
| OGYSGA1798 | *MATa, his3Δ1, leu2Δ0, ura3Δ0, LYS+, can1Δ::STE2pr-LEU2, lyp1Δ::, tor1-1, fpr1Δ::klURA, Tub4-(6)-RFP-(24)-FKBP::natNT2, COG6-FRB::hphNT1, YDR297W-myeGFP::HIS3* | This study |
| OGYSGA1799 | *MATa, his3Δ1, leu2Δ0, ura3Δ0, LYS+, can1Δ::STE2pr-LEU2, lyp1Δ::, tor1-1, fpr1Δ::klURA, Tub4-(6)-RFP-(24)-FKBP::natNT2, COG6-FRB::hphNT1, YER089C-myeGFP::HIS3* | This study |
| OGYSGA1800 | *MATa, his3Δ1, leu2Δ0, ura3Δ0, LYS+, can1Δ::STE2pr-LEU2, lyp1Δ::, tor1-1, fpr1Δ::klURA, Tub4-(6)-RFP-(24)-FKBP::natNT2, COG6-FRB::hphNT1, YLR110C-myeGFP::HIS3* | This study |

## APPENDIX I – YEAST STRAINS

| | | |
|---|---|---|
| OGYSGA1801 | *MATa, his3Δ1, leu2Δ0, ura3Δ0, LYS+, can1Δ::STE2pr-LEU2, lyp1Δ::, tor1-1, fpr1Δ::klURA, Tub4-(6)-RFP-(24)-FKBP::natNT2, COG6-FRB::hphNT1, YNL141W-myeGFP::HIS3* | This study |
| OGYSGA1802 | *MATa, his3Δ1, leu2Δ0, ura3Δ0, LYS+, can1Δ::STE2pr-LEU2, lyp1Δ::, tor1-1, fpr1Δ::klURA, Tub4-(6)-RFP-(24)-FKBP::natNT2, COG6-FRB::hphNT1, YNL238W-myeGFP::HIS3* | This study |
| OGYSGA1803 | *MATa, his3Δ1, leu2Δ0, ura3Δ0, LYS+, can1Δ::STE2pr-LEU2, lyp1Δ::, tor1-1, fpr1Δ::klURA, Tub4-(6)-RFP-(24)-FKBP::natNT2, COG6-FRB::hphNT1, YKL006W-myeGFP::HIS3* | This study |
| OGYSGA1804 | *MATa, his3Δ1, leu2Δ0, ura3Δ0, LYS+, can1Δ::STE2pr-LEU2, lyp1Δ::, tor1-1, fpr1Δ::klURA, Tub4-(6)-RFP-(24)-FKBP::natNT2, COG6-FRB::hphNT1, YDL226C-myeGFP::HIS3* | This study |
| OGYSGA1805 | *MATa, his3Δ1, leu2Δ0, ura3Δ0, LYS+, can1Δ::STE2pr-LEU2, lyp1Δ::, tor1-1, fpr1Δ::klURA, Tub4-(6)-RFP-(24)-FKBP::natNT2, COG6-FRB::hphNT1, YNL251C-myeGFP::HIS3* | This study |
| OGYSGA6452 | *MATa, his3Δ1, leu2Δ0, ura3Δ0, LYS+, can1Δ::STE2pr-LEU2, lyp1Δ::, tor1-1, fpr1Δ::klURA, Tub4-(6)-RFP-(24)-FKBP::natNT2, VPS3-FRB::hphNT1, YDR150W-myeGFP::HIS3* | This study |
| OGYSGA6453 | *MATa, his3Δ1, leu2Δ0, ura3Δ0, LYS+, can1Δ::STE2pr-LEU2, lyp1Δ::, tor1-1, fpr1Δ::klURA, Tub4-(6)-RFP-(24)-FKBP::natNT2, VPS3-FRB::hphNT1, YDL040C-myeGFP::HIS3* | This study |
| OGYSGA6454 | *MATa, his3Δ1, leu2Δ0, ura3Δ0, LYS+, can1Δ::STE2pr-LEU2, lyp1Δ::, tor1-1, fpr1Δ::klURA, Tub4-(6)-RFP-(24)-FKBP::natNT2, VPS3-FRB::hphNT1, YPL084W-myeGFP::HIS3* | This study |
| OGYSGA6455 | *MATa, his3Δ1, leu2Δ0, ura3Δ0, LYS+, can1Δ::STE2pr-LEU2, lyp1Δ::, tor1-1, fpr1Δ::klURA, Tub4-(6)-RFP-(24)-FKBP::natNT2, VPS3-FRB::hphNT1, YGR198W-myeGFP::HIS3* | This study |
| OGYSGA6456 | *MATa, his3Δ1, leu2Δ0, ura3Δ0, LYS+, can1Δ::STE2pr-LEU2, lyp1Δ::, tor1-1, fpr1Δ::klURA, Tub4-(6)-RFP-(24)-FKBP::natNT2, VPS3-FRB::hphNT1, YFL024C-myeGFP::HIS3* | This study |
| OGYSGA6457 | *MATa, his3Δ1, leu2Δ0, ura3Δ0, LYS+, can1Δ::STE2pr-LEU2, lyp1Δ::, tor1-1, fpr1Δ::klURA, Tub4-(6)-RFP-(24)-FKBP::natNT2, VPS3-FRB::hphNT1, YPL153C-myeGFP::HIS3* | This study |
| OGYSGA6458 | *MATa, his3Δ1, leu2Δ0, ura3Δ0, LYS+, can1Δ::STE2pr-LEU2, lyp1Δ::, tor1-1, fpr1Δ::klURA, Tub4-(6)-RFP-(24)-FKBP::natNT2, VPS3-FRB::hphNT1, YMR078C-myeGFP::HIS3* | This study |
| OGYSGA6459 | *MATa, his3Δ1, leu2Δ0, ura3Δ0, LYS+, can1Δ::STE2pr-LEU2, lyp1Δ::, tor1-1, fpr1Δ::klURA, Tub4-(6)-RFP-(24)-FKBP::natNT2, VPS3-FRB::hphNT1, YDL074C-myeGFP::HIS3* | This study |
| OGYSGA6460 | *MATa, his3Δ1, leu2Δ0, ura3Δ0, LYS+, can1Δ::STE2pr-LEU2, lyp1Δ::, tor1-1, fpr1Δ::klURA, Tub4-(6)-RFP-(24)-FKBP::natNT2, VPS3-FRB::hphNT1, YNL021W-myeGFP::HIS3* | This study |
| OGYSGA6461 | *MATa, his3Δ1, leu2Δ0, ura3Δ0, LYS+, can1Δ::STE2pr-LEU2, lyp1Δ::, tor1-1, fpr1Δ::klURA, Tub4-(6)-RFP-(24)-FKBP::natNT2, VPS3-FRB::hphNT1, YLR153C-myeGFP::HIS3* | This study |
| OGYSGA6462 | *MATa, his3Δ1, leu2Δ0, ura3Δ0, LYS+, can1Δ::STE2pr-LEU2, lyp1Δ::, tor1-1, fpr1Δ::klURA, Tub4-(6)-RFP-(24)-FKBP::natNT2, VPS3-FRB::hphNT1, YOL115W-myeGFP::HIS3* | This study |
| OGYSGA6463 | *MATa, his3Δ1, leu2Δ0, ura3Δ0, LYS+, can1Δ::STE2pr-LEU2, lyp1Δ::, tor1-1, fpr1Δ::klURA, Tub4-(6)-RFP-(24)-FKBP::natNT2, VPS3-FRB::hphNT1, YGL116W-myeGFP::HIS3* | This study |
| OGYSGA6464 | *MATa, his3Δ1, leu2Δ0, ura3Δ0, LYS+, can1Δ::STE2pr-LEU2, lyp1Δ::, tor1-1, fpr1Δ::klURA, Tub4-(6)-RFP-(24)-FKBP::natNT2, VPS3-FRB::hphNT1, YPL086C-myeGFP::HIS3* | This study |
| OGYSGA6465 | *MATa, his3Δ1, leu2Δ0, ura3Δ0, LYS+, can1Δ::STE2pr-LEU2, lyp1Δ::, tor1-1, fpr1Δ::klURA, Tub4-(6)-RFP-(24)-FKBP::natNT2, VPS3-FRB::hphNT1, YDL020C-myeGFP::HIS3* | This study |
| OGYSGA6466 | *MATa, his3Δ1, leu2Δ0, ura3Δ0, LYS+, can1Δ::STE2pr-LEU2, lyp1Δ::, tor1-1, fpr1Δ::klURA, Tub4-(6)-RFP-(24)-FKBP::natNT2, VPS3-FRB::hphNT1, YJL081C-myeGFP::HIS3* | This study |
| OGYSGA6467 | *MATa, his3Δ1, leu2Δ0, ura3Δ0, LYS+, can1Δ::STE2pr-LEU2, lyp1Δ::, tor1-1, fpr1Δ::klURA, Tub4-(6)-RFP-(24)-FKBP::natNT2, VPS3-FRB::hphNT1, YGR002C-myeGFP::HIS3* | This study |
| OGYSGA6468 | *MATa, his3Δ1, leu2Δ0, ura3Δ0, LYS+, can1Δ::STE2pr-LEU2, lyp1Δ::, tor1-1, fpr1Δ::klURA, Tub4-(6)-RFP-(24)-FKBP::natNT2, VPS3-FRB::hphNT1, YML097C-myeGFP::HIS3* | This study |
| OGYSGA6469 | *MATa, his3Δ1, leu2Δ0, ura3Δ0, LYS+, can1Δ::STE2pr-LEU2, lyp1Δ::, tor1-1, fpr1Δ::klURA, Tub4-(6)-RFP-(24)-FKBP::natNT2, VPS3-FRB::hphNT1, YHL002W-myeGFP::HIS3* | This study |
| OGYSGA6470 | *MATa, his3Δ1, leu2Δ0, ura3Δ0, LYS+, can1Δ::STE2pr-LEU2, lyp1Δ::, tor1-1, fpr1Δ::klURA, Tub4-(6)-RFP-(24)-FKBP::natNT2, VPS3-FRB::hphNT1, YOR244W-myeGFP::HIS3* | This study |
| OGYSGA6471 | *MATa, his3Δ1, leu2Δ0, ura3Δ0, LYS+, can1Δ::STE2pr-LEU2, lyp1Δ::, tor1-1, fpr1Δ::klURA, Tub4-(6)-RFP-(24)-FKBP::natNT2, VPS3-FRB::hphNT1, YGR122W-myeGFP::HIS3* | This study |
| OGYSGA6472 | *MATa, his3Δ1, leu2Δ0, ura3Δ0, LYS+, can1Δ::STE2pr-LEU2, lyp1Δ::, tor1-1, fpr1Δ::klURA, Tub4-(6)-RFP-(24)-FKBP::natNT2, VPS3-FRB::hphNT1, YKL113C-myeGFP::HIS3* | This study |
| OGYSGA6473 | *MATa, his3Δ1, leu2Δ0, ura3Δ0, LYS+, can1Δ::STE2pr-LEU2, lyp1Δ::, tor1-1, fpr1Δ::klURA, Tub4-(6)-RFP-(24)-FKBP::natNT2, VPS3-FRB::hphNT1, YCL016C-myeGFP::HIS3* | This study |

## APPENDIX I – YEAST STRAINS

| | | |
|---|---|---|
| OGYSGA6474 | *MATa, his3Δ1, leu2Δ0, ura3Δ0, LYS+, can1Δ::STE2pr-LEU2, lyp1Δ::, tor1-1, fpr1Δ::klURA, Tub4-(6)-RFP-(24)-FKBP::natNT2, VPS3-FRB::hphNT1, YJR043C-myeGFP::HIS3* | This study |
| OGYSGA6475 | *MATa, his3Δ1, leu2Δ0, ura3Δ0, LYS+, can1Δ::STE2pr-LEU2, lyp1Δ::, tor1-1, fpr1Δ::klURA, Tub4-(6)-RFP-(24)-FKBP::natNT2, VPS3-FRB::hphNT1, YPL055C-myeGFP::HIS3* | This study |
| OGYSGA6476 | *MATa, his3Δ1, leu2Δ0, ura3Δ0, LYS+, can1Δ::STE2pr-LEU2, lyp1Δ::, tor1-1, fpr1Δ::klURA, Tub4-(6)-RFP-(24)-FKBP::natNT2, VPS3-FRB::hphNT1, YER083C-myeGFP::HIS3* | This study |
| OGYSGA6477 | *MATa, his3Δ1, leu2Δ0, ura3Δ0, LYS+, can1Δ::STE2pr-LEU2, lyp1Δ::, tor1-1, fpr1Δ::klURA, Tub4-(6)-RFP-(24)-FKBP::natNT2, VPS3-FRB::hphNT1, YPR066W-myeGFP::HIS3* | This study |
| OGYSGA6478 | *MATa, his3Δ1, leu2Δ0, ura3Δ0, LYS+, can1Δ::STE2pr-LEU2, lyp1Δ::, tor1-1, fpr1Δ::klURA, Tub4-(6)-RFP-(24)-FKBP::natNT2, VPS3-FRB::hphNT1, YJL115W-myeGFP::HIS3* | This study |
| OGYSGA6479 | *MATa, his3Δ1, leu2Δ0, ura3Δ0, LYS+, can1Δ::STE2pr-LEU2, lyp1Δ::, tor1-1, fpr1Δ::klURA, Tub4-(6)-RFP-(24)-FKBP::natNT2, VPS3-FRB::hphNT1, YHR200W-myeGFP::HIS3* | This study |
| OGYSGA6480 | *MATa, his3Δ1, leu2Δ0, ura3Δ0, LYS+, can1Δ::STE2pr-LEU2, lyp1Δ::, tor1-1, fpr1Δ::klURA, Tub4-(6)-RFP-(24)-FKBP::natNT2, VPS3-FRB::hphNT1, YMR161W-myeGFP::HIS3* | This study |
| OGYSGA6481 | *MATa, his3Δ1, leu2Δ0, ura3Δ0, LYS+, can1Δ::STE2pr-LEU2, lyp1Δ::, tor1-1, fpr1Δ::klURA, Tub4-(6)-RFP-(24)-FKBP::natNT2, VPS3-FRB::hphNT1, YHR013C-myeGFP::HIS3* | This study |
| OGYSGA6482 | *MATa, his3Δ1, leu2Δ0, ura3Δ0, LYS+, can1Δ::STE2pr-LEU2, lyp1Δ::, tor1-1, fpr1Δ::klURA, Tub4-(6)-RFP-(24)-FKBP::natNT2, VPS3-FRB::hphNT1, YGL058W-myeGFP::HIS3* | This study |
| OGYSGA6483 | *MATa, his3Δ1, leu2Δ0, ura3Δ0, LYS+, can1Δ::STE2pr-LEU2, lyp1Δ::, tor1-1, fpr1Δ::klURA, Tub4-(6)-RFP-(24)-FKBP::natNT2, VPS3-FRB::hphNT1, YMR022W-myeGFP::HIS3* | This study |
| OGYSGA6484 | *MATa, his3Δ1, leu2Δ0, ura3Δ0, LYS+, can1Δ::STE2pr-LEU2, lyp1Δ::, tor1-1, fpr1Δ::klURA, Tub4-(6)-RFP-(24)-FKBP::natNT2, VPS3-FRB::hphNT1, YMR236W-myeGFP::HIS3* | This study |
| OGYSGA6485 | *MATa, his3Δ1, leu2Δ0, ura3Δ0, LYS+, can1Δ::STE2pr-LEU2, lyp1Δ::, tor1-1, fpr1Δ::klURA, Tub4-(6)-RFP-(24)-FKBP::natNT2, VPS3-FRB::hphNT1, YNL243W-myeGFP::HIS3* | This study |
| OGYSGA6486 | *MATa, his3Δ1, leu2Δ0, ura3Δ0, LYS+, can1Δ::STE2pr-LEU2, lyp1Δ::, tor1-1, fpr1Δ::klURA, Tub4-(6)-RFP-(24)-FKBP::natNT2, VPS3-FRB::hphNT1, YDL185W-myeGFP::HIS3* | This study |
| OGYSGA6487 | *MATa, his3Δ1, leu2Δ0, ura3Δ0, LYS+, can1Δ::STE2pr-LEU2, lyp1Δ::, tor1-1, fpr1Δ::klURA, Tub4-(6)-RFP-(24)-FKBP::natNT2, VPS3-FRB::hphNT1, YJL062W-myeGFP::HIS3* | This study |
| OGYSGA6488 | *MATa, his3Δ1, leu2Δ0, ura3Δ0, LYS+, can1Δ::STE2pr-LEU2, lyp1Δ::, tor1-1, fpr1Δ::klURA, Tub4-(6)-RFP-(24)-FKBP::natNT2, VPS3-FRB::hphNT1, YGL095C-myeGFP::HIS3* | This study |
| OGYSGA6489 | *MATa, his3Δ1, leu2Δ0, ura3Δ0, LYS+, can1Δ::STE2pr-LEU2, lyp1Δ::, tor1-1, fpr1Δ::klURA, Tub4-(6)-RFP-(24)-FKBP::natNT2, VPS3-FRB::hphNT1, YNL323W-myeGFP::HIS3* | This study |
| OGYSGA6490 | *MATa, his3Δ1, leu2Δ0, ura3Δ0, LYS+, can1Δ::STE2pr-LEU2, lyp1Δ::, tor1-1, fpr1Δ::klURA, Tub4-(6)-RFP-(24)-FKBP::natNT2, VPS3-FRB::hphNT1, YCR044C-myeGFP::HIS3* | This study |
| OGYSGA6491 | *MATa, his3Δ1, leu2Δ0, ura3Δ0, LYS+, can1Δ::STE2pr-LEU2, lyp1Δ::, tor1-1, fpr1Δ::klURA, Tub4-(6)-RFP-(24)-FKBP::natNT2, VPS3-FRB::hphNT1, YGL020C-myeGFP::HIS3* | This study |
| OGYSGA6492 | *MATa, his3Δ1, leu2Δ0, ura3Δ0, LYS+, can1Δ::STE2pr-LEU2, lyp1Δ::, tor1-1, fpr1Δ::klURA, Tub4-(6)-RFP-(24)-FKBP::natNT2, VPS3-FRB::hphNT1, YGR105W-myeGFP::HIS3* | This study |
| OGYSGA1847 | *MATa, his3Δ1, leu2Δ0, ura3Δ0, LYS+, can1Δ::STE2pr-LEU2, lyp1Δ::, tor1-1, fpr1Δ::klURA, Tub4-(6)-RFP-(24)-FKBP::natNT2, VAM6-FRB::hphNT1, YNL243W-myeGFP::HIS3* | This study |
| OGYSGA1848 | *MATa, his3Δ1, leu2Δ0, ura3Δ0, LYS+, can1Δ::STE2pr-LEU2, lyp1Δ::, tor1-1, fpr1Δ::klURA, Tub4-(6)-RFP-(24)-FKBP::natNT2, VAM6-FRB::hphNT1, YDL185W-myeGFP::HIS3* | This study |
| OGYSGA1849 | *MATa, his3Δ1, leu2Δ0, ura3Δ0, LYS+, can1Δ::STE2pr-LEU2, lyp1Δ::, tor1-1, fpr1Δ::klURA, Tub4-(6)-RFP-(24)-FKBP::natNT2, VAM6-FRB::hphNT1, YOR244W-myeGFP::HIS3* | This study |
| OGYSGA1850 | *MATa, his3Δ1, leu2Δ0, ura3Δ0, LYS+, can1Δ::STE2pr-LEU2, lyp1Δ::, tor1-1, fpr1Δ::klURA, Tub4-(6)-RFP-(24)-FKBP::natNT2, VAM6-FRB::hphNT1, YGL020C-myeGFP::HIS3* | This study |
| OGYSGA1851 | *MATa, his3Δ1, leu2Δ0, ura3Δ0, LYS+, can1Δ::STE2pr-LEU2, lyp1Δ::, tor1-1, fpr1Δ::klURA, Tub4-(6)-RFP-(24)-FKBP::natNT2, VAM6-FRB::hphNT1, YER083C-myeGFP::HIS3* | This study |
| OGYSGA1852 | *MATa, his3Δ1, leu2Δ0, ura3Δ0, LYS+, can1Δ::STE2pr-LEU2, lyp1Δ::, tor1-1, fpr1Δ::klURA, Tub4-(6)-RFP-(24)-FKBP::natNT2, VAM6-FRB::hphNT1, YJL115W-myeGFP::HIS3* | This study |
| OGYSGA1853 | *MATa, his3Δ1, leu2Δ0, ura3Δ0, LYS+, can1Δ::STE2pr-LEU2, lyp1Δ::, tor1-1, fpr1Δ::klURA, Tub4-(6)-RFP-(24)-FKBP::natNT2, VAM6-FRB::hphNT1, YKL113C-myeGFP::HIS3* | This study |
| OGYSGA1854 | *MATa, his3Δ1, leu2Δ0, ura3Δ0, LYS+, can1Δ::STE2pr-LEU2, lyp1Δ::, tor1-1, fpr1Δ::klURA, Tub4-(6)-RFP-(24)-FKBP::natNT2, VAM6-FRB::hphNT1, YGL095C-myeGFP::HIS3* | This study |

## APPENDIX I – YEAST STRAINS

| | | |
|---|---|---|
| OGYSGA1855 | *MATa, his3Δ1, leu2Δ0, ura3Δ0, LYS+, can1Δ::STE2pr-LEU2, lyp1Δ::, tor1-1, fpr1Δ::klURA, Tub4-(6)-RFP-(24)-FKBP::natNT2, VAM6-FRB::hphNT1, YFL024C-myeGFP::HIS3* | This study |
| OGYSGA1856 | *MATa, his3Δ1, leu2Δ0, ura3Δ0, LYS+, can1Δ::STE2pr-LEU2, lyp1Δ::, tor1-1, fpr1Δ::klURA, Tub4-(6)-RFP-(24)-FKBP::natNT2, VAM6-FRB::hphNT1, YDL040C-myeGFP::HIS3* | This study |
| OGYSGA1857 | *MATa, his3Δ1, leu2Δ0, ura3Δ0, LYS+, can1Δ::STE2pr-LEU2, lyp1Δ::, tor1-1, fpr1Δ::klURA, Tub4-(6)-RFP-(24)-FKBP::natNT2, VAM6-FRB::hphNT1, YGL116W-myeGFP::HIS3* | This study |
| OGYSGA1858 | *MATa, his3Δ1, leu2Δ0, ura3Δ0, LYS+, can1Δ::STE2pr-LEU2, lyp1Δ::, tor1-1, fpr1Δ::klURA, Tub4-(6)-RFP-(24)-FKBP::natNT2, VAM6-FRB::hphNT1, YPL153C-myeGFP::HIS3* | This study |
| OGYSGA1859 | *MATa, his3Δ1, leu2Δ0, ura3Δ0, LYS+, can1Δ::STE2pr-LEU2, lyp1Δ::, tor1-1, fpr1Δ::klURA, Tub4-(6)-RFP-(24)-FKBP::natNT2, VAM6-FRB::hphNT1, YHR090C-myeGFP::HIS3* | This study |
| OGYSGA1860 | *MATa, his3Δ1, leu2Δ0, ura3Δ0, LYS+, can1Δ::STE2pr-LEU2, lyp1Δ::, tor1-1, fpr1Δ::klURA, Tub4-(6)-RFP-(24)-FKBP::natNT2, VAM6-FRB::hphNT1, YCL016C-myeGFP::HIS3* | This study |
| OGYSGA1861 | *MATa, his3Δ1, leu2Δ0, ura3Δ0, LYS+, can1Δ::STE2pr-LEU2, lyp1Δ::, tor1-1, fpr1Δ::klURA, Tub4-(6)-RFP-(24)-FKBP::natNT2, VAM6-FRB::hphNT1, YGL058W-myeGFP::HIS3* | This study |
| OGYSGA1862 | *MATa, his3Δ1, leu2Δ0, ura3Δ0, LYS+, can1Δ::STE2pr-LEU2, lyp1Δ::, tor1-1, fpr1Δ::klURA, Tub4-(6)-RFP-(24)-FKBP::natNT2, VAM6-FRB::hphNT1, YHR013C-myeGFP::HIS3* | This study |
| OGYSGA1863 | *MATa, his3Δ1, leu2Δ0, ura3Δ0, LYS+, can1Δ::STE2pr-LEU2, lyp1Δ::, tor1-1, fpr1Δ::klURA, Tub4-(6)-RFP-(24)-FKBP::natNT2, VAM6-FRB::hphNT1, YMR078C-myeGFP::HIS3* | This study |
| OGYSGA1864 | *MATa, his3Δ1, leu2Δ0, ura3Δ0, LYS+, can1Δ::STE2pr-LEU2, lyp1Δ::, tor1-1, fpr1Δ::klURA, Tub4-(6)-RFP-(24)-FKBP::natNT2, VAM6-FRB::hphNT1, YHR200W-myeGFP::HIS3* | This study |
| OGYSGA1865 | *MATa, his3Δ1, leu2Δ0, ura3Δ0, LYS+, can1Δ::STE2pr-LEU2, lyp1Δ::, tor1-1, fpr1Δ::klURA, Tub4-(6)-RFP-(24)-FKBP::natNT2, VAM6-FRB::hphNT1, YDR023W-myeGFP::HIS3* | This study |
| OGYSGA1866 | *MATa, his3Δ1, leu2Δ0, ura3Δ0, LYS+, can1Δ::STE2pr-LEU2, lyp1Δ::, tor1-1, fpr1Δ::klURA, Tub4-(6)-RFP-(24)-FKBP::natNT2, VAM6-FRB::hphNT1, YDL074C-myeGFP::HIS3* | This study |
| OGYSGA1867 | *MATa, his3Δ1, leu2Δ0, ura3Δ0, LYS+, can1Δ::STE2pr-LEU2, lyp1Δ::, tor1-1, fpr1Δ::klURA, Tub4-(6)-RFP-(24)-FKBP::natNT2, VAM6-FRB::hphNT1, YPL055C-myeGFP::HIS3* | This study |
| OGYSGA1868 | *MATa, his3Δ1, leu2Δ0, ura3Δ0, LYS+, can1Δ::STE2pr-LEU2, lyp1Δ::, tor1-1, fpr1Δ::klURA, Tub4-(6)-RFP-(24)-FKBP::natNT2, VAM6-FRB::hphNT1, YBR164C-myeGFP::HIS3* | This study |
| OGYSGA1869 | *MATa, his3Δ1, leu2Δ0, ura3Δ0, LYS+, can1Δ::STE2pr-LEU2, lyp1Δ::, tor1-1, fpr1Δ::klURA, Tub4-(6)-RFP-(24)-FKBP::natNT2, VAM6-FRB::hphNT1, YJL092W-myeGFP::HIS3* | This study |
| OGYSGA1870 | *MATa, his3Δ1, leu2Δ0, ura3Δ0, LYS+, can1Δ::STE2pr-LEU2, lyp1Δ::, tor1-1, fpr1Δ::klURA, Tub4-(6)-RFP-(24)-FKBP::natNT2, VAM6-FRB::hphNT1, YOR141C-myeGFP::HIS3* | This study |
| OGYSGA1871 | *MATa, his3Δ1, leu2Δ0, ura3Δ0, LYS+, can1Δ::STE2pr-LEU2, lyp1Δ::, tor1-1, fpr1Δ::klURA, Tub4-(6)-RFP-(24)-FKBP::natNT2, VAM6-FRB::hphNT1, YGR106C-myeGFP::HIS3* | This study |
| OGYSGA1872 | *MATa, his3Δ1, leu2Δ0, ura3Δ0, LYS+, can1Δ::STE2pr-LEU2, lyp1Δ::, tor1-1, fpr1Δ::klURA, Tub4-(6)-RFP-(24)-FKBP::natNT2, VAM6-FRB::hphNT1, YGR198W-myeGFP::HIS3* | This study |
| OGYSGA1873 | *MATa, his3Δ1, leu2Δ0, ura3Δ0, LYS+, can1Δ::STE2pr-LEU2, lyp1Δ::, tor1-1, fpr1Δ::klURA, Tub4-(6)-RFP-(24)-FKBP::natNT2, VAM6-FRB::hphNT1, YGR105W-myeGFP::HIS3* | This study |
| OGYSGA1874 | *MATa, his3Δ1, leu2Δ0, ura3Δ0, LYS+, can1Δ::STE2pr-LEU2, lyp1Δ::, tor1-1, fpr1Δ::klURA, Tub4-(6)-RFP-(24)-FKBP::natNT2, VAM6-FRB::hphNT1, YDR150W-myeGFP::HIS3* | This study |
| OGYSGA1875 | *MATa, his3Δ1, leu2Δ0, ura3Δ0, LYS+, can1Δ::STE2pr-LEU2, lyp1Δ::, tor1-1, fpr1Δ::klURA, Tub4-(6)-RFP-(24)-FKBP::natNT2, VAM6-FRB::hphNT1, YGR061C-myeGFP::HIS3* | This study |
| OGYSGA1876 | *MATa, his3Δ1, leu2Δ0, ura3Δ0, LYS+, can1Δ::STE2pr-LEU2, lyp1Δ::, tor1-1, fpr1Δ::klURA, Tub4-(6)-RFP-(24)-FKBP::natNT2, VAM6-FRB::hphNT1, YBR152W-myeGFP::HIS3* | This study |
| OGYSGA1877 | *MATa, his3Δ1, leu2Δ0, ura3Δ0, LYS+, can1Δ::STE2pr-LEU2, lyp1Δ::, tor1-1, fpr1Δ::klURA, Tub4-(6)-RFP-(24)-FKBP::natNT2, VAM6-FRB::hphNT1, YLL029W-myeGFP::HIS3* | This study |
| OGYSGA1878 | *MATa, his3Δ1, leu2Δ0, ura3Δ0, LYS+, can1Δ::STE2pr-LEU2, lyp1Δ::, tor1-1, fpr1Δ::klURA, Tub4-(6)-RFP-(24)-FKBP::natNT2, VAM6-FRB::hphNT1, YGR002C-myeGFP::HIS3* | This study |
| OGYSGA1879 | *MATa, his3Δ1 leu2Δ0 ura3Δ0 LYS+, can1Δ::STE2pr-LEU2, lyp1Δ::, tor1-1, fpr1Δ::klURA, Tub4-(6)-RFP-(24)-FKBP::natNT2, VAM6-FRB::hphNT1, YJL081C-myeGFP::HIS3* | This study |
| OGYSGA1880 | *MATa, his3Δ1 leu2Δ0 ura3Δ0 LYS+, can1Δ::STE2pr-LEU2, lyp1Δ::, tor1-1, fpr1Δ::klURA, Tub4-(6)-RFP-(24)-FKBP::natNT2, VAM6-FRB::hphNT1, YLR114C-myeGFP::HIS3* | This study |
| OGYSGA1881 | *MATa, his3Δ1 leu2Δ0 ura3Δ0 LYS+, can1Δ::STE2pr-LEU2, lyp1Δ::, tor1-1, fpr1Δ::klURA, Tub4-(6)-RFP-(24)-FKBP::natNT2, VAM6-FRB::hphNT1, YJR043C-myeGFP::HIS3* | This study |

## APPENDIX I – YEAST STRAINS

| | | |
|---|---|---|
| OGYSGA1882 | *MATa, his3Δ1 leu2Δ0 ura3Δ0 LYS+, can1Δ::STE2pr-LEU2, lyp1Δ::, tor1-1, fpr1Δ::klURA, Tub4-(6)-RFP-(24)-FKBP::natNT2, VAM6-FRB::hphNT1, YLR153C-myeGFP::HIS3* | This study |
| OGYSGA1883 | *MATa, his3Δ1 leu2Δ0 ura3Δ0 LYS+, can1Δ::STE2pr-LEU2, lyp1Δ::, tor1-1, fpr1Δ::klURA, Tub4-(6)-RFP-(24)-FKBP::natNT2, VAM6-FRB::hphNT1, YNL056W-myeGFP::HIS3* | This study |
| OGYSGA1884 | *MATa, his3Δ1 leu2Δ0 ura3Δ0 LYS+, can1Δ::STE2pr-LEU2, lyp1Δ::, tor1-1, fpr1Δ::klURA, Tub4-(6)-RFP-(24)-FKBP::natNT2, VAM6-FRB::hphNT1, YGR155W-myeGFP::HIS3* | This study |
| OGYSGA1885 | *MATa, his3Δ1 leu2Δ0 ura3Δ0 LYS+, can1Δ::STE2pr-LEU2, lyp1Δ::, tor1-1, fpr1Δ::klURA, Tub4-(6)-RFP-(24)-FKBP::natNT2, VAM6-FRB::hphNT1, YNL032W-myeGFP::HIS3* | This study |
| OGYSGA1886 | *MATa, his3Δ1 leu2Δ0 ura3Δ0 LYS+, can1Δ::STE2pr-LEU2, lyp1Δ::, tor1-1, fpr1Δ::klURA, Tub4-(6)-RFP-(24)-FKBP::natNT2, VAM6-FRB::hphNT1, YOL115W-myeGFP::HIS3* | This study |
| OGYSGA1887 | *MATa, his3Δ1 leu2Δ0 ura3Δ0 LYS+, can1Δ::STE2pr-LEU2, lyp1Δ::, tor1-1, fpr1Δ::klURA, Tub4-(6)-RFP-(24)-FKBP::natNT2, VAM6-FRB::hphNT1, YJL154C-myeGFP::HIS3* | This study |
| OGYSGA1888 | *MATa, his3Δ1 leu2Δ0 ura3Δ0 LYS+, can1Δ::STE2pr-LEU2, lyp1Δ::, tor1-1, fpr1Δ::klURA, Tub4-(6)-RFP-(24)-FKBP::natNT2, VAM6-FRB::hphNT1, YOR069W-myeGFP::HIS3* | This study |
| OGYSGA1889 | *MATa, his3Δ1 leu2Δ0 ura3Δ0 LYS+, can1Δ::STE2pr-LEU2, lyp1Δ::, tor1-1, fpr1Δ::klURA, Tub4-(6)-RFP-(24)-FKBP::natNT2, VAM6-FRB::hphNT1, YKL009W-myeGFP::HIS3* | This study |
| OGYSGA1890 | *MATa, his3Δ1 leu2Δ0 ura3Δ0 LYS+, can1Δ::STE2pr-LEU2, lyp1Δ::, tor1-1, fpr1Δ::klURA, Tub4-(6)-RFP-(24)-FKBP::natNT2, VAM6-FRB::hphNT1, YNL021W-myeGFP::HIS3* | This study |
| OGYSGA1891 | *MATa, his3Δ1 leu2Δ0 ura3Δ0 LYS+, can1Δ::STE2pr-LEU2, lyp1Δ::, tor1-1, fpr1Δ::klURA, Tub4-(6)-RFP-(24)-FKBP::natNT2, VAM6-FRB::hphNT1, YHR012W-myeGFP::HIS3* | This study |
| OGYSGA1892 | *MATa, his3Δ1 leu2Δ0 ura3Δ0 LYS+, can1Δ::STE2pr-LEU2, lyp1Δ::, tor1-1, fpr1Δ::klURA, Tub4-(6)-RFP-(24)-FKBP::natNT2, VAM6-FRB::hphNT1, YGL061C-myeGFP::HIS3* | This study |
| OGYSGA1893 | *MATa, his3Δ1 leu2Δ0 ura3Δ0 LYS+, can1Δ::STE2pr-LEU2, lyp1Δ::, tor1-1, fpr1Δ::klURA, Tub4-(6)-RFP-(24)-FKBP::natNT2, VAM6-FRB::hphNT1, YPL145C-myeGFP::HIS3* | This study |
| OGYSGA1894 | *MATa, his3Δ1 leu2Δ0 ura3Δ0 LYS+, can1Δ::STE2pr-LEU2, lyp1Δ::, tor1-1, fpr1Δ::klURA, Tub4-(6)-RFP-(24)-FKBP::natNT2, VAM6-FRB::hphNT1, YDL020C-myeGFP::HIS3* | This study |
| OGYSGA1895 | *MATa, his3Δ1 leu2Δ0 ura3Δ0 LYS+, can1Δ::STE2pr-LEU2, lyp1Δ::, tor1-1, fpr1Δ::klURA, Tub4-(6)-RFP-(24)-FKBP::natNT2, VAM6-FRB::hphNT1, YLR190W-myeGFP::HIS3* | This study |
| OGYSGA1896 | *MATa, his3Δ1 leu2Δ0 ura3Δ0 LYS+, can1Δ::STE2pr-LEU2, lyp1Δ::, tor1-1, fpr1Δ::klURA, Tub4-(6)-RFP-(24)-FKBP::natNT2, VAM6-FRB::hphNT1, YJL004C-myeGFP::HIS3* | This study |
| OGYSGA1897 | *MATa, his3Δ1 leu2Δ0 ura3Δ0 LYS+, can1Δ::STE2pr-LEU2, lyp1Δ::, tor1-1, fpr1Δ::klURA, Tub4-(6)-RFP-(24)-FKBP::natNT2, VAM6-FRB::hphNT1, YAL010C-myeGFP::HIS3* | This study |
| OGYSGA1898 | *MATa, his3Δ1 leu2Δ0 ura3Δ0 LYS+, can1Δ::STE2pr-LEU2, lyp1Δ::, tor1-1, fpr1Δ::klURA, Tub4-(6)-RFP-(24)-FKBP::natNT2, VAM6-FRB::hphNT1, YPL051W-myeGFP::HIS3* | This study |
| OGYSGA1899 | *MATa, his3Δ1 leu2Δ0 ura3Δ0 LYS+, can1Δ::STE2pr-LEU2, lyp1Δ::, tor1-1, fpr1Δ::klURA, Tub4-(6)-RFP-(24)-FKBP::natNT2, VAM6-FRB::hphNT1, YJL166W-myeGFP::HIS3* | This study |
| OGYSGA1900 | *MATa, his3Δ1 leu2Δ0 ura3Δ0 LYS+, can1Δ::STE2pr-LEU2, lyp1Δ::, tor1-1, fpr1Δ::klURA, Tub4-(6)-RFP-(24)-FKBP::natNT2, TRS23-FRB::hphNT1, YOR216C-myeGFP::HIS3* | This study |
| OGYSGA1901 | *MATa, his3Δ1 leu2Δ0 ura3Δ0 LYS+, can1Δ::STE2pr-LEU2, lyp1Δ::, tor1-1, fpr1Δ::klURA, Tub4-(6)-RFP-(24)-FKBP::natNT2, TRS23-FRB::hphNT1, YMR307W-myeGFP::HIS3* | This study |
| OGYSGA1902 | *MATa, his3Δ1 leu2Δ0 ura3Δ0 LYS+, can1Δ::STE2pr-LEU2, lyp1Δ::, tor1-1, fpr1Δ::klURA, Tub4-(6)-RFP-(24)-FKBP::natNT2, TRS23-FRB::hphNT1, YMR272C-myeGFP::HIS3* | This study |
| OGYSGA1903 | *MATa, his3Δ1 leu2Δ0 ura3Δ0 LYS+, can1Δ::STE2pr-LEU2, lyp1Δ::, tor1-1, fpr1Δ::klURA, Tub4-(6)-RFP-(24)-FKBP::natNT2, TRS23-FRB::hphNT1, YLR262C-myeGFP::HIS3* | This study |
| OGYSGA1904 | *MATa, his3Δ1 leu2Δ0 ura3Δ0 LYS+, can1Δ::STE2pr-LEU2, lyp1Δ::, tor1-1, fpr1Δ::klURA, Tub4-(6)-RFP-(24)-FKBP::natNT2, TRS23-FRB::hphNT1, YPL051W-myeGFP::HIS3* | This study |
| OGYSGA1905 | *MATa, his3Δ1 leu2Δ0 ura3Δ0 LYS+, can1Δ::STE2pr-LEU2, lyp1Δ::, tor1-1, fpr1Δ::klURA, Tub4-(6)-RFP-(24)-FKBP::natNT2, TRS23-FRB::hphNT1, YGL054C-myeGFP::HIS3* | This study |
| OGYSGA1906 | *MATa, his3Δ1 leu2Δ0 ura3Δ0 LYS+, can1Δ::STE2pr-LEU2, lyp1Δ::, tor1-1, fpr1Δ::klURA, Tub4-(6)-RFP-(24)-FKBP::natNT2, TRS23-FRB::hphNT1, YPL234C-myeGFP::HIS3* | This study |
| OGYSGA1907 | *MATa, his3Δ1 leu2Δ0 ura3Δ0 LYS+, can1Δ::STE2pr-LEU2, lyp1Δ::, tor1-1, fpr1Δ::klURA, Tub4-(6)-RFP-(24)-FKBP::natNT2, TRS23-FRB::hphNT1, YKL119C-myeGFP::HIS3* | This study |
| OGYSGA1908 | *MATa, his3Δ1 leu2Δ0 ura3Δ0 LYS+, can1Δ::STE2pr-LEU2, lyp1Δ::, tor1-1, fpr1Δ::klURA, Tub4-(6)-RFP-(24)-FKBP::natNT2, TRS23-FRB::hphNT1, YMR123W-myeGFP::HIS3* | This study |

## APPENDIX I – YEAST STRAINS

| | | |
|---|---|---|
| OGYSGA1909 | *MATa, his3Δ1 leu2Δ0 ura3Δ0 LYS+, can1Δ::STE2pr-LEU2, lyp1Δ::, tor1-1, fpr1Δ::klURA, Tub4-(6)-RFP-(24)-FKBP::natNT2, TRS23-FRB::hphNT1, YBR164C-myeGFP::HIS3* | This study |
| OGYSGA1910 | *MATa, his3Δ1 leu2Δ0 ura3Δ0 LYS+, can1Δ::STE2pr-LEU2, lyp1Δ::, tor1-1, fpr1Δ::klURA, Tub4-(6)-RFP-(24)-FKBP::natNT2, TRS23-FRB::hphNT1, YOR070C-myeGFP::HIS3* | This study |
| OGYSGA1911 | *MATa, his3Δ1 leu2Δ0 ura3Δ0 LYS+, can1Δ::STE2pr-LEU2, lyp1Δ::, tor1-1, fpr1Δ::klURA, Tub4-(6)-RFP-(24)-FKBP::natNT2, TRS23-FRB::hphNT1, YKR001C-myeGFP::HIS3* | This study |
| OGYSGA1912 | *MATa, his3Δ1 leu2Δ0 ura3Δ0 LYS+, can1Δ::STE2pr-LEU2, lyp1Δ::, tor1-1, fpr1Δ::klURA, Tub4-(6)-RFP-(24)-FKBP::natNT2, TRS23-FRB::hphNT1, YPL057C-myeGFP::HIS3* | This study |
| OGYSGA1913 | *MATa, his3Δ1 leu2Δ0 ura3Δ0 LYS+, can1Δ::STE2pr-LEU2, lyp1Δ::, tor1-1, fpr1Δ::klURA, Tub4-(6)-RFP-(24)-FKBP::natNT2, TRS23-FRB::hphNT1, YLR350W-myeGFP::HIS3* | This study |
| OGYSGA1914 | *MATa, his3Δ1 leu2Δ0 ura3Δ0 LYS+, can1Δ::STE2pr-LEU2, lyp1Δ::, tor1-1, fpr1Δ::klURA, Tub4-(6)-RFP-(24)-FKBP::natNT2, TRS23-FRB::hphNT1, YLR268W-myeGFP::HIS3* | This study |
| OGYSGA1915 | *MATa, his3Δ1 leu2Δ0 ura3Δ0 LYS+, can1Δ::STE2pr-LEU2, lyp1Δ::, tor1-1, fpr1Δ::klURA, Tub4-(6)-RFP-(24)-FKBP::natNT2, TRS23-FRB::hphNT1, YJR118C-myeGFP::HIS3* | This study |
| OGYSGA1916 | *MATa, his3Δ1 leu2Δ0 ura3Δ0 LYS+, can1Δ::STE2pr-LEU2, lyp1Δ::, tor1-1, fpr1Δ::klURA, Tub4-(6)-RFP-(24)-FKBP::natNT2, TRS23-FRB::hphNT1, YMR190C-myeGFP::HIS3* | This study |
| OGYSGA1917 | *MATa, his3Δ1 leu2Δ0 ura3Δ0 LYS+, can1Δ::STE2pr-LEU2, lyp1Δ::, tor1-1, fpr1Δ::klURA, Tub4-(6)-RFP-(24)-FKBP::natNT2, TRS23-FRB::hphNT1, YLR039C-myeGFP::HIS3* | This study |
| OGYSGA1918 | *MATa, his3Δ1 leu2Δ0 ura3Δ0 LYS+, can1Δ::STE2pr-LEU2, lyp1Δ::, tor1-1, fpr1Δ::klURA, Tub4-(6)-RFP-(24)-FKBP::natNT2, TRS23-FRB::hphNT1, YIL004C-myeGFP::HIS3* | This study |
| OGYSGA1919 | *MATa, his3Δ1 leu2Δ0 ura3Δ0 LYS+, can1Δ::STE2pr-LEU2, lyp1Δ::, tor1-1, fpr1Δ::klURA, Tub4-(6)-RFP-(24)-FKBP::natNT2, TRS23-FRB::hphNT1, YBR080C-myeGFP::HIS3* | This study |
| OGYSGA1920 | *MATa, his3Δ1 leu2Δ0 ura3Δ0 LYS+, can1Δ::STE2pr-LEU2, lyp1Δ::, tor1-1, fpr1Δ::klURA, Tub4-(6)-RFP-(24)-FKBP::natNT2, TRS23-FRB::hphNT1, YJL123C-myeGFP::HIS3* | This study |
| OGYSGA1921 | *MATa, his3Δ1 leu2Δ0 ura3Δ0 LYS+, can1Δ::STE2pr-LEU2, lyp1Δ::, tor1-1, fpr1Δ::klURA, Tub4-(6)-RFP-(24)-FKBP::natNT2, TRS23-FRB::hphNT1, YNL267W-myeGFP::HIS3* | This study |
| OGYSGA1922 | *MATa, his3Δ1 leu2Δ0 ura3Δ0 LYS+, can1Δ::STE2pr-LEU2, lyp1Δ::, tor1-1, fpr1Δ::klURA, Tub4-(6)-RFP-(24)-FKBP::natNT2, TRS23-FRB::hphNT1, YLL040C-myeGFP::HIS3* | This study |
| OGYSGA1923 | *MATa, his3Δ1 leu2Δ0 ura3Δ0 LYS+, can1Δ::STE2pr-LEU2, lyp1Δ::, tor1-1, fpr1Δ::klURA, Tub4-(6)-RFP-(24)-FKBP::natNT2, TRS23-FRB::hphNT1, YPL120W-myeGFP::HIS3* | This study |
| OGYSGA1924 | *MATa, his3Δ1 leu2Δ0 ura3Δ0 LYS+, can1Δ::STE2pr-LEU2, lyp1Δ::, tor1-1, fpr1Δ::klURA, Tub4-(6)-RFP-(24)-FKBP::natNT2, TRS23-FRB::hphNT1, YAL026C-myeGFP::HIS3* | This study |
| OGYSGA1925 | *MATa, his3Δ1 leu2Δ0 ura3Δ0 LYS+, can1Δ::STE2pr-LEU2, lyp1Δ::, tor1-1, fpr1Δ::klURA, Tub4-(6)-RFP-(24)-FKBP::natNT2, TRS23-FRB::hphNT1, YKL004W-myeGFP::HIS3* | This study |
| OGYSGA1926 | *MATa, his3Δ1 leu2Δ0 ura3Δ0 LYS+, can1Δ::STE2pr-LEU2, lyp1Δ::, tor1-1, fpr1Δ::klURA, Tub4-(6)-RFP-(24)-FKBP::natNT2, TRS23-FRB::hphNT1, YGL086W-myeGFP::HIS3* | This study |
| OGYSGA1927 | *MATa, his3Δ1 leu2Δ0 ura3Δ0 LYS+, can1Δ::STE2pr-LEU2, lyp1Δ::, tor1-1, fpr1Δ::klURA, Tub4-(6)-RFP-(24)-FKBP::natNT2, TRS23-FRB::hphNT1, YDR137W-myeGFP::HIS3* | This study |
| OGYSGA1928 | *MATa, his3Δ1 leu2Δ0 ura3Δ0 LYS+, can1Δ::STE2pr-LEU2, lyp1Δ::, tor1-1, fpr1Δ::klURA, Tub4-(6)-RFP-(24)-FKBP::natNT2, TRS23-FRB::hphNT1, YML008C-myeGFP::HIS3* | This study |
| OGYSGA1929 | *MATa, his3Δ1 leu2Δ0 ura3Δ0 LYS+, can1Δ::STE2pr-LEU2, lyp1Δ::, tor1-1, fpr1Δ::klURA, Tub4-(6)-RFP-(24)-FKBP::natNT2, TRS23-FRB::hphNT1, YPL158C-myeGFP::HIS3* | This study |
| OGYSGA1930 | *MATa, his3Δ1 leu2Δ0 ura3Δ0 LYS+, can1Δ::STE2pr-LEU2, lyp1Δ::, tor1-1, fpr1Δ::klURA, Tub4-(6)-RFP-(24)-FKBP::natNT2, TRS23-FRB::hphNT1, YNL169C-myeGFP::HIS3* | This study |
| OGYSGA1931 | *MATa, his3Δ1 leu2Δ0 ura3Δ0 LYS+, can1Δ::STE2pr-LEU2, lyp1Δ::, tor1-1, fpr1Δ::klURA, Tub4-(6)-RFP-(24)-FKBP::natNT2, TRS23-FRB::hphNT1, YLL006W-myeGFP::HIS3* | This study |
| OGYSGA1932 | *MATa, his3Δ1 leu2Δ0 ura3Δ0 LYS+, can1Δ::STE2pr-LEU2, lyp1Δ::, tor1-1, fpr1Δ::klURA, Tub4-(6)-RFP-(24)-FKBP::natNT2, TRS23-FRB::hphNT1, YML041C-myeGFP::HIS3* | This study |
| OGYSGA1933 | *MATa, his3Δ1 leu2Δ0 ura3Δ0 LYS+, can1Δ::STE2pr-LEU2, lyp1Δ::, tor1-1, fpr1Δ::klURA, Tub4-(6)-RFP-(24)-FKBP::natNT2, TRS23-FRB::hphNT1, YGL020C-myeGFP::HIS3* | This study |
| OGYSGA1934 | *MATa, his3Δ1 leu2Δ0 ura3Δ0 LYS+, can1Δ::STE2pr-LEU2, lyp1Δ::, tor1-1, fpr1Δ::klURA, Tub4-(6)-RFP-(24)-FKBP::natNT2, TRS23-FRB::hphNT1, YOL012C-myeGFP::HIS3* | This study |
| OGYSGA6402 | *MATa, his3Δ1, leu2Δ0, ura3Δ0, LYS+, can1Δ::STE2pr-LEU2, lyp1Δ::, tor1-1, fpr1Δ::klURA, Tub4-(6)-RFP-(24)-FKBP::natNT2, TRS130-FRB::hphNT1, YGL086W-myeGFP::HIS3* | This study |

## APPENDIX I – YEAST STRAINS

| | | |
|---|---|---|
| OGYSGA6403 | *MATa, his3Δ1, leu2Δ0, ura3Δ0, LYS+, can1Δ::STE2pr-LEU2, lyp1Δ::, tor1-1, fpr1Δ::klURA, Tub4-(6)-RFP-(24)-FKBP::natNT2, TRS130-FRB::hphNT1, YDR137W-myeGFP::HIS3* | This study |
| OGYSGA6404 | *MATa, his3Δ1, leu2Δ0, ura3Δ0, LYS+, can1Δ::STE2pr-LEU2, lyp1Δ::, tor1-1, fpr1Δ::klURA, Tub4-(6)-RFP-(24)-FKBP::natNT2, TRS130-FRB::hphNT1, YOR070C-myeGFP::HIS3* | This study |
| OGYSGA6405 | *MATa, his3Δ1, leu2Δ0, ura3Δ0, LYS+, can1Δ::STE2pr-LEU2, lyp1Δ::, tor1-1, fpr1Δ::klURA, Tub4-(6)-RFP-(24)-FKBP::natNT2, TRS130-FRB::hphNT1, YOR216C-myeGFP::HIS3* | This study |
| OGYSGA6406 | *MATa, his3Δ1, leu2Δ0, ura3Δ0, LYS+, can1Δ::STE2pr-LEU2, lyp1Δ::, tor1-1, fpr1Δ::klURA, Tub4-(6)-RFP-(24)-FKBP::natNT2, TRS130-FRB::hphNT1, YJL123C-myeGFP::HIS3* | This study |
| OGYSGA6407 | *MATa, his3Δ1, leu2Δ0, ura3Δ0, LYS+, can1Δ::STE2pr-LEU2, lyp1Δ::, tor1-1, fpr1Δ::klURA, Tub4-(6)-RFP-(24)-FKBP::natNT2, TRS130-FRB::hphNT1, YMR272C-myeGFP::HIS3* | This study |
| OGYSGA6414 | *MATa, his3Δ1, leu2Δ0, ura3Δ0, LYS+, can1Δ::STE2pr-LEU2, lyp1Δ::, tor1-1, fpr1Δ::klURA, Tub4-(6)-RFP-(24)-FKBP::natNT2, TRS130-FRB::hphNT1, YLL040C-myeGFP::HIS3* | This study |
| OGYSGA6415 | *MATa, his3Δ1, leu2Δ0, ura3Δ0, LYS+, can1Δ::STE2pr-LEU2, lyp1Δ::, tor1-1, fpr1Δ::klURA, Tub4-(6)-RFP-(24)-FKBP::natNT2, TRS130-FRB::hphNT1, YAL026C-myeGFP::HIS3* | This study |
| OGYSGA6416 | *MATa, his3Δ1, leu2Δ0, ura3Δ0, LYS+, can1Δ::STE2pr-LEU2, lyp1Δ::, tor1-1, fpr1Δ::klURA, Tub4-(6)-RFP-(24)-FKBP::natNT2, TRS130-FRB::hphNT1, YBR080C-myeGFP::HIS3* | This study |
| OGYSGA6417 | *MATa, his3Δ1, leu2Δ0, ura3Δ0, LYS+, can1Δ::STE2pr-LEU2, lyp1Δ::, tor1-1, fpr1Δ::klURA, Tub4-(6)-RFP-(24)-FKBP::natNT2, TRS130-FRB::hphNT1, YKR001C-myeGFP::HIS3* | This study |
| OGYSGA6418 | *MATa, his3Δ1, leu2Δ0, ura3Δ0, LYS+, can1Δ::STE2pr-LEU2, lyp1Δ::, tor1-1, fpr1Δ::klURA, Tub4-(6)-RFP-(24)-FKBP::natNT2, TRS130-FRB::hphNT1, YNL238W-myeGFP::HIS3* | This study |
| OGYSGA6419 | *MATa, his3Δ1, leu2Δ0, ura3Δ0, LYS+, can1Δ::STE2pr-LEU2, lyp1Δ::, tor1-1, fpr1Δ::klURA, Tub4-(6)-RFP-(24)-FKBP::natNT2, TRS130-FRB::hphNT1, YPL120W-myeGFP::HIS3* | This study |
| OGYSGA6420 | *MATa, his3Δ1, leu2Δ0, ura3Δ0, LYS+, can1Δ::STE2pr-LEU2, lyp1Δ::, tor1-1, fpr1Δ::klURA, Tub4-(6)-RFP-(24)-FKBP::natNT2, TRS130-FRB::hphNT1, YMR190C-myeGFP::HIS3* | This study |
| OGYSGA6421 | *MATa, his3Δ1, leu2Δ0, ura3Δ0, LYS+, can1Δ::STE2pr-LEU2, lyp1Δ::, tor1-1, fpr1Δ::klURA, Tub4-(6)-RFP-(24)-FKBP::natNT2, TRS130-FRB::hphNT1, YNL267W-myeGFP::HIS3* | This study |
| OGYSGA6422 | *MATa, his3Δ1, leu2Δ0, ura3Δ0, LYS+, can1Δ::STE2pr-LEU2, lyp1Δ::, tor1-1, fpr1Δ::klURA, Tub4-(6)-RFP-(24)-FKBP::natNT2, TRS130-FRB::hphNT1, YLR039C-myeGFP::HIS3* | This study |
| OGYSGA6423 | *MATa, his3Δ1, leu2Δ0, ura3Δ0, LYS+, can1Δ::STE2pr-LEU2, lyp1Δ::, tor1-1, fpr1Δ::klURA, Tub4-(6)-RFP-(24)-FKBP::natNT2, TRS130-FRB::hphNT1, YGL180W-myeGFP::HIS3* | This study |
| OGYSGA6424 | *MATa, his3Δ1, leu2Δ0, ura3Δ0, LYS+, can1Δ::STE2pr-LEU2, lyp1Δ::, tor1-1, fpr1Δ::klURA, Tub4-(6)-RFP-(24)-FKBP::natNT2, TRS130-FRB::hphNT1, YOR144C-myeGFP::HIS3* | This study |
| OGYSGA6425 | *MATa, his3Δ1, leu2Δ0, ura3Δ0, LYS+, can1Δ::STE2pr-LEU2, lyp1Δ::, tor1-1, fpr1Δ::klURA, Tub4-(6)-RFP-(24)-FKBP::natNT2, TRS130-FRB::hphNT1, YPL158C-myeGFP::HIS3* | This study |
| OGYSGA6426 | *MATa, his3Δ1, leu2Δ0, ura3Δ0, LYS+, can1Δ::STE2pr-LEU2, lyp1Δ::, tor1-1, fpr1Δ::klURA, Tub4-(6)-RFP-(24)-FKBP::natNT2, TRS130-FRB::hphNT1, YMR079W-myeGFP::HIS3* | This study |
| OGYSGA6427 | *MATa, his3Δ1, leu2Δ0, ura3Δ0, LYS+, can1Δ::STE2pr-LEU2, lyp1Δ::, tor1-1, fpr1Δ::klURA, Tub4-(6)-RFP-(24)-FKBP::natNT2, TRS130-FRB::hphNT1, YML008C-myeGFP::HIS3* | This study |
| OGYSGA6428 | *MATa, his3Δ1, leu2Δ0, ura3Δ0, LYS+, can1Δ::STE2pr-LEU2, lyp1Δ::, tor1-1, fpr1Δ::klURA, Tub4-(6)-RFP-(24)-FKBP::natNT2, TRS130-FRB::hphNT1, YPL057C-myeGFP::HIS3* | This study |
| OGYSGA6429 | *MATa, his3Δ1, leu2Δ0, ura3Δ0, LYS+, can1Δ::STE2pr-LEU2, lyp1Δ::, tor1-1, fpr1Δ::klURA, Tub4-(6)-RFP-(24)-FKBP::natNT2, TRS130-FRB::hphNT1, YJR077C-myeGFP::HIS3* | This study |
| OGYSGA6430 | *MATa, his3Δ1, leu2Δ0, ura3Δ0, LYS+, can1Δ::STE2pr-LEU2, lyp1Δ::, tor1-1, fpr1Δ::klURA, Tub4-(6)-RFP-(24)-FKBP::natNT2, TRS130-FRB::hphNT1, YLR350W-myeGFP::HIS3* | This study |
| OGYSGA6431 | *MATa, his3Δ1, leu2Δ0, ura3Δ0, LYS+, can1Δ::STE2pr-LEU2, lyp1Δ::, tor1-1, fpr1Δ::klURA, Tub4-(6)-RFP-(24)-FKBP::natNT2, TRS130-FRB::hphNT1, YJR118C-myeGFP::HIS3* | This study |
| OGYSGA6432 | *MATa, his3Δ1, leu2Δ0, ura3Δ0, LYS+, can1Δ::STE2pr-LEU2, lyp1Δ::, tor1-1, fpr1Δ::klURA, Tub4-(6)-RFP-(24)-FKBP::natNT2, TRS130-FRB::hphNT1, YDL226C-myeGFP::HIS3* | This study |

## APPENDIX I – YEAST STRAINS

| | | |
|---|---|---|
| OGYSGA6433 | *MATa, his3Δ1, leu2Δ0, ura3Δ0, LYS+, can1Δ::STE2pr-LEU2, lyp1Δ::, tor1-1, fpr1Δ::klURA, Tub4-(6)-RFP-(24)-FKBP::natNT2, TRS130-FRB::hphNT1, YDR372C-myeGFP::HIS3* | This study |
| OGYSGA6434 | *MATa, his3Δ1, leu2Δ0, ura3Δ0, LYS+, can1Δ::STE2pr-LEU2, lyp1Δ::, tor1-1, fpr1Δ::klURA, Tub4-(6)-RFP-(24)-FKBP::natNT2, TRS130-FRB::hphNT1, YML041C-myeGFP::HIS3* | This study |
| OGYSGA6435 | *MATa, his3Δ1, leu2Δ0, ura3Δ0, LYS+, can1Δ::STE2pr-LEU2, lyp1Δ::, tor1-1, fpr1Δ::klURA, Tub4-(6)-RFP-(24)-FKBP::natNT2, TRS130-FRB::hphNT1, YPL051W-myeGFP::HIS3* | This study |
| OGYSGA6436 | *MATa, his3Δ1, leu2Δ0, ura3Δ0, LYS+, can1Δ::STE2pr-LEU2, lyp1Δ::, tor1-1, fpr1Δ::klURA, Tub4-(6)-RFP-(24)-FKBP::natNT2, TRS130-FRB::hphNT1, YOL012C-myeGFP::HIS3* | This study |
| OGYSGA6437 | *MATa, his3Δ1, leu2Δ0, ura3Δ0, LYS+, can1Δ::STE2pr-LEU2, lyp1Δ::, tor1-1, fpr1Δ::klURA, Tub4-(6)-RFP-(24)-FKBP::natNT2, TRS130-FRB::hphNT1, YMR123W-myeGFP::HIS3* | This study |
| OGYSGA6438 | *MATa, his3Δ1, leu2Δ0, ura3Δ0, LYS+, can1Δ::STE2pr-LEU2, lyp1Δ::, tor1-1, fpr1Δ::klURA, Tub4-(6)-RFP-(24)-FKBP::natNT2, TRS130-FRB::hphNT1, YIL004C-myeGFP::HIS3* | This study |
| OGYSGA6439 | *MATa, his3Δ1, leu2Δ0, ura3Δ0, LYS+, can1Δ::STE2pr-LEU2, lyp1Δ::, tor1-1, fpr1Δ::klURA, Tub4-(6)-RFP-(24)-FKBP::natNT2, TRS130-FRB::hphNT1, YGL210W-myeGFP::HIS3* | This study |
| OGYSGA6440 | *MATa, his3Δ1, leu2Δ0, ura3Δ0, LYS+, can1Δ::STE2pr-LEU2, lyp1Δ::, tor1-1, fpr1Δ::klURA, Tub4-(6)-RFP-(24)-FKBP::natNT2, TRS130-FRB::hphNT1, YLR262C-myeGFP::HIS3* | This study |
| OGYSGA6441 | *MATa, his3Δ1, leu2Δ0, ura3Δ0, LYS+, can1Δ::STE2pr-LEU2, lyp1Δ::, tor1-1, fpr1Δ::klURA, Tub4-(6)-RFP-(24)-FKBP::natNT2, TRS130-FRB::hphNT1, YLR268W-myeGFP::HIS3* | This study |
| OGYSGA6442 | *MATa, his3Δ1, leu2Δ0, ura3Δ0, LYS+, can1Δ::STE2pr-LEU2, lyp1Δ::, tor1-1, fpr1Δ::klURA, Tub4-(6)-RFP-(24)-FKBP::natNT2, TRS130-FRB::hphNT1, YBR164C-myeGFP::HIS3* | This study |
| OGYSGA6443 | *MATa, his3Δ1, leu2Δ0, ura3Δ0, LYS+, can1Δ::STE2pr-LEU2, lyp1Δ::, tor1-1, fpr1Δ::klURA, Tub4-(6)-RFP-(24)-FKBP::natNT2, TRS130-FRB::hphNT1, YGL054C-myeGFP::HIS3* | This study |
| OGYSGA6444 | *MATa, his3Δ1, leu2Δ0, ura3Δ0, LYS+, can1Δ::STE2pr-LEU2, lyp1Δ::, tor1-1, fpr1Δ::klURA, Tub4-(6)-RFP-(24)-FKBP::natNT2, TRS130-FRB::hphNT1, YGL084C-myeGFP::HIS3* | This study |
| OGYSGA6445 | *MATa, his3Δ1, leu2Δ0, ura3Δ0, LYS+, can1Δ::STE2pr-LEU2, lyp1Δ::, tor1-1, fpr1Δ::klURA, Tub4-(6)-RFP-(24)-FKBP::natNT2, TRS130-FRB::hphNT1, YMR307W-myeGFP::HIS3* | This study |
| OGYSGA6446 | *MATa, his3Δ1, leu2Δ0, ura3Δ0, LYS+, can1Δ::STE2pr-LEU2, lyp1Δ::, tor1-1, fpr1Δ::klURA, Tub4-(6)-RFP-(24)-FKBP::natNT2, TRS130-FRB::hphNT1, YNL169C-myeGFP::HIS3* | This study |
| OGYSGA6447 | *MATa, his3Δ1, leu2Δ0, ura3Δ0, LYS+, can1Δ::STE2pr-LEU2, lyp1Δ::, tor1-1, fpr1Δ::klURA, Tub4-(6)-RFP-(24)-FKBP::natNT2, TRS130-FRB::hphNT1, YLL006W-myeGFP::HIS3* | This study |
| OGYSGA6448 | *MATa, his3Δ1, leu2Δ0, ura3Δ0, LYS+, can1Δ::STE2pr-LEU2, lyp1Δ::, tor1-1, fpr1Δ::klURA, Tub4-(6)-RFP-(24)-FKBP::natNT2, TRS130-FRB::hphNT1, YCR044C-myeGFP::HIS3* | This study |
| OGYSGA6449 | *MATa, his3Δ1, leu2Δ0, ura3Δ0, LYS+, can1Δ::STE2pr-LEU2, lyp1Δ::, tor1-1, fpr1Δ::klURA, Tub4-(6)-RFP-(24)-FKBP::natNT2, TRS130-FRB::hphNT1, YKL004W-myeGFP::HIS3* | This study |
| OGYSGA6450 | *MATa, his3Δ1, leu2Δ0, ura3Δ0, LYS+, can1Δ::STE2pr-LEU2, lyp1Δ::, tor1-1, fpr1Δ::klURA, Tub4-(6)-RFP-(24)-FKBP::natNT2, TRS130-FRB::hphNT1, YPL234C-myeGFP::HIS3* | This study |
| OGYSGA6451 | *MATa, his3Δ1, leu2Δ0, ura3Δ0, LYS+, can1Δ::STE2pr-LEU2, lyp1Δ::, tor1-1, fpr1Δ::klURA, Tub4-(6)-RFP-(24)-FKBP::natNT2, TRS130-FRB::hphNT1, YKL119C-myeGFP::HIS3* | This study |
| OGYSGA1979 | *MATa, his3Δ1 leu2Δ0 ura3Δ0 LYS+, can1Δ::STE2pr-LEU2, lyp1Δ::, tor1-1, fpr1Δ::klURA, Tub4-(6)-RFP-(24)-FKBP::natNT2, TRS85-FRB::hphNT1, YOR216C-myeGFP::HIS3* | This study |
| OGYSGA1980 | *MATa, his3Δ1 leu2Δ0 ura3Δ0 LYS+, can1Δ::STE2pr-LEU2, lyp1Δ::, tor1-1, fpr1Δ::klURA, Tub4-(6)-RFP-(24)-FKBP::natNT2, TRS85-FRB::hphNT1, YMR307W-myeGFP::HIS3* | This study |
| OGYSGA1981 | *MATa, his3Δ1 leu2Δ0 ura3Δ0 LYS+, can1Δ::STE2pr-LEU2, lyp1Δ::, tor1-1, fpr1Δ::klURA, Tub4-(6)-RFP-(24)-FKBP::natNT2, TRS85-FRB::hphNT1, YMR272C-myeGFP::HIS3* | This study |
| OGYSGA1982 | *MATa, his3Δ1 leu2Δ0 ura3Δ0 LYS+, can1Δ::STE2pr-LEU2, lyp1Δ::, tor1-1, fpr1Δ::klURA, Tub4-(6)-RFP-(24)-FKBP::natNT2, TRS85-FRB::hphNT1, YLR262C-myeGFP::HIS3* | This study |
| OGYSGA1983 | *MATa, his3Δ1 leu2Δ0 ura3Δ0 LYS+, can1Δ::STE2pr-LEU2, lyp1Δ::, tor1-1, fpr1Δ::klURA, Tub4-(6)-RFP-(24)-FKBP::natNT2, TRS85-FRB::hphNT1, YGL054C-myeGFP::HIS3* | This study |
| OGYSGA1984 | *MATa, his3Δ1 leu2Δ0 ura3Δ0 LYS+, can1Δ::STE2pr-LEU2, lyp1Δ::, tor1-1, fpr1Δ::klURA, Tub4-(6)-RFP-(24)-FKBP::natNT2, TRS85-FRB::hphNT1, YPL051W-myeGFP::HIS3* | This study |

## APPENDIX I – YEAST STRAINS

| | | |
|---|---|---|
| OGYSGA1985 | *MATa, his3Δ1 leu2Δ0 ura3Δ0 LYS+, can1Δ::STE2pr-LEU2, lyp1Δ::, tor1-1, fpr1Δ::klURA, Tub4-(6)-RFP-(24)-FKBP::natNT2, TRS85-FRB::hphNT1, YMR123W-myeGFP::HIS3* | This study |
| OGYSGA1986 | *MATa, his3Δ1 leu2Δ0 ura3Δ0 LYS+, can1Δ::STE2pr-LEU2, lyp1Δ::, tor1-1, fpr1Δ::klURA, Tub4-(6)-RFP-(24)-FKBP::natNT2, TRS85-FRB::hphNT1, YBR164C-myeGFP::HIS3* | This study |
| OGYSGA1987 | *MATa, his3Δ1 leu2Δ0 ura3Δ0 LYS+, can1Δ::STE2pr-LEU2, lyp1Δ::, tor1-1, fpr1Δ::klURA, Tub4-(6)-RFP-(24)-FKBP::natNT2, TRS85-FRB::hphNT1, YOR070C-myeGFP::HIS3* | This study |
| OGYSGA1988 | *MATa, his3Δ1 leu2Δ0 ura3Δ0 LYS+, can1Δ::STE2pr-LEU2, lyp1Δ::, tor1-1, fpr1Δ::klURA, Tub4-(6)-RFP-(24)-FKBP::natNT2, TRS85-FRB::hphNT1, YKR001C-myeGFP::HIS3* | This study |
| OGYSGA1989 | *MATa, his3Δ1 leu2Δ0 ura3Δ0 LYS+, can1Δ::STE2pr-LEU2, lyp1Δ::, tor1-1, fpr1Δ::klURA, Tub4-(6)-RFP-(24)-FKBP::natNT2, TRS85-FRB::hphNT1, YPL057C-myeGFP::HIS3* | This study |
| OGYSGA1990 | *MATa, his3Δ1 leu2Δ0 ura3Δ0 LYS+, can1Δ::STE2pr-LEU2, lyp1Δ::, tor1-1, fpr1Δ::klURA, Tub4-(6)-RFP-(24)-FKBP::natNT2, TRS85-FRB::hphNT1, YLR350W-myeGFP::HIS3* | This study |
| OGYSGA1991 | *MATa, his3Δ1 leu2Δ0 ura3Δ0 LYS+, can1Δ::STE2pr-LEU2, lyp1Δ::, tor1-1, fpr1Δ::klURA, Tub4-(6)-RFP-(24)-FKBP::natNT2, TRS85-FRB::hphNT1, YLR268W-myeGFP::HIS3* | This study |
| OGYSGA1992 | *MATa, his3Δ1 leu2Δ0 ura3Δ0 LYS+, can1Δ::STE2pr-LEU2, lyp1Δ::, tor1-1, fpr1Δ::klURA, Tub4-(6)-RFP-(24)-FKBP::natNT2, TRS85-FRB::hphNT1, YJR118C-myeGFP::HIS3* | This study |
| OGYSGA1993 | *MATa, his3Δ1 leu2Δ0 ura3Δ0 LYS+, can1Δ::STE2pr-LEU2, lyp1Δ::, tor1-1, fpr1Δ::klURA, Tub4-(6)-RFP-(24)-FKBP::natNT2, TRS85-FRB::hphNT1, YLR039C-myeGFP::HIS3* | This study |
| OGYSGA1994 | *MATa, his3Δ1 leu2Δ0 ura3Δ0 LYS+, can1Δ::STE2pr-LEU2, lyp1Δ::, tor1-1, fpr1Δ::klURA, Tub4-(6)-RFP-(24)-FKBP::natNT2, TRS85-FRB::hphNT1, YBR080C-myeGFP::HIS3* | This study |
| OGYSGA1995 | *MATa, his3Δ1 leu2Δ0 ura3Δ0 LYS+, can1Δ::STE2pr-LEU2, lyp1Δ::, tor1-1, fpr1Δ::klURA, Tub4-(6)-RFP-(24)-FKBP::natNT2, TRS85-FRB::hphNT1, YJL123C-myeGFP::HIS3* | This study |
| OGYSGA1996 | *MATa, his3Δ1 leu2Δ0 ura3Δ0 LYS+, can1Δ::STE2pr-LEU2, lyp1Δ::, tor1-1, fpr1Δ::klURA, Tub4-(6)-RFP-(24)-FKBP::natNT2, TRS85-FRB::hphNT1, YPL234C-myeGFP::HIS3* | This study |
| OGYSGA1997 | *MATa, his3Δ1 leu2Δ0 ura3Δ0 LYS+, can1Δ::STE2pr-LEU2, lyp1Δ::, tor1-1, fpr1Δ::klURA, Tub4-(6)-RFP-(24)-FKBP::natNT2, TRS85-FRB::hphNT1, YKL119C-myeGFP::HIS3* | This study |
| OGYSGA1998 | *MATa, his3Δ1 leu2Δ0 ura3Δ0 LYS+, can1Δ::STE2pr-LEU2, lyp1Δ::, tor1-1, fpr1Δ::klURA, Tub4-(6)-RFP-(24)-FKBP::natNT2, TRS85-FRB::hphNT1, YLL040C-myeGFP::HIS3* | This study |
| OGYSGA1999 | *MATa, his3Δ1 leu2Δ0 ura3Δ0 LYS+, can1Δ::STE2pr-LEU2, lyp1Δ::, tor1-1, fpr1Δ::klURA, Tub4-(6)-RFP-(24)-FKBP::natNT2, TRS85-FRB::hphNT1, YPL120W-myeGFP::HIS3* | This study |
| OGYSGA2000 | *MATa, his3Δ1 leu2Δ0 ura3Δ0 LYS+, can1Δ::STE2pr-LEU2, lyp1Δ::, tor1-1, fpr1Δ::klURA, Tub4-(6)-RFP-(24)-FKBP::natNT2, TRS85-FRB::hphNT1, YAL026C-myeGFP::HIS3* | This study |
| OGYSGA2001 | *MATa, his3Δ1 leu2Δ0 ura3Δ0 LYS+, can1Δ::STE2pr-LEU2, lyp1Δ::, tor1-1, fpr1Δ::klURA, Tub4-(6)-RFP-(24)-FKBP::natNT2, TRS85-FRB::hphNT1, YKL004W-myeGFP::HIS3* | This study |
| OGYSGA2002 | *MATa, his3Δ1 leu2Δ0 ura3Δ0 LYS+, can1Δ::STE2pr-LEU2, lyp1Δ::, tor1-1, fpr1Δ::klURA, Tub4-(6)-RFP-(24)-FKBP::natNT2, TRS85-FRB::hphNT1, YMR190C-myeGFP::HIS3* | This study |
| OGYSGA2003 | *MATa, his3Δ1 leu2Δ0 ura3Δ0 LYS+, can1Δ::STE2pr-LEU2, lyp1Δ::, tor1-1, fpr1Δ::klURA, Tub4-(6)-RFP-(24)-FKBP::natNT2, TRS85-FRB::hphNT1, YDR137W-myeGFP::HIS3* | This study |
| OGYSGA2004 | *MATa, his3Δ1 leu2Δ0 ura3Δ0 LYS+, can1Δ::STE2pr-LEU2, lyp1Δ::, tor1-1, fpr1Δ::klURA, Tub4-(6)-RFP-(24)-FKBP::natNT2, TRS85-FRB::hphNT1, YIL004C-myeGFP::HIS3* | This study |
| OGYSGA2005 | *MATa, his3Δ1 leu2Δ0 ura3Δ0 LYS+, can1Δ::STE2pr-LEU2, lyp1Δ::, tor1-1, fpr1Δ::klURA, Tub4-(6)-RFP-(24)-FKBP::natNT2, TRS85-FRB::hphNT1, YPL158C-myeGFP::HIS3* | This study |
| OGYSGA2006 | *MATa, his3Δ1 leu2Δ0 ura3Δ0 LYS+, can1Δ::STE2pr-LEU2, lyp1Δ::, tor1-1, fpr1Δ::klURA, Tub4-(6)-RFP-(24)-FKBP::natNT2, TRS85-FRB::hphNT1, YNL169C-myeGFP::HIS3* | This study |
| OGYSGA2007 | *MATa, his3Δ1 leu2Δ0 ura3Δ0 LYS+, can1Δ::STE2pr-LEU2, lyp1Δ::, tor1-1, fpr1Δ::klURA, Tub4-(6)-RFP-(24)-FKBP::natNT2, TRS85-FRB::hphNT1, YML041C-myeGFP::HIS3* | This study |
| OGYSGA2008 | *MATa, his3Δ1 leu2Δ0 ura3Δ0 LYS+, can1Δ::STE2pr-LEU2, lyp1Δ::, tor1-1, fpr1Δ::klURA, Tub4-(6)-RFP-(24)-FKBP::natNT2, TRS85-FRB::hphNT1, YGL020C-myeGFP::HIS3* | This study |
| OGYSGA2009 | *MATa, his3Δ1 leu2Δ0 ura3Δ0 LYS+, can1Δ::STE2pr-LEU2, lyp1Δ::, tor1-1, fpr1Δ::klURA, Tub4-(6)-RFP-(24)-FKBP::natNT2, TRS85-FRB::hphNT1, YOL012C-myeGFP::HIS3* | This study |
| OGYSGA2010 | *MATa, his3Δ1 leu2Δ0 ura3Δ0 LYS+, can1Δ::STE2pr-LEU2, lyp1Δ::, tor1-1, fpr1Δ::klURA, Tub4-(6)-RFP-(24)-FKBP::natNT2, TRS85-FRB::hphNT1, YNR051C-myeGFP::HIS3* | This study |
| OGYSGA2011 | *MATa, his3Δ1 leu2Δ0 ura3Δ0 LYS+, can1Δ::STE2pr-LEU2, lyp1Δ::, tor1-1, fpr1Δ::klURA, Tub4-(6)-RFP-(24)-FKBP::natNT2, TRS85-FRB::hphNT1, YKL212W-myeGFP::HIS3* | This study |

## APPENDIX I – YEAST STRAINS

| | | |
|---|---|---|
| OGYSGA2012 | *MATa, his3Δ1 leu2Δ0 ura3Δ0 LYS+, can1Δ::STE2pr-LEU2, lyp1Δ::, tor1-1, fpr1Δ::klURA, Tub4-(6)-RFP-(24)-FKBP::natNT2, TRS85-FRB::hphNT1, YLR418C-myeGFP::HIS3* | This study |
| OGYSGA2013 | *MATa, his3Δ1 leu2Δ0 ura3Δ0 LYS+, can1Δ::STE2pr-LEU2, lyp1Δ::, tor1-1, fpr1Δ::klURA, Tub4-(6)-RFP-(24)-FKBP::natNT2, TRS85-FRB::hphNT1, YNL044W-myeGFP::HIS3* | This study |
| OGYSGA2014 | *MATa, his3Δ1 leu2Δ0 ura3Δ0 LYS+, can1Δ::STE2pr-LEU2, lyp1Δ::, tor1-1, fpr1Δ::klURA, Tub4-(6)-RFP-(24)-FKBP::natNT2, TRS85-FRB::hphNT1, YMR010W-myeGFP::HIS3* | This study |
| OGYSGA2015 | *MATa, his3Δ1 leu2Δ0 ura3Δ0 LYS+, can1Δ::STE2pr-LEU2, lyp1Δ::, tor1-1, fpr1Δ::klURA, Tub4-(6)-RFP-(24)-FKBP::natNT2, TRS85-FRB::hphNT1, YEL043W-myeGFP::HIS3* | This study |
| OGYSGA2016 | *MATa, his3Δ1 leu2Δ0 ura3Δ0 LYS+, can1Δ::STE2pr-LEU2, lyp1Δ::, tor1-1, fpr1Δ::klURA, Tub4-(6)-RFP-(24)-FKBP::natNT2, TRS85-FRB::hphNT1, YDL058W-myeGFP::HIS3* | This study |
| OGYSGA2017 | *MATa, his3Δ1 leu2Δ0 ura3Δ0 LYS+, can1Δ::STE2pr-LEU2, lyp1Δ::, tor1-1, fpr1Δ::klURA, Tub4-(6)-RFP-(24)-FKBP::natNT2, TRS85-FRB::hphNT1, YNL267W-myeGFP::HIS3* | This study |
| OGYSGA2018 | *MATa, his3Δ1 leu2Δ0 ura3Δ0 LYS+, can1Δ::STE2pr-LEU2, lyp1Δ::, tor1-1, fpr1Δ::klURA, Tub4-(6)-RFP-(24)-FKBP::natNT2, TRS85-FRB::hphNT1, YDL099W-myeGFP::HIS3* | This study |
| OGYSGA2019 | *MATa, his3Δ1 leu2Δ0 ura3Δ0 LYS+, can1Δ::STE2pr-LEU2, lyp1Δ::, tor1-1, fpr1Δ::klURA, Tub4-(6)-RFP-(24)-FKBP::natNT2, TRS85-FRB::hphNT1, YIL039W-myeGFP::HIS3* | This study |
| OGYSGA2020 | *MATa, his3Δ1 leu2Δ0 ura3Δ0 LYS+, can1Δ::STE2pr-LEU2, lyp1Δ::, tor1-1, fpr1Δ::klURA, Tub4-(6)-RFP-(24)-FKBP::natNT2, TRS85-FRB::hphNT1, YML012W-myeGFP::HIS3* | This study |
| OGYSGA2021 | *MATa, his3Δ1 leu2Δ0 ura3Δ0 LYS+, can1Δ::STE2pr-LEU2, lyp1Δ::, tor1-1, fpr1Δ::klURA, Tub4-(6)-RFP-(24)-FKBP::natNT2, TRS85-FRB::hphNT1, YDR372C-myeGFP::HIS3* | This study |
| OGYSGA2022 | *MATa, his3Δ1 leu2Δ0 ura3Δ0 LYS+, can1Δ::STE2pr-LEU2, lyp1Δ::, tor1-1, fpr1Δ::klURA, Tub4-(6)-RFP-(24)-FKBP::natNT2, TRS85-FRB::hphNT1, YGL200C-myeGFP::HIS3* | This study |
| OGYSGA2023 | *MATa, his3Δ1 leu2Δ0 ura3Δ0 LYS+, can1Δ::STE2pr-LEU2, lyp1Δ::, tor1-1, fpr1Δ::klURA, Tub4-(6)-RFP-(24)-FKBP::natNT2, TRS85-FRB::hphNT1, YJL117W-myeGFP::HIS3* | This study |
| OGYSGA2024 | *MATa, his3Δ1 leu2Δ0 ura3Δ0 LYS+, can1Δ::STE2pr-LEU2, lyp1Δ::, tor1-1, fpr1Δ::klURA, Tub4-(6)-RFP-(24)-FKBP::natNT2, TRS85-FRB::hphNT1, YEL042W-myeGFP::HIS3* | This study |
| OGYSGA2025 | *MATa, his3Δ1 leu2Δ0 ura3Δ0 LYS+, can1Δ::STE2pr-LEU2, lyp1Δ::, tor1-1, fpr1Δ::klURA, Tub4-(6)-RFP-(24)-FKBP::natNT2, TRS85-FRB::hphNT1, YKL069W-myeGFP::HIS3* | This study |
| OGYSGA2026 | *MATa, his3Δ1 leu2Δ0 ura3Δ0 LYS+, can1Δ::STE2pr-LEU2, lyp1Δ::, tor1-1, fpr1Δ::klURA, Tub4-(6)-RFP-(24)-FKBP::natNT2, TRS85-FRB::hphNT1, YJR032W-myeGFP::HIS3* | This study |
| OGYSGA2027 | *MATa, his3Δ1 leu2Δ0 ura3Δ0 LYS+, can1Δ::STE2pr-LEU2, lyp1Δ::, tor1-1, fpr1Δ::klURA, Tub4-(6)-RFP-(24)-FKBP::natNT2, TRS85-FRB::hphNT1, YLR260W-myeGFP::HIS3* | This study |
| OGYSGA2028 | *MATa, his3Δ1 leu2Δ0 ura3Δ0 LYS+, can1Δ::STE2pr-LEU2, lyp1Δ::, tor1-1, fpr1Δ::klURA, Tub4-(6)-RFP-(24)-FKBP::natNT2, TRS85-FRB::hphNT1, YEL051W-myeGFP::HIS3* | This study |
| OGYSGA2029 | *MATa, his3Δ1 leu2Δ0 ura3Δ0 LYS+, can1Δ::STE2pr-LEU2, lyp1Δ::, tor1-1, fpr1Δ::klURA, Tub4-(6)-RFP-(24)-FKBP::natNT2, TRS85-FRB::hphNT1, YNL238W-myeGFP::HIS3* | This study |
| OGYSGA2030 | *MATa, his3Δ1 leu2Δ0 ura3Δ0 LYS+, can1Δ::STE2pr-LEU2, lyp1Δ::, tor1-1, fpr1Δ::klURA, Tub4-(6)-RFP-(24)-FKBP::natNT2, TRS85-FRB::hphNT1, YMR079W-myeGFP::HIS3* | This study |
| OGYSGA2031 | *MATa, his3Δ1 leu2Δ0 ura3Δ0 LYS+, can1Δ::STE2pr-LEU2, lyp1Δ::, tor1-1, fpr1Δ::klURA, Tub4-(6)-RFP-(24)-FKBP::natNT2, TRS85-FRB::hphNT1, YGL086W-myeGFP::HIS3* | This study |
| OGYSGA2032 | *MATa, his3Δ1 leu2Δ0 ura3Δ0 LYS+, can1Δ::STE2pr-LEU2, lyp1Δ::, tor1-1, fpr1Δ::klURA, Tub4-(6)-RFP-(24)-FKBP::natNT2, TRS85-FRB::hphNT1, YML008C-myeGFP::HIS3* | This study |
| OGYSGA2033 | *MATa, his3Δ1 leu2Δ0 ura3Δ0 LYS+, can1Δ::STE2pr-LEU2, lyp1Δ::, tor1-1, fpr1Δ::klURA, Tub4-(6)-RFP-(24)-FKBP::natNT2, TRS85-FRB::hphNT1, YJL004C-myeGFP::HIS3* | This study |
| OGYSGA2034 | *MATa, his3Δ1 leu2Δ0 ura3Δ0 LYS+, can1Δ::STE2pr-LEU2, lyp1Δ::, tor1-1, fpr1Δ::klURA, Tub4-(6)-RFP-(24)-FKBP::natNT2, TRS85-FRB::hphNT1, YDR320C-myeGFP::HIS3* | This study |
| OGYSGA2035 | *MATa, his3Δ1 leu2Δ0 ura3Δ0 LYS+, can1Δ::STE2pr-LEU2, lyp1Δ::, tor1-1, fpr1Δ::klURA, Tub4-(6)-RFP-(24)-FKBP::natNT2, TRS85-FRB::hphNT1, YMR216C-myeGFP::HIS3* | This study |
| OGYSGA2036 | *MATa, his3Δ1 leu2Δ0 ura3Δ0 LYS+, can1Δ::STE2pr-LEU2, lyp1Δ::, tor1-1, fpr1Δ::klURA, Tub4-(6)-RFP-(24)-FKBP::natNT2, TRS85-FRB::hphNT1, YGL084C-myeGFP::HIS3* | This study |
| OGYSGA2037 | *MATa, his3Δ1 leu2Δ0 ura3Δ0 LYS+, can1Δ::STE2pr-LEU2, lyp1Δ::, tor1-1, fpr1Δ::klURA, Tub4-(6)-RFP-(24)-FKBP::natNT2, TRS85-FRB::hphNT1, YOR254C-myeGFP::HIS3* | This study |
| OGYSGA2038 | *MATa, his3Δ1 leu2Δ0 ura3Δ0 LYS+, can1Δ::STE2pr-LEU2, lyp1Δ::, tor1-1, fpr1Δ::klURA, Tub4-(6)-RFP-(24)-FKBP::natNT2, TRS85-FRB::hphNT1, YGR092W-myeGFP::HIS3* | This study |

## APPENDIX I – YEAST STRAINS

| | | |
|---|---|---|
| OGYSGA2039 | *MATa, his3Δ1 leu2Δ0 ura3Δ0 LYS+, can1Δ::STE2pr-LEU2, lyp1Δ::, tor1-1, fpr1Δ::klURA, Tub4-(6)-RFP-(24)-FKBP::natNT2, TRS85-FRB::hphNT1, YJR060W-myeGFP::HIS3* | This study |
| OGYSGA2040 | *MATa, his3Δ1 leu2Δ0 ura3Δ0 LYS+, can1Δ::STE2pr-LEU2, lyp1Δ::, tor1-1, fpr1Δ::klURA, Tub4-(6)-RFP-(24)-FKBP::natNT2, TRS85-FRB::hphNT1, YLL006W-myeGFP::HIS3* | This study |
| OGYSGA2041 | *MATa, his3Δ1 leu2Δ0 ura3Δ0 LYS+, can1Δ::STE2pr-LEU2, lyp1Δ::, tor1-1, fpr1Δ::klURA, Tub4-(6)-RFP-(24)-FKBP::natNT2, TRS85-FRB::hphNT1, YCR044C-myeGFP::HIS3* | This study |
| OGYSGA2042 | *MATa, his3Δ1 leu2Δ0 ura3Δ0 LYS+, can1Δ::STE2pr-LEU2, lyp1Δ::, tor1-1, fpr1Δ::klURA, Tub4-(6)-RFP-(24)-FKBP::natNT2, TRS85-FRB::hphNT1, YNL297C-myeGFP::HIS3* | This study |
| OGYSGA2043 | *MATa, his3Δ1 leu2Δ0 ura3Δ0 LYS+, can1Δ::STE2pr-LEU2, lyp1Δ::, tor1-1, fpr1Δ::klURA, Tub4-(6)-RFP-(24)-FKBP::natNT2, TRS85-FRB::hphNT1, YCR034W-myeGFP::HIS3* | This study |
| OGYSGA2044 | *MATa, his3Δ1 leu2Δ0 ura3Δ0 LYS+, can1Δ::STE2pr-LEU2, lyp1Δ::, tor1-1, fpr1Δ::klURA, Tub4-(6)-RFP-(24)-FKBP::natNT2, VPS53-FRB::hphNT1, YCR017C-myeGFP::HIS3* | This study |
| OGYSGA2045 | *MATa, his3Δ1 leu2Δ0 ura3Δ0 LYS+, can1Δ::STE2pr-LEU2, lyp1Δ::, tor1-1, fpr1Δ::klURA, Tub4-(6)-RFP-(24)-FKBP::natNT2, VPS53-FRB::hphNT1, YNL243W-myeGFP::HIS3* | This study |
| OGYSGA2046 | *MATa, his3Δ1 leu2Δ0 ura3Δ0 LYS+, can1Δ::STE2pr-LEU2, lyp1Δ::, tor1-1, fpr1Δ::klURA, Tub4-(6)-RFP-(24)-FKBP::natNT2, VPS53-FRB::hphNT1, YOR164C-myeGFP::HIS3* | This study |
| OGYSGA2047 | *MATa, his3Δ1 leu2Δ0 ura3Δ0 LYS+, can1Δ::STE2pr-LEU2, lyp1Δ::, tor1-1, fpr1Δ::klURA, Tub4-(6)-RFP-(24)-FKBP::natNT2, VPS53-FRB::hphNT1, YCL001W-myeGFP::HIS3* | This study |
| OGYSGA2048 | *MATa, his3Δ1 leu2Δ0 ura3Δ0 LYS+, can1Δ::STE2pr-LEU2, lyp1Δ::, tor1-1, fpr1Δ::klURA, Tub4-(6)-RFP-(24)-FKBP::natNT2, VPS53-FRB::hphNT1, YBR245C-myeGFP::HIS3* | This study |
| OGYSGA2049 | *MATa, his3Δ1 leu2Δ0 ura3Δ0 LYS+, can1Δ::STE2pr-LEU2, lyp1Δ::, tor1-1, fpr1Δ::klURA, Tub4-(6)-RFP-(24)-FKBP::natNT2, VPS53-FRB::hphNT1, YMR079W-myeGFP::HIS3* | This study |
| OGYSGA2050 | *MATa, his3Δ1 leu2Δ0 ura3Δ0 LYS+, can1Δ::STE2pr-LEU2, lyp1Δ::, tor1-1, fpr1Δ::klURA, Tub4-(6)-RFP-(24)-FKBP::natNT2, VPS53-FRB::hphNT1, YMR216C-myeGFP::HIS3* | This study |
| OGYSGA2051 | *MATa, his3Δ1 leu2Δ0 ura3Δ0 LYS+, can1Δ::STE2pr-LEU2, lyp1Δ::, tor1-1, fpr1Δ::klURA, Tub4-(6)-RFP-(24)-FKBP::natNT2, VPS53-FRB::hphNT1, YKR001C-myeGFP::HIS3* | This study |
| OGYSGA2052 | *MATa, his3Δ1 leu2Δ0 ura3Δ0 LYS+, can1Δ::STE2pr-LEU2, lyp1Δ::, tor1-1, fpr1Δ::klURA, Tub4-(6)-RFP-(24)-FKBP::natNT2, VPS53-FRB::hphNT1, YLR372W-myeGFP::HIS3* | This study |
| OGYSGA2053 | *MATa, his3Δ1 leu2Δ0 ura3Δ0 LYS+, can1Δ::STE2pr-LEU2, lyp1Δ::, tor1-1, fpr1Δ::klURA, Tub4-(6)-RFP-(24)-FKBP::natNT2, VPS53-FRB::hphNT1, YLR350W-myeGFP::HIS3* | This study |
| OGYSGA2054 | *MATa, his3Δ1 leu2Δ0 ura3Δ0 LYS+, can1Δ::STE2pr-LEU2, lyp1Δ::, tor1-1, fpr1Δ::klURA, Tub4-(6)-RFP-(24)-FKBP::natNT2, VPS53-FRB::hphNT1, YGL020C-myeGFP::HIS3* | This study |
| OGYSGA2055 | *MATa, his3Δ1 leu2Δ0 ura3Δ0 LYS+, can1Δ::STE2pr-LEU2, lyp1Δ::, tor1-1, fpr1Δ::klURA, Tub4-(6)-RFP-(24)-FKBP::natNT2, VPS53-FRB::hphNT1, YER083C-myeGFP::HIS3* | This study |
| OGYSGA2056 | *MATa, his3Δ1 leu2Δ0 ura3Δ0 LYS+, can1Δ::STE2pr-LEU2, lyp1Δ::, tor1-1, fpr1Δ::klURA, Tub4-(6)-RFP-(24)-FKBP::natNT2, VPS53-FRB::hphNT1, YMR161W-myeGFP::HIS3* | This study |
| OGYSGA2057 | *MATa, his3Δ1 leu2Δ0 ura3Δ0 LYS+, can1Δ::STE2pr-LEU2, lyp1Δ::, tor1-1, fpr1Δ::klURA, Tub4-(6)-RFP-(24)-FKBP::natNT2, VPS53-FRB::hphNT1, YER122C-myeGFP::HIS3* | This study |
| OGYSGA2058 | *MATa, his3Δ1 leu2Δ0 ura3Δ0 LYS+, can1Δ::STE2pr-LEU2, lyp1Δ::, tor1-1, fpr1Δ::klURA, Tub4-(6)-RFP-(24)-FKBP::natNT2, VPS53-FRB::hphNT1, YJR117W-myeGFP::HIS3* | This study |
| OGYSGA2059 | *MATa, his3Δ1 leu2Δ0 ura3Δ0 LYS+, can1Δ::STE2pr-LEU2, lyp1Δ::, tor1-1, fpr1Δ::klURA, Tub4-(6)-RFP-(24)-FKBP::natNT2, VPS53-FRB::hphNT1, YKR029C-myeGFP::HIS3* | This study |
| OGYSGA2060 | *MATa, his3Δ1 leu2Δ0 ura3Δ0 LYS+, can1Δ::STE2pr-LEU2, lyp1Δ::, tor1-1, fpr1Δ::klURA, Tub4-(6)-RFP-(24)-FKBP::natNT2, VPS53-FRB::hphNT1, YGR063C-myeGFP::HIS3* | This study |
| OGYSGA2061 | *MATa, his3Δ1 leu2Δ0 ura3Δ0 LYS+, can1Δ::STE2pr-LEU2, lyp1Δ::, tor1-1, fpr1Δ::klURA, Tub4-(6)-RFP-(24)-FKBP::natNT2, VPS53-FRB::hphNT1, YML097C-myeGFP::HIS3* | This study |
| OGYSGA2062 | *MATa, his3Δ1 leu2Δ0 ura3Δ0 LYS+, can1Δ::STE2pr-LEU2, lyp1Δ::, tor1-1, fpr1Δ::klURA, Tub4-(6)-RFP-(24)-FKBP::natNT2, VPS53-FRB::hphNT1, YOL001W-myeGFP::HIS3* | This study |
| OGYSGA2063 | *MATa, his3Δ1 leu2Δ0 ura3Δ0 LYS+, can1Δ::STE2pr-LEU2, lyp1Δ::, tor1-1, fpr1Δ::klURA, Tub4-(6)-RFP-(24)-FKBP::natNT2, VPS53-FRB::hphNT1, YOR070C-myeGFP::HIS3* | This study |
| OGYSGA2064 | *MATa, his3Δ1 leu2Δ0 ura3Δ0 LYS+, can1Δ::STE2pr-LEU2, lyp1Δ::, tor1-1, fpr1Δ::klURA, Tub4-(6)-RFP-(24)-FKBP::natNT2, VPS53-FRB::hphNT1, YLR056W-myeGFP::HIS3* | This study |
| OGYSGA2065 | *MATa, his3Δ1 leu2Δ0 ura3Δ0 LYS+, can1Δ::STE2pr-LEU2, lyp1Δ::, tor1-1, fpr1Δ::klURA, Tub4-(6)-RFP-(24)-FKBP::natNT2, VPS53-FRB::hphNT1, YDL185W-myeGFP::HIS3* | This study |

## APPENDIX I – YEAST STRAINS

| | | |
|---|---|---|
| OGYSGA2066 | *MATa, his3Δ1 leu2Δ0 ura3Δ0 LYS+, can1Δ::STE2pr-LEU2, lyp1Δ::, tor1-1, fpr1Δ::klURA, Tub4-(6)-RFP-(24)-FKBP::natNT2, VPS53-FRB::hphNT1, YGL058W-myeGFP::HIS3* | This study |
| OGYSGA2067 | *MATa, his3Δ1 leu2Δ0 ura3Δ0 LYS+, can1Δ::STE2pr-LEU2, lyp1Δ::, tor1-1, fpr1Δ::klURA, Tub4-(6)-RFP-(24)-FKBP::natNT2, VPS53-FRB::hphNT1, YJR073C-myeGFP::HIS3* | This study |
| OGYSGA2068 | *MATa, his3Δ1 leu2Δ0 ura3Δ0 LYS+, can1Δ::STE2pr-LEU2, lyp1Δ::, tor1-1, fpr1Δ::klURA, Tub4-(6)-RFP-(24)-FKBP::natNT2, VPS53-FRB::hphNT1, YDL074C-myeGFP::HIS3* | This study |
| OGYSGA2069 | *MATa, his3Δ1 leu2Δ0 ura3Δ0 LYS+, can1Δ::STE2pr-LEU2, lyp1Δ::, tor1-1, fpr1Δ::klURA, Tub4-(6)-RFP-(24)-FKBP::natNT2, VPS53-FRB::hphNT1, YPL055C-myeGFP::HIS3* | This study |
| OGYSGA2070 | *MATa, his3Δ1 leu2Δ0 ura3Δ0 LYS+, can1Δ::STE2pr-LEU2, lyp1Δ::, tor1-1, fpr1Δ::klURA, Tub4-(6)-RFP-(24)-FKBP::natNT2, VPS53-FRB::hphNT1, YDR056C-myeGFP::HIS3* | This study |
| OGYSGA2071 | *MATa, his3Δ1 leu2Δ0 ura3Δ0 LYS+, can1Δ::STE2pr-LEU2, lyp1Δ::, tor1-1, fpr1Δ::klURA, Tub4-(6)-RFP-(24)-FKBP::natNT2, VPS53-FRB::hphNT1, YOR244W-myeGFP::HIS3* | This study |
| OGYSGA2072 | *MATa, his3Δ1 leu2Δ0 ura3Δ0 LYS+, can1Δ::STE2pr-LEU2, lyp1Δ::, tor1-1, fpr1Δ::klURA, Tub4-(6)-RFP-(24)-FKBP::natNT2, VPS53-FRB::hphNT1, YGR105W-myeGFP::HIS3* | This study |
| OGYSGA2073 | *MATa, his3Δ1 leu2Δ0 ura3Δ0 LYS+, can1Δ::STE2pr-LEU2, lyp1Δ::, tor1-1, fpr1Δ::klURA, Tub4-(6)-RFP-(24)-FKBP::natNT2, VPS53-FRB::hphNT1, YAR002C-A -myeGFP::HIS3* | This study |
| OGYSGA2074 | *MATa, his3Δ1 leu2Δ0 ura3Δ0 LYS+, can1Δ::STE2pr-LEU2, lyp1Δ::, tor1-1, fpr1Δ::klURA, Tub4-(6)-RFP-(24)-FKBP::natNT2, VPS53-FRB::hphNT1, YBR041W-myeGFP::HIS3* | This study |
| OGYSGA2075 | *MATa, his3Δ1 leu2Δ0 ura3Δ0 LYS+, can1Δ::STE2pr-LEU2, lyp1Δ::, tor1-1, fpr1Δ::klURA, Tub4-(6)-RFP-(24)-FKBP::natNT2, VPS53-FRB::hphNT1, YDL099W-myeGFP::HIS3* | This study |
| OGYSGA2076 | *MATa, his3Δ1 leu2Δ0 ura3Δ0 LYS+, can1Δ::STE2pr-LEU2, lyp1Δ::, tor1-1, fpr1Δ::klURA, Tub4-(6)-RFP-(24)-FKBP::natNT2, VPS53-FRB::hphNT1, YML075C-myeGFP::HIS3* | This study |
| OGYSGA2077 | *MATa, his3Δ1 leu2Δ0 ura3Δ0 LYS+, can1Δ::STE2pr-LEU2, lyp1Δ::, tor1-1, fpr1Δ::klURA, Tub4-(6)-RFP-(24)-FKBP::natNT2, VPS53-FRB::hphNT1, YNL323W-myeGFP::HIS3* | This study |
| OGYSGA2078 | *MATa, his3Δ1 leu2Δ0 ura3Δ0 LYS+, can1Δ::STE2pr-LEU2, lyp1Δ::, tor1-1, fpr1Δ::klURA, Tub4-(6)-RFP-(24)-FKBP::natNT2, VPS53-FRB::hphNT1, YAL058W-myeGFP::HIS3* | This study |
| OGYSGA2079 | *MATa, his3Δ1 leu2Δ0 ura3Δ0 LYS+, can1Δ::STE2pr-LEU2, lyp1Δ::, tor1-1, fpr1Δ::klURA, Tub4-(6)-RFP-(24)-FKBP::natNT2, VPS53-FRB::hphNT1, YOL111C-myeGFP::HIS3* | This study |
| OGYSGA2080 | *MATa, his3Δ1 leu2Δ0 ura3Δ0 LYS+, can1Δ::STE2pr-LEU2, lyp1Δ::, tor1-1, fpr1Δ::klURA, Tub4-(6)-RFP-(24)-FKBP::natNT2, VPS53-FRB::hphNT1, YIL030C-myeGFP::HIS3* | This study |
| OGYSGA2081 | *MATa, his3Δ1 leu2Δ0 ura3Δ0 LYS+, can1Δ::STE2pr-LEU2, lyp1Δ::, tor1-1, fpr1Δ::klURA, Tub4-(6)-RFP-(24)-FKBP::natNT2, VPS53-FRB::hphNT1, YOL013C-myeGFP::HIS3* | This study |
| OGYSGA2082 | *MATa, his3Δ1 leu2Δ0 ura3Δ0 LYS+, can1Δ::STE2pr-LEU2, lyp1Δ::, tor1-1, fpr1Δ::klURA, Tub4-(6)-RFP-(24)-FKBP::natNT2, VPS53-FRB::hphNT1, YMR015C-myeGFP::HIS3* | This study |
| OGYSGA2083 | *MATa, his3Δ1 leu2Δ0 ura3Δ0 LYS+, can1Δ::STE2pr-LEU2, lyp1Δ::, tor1-1, fpr1Δ::klURA, Tub4-(6)-RFP-(24)-FKBP::natNT2, VPS53-FRB::hphNT1, YBR283C-myeGFP::HIS3* | This study |
| OGYSGA2084 | *MATa, his3Δ1 leu2Δ0 ura3Δ0 LYS+, can1Δ::STE2pr-LEU2, lyp1Δ::, tor1-1, fpr1Δ::klURA, Tub4-(6)-RFP-(24)-FKBP::natNT2, VPS53-FRB::hphNT1, YOR085W-myeGFP::HIS3* | This study |
| OGYSGA2085 | *MATa, his3Δ1 leu2Δ0 ura3Δ0 LYS+, can1Δ::STE2pr-LEU2, lyp1Δ::, tor1-1, fpr1Δ::klURA, Tub4-(6)-RFP-(24)-FKBP::natNT2, VPS53-FRB::hphNT1, YNL267W-myeGFP::HIS3* | This study |
| OGYSGA2086 | *MATa, his3Δ1 leu2Δ0 ura3Δ0 LYS+, can1Δ::STE2pr-LEU2, lyp1Δ::, tor1-1, fpr1Δ::klURA, Tub4-(6)-RFP-(24)-FKBP::natNT2, VPS53-FRB::hphNT1, YNR052C-myeGFP::HIS3* | This study |
| OGYSGA2087 | *MATa, his3Δ1 leu2Δ0 ura3Δ0 LYS+, can1Δ::STE2pr-LEU2, lyp1Δ::, tor1-1, fpr1Δ::klURA, Tub4-(6)-RFP-(24)-FKBP::natNT2, VPS53-FRB::hphNT1, YAL023C-myeGFP::HIS3* | This study |
| OGYSGA2088 | *MATa, his3Δ1 leu2Δ0 ura3Δ0 LYS+, can1Δ::STE2pr-LEU2, lyp1Δ::, tor1-1, fpr1Δ::klURA, Tub4-(6)-RFP-(24)-FKBP::natNT2, VPS53-FRB::hphNT1, YGR060W-myeGFP::HIS3* | This study |
| OGYSGA2089 | *MATa, his3Δ1 leu2Δ0 ura3Δ0 LYS+, can1Δ::STE2pr-LEU2, lyp1Δ::, tor1-1, fpr1Δ::klURA, Tub4-(6)-RFP-(24)-FKBP::natNT2, VPS53-FRB::hphNT1, YLL040C-myeGFP::HIS3* | This study |
| OGYSGA2090 | *MATa, his3Δ1 leu2Δ0 ura3Δ0 LYS+, can1Δ::STE2pr-LEU2, lyp1Δ::, tor1-1, fpr1Δ::klURA, Tub4-(6)-RFP-(24)-FKBP::natNT2, VPS53-FRB::hphNT1, YOR216C-myeGFP::HIS3* | This study |
| OGYSGA2091 | *MATa, his3Δ1 leu2Δ0 ura3Δ0 LYS+, can1Δ::STE2pr-LEU2, lyp1Δ::, tor1-1, fpr1Δ::klURA, Tub4-(6)-RFP-(24)-FKBP::natNT2, VPS53-FRB::hphNT1, YFL024C-myeGFP::HIS3* | This study |
| OGYSGA2092 | *MATa, his3Δ1 leu2Δ0 ura3Δ0 LYS+, can1Δ::STE2pr-LEU2, lyp1Δ::, tor1-1, fpr1Δ::klURA, Tub4-(6)-RFP-(24)-FKBP::natNT2, VPS53-FRB::hphNT1, YAL021C-myeGFP::HIS3* | This study |

## APPENDIX I – YEAST STRAINS

| | | |
|---|---|---|
| OGYSGA2093 | *MATa, his3Δ1 leu2Δ0 ura3Δ0 LYS+, can1Δ::STE2pr-LEU2, lyp1Δ::, tor1-1, fpr1Δ::klURA, Tub4-(6)-RFP-(24)-FKBP::natNT2, VPS53-FRB::hphNT1, YPL120W-myeGFP::HIS3* | This study |
| OGYSGA2094 | *MATa, his3Δ1 leu2Δ0 ura3Δ0 LYS+, can1Δ::STE2pr-LEU2, lyp1Δ::, tor1-1, fpr1Δ::klURA, Tub4-(6)-RFP-(24)-FKBP::natNT2, VPS53-FRB::hphNT1, YPR032W-myeGFP::HIS3* | This study |
| OGYSGA2095 | *MATa, his3Δ1 leu2Δ0 ura3Δ0 LYS+, can1Δ::STE2pr-LEU2, lyp1Δ::, tor1-1, fpr1Δ::klURA, Tub4-(6)-RFP-(24)-FKBP::natNT2, VPS53-FRB::hphNT1, YGL054C-myeGFP::HIS3* | This study |
| OGYSGA2096 | *MATa, his3Δ1 leu2Δ0 ura3Δ0 LYS+, can1Δ::STE2pr-LEU2, lyp1Δ::, tor1-1, fpr1Δ::klURA, Tub4-(6)-RFP-(24)-FKBP::natNT2, VPS53-FRB::hphNT1, YDL100C-myeGFP::HIS3* | This study |
| OGYSGA2097 | *MATa, his3Δ1 leu2Δ0 ura3Δ0 LYS+, can1Δ::STE2pr-LEU2, lyp1Δ::, tor1-1, fpr1Δ::klURA, Tub4-(6)-RFP-(24)-FKBP::natNT2, VPS53-FRB::hphNT1, YJL004C-myeGFP::HIS3* | This study |
| OGYSGA2098 | *MATa, his3Δ1 leu2Δ0 ura3Δ0 LYS+, can1Δ::STE2pr-LEU2, lyp1Δ::, tor1-1, fpr1Δ::klURA, Tub4-(6)-RFP-(24)-FKBP::natNT2, VPS53-FRB::hphNT1, YCR044C-myeGFP::HIS3* | This study |
| OGYSGA2099 | *MATa, his3Δ1 leu2Δ0 ura3Δ0 LYS+, can1Δ::STE2pr-LEU2, lyp1Δ::, tor1-1, fpr1Δ::klURA, Tub4-(6)-RFP-(24)-FKBP::natNT2, VPS53-FRB::hphNT1, YGL084C-myeGFP::HIS3* | This study |
| OGYSGA2100 | *MATa, his3Δ1 leu2Δ0 ura3Δ0 LYS+, can1Δ::STE2pr-LEU2, lyp1Δ::, tor1-1, fpr1Δ::klURA, Tub4-(6)-RFP-(24)-FKBP::natNT2, VPS53-FRB::hphNT1, YMR123W-myeGFP::HIS3* | This study |
| OGYSGA2101 | *MATa, his3Δ1 leu2Δ0 ura3Δ0 LYS+, can1Δ::STE2pr-LEU2, lyp1Δ::, tor1-1, fpr1Δ::klURA, Tub4-(6)-RFP-(24)-FKBP::natNT2, VPS53-FRB::hphNT1, YNL271C-myeGFP::HIS3* | This study |
| OGYSGA2102 | *MATa, his3Δ1 leu2Δ0 ura3Δ0 LYS+, can1Δ::STE2pr-LEU2, lyp1Δ::, tor1-1, fpr1Δ::klURA, Tub4-(6)-RFP-(24)-FKBP::natNT2, VPS53-FRB::hphNT1, YJR118C-myeGFP::HIS3* | This study |
| OGYSGA4423 | *MATa, his3Δ1 leu2Δ0 ura3Δ0 LYS+, can1Δ::STE2pr-LEU2, lyp1Δ::, tor1-1, fpr1Δ::klURA, Tub4-(6)-RFP-(24)-FKBP::natNT2, SEC3-FRB::hphNT1, YMR183C-myeGFP::HIS3* | This study |
| OGYSGA4424 | *MATa, his3Δ1 leu2Δ0 ura3Δ0 LYS+, can1Δ::STE2pr-LEU2, lyp1Δ::, tor1-1, fpr1Δ::klURA, Tub4-(6)-RFP-(24)-FKBP::natNT2, SEC3-FRB::hphNT1, YDR086C-myeGFP::HIS3* | This study |
| OGYSGA4425 | *MATa, his3Δ1 leu2Δ0 ura3Δ0 LYS+, can1Δ::STE2pr-LEU2, lyp1Δ::, tor1-1, fpr1Δ::klURA, Tub4-(6)-RFP-(24)-FKBP::natNT2, SEC3-FRB::hphNT1, YOR327C-myeGFP::HIS3* | This study |
| OGYSGA4426 | *MATa, his3Δ1 leu2Δ0 ura3Δ0 LYS+, can1Δ::STE2pr-LEU2, lyp1Δ::, tor1-1, fpr1Δ::klURA, Tub4-(6)-RFP-(24)-FKBP::natNT2, SEC3-FRB::hphNT1, YNL267W-myeGFP::HIS3* | This study |
| OGYSGA4427 | *MATa, his3Δ1 leu2Δ0 ura3Δ0 LYS+, can1Δ::STE2pr-LEU2, lyp1Δ::, tor1-1, fpr1Δ::klURA, Tub4-(6)-RFP-(24)-FKBP::natNT2, SEC3-FRB::hphNT1, YJL145W-myeGFP::HIS3* | This study |
| OGYSGA4428 | *MATa, his3Δ1 leu2Δ0 ura3Δ0 LYS+, can1Δ::STE2pr-LEU2, lyp1Δ::, tor1-1, fpr1Δ::klURA, Tub4-(6)-RFP-(24)-FKBP::natNT2, SEC3-FRB::hphNT1, YPL232W-myeGFP::HIS3* | This study |
| OGYSGA4429 | *MATa, his3Δ1 leu2Δ0 ura3Δ0 LYS+, can1Δ::STE2pr-LEU2, lyp1Δ::, tor1-1, fpr1Δ::klURA, Tub4-(6)-RFP-(24)-FKBP::natNT2, SEC3-FRB::hphNT1, YPR017C-myeGFP::HIS3* | This study |
| OGYSGA4430 | *MATa, his3Δ1 leu2Δ0 ura3Δ0 LYS+, can1Δ::STE2pr-LEU2, lyp1Δ::, tor1-1, fpr1Δ::klURA, Tub4-(6)-RFP-(24)-FKBP::natNT2, SEC3-FRB::hphNT1, YDR363W-A-myeGFP::HIS3* | This study |
| OGYSGA4431 | *MATa, his3Δ1 leu2Δ0 ura3Δ0 LYS+, can1Δ::STE2pr-LEU2, lyp1Δ::, tor1-1, fpr1Δ::klURA, Tub4-(6)-RFP-(24)-FKBP::natNT2, SEC3-FRB::hphNT1, YPL069C-myeGFP::HIS3* | This study |
| OGYSGA4432 | *MATa, his3Δ1 leu2Δ0 ura3Δ0 LYS+, can1Δ::STE2pr-LEU2, lyp1Δ::, tor1-1, fpr1Δ::klURA, Tub4-(6)-RFP-(24)-FKBP::natNT2, SEC3-FRB::hphNT1, YOR122C-myeGFP::HIS3* | This study |
| OGYSGA4433 | *MATa, his3Δ1 leu2Δ0 ura3Δ0 LYS+, can1Δ::STE2pr-LEU2, lyp1Δ::, tor1-1, fpr1Δ::klURA, Tub4-(6)-RFP-(24)-FKBP::natNT2, SEC3-FRB::hphNT1, YLR096W-myeGFP::HIS3* | This study |
| OGYSGA4434 | *MATa, his3Δ1 leu2Δ0 ura3Δ0 LYS+, can1Δ::STE2pr-LEU2, lyp1Δ::, tor1-1, fpr1Δ::klURA, Tub4-(6)-RFP-(24)-FKBP::natNT2, SEC3-FRB::hphNT1, YLR378C-myeGFP::HIS3* | This study |
| OGYSGA4435 | *MATa, his3Δ1 leu2Δ0 ura3Δ0 LYS+, can1Δ::STE2pr-LEU2, lyp1Δ::, tor1-1, fpr1Δ::klURA, Tub4-(6)-RFP-(24)-FKBP::natNT2, SEC3-FRB::hphNT1, YDR122W-myeGFP::HIS3* | This study |
| OGYSGA4436 | *MATa, his3Δ1 leu2Δ0 ura3Δ0 LYS+, can1Δ::STE2pr-LEU2, lyp1Δ::, tor1-1, fpr1Δ::klURA, Tub4-(6)-RFP-(24)-FKBP::natNT2, SEC3-FRB::hphNT1, YER155C-myeGFP::HIS3* | This study |
| OGYSGA4437 | *MATa, his3Δ1 leu2Δ0 ura3Δ0 LYS+, can1Δ::STE2pr-LEU2, lyp1Δ::, tor1-1, fpr1Δ::klURA, Tub4-(6)-RFP-(24)-FKBP::natNT2, SEC3-FRB::hphNT1, YNL271C-myeGFP::HIS3* | This study |
| OGYSGA4438 | *MATa, his3Δ1 leu2Δ0 ura3Δ0 LYS+, can1Δ::STE2pr-LEU2, lyp1Δ::, tor1-1, fpr1Δ::klURA, Tub4-(6)-RFP-(24)-FKBP::natNT2, SEC3-FRB::hphNT1, YGL167C-myeGFP::HIS3* | This study |
| OGYSGA4439 | *MATa, his3Δ1 leu2Δ0 ura3Δ0 LYS+, can1Δ::STE2pr-LEU2, lyp1Δ::, tor1-1, fpr1Δ::klURA, Tub4-(6)-RFP-(24)-FKBP::natNT2, SEC3-FRB::hphNT1, YDR293C-myeGFP::HIS3* | This study |

## APPENDIX I – YEAST STRAINS

| | | |
|---|---|---|
| OGYSGA4440 | *MATa, his3Δ1 leu2Δ0 ura3Δ0 LYS+, can1Δ::STE2pr-LEU2, lyp1Δ::, tor1-1, fpr1Δ::klURA, Tub4-(6)-RFP-(24)-FKBP::natNT2, SEC3-FRB::hphNT1, YKL212W-myeGFP::HIS3* | This study |
| OGYSGA4441 | *MATa, his3Δ1 leu2Δ0 ura3Δ0 LYS+, can1Δ::STE2pr-LEU2, lyp1Δ::, tor1-1, fpr1Δ::klURA, Tub4-(6)-RFP-(24)-FKBP::natNT2, SEC3-FRB::hphNT1, YHR030C-myeGFP::HIS3* | This study |
| OGYSGA4442 | *MATa, his3Δ1 leu2Δ0 ura3Δ0 LYS+, can1Δ::STE2pr-LEU2, lyp1Δ::, tor1-1, fpr1Δ::klURA, Tub4-(6)-RFP-(24)-FKBP::natNT2, SEC3-FRB::hphNT1, YMR307W-myeGFP::HIS3* | This study |
| OGYSGA4443 | *MATa, his3Δ1 leu2Δ0 ura3Δ0 LYS+, can1Δ::STE2pr-LEU2, lyp1Δ::, tor1-1, fpr1Δ::klURA, Tub4-(6)-RFP-(24)-FKBP::natNT2, SEC3-FRB::hphNT1, YDL019C-myeGFP::HIS3* | This study |
| OGYSGA4444 | *MATa, his3Δ1 leu2Δ0 ura3Δ0 LYS+, can1Δ::STE2pr-LEU2, lyp1Δ::, tor1-1, fpr1Δ::klURA, Tub4-(6)-RFP-(24)-FKBP::natNT2, SEC3-FRB::hphNT1, YER098W-myeGFP::HIS3* | This study |
| OGYSGA4445 | *MATa, his3Δ1 leu2Δ0 ura3Δ0 LYS+, can1Δ::STE2pr-LEU2, lyp1Δ::, tor1-1, fpr1Δ::klURA, Tub4-(6)-RFP-(24)-FKBP::natNT2, SEC3-FRB::hphNT1, YER019C-A-myeGFP::HIS3* | This study |
| OGYSGA4446 | *MATa, his3Δ1 leu2Δ0 ura3Δ0 LYS+, can1Δ::STE2pr-LEU2, lyp1Δ::, tor1-1, fpr1Δ::klURA, Tub4-(6)-RFP-(24)-FKBP::natNT2, SEC3-FRB::hphNT1, YDR116C-myeGFP::HIS3* | This study |
| OGYSGA4447 | *MATa, his3Δ1 leu2Δ0 ura3Δ0 LYS+, can1Δ::STE2pr-LEU2, lyp1Δ::, tor1-1, fpr1Δ::klURA, Tub4-(6)-RFP-(24)-FKBP::natNT2, SEC3-FRB::hphNT1, YER114C-myeGFP::HIS3* | This study |
| OGYSGA4448 | *MATa, his3Δ1 leu2Δ0 ura3Δ0 LYS+, can1Δ::STE2pr-LEU2, lyp1Δ::, tor1-1, fpr1Δ::klURA, Tub4-(6)-RFP-(24)-FKBP::natNT2, SEC3-FRB::hphNT1, YIL046W-myeGFP::HIS3* | This study |
| OGYSGA4449 | *MATa, his3Δ1 leu2Δ0 ura3Δ0 LYS+, can1Δ::STE2pr-LEU2, lyp1Δ::, tor1-1, fpr1Δ::klURA, Tub4-(6)-RFP-(24)-FKBP::natNT2, SEC3-FRB::hphNT1, YNL293W-myeGFP::HIS3* | This study |
| OGYSGA4450 | *MATa, his3Δ1 leu2Δ0 ura3Δ0 LYS+, can1Δ::STE2pr-LEU2, lyp1Δ::, tor1-1, fpr1Δ::klURA, Tub4-(6)-RFP-(24)-FKBP::natNT2, SEC3-FRB::hphNT1, YBR135W-myeGFP::HIS3* | This study |
| OGYSGA4451 | *MATa, his3Δ1 leu2Δ0 ura3Δ0 LYS+, can1Δ::STE2pr-LEU2, lyp1Δ::, tor1-1, fpr1Δ::klURA, Tub4-(6)-RFP-(24)-FKBP::natNT2, SEC3-FRB::hphNT1, YDR099W-myeGFP::HIS3* | This study |
| OGYSGA4452 | *MATa, his3Δ1 leu2Δ0 ura3Δ0 LYS+, can1Δ::STE2pr-LEU2, lyp1Δ::, tor1-1, fpr1Δ::klURA, Tub4-(6)-RFP-(24)-FKBP::natNT2, SEC3-FRB::hphNT1, YMR149W-myeGFP::HIS3* | This study |
| OGYSGA4453 | *MATa, his3Δ1 leu2Δ0 ura3Δ0 LYS+, can1Δ::STE2pr-LEU2, lyp1Δ::, tor1-1, fpr1Δ::klURA, Tub4-(6)-RFP-(24)-FKBP::natNT2, SEC3-FRB::hphNT1, YBR088C-myeGFP::HIS3* | This study |
| OGYSGA4454 | *MATa, his3Δ1 leu2Δ0 ura3Δ0 LYS+, can1Δ::STE2pr-LEU2, lyp1Δ::, tor1-1, fpr1Δ::klURA, Tub4-(6)-RFP-(24)-FKBP::natNT2, SEC3-FRB::hphNT1, YMR079W-myeGFP::HIS3* | This study |
| OGYSGA4455 | *MATa, his3Δ1 leu2Δ0 ura3Δ0 LYS+, can1Δ::STE2pr-LEU2, lyp1Δ::, tor1-1, fpr1Δ::klURA, Tub4-(6)-RFP-(24)-FKBP::natNT2, SEC3-FRB::hphNT1, YBR126C-myeGFP::HIS3* | This study |
| OGYSGA4456 | *MATa, his3Δ1 leu2Δ0 ura3Δ0 LYS+, can1Δ::STE2pr-LEU2, lyp1Δ::, tor1-1, fpr1Δ::klURA, Tub4-(6)-RFP-(24)-FKBP::natNT2, SEC3-FRB::hphNT1, YPR024W-myeGFP::HIS3* | This study |
| OGYSGA4457 | *MATa, his3Δ1 leu2Δ0 ura3Δ0 LYS+, can1Δ::STE2pr-LEU2, lyp1Δ::, tor1-1, fpr1Δ::klURA, Tub4-(6)-RFP-(24)-FKBP::natNT2, SEC3-FRB::hphNT1, YER177W-myeGFP::HIS3* | This study |
| OGYSGA4458 | *MATa, his3Δ1 leu2Δ0 ura3Δ0 LYS+, can1Δ::STE2pr-LEU2, lyp1Δ::, tor1-1, fpr1Δ::klURA, Tub4-(6)-RFP-(24)-FKBP::natNT2, SEC3-FRB::hphNT1, YDR217C-myeGFP::HIS3* | This study |
| OGYSGA4459 | *MATa, his3Δ1 leu2Δ0 ura3Δ0 LYS+, can1Δ::STE2pr-LEU2, lyp1Δ::, tor1-1, fpr1Δ::klURA, Tub4-(6)-RFP-(24)-FKBP::natNT2, SEC3-FRB::hphNT1, YDR477W-myeGFP::HIS3* | This study |
| OGYSGA4460 | *MATa, his3Δ1 leu2Δ0 ura3Δ0 LYS+, can1Δ::STE2pr-LEU2, lyp1Δ::, tor1-1, fpr1Δ::klURA, Tub4-(6)-RFP-(24)-FKBP::natNT2, SEC3-FRB::hphNT1, YBR095C-myeGFP::HIS3* | This study |
| OGYSGA4461 | *MATa, his3Δ1 leu2Δ0 ura3Δ0 LYS+, can1Δ::STE2pr-LEU2, lyp1Δ::, tor1-1, fpr1Δ::klURA, Tub4-(6)-RFP-(24)-FKBP::natNT2, SEC3-FRB::hphNT1, YGL173C-myeGFP::HIS3* | This study |
| OGYSGA4462 | *MATa, his3Δ1 leu2Δ0 ura3Δ0 LYS+, can1Δ::STE2pr-LEU2, lyp1Δ::, tor1-1, fpr1Δ::klURA, Tub4-(6)-RFP-(24)-FKBP::natNT2, SEC3-FRB::hphNT1, YKL033W-myeGFP::HIS3* | This study |
| OGYSGA4463 | *MATa, his3Δ1 leu2Δ0 ura3Δ0 LYS+, can1Δ::STE2pr-LEU2, lyp1Δ::, tor1-1, fpr1Δ::klURA, Tub4-(6)-RFP-(24)-FKBP::natNT2, SEC3-FRB::hphNT1, YIL084C-myeGFP::HIS3* | This study |
| OGYSGA4464 | *MATa, his3Δ1 leu2Δ0 ura3Δ0 LYS+, can1Δ::STE2pr-LEU2, lyp1Δ::, tor1-1, fpr1Δ::klURA, Tub4-(6)-RFP-(24)-FKBP::natNT2, DSL1-FRB::hphNT1, YNL048W-myeGFP::HIS3* | This study |
| OGYSGA4465 | *MATa, his3Δ1 leu2Δ0 ura3Δ0 LYS+, can1Δ::STE2pr-LEU2, lyp1Δ::, tor1-1, fpr1Δ::klURA, Tub4-(6)-RFP-(24)-FKBP::natNT2, DSL1-FRB::hphNT1, YGL145W-myeGFP::HIS3* | This study |
| OGYSGA4466 | *MATa, his3Δ1 leu2Δ0 ura3Δ0 LYS+, can1Δ::STE2pr-LEU2, lyp1Δ::, tor1-1, fpr1Δ::klURA, Tub4-(6)-RFP-(24)-FKBP::natNT2, COG6-FRB::hphNT1, YPL050C-myeGFP::HIS3* | This study |

## APPENDIX I – YEAST STRAINS

| | | |
|---|---|---|
| OGYSGA4467 | *MATa, his3Δ1 leu2Δ0 ura3Δ0 LYS+, can1Δ::STE2pr-LEU2, lyp1Δ::, tor1-1, fpr1Δ::klURA, Tub4-(6)-RFP-(24)-FKBP::natNT2, COG6-FRB::hphNT1, YGL223C-myeGFP::HIS3* | This study |
| OGYSGA4468 | *MATa, his3Δ1 leu2Δ0 ura3Δ0 LYS+, can1Δ::STE2pr-LEU2, lyp1Δ::, tor1-1, fpr1Δ::klURA, Tub4-(6)-RFP-(24)-FKBP::natNT2, VPS3-FRB::hphNT1, YDR456W-myeGFP::HIS3* | This study |
| OGYSGA4469 | *MATa, his3Δ1 leu2Δ0 ura3Δ0 LYS+, can1Δ::STE2pr-LEU2, lyp1Δ::, tor1-1, fpr1Δ::klURA, Tub4-(6)-RFP-(24)-FKBP::natNT2, VPS3-FRB::hphNT1, YAL002W-myeGFP::HIS3* | This study |
| OGYSGA4470 | *MATa, his3Δ1 leu2Δ0 ura3Δ0 LYS+, can1Δ::STE2pr-LEU2, lyp1Δ::, tor1-1, fpr1Δ::klURA, Tub4-(6)-RFP-(24)-FKBP::natNT2, VAM6-FRB::hphNT1, YOR270C-myeGFP::HIS3* | This study |
| OGYSGA4471 | *MATa, his3Δ1 leu2Δ0 ura3Δ0 LYS+, can1Δ::STE2pr-LEU2, lyp1Δ::, tor1-1, fpr1Δ::klURA, Tub4-(6)-RFP-(24)-FKBP::natNT2, VAM6-FRB::hphNT1, YDR080W-myeGFP::HIS3* | This study |
| OGYSGA4472 | *MATa, his3Δ1 leu2Δ0 ura3Δ0 LYS+, can1Δ::STE2pr-LEU2, lyp1Δ::, tor1-1, fpr1Δ::klURA, Tub4-(6)-RFP-(24)-FKBP::natNT2, TRS23-FRB::hphNT1, YDR264C-myeGFP::HIS3* | This study |
| OGYSGA4473 | *MATa, his3Δ1 leu2Δ0 ura3Δ0 LYS+, can1Δ::STE2pr-LEU2, lyp1Δ::, tor1-1, fpr1Δ::klURA, Tub4-(6)-RFP-(24)-FKBP::natNT2, TRS23-FRB::hphNT1, YKR068C-myeGFP::HIS3* | This study |
| OGYSGA4474 | *MATa, his3Δ1 leu2Δ0 ura3Δ0 LYS+, can1Δ::STE2pr-LEU2, lyp1Δ::, tor1-1, fpr1Δ::klURA, Tub4-(6)-RFP-(24)-FKBP::natNT2, TRS130-FRB::hphNT1, YDR264C-myeGFP::HIS3* | This study |
| OGYSGA4475 | *MATa, his3Δ1 leu2Δ0 ura3Δ0 LYS+, can1Δ::STE2pr-LEU2, lyp1Δ::, tor1-1, fpr1Δ::klURA, Tub4-(6)-RFP-(24)-FKBP::natNT2, TRS130-FRB::hphNT1, YGR166W-myeGFP::HIS3* | This study |
| OGYSGA4476 | *MATa, his3Δ1 leu2Δ0 ura3Δ0 LYS+, can1Δ::STE2pr-LEU2, lyp1Δ::, tor1-1, fpr1Δ::klURA, Tub4-(6)-RFP-(24)-FKBP::natNT2, TRS85-FRB::hphNT1, YMR159C-myeGFP::HIS3* | This study |
| OGYSGA4477 | *MATa, his3Δ1 leu2Δ0 ura3Δ0 LYS+, can1Δ::STE2pr-LEU2, lyp1Δ::, tor1-1, fpr1Δ::klURA, Tub4-(6)-RFP-(24)-FKBP::natNT2, TRS85-FRB::hphNT1, YKR068C-myeGFP::HIS3* | This study |
| OGYSGA4478 | *MATa, his3Δ1 leu2Δ0 ura3Δ0 LYS+, can1Δ::STE2pr-LEU2, lyp1Δ::, tor1-1, fpr1Δ::klURA, Tub4-(6)-RFP-(24)-FKBP::natNT2, VPS53-FRB::hphNT1, YDR170C-myeGFP::HIS3* | This study |
| OGYSGA4479 | *MATa, his3Δ1 leu2Δ0 ura3Δ0 LYS+, can1Δ::STE2pr-LEU2, lyp1Δ::, tor1-1, fpr1Δ::klURA, Tub4-(6)-RFP-(24)-FKBP::natNT2, VPS53-FRB::hphNT1, YDR027C-myeGFP::HIS3* | This study |
| OGYSGA4480 | *MATa, his3Δ1 leu2Δ0 ura3Δ0 LYS+, can1Δ::STE2pr-LEU2, lyp1Δ::, tor1-1, fpr1Δ::klURA, Tub4-(6)-RFP-(24)-FKBP::natNT2, SEC3-FRB::hphNT1, YGL008C-myeGFP::HIS3* | This study |
| OGYSGA4481 | *MATa, his3Δ1 leu2Δ0 ura3Δ0 LYS+, can1Δ::STE2pr-LEU2, lyp1Δ::, tor1-1, fpr1Δ::klURA, Tub4-(6)-RFP-(24)-FKBP::natNT2, VPS53-FRB::hphNT1, YER136W-myeGFP::HIS3* | This study |
| OGYSGA4482 | *MATa, his3Δ1 leu2Δ0 ura3Δ0 LYS+, can1Δ::STE2pr-LEU2, lyp1Δ::, tor1-1, fpr1Δ::klURA, Tub4-(6)-RFP-(24)-FKBP::natNT2, VPS53-FRB::hphNT1, YJR118C-myeGFP::HIS3* | This study |
| OGYSGA6330 | *MATa, his3Δ1, leu2Δ0, ura3Δ0, LYS+, can1Δ::STE2pr-LEU2, lyp1Δ::, tor1-1, fpr1Δ::klURA, Tub4-(6)-RFP-(24)-FKBP::natNT2, DSL1-FRB::hphNT1, YER166W-myeGFP::HIS3* | This study |
| OGYSGA6331 | *MATa, his3Δ1, leu2Δ0, ura3Δ0, LYS+, can1Δ::STE2pr-LEU2, lyp1Δ::, tor1-1, fpr1Δ::klURA, Tub4-(6)-RFP-(24)-FKBP::natNT2, COG6-FRB::hphNT1, YER166W-myeGFP::HIS3* | This study |
| OGY0858 | *MATa, his3Δ1, leu2Δ0, ura3Δ0, LYS+, can1Δ::STE2pr-LEU2, lyp1Δ::, tor1-1, fpr1Δ::klURA, Tub4-(6)-RFP-(24)-FKBP::natNT2, VPS3-FRB::hphNT1, YER166W-myeGFP::HIS3* | This study |
| OGYSGA6333 | *MATa, his3Δ1, leu2Δ0, ura3Δ0, LYS+, can1Δ::STE2pr-LEU2, lyp1Δ::, tor1-1, fpr1Δ::klURA, Tub4-(6)-RFP-(24)-FKBP::natNT2, VAM6-FRB::hphNT1, YER166W-myeGFP::HIS3* | This study |
| OGYSGA6334 | *MATa, his3Δ1, leu2Δ0, ura3Δ0, LYS+, can1Δ::STE2pr-LEU2, lyp1Δ::, tor1-1, fpr1Δ::klURA, Tub4-(6)-RFP-(24)-FKBP::natNT2, MTC23-FRB::hphNT1, YER166W-myeGFP::HIS3* | This study |
| OGY0863 | *MATa, his3Δ1, leu2Δ0, ura3Δ0, LYS+, can1Δ::STE2pr-LEU2, lyp1Δ::, tor1-1, fpr1Δ::klURA, Tub4-(6)-RFP-(24)-FKBP::natNT2, TRS130-FRB::hphNT1, YER166W-myeGFP::HIS3* | This study |
| OGYSGA6336 | *MATa, his3Δ1, leu2Δ0, ura3Δ0, LYS+, can1Δ::STE2pr-LEU2, lyp1Δ::, tor1-1, fpr1Δ::klURA, Tub4-(6)-RFP-(24)-FKBP::natNT2, TRS85-FRB::hphNT1, YER166W-myeGFP::HIS3* | This study |
| OGYSGA6337 | *MATa, his3Δ1, leu2Δ0, ura3Δ0, LYS+, can1Δ::STE2pr-LEU2, lyp1Δ::, tor1-1, fpr1Δ::klURA, Tub4-(6)-RFP-(24)-FKBP::natNT2, VPS53-FRB::hphNT1, YER166W-myeGFP::HIS3* | This study |
| OGYSGA6338 | *MATa, his3Δ1, leu2Δ0, ura3Δ0, LYS+, can1Δ::STE2pr-LEU2, lyp1Δ::, tor1-1, fpr1Δ::klURA, Tub4-(6)-RFP-(24)-FKBP::natNT2, SEC3-FRB::hphNT1, YER166W-myeGFP::HIS3* | This study |
| OGYSGA6339 | *MATa, his3Δ1, leu2Δ0, ura3Δ0, LYS+, can1Δ::STE2pr-LEU2, lyp1Δ::, tor1-1, fpr1Δ::klURA, Tub4-(6)-RFP-(24)-FKBP::natNT2, DSL1-FRB::hphNT1, YDR093W-myeGFP::HIS3* | This study |
| OGYSGA6340 | *MATa, his3Δ1, leu2Δ0, ura3Δ0, LYS+, can1Δ::STE2pr-LEU2, lyp1Δ::, tor1-1, fpr1Δ::klURA, Tub4-(6)-RFP-(24)-FKBP::natNT2, COG6-FRB::hphNT1, YDR093W-myeGFP::HIS3* | This study |

## APPENDIX I – YEAST STRAINS

| | | |
|---|---|---|
| OGY0859 | *MATa, his3Δ1, leu2Δ0, ura3Δ0, LYS+, can1Δ::STE2pr-LEU2, lyp1Δ::, tor1-1, fpr1Δ::klURA, Tub4-(6)-RFP-(24)-FKBP::natNT2, VPS3-FRB::hphNT1, YDR093W-myeGFP::HIS3* | This study |
| OGYSGA6342 | *MATa, his3Δ1, leu2Δ0, ura3Δ0, LYS+, can1Δ::STE2pr-LEU2, lyp1Δ::, tor1-1, fpr1Δ::klURA, Tub4-(6)-RFP-(24)-FKBP::natNT2, VAM6-FRB::hphNT1, YDR093W-myeGFP::HIS3* | This study |
| OGYSGA6343 | *MATa, his3Δ1, leu2Δ0, ura3Δ0, LYS+, can1Δ::STE2pr-LEU2, lyp1Δ::, tor1-1, fpr1Δ::klURA, Tub4-(6)-RFP-(24)-FKBP::natNT2, MTC23-FRB::hphNT1, YDR093W-myeGFP::HIS3* | This study |
| OGY0864 | *MATa, his3Δ1, leu2Δ0, ura3Δ0, LYS+, can1Δ::STE2pr-LEU2, lyp1Δ::, tor1-1, fpr1Δ::klURA, Tub4-(6)-RFP-(24)-FKBP::natNT2, TRS130-FRB::hphNT1, YDR093W-myeGFP::HIS3* | This study |
| OGYSGA6345 | *MATa, his3Δ1, leu2Δ0, ura3Δ0, LYS+, can1Δ::STE2pr-LEU2, lyp1Δ::, tor1-1, fpr1Δ::klURA, Tub4-(6)-RFP-(24)-FKBP::natNT2, TRS85-FRB::hphNT1, YDR093W-myeGFP::HIS3* | This study |
| OGYSGA6346 | *MATa, his3Δ1, leu2Δ0, ura3Δ0, LYS+, can1Δ::STE2pr-LEU2, lyp1Δ::, tor1-1, fpr1Δ::klURA, Tub4-(6)-RFP-(24)-FKBP::natNT2, VPS53-FRB::hphNT1, YDR093W-myeGFP::HIS3* | This study |
| OGYSGA6347 | *MATa, his3Δ1, leu2Δ0, ura3Δ0, LYS+, can1Δ::STE2pr-LEU2, lyp1Δ::, tor1-1, fpr1Δ::klURA, Tub4-(6)-RFP-(24)-FKBP::natNT2, SEC3-FRB::hphNT1, YDR093W-myeGFP::HIS3* | This study |
| OGYSGA6348 | *MATa, his3Δ1, leu2Δ0, ura3Δ0, LYS+, can1Δ::STE2pr-LEU2, lyp1Δ::, tor1-1, fpr1Δ::klURA, Tub4-(6)-RFP-(24)-FKBP::natNT2, DSL1-FRB::hphNT1, YMR162C-myeGFP::HIS3* | This study |
| OGYSGA6349 | *MATa, his3Δ1, leu2Δ0, ura3Δ0, LYS+, can1Δ::STE2pr-LEU2, lyp1Δ::, tor1-1, fpr1Δ::klURA, Tub4-(6)-RFP-(24)-FKBP::natNT2, COG6-FRB::hphNT1, YMR162C-myeGFP::HIS3* | This study |
| OGY0855 | *MATa, his3Δ1, leu2Δ0, ura3Δ0, LYS+, can1Δ::STE2pr-LEU2, lyp1Δ::, tor1-1, fpr1Δ::klURA, Tub4-(6)-RFP-(24)-FKBP::natNT2, VPS3-FRB::hphNT1, YMR162C-myeGFP::HIS3* | This study |
| OGYSGA6351 | *MATa, his3Δ1, leu2Δ0, ura3Δ0, LYS+, can1Δ::STE2pr-LEU2, lyp1Δ::, tor1-1, fpr1Δ::klURA, Tub4-(6)-RFP-(24)-FKBP::natNT2, VAM6-FRB::hphNT1, YMR162C-myeGFP::HIS3* | This study |
| OGYSGA6352 | *MATa, his3Δ1, leu2Δ0, ura3Δ0, LYS+, can1Δ::STE2pr-LEU2, lyp1Δ::, tor1-1, fpr1Δ::klURA, Tub4-(6)-RFP-(24)-FKBP::natNT2, MTC23-FRB::hphNT1, YMR162C-myeGFP::HIS3* | This study |
| OGY0860 | *MATa, his3Δ1, leu2Δ0, ura3Δ0, LYS+, can1Δ::STE2pr-LEU2, lyp1Δ::, tor1-1, fpr1Δ::klURA, Tub4-(6)-RFP-(24)-FKBP::natNT2, TRS130-FRB::hphNT1, YMR162C-myeGFP::HIS3* | This study |
| OGYSGA6354 | *MATa, his3Δ1, leu2Δ0, ura3Δ0, LYS+, can1Δ::STE2pr-LEU2, lyp1Δ::, tor1-1, fpr1Δ::klURA, Tub4-(6)-RFP-(24)-FKBP::natNT2, TRS85-FRB::hphNT1, YMR162C-myeGFP::HIS3* | This study |
| OGYSGA6355 | *MATa, his3Δ1, leu2Δ0, ura3Δ0, LYS+, can1Δ::STE2pr-LEU2, lyp1Δ::, tor1-1, fpr1Δ::klURA, Tub4-(6)-RFP-(24)-FKBP::natNT2, VPS53-FRB::hphNT1, YMR162C-myeGFP::HIS3* | This study |
| OGYSGA6356 | *MATa, his3Δ1, leu2Δ0, ura3Δ0, LYS+, can1Δ::STE2pr-LEU2, lyp1Δ::, tor1-1, fpr1Δ::klURA, Tub4-(6)-RFP-(24)-FKBP::natNT2, SEC3-FRB::hphNT1, YMR162C-myeGFP::HIS3* | This study |
| OGYSGA6357 | *MATa, his3Δ1, leu2Δ0, ura3Δ0, LYS+, can1Δ::STE2pr-LEU2, lyp1Δ::, tor1-1, fpr1Δ::klURA, Tub4-(6)-RFP-(24)-FKBP::natNT2, DSL1-FRB::hphNT1, YIL048W-myeGFP::HIS3* | This study |
| OGYSGA6358 | *MATa, his3Δ1, leu2Δ0, ura3Δ0, LYS+, can1Δ::STE2pr-LEU2, lyp1Δ::, tor1-1, fpr1Δ::klURA, Tub4-(6)-RFP-(24)-FKBP::natNT2, COG6-FRB::hphNT1, YIL048W-myeGFP::HIS3* | This study |
| OGY0856 | *MATa, his3Δ1, leu2Δ0, ura3Δ0, LYS+, can1Δ::STE2pr-LEU2, lyp1Δ::, tor1-1, fpr1Δ::klURA, Tub4-(6)-RFP-(24)-FKBP::natNT2, VPS3-FRB::hphNT1, YIL048W-myeGFP::HIS3* | This study |
| OGYSGA6360 | *MATa, his3Δ1, leu2Δ0, ura3Δ0, LYS+, can1Δ::STE2pr-LEU2, lyp1Δ::, tor1-1, fpr1Δ::klURA, Tub4-(6)-RFP-(24)-FKBP::natNT2, VAM6-FRB::hphNT1, YIL048W-myeGFP::HIS3* | This study |
| OGYSGA6361 | *MATa, his3Δ1, leu2Δ0, ura3Δ0, LYS+, can1Δ::STE2pr-LEU2, lyp1Δ::, tor1-1, fpr1Δ::klURA, Tub4-(6)-RFP-(24)-FKBP::natNT2, MTC23-FRB::hphNT1, YIL048W-myeGFP::HIS3* | This study |
| OGY0861 | *MATa, his3Δ1, leu2Δ0, ura3Δ0, LYS+, can1Δ::STE2pr-LEU2, lyp1Δ::, tor1-1, fpr1Δ::klURA, Tub4-(6)-RFP-(24)-FKBP::natNT2, TRS130-FRB::hphNT1, YIL048W-myeGFP::HIS3* | This study |
| OGYSGA6363 | *MATa, his3Δ1, leu2Δ0, ura3Δ0, LYS+, can1Δ::STE2pr-LEU2, lyp1Δ::, tor1-1, fpr1Δ::klURA, Tub4-(6)-RFP-(24)-FKBP::natNT2, TRS85-FRB::hphNT1, YIL048W-myeGFP::HIS3* | This study |
| OGYSGA6364 | *MATa, his3Δ1, leu2Δ0, ura3Δ0, LYS+, can1Δ::STE2pr-LEU2, lyp1Δ::, tor1-1, fpr1Δ::klURA, Tub4-(6)-RFP-(24)-FKBP::natNT2, VPS53-FRB::hphNT1, YIL048W-myeGFP::HIS3* | This study |
| OGYSGA6365 | *MATa, his3Δ1, leu2Δ0, ura3Δ0, LYS+, can1Δ::STE2pr-LEU2, lyp1Δ::, tor1-1, fpr1Δ::klURA, Tub4-(6)-RFP-(24)-FKBP::natNT2, SEC3-FRB::hphNT1, YIL048W-myeGFP::HIS3* | This study |
| OGY0847 | *MATa, his3Δ1, leu2Δ0, ura3Δ0, LYS+, can1Δ::STE2pr-LEU2, lyp1Δ::, tor1-1, fpr1Δ::klURA, Tub4-(6)-RFP-(24)-FKBP::natNT2, DSL1-FRB::hphNT1, YAL026C-myeGFP::HIS3* | This study |

## APPENDIX I – YEAST STRAINS

| | | |
|---|---|---|
| OGY0848 | *MATa, his3Δ1, leu2Δ0, ura3Δ0, LYS+, can1Δ::STE2pr-LEU2, lyp1Δ::, tor1-1, fpr1Δ::klURA, Tub4-(6)-RFP-(24)-FKBP::natNT2, COG6-FRB::hphNT1, YAL026C-myeGFP::HIS3* | This study |
| OGY0857 | *MATa, his3Δ1, leu2Δ0, ura3Δ0, LYS+, can1Δ::STE2pr-LEU2, lyp1Δ::, tor1-1, fpr1Δ::klURA, Tub4-(6)-RFP-(24)-FKBP::natNT2, VPS3-FRB::hphNT1, YAL026C-myeGFP::HIS3* | This study |
| OGY0850 | *MATa, his3Δ1, leu2Δ0, ura3Δ0, LYS+, can1Δ::STE2pr-LEU2, lyp1Δ::, tor1-1, fpr1Δ::klURA, Tub4-(6)-RFP-(24)-FKBP::natNT2, VAM6-FRB::hphNT1, YAL026C-myeGFP::HIS3* | This study |
| OGY0851 | *MATa, his3Δ1, leu2Δ0, ura3Δ0, LYS+, can1Δ::STE2pr-LEU2, lyp1Δ::, tor1-1, fpr1Δ::klURA, Tub4-(6)-RFP-(24)-FKBP::natNT2, MTC23-FRB::hphNT1, YAL026C-myeGFP::HIS3* | This study |
| OGY0862 | *MATa, his3Δ1, leu2Δ0, ura3Δ0, LYS+, can1Δ::STE2pr-LEU2, lyp1Δ::, tor1-1, fpr1Δ::klURA, Tub4-(6)-RFP-(24)-FKBP::natNT2, TRS130-FRB::hphNT1, YAL026C-myeGFP::HIS3* | This study |
| OGY0853 | *MATa, his3Δ1, leu2Δ0, ura3Δ0, LYS+, can1Δ::STE2pr-LEU2, lyp1Δ::, tor1-1, fpr1Δ::klURA, Tub4-(6)-RFP-(24)-FKBP::natNT2, TRS85-FRB::hphNT1, YAL026C-myeGFP::HIS3* | This study |
| | *MATa, his3Δ1, leu2Δ0, ura3Δ0, LYS+, can1Δ::STE2pr-LEU2, lyp1Δ::, tor1-1, fpr1Δ::klURA, Tub4-(6)-RFP-(24)-FKBP::natNT2, VPS53-FRB::hphNT1, YAL026C-myeGFP::HIS3* | This study |
| OGY0854 | *MATa, his3Δ1, leu2Δ0, ura3Δ0, LYS+, can1Δ::STE2pr-LEU2, lyp1Δ::, tor1-1, fpr1Δ::klURA, Tub4-(6)-RFP-(24)-FKBP::natNT2, SEC3-FRB::hphNT1, YAL026C-myeGFP::HIS3* | This study |
| OGY0636 | *MATa, his3Δ1, leu2Δ0, ura3Δ0, LYS+, can1Δ::STE2pr-LEU2, lyp1Δ::, tor1-1, fpr1Δ::klURA, Tub4-(6)-RFP-(24)-FKBP::natNT2, MTC33-FRB::hphNT1, DNF1-myeGFP::HIS3* | This study |
| OGYSGA5730 | *MATa, his3Δ1, leu2Δ0, ura3Δ0, LYS+, can1Δ::STE2pr-LEU2, lyp1Δ::, tor1-1, fpr1Δ::klURA, Tub4-(6)-RFP-(24)-FKBP::natNT2, MTC30-FRB::hphNT1, ATG9-myeGFP::HIS3* | This study |

# APPENDIX II – PLASMIDS

| Cassettes | | |
|---|---|---|
| **Vector number** | **Name** | **Source** |
| pOG010 | pFA6a-FRB::hphNT1 | Gallego et at. 2013 |
| pOG019 | pFA6a-(6)-RFP-(24)-FKBP::natNT2 | Gallego et at. 2013 |
| pOG026 | pFA6a-eGFP::His | Provided by Dr. Knop M. |
| pOG029 | pFA6a-3xmyeGFP::kanMX4 | Provided by Dr. Knop M. |
| pOG0201 | pFA6a-3mCherry::natNT2 | Provided by Dr. Knop M. |
| pOG038 | pFA6a-kanMX4 | Provided by Dr. Knop M. |
| pOG039 | pFA6a-hphNT1 | Provided by Dr. Knop M. |
| pOG040 | pFA6a-klURA | Provided by Dr. Knop M. |
| pOG0226 | pFA6a-LEU2 | Provided by Dr. Knop M. |

| Centromeric plasmids | | |
|---|---|---|
| **Vector number** | **Name** | **Source** |
| pOG0190 | pRS416-prAPE1-Ape1-mCherry | Provided by Dr. Malhotra V. |
| pOG001 | pRS313 | Provided by Dr. Kaksonen M. |
| pOG0161 | pRS313-DRS2 | Provided by Dr. Graham T. |
| pOG0169 | pRS313-*drs2-GA* | Provided by Dr. Graham T. |
| pOG0191 | pRS315-*drs2*-ΔGIM | Provided by Dr. Graham T. |
| pOG0192 | pRS315-*drs2*-ΔCM | Provided by Dr. Graham T. |
| pOG0193 | pRS315-*drs2*-ΔCT | Provided by Dr. Graham T. |
| pOG0194 | pRS315-*drs2*-ΔGIM-ΔNPF | Provided by Dr. Graham T. |
| pOG0274 | pRS313-GFP-DRS2 | DC BIOSCIENCES Ltd |
| pOG0275 | pRS313-GFP-*drs2-5A* | DC BIOSCIENCES Ltd |
| pOG0179 | pDDFGP_N-term_DRS2 | This study |
| pOG0264 | pRS313-*drs2*-5A | This study |

| Yeast two-hybrid vectors | | | | |
|---|---|---|---|---|
| **Vector number** | **Name** | **Fusion** | **Yeast Selection** | **Source** |
| pOG0255 | pGADT7 | AD/library | *LEU2* | Provided by Dr. Hamasaki M |
| pOG0257 | pGBKT7 | DNA/bait | *TRP1* | Provided by Dr. Hamasaki M |
| pOG0259 | pGADT7_T | AD/T-antigen | *LEU2* | Provided by Dr. Hamasaki M |
| pOG0260 | pGBKT7_53 | DNA-BD/p53 | *TRP1* | Provided by Dr. Hamasaki M |
| pOG0279 | pGADT7_N-term_DRS2 | AD/N-terminal (633bp)_DRS2 | *LEU2* | This study |
| pOG0280 | pGBKT7_BET3 | DNA-BD/BET3 | *TRP1* | This study |
| pOG0282 | pGBKT7_TRS31 | DNA-BD/TRS31 | *TRP1* | This study |